Spatio-temporal mathematical models of insect trapping: analysis, parameter estimation and applications to control

Claire Chantal Dufourd

Spatio-temporal mathematical models of insect trapping: analysis, parameter estimation and applications to control

by

Claire Chantal Dufourd

Submitted in partial fulfillment of the requirements for the degree

Philosophiae Doctor

in the Department of Mathematics and Applied Mathematics
in the Faculty of Natural and Agricultural Sciences

University of Pretoria
Pretoria

November 2016

Declaration

I, Claire Chantal Dufourd declare that the thesis, which I hereby submit for the degree Philosophiae Doctor at the University of Pretoria, is my own work and has not previously been submitted by me for a degree at this or any other tertiary institution.

SIGNATURE:

NAME: Claire Chantal Dufourd

DATE:

Title	Spatio-temporal mathematical models of insect trapping: analysis, parameter estimation and applications to control
Name	Claire Chantal Dufourd
Supervisor	Prof Roumen Anguelov
Co-Supervisor	Dr Yves Dumont
Department	Mathematics & Applied Mathematics
Degree	Philosophiae Doctor

Summary

Pest insects represent a major threat to public health, to food security as well as to the economy. Constant effort is being made to develop or improve control strategies in the framework of Integrated Pest Management (IPM). IPM aims to maintain pests at low levels that do not represent risks for health or economy, while satisfying environmentally respectful toxicological and ecological requirements. Planning of efficient control strategies requires in-depth knowledge of the pest's biology and ecology. In particular, it is essential to have accurate estimates of parameters of biological and ecological relevance like population size and distribution, dispersal capacity, as well as good understanding of the underlying processes governing the dynamics of the population in time and space.

The aim of this thesis is to provide a mathematical framework for the development of efficient IPM control strategies. This mathematical framework is based on a dynamical system approach and comprises the construction of mathematical models, their theoretical study, the development of adequate schemes for numerical solutions and reliable procedures for parameter identification. The first objective of this thesis is to develop mathematical methods and practical protocols to estimate a pest population size and distribution. The second objective is to predict the impact of a specific control strategy on a pest population and identify how full control of the population can be achieved.

Typically, the only data available on the field is trapping data. Further, to increase the capture of insects, those traps are often combined with a chemical attractant.

The first objective of this thesis is addressed by constructing a generic 2-dimensional spatio-temporal Trap-Insect-Model (TIM) based on biological and ecological knowledge of the pest. This model is formulated by Advection-Diffusion-Reaction (ADR) equations which account for the dispersal capacity of the insects, their attractiveness towards the traps and their demography and trapping. The unknown insect population size and distribution is the initial condition of the model. Usually, the dispersal capacity as well as the parameters related to the traps are also unknown and may vary in time. A major outcome of this thesis is a protocol to identify a set of parameters using trap data collected over a short period of time during which the parameters can be assumed constant.

To address the second objective, we consider a model for the control of crop-pest insects via mating disruption, using a female pheromone, and trapping. Here, males are diverted from females compromising their insemination. The model uses compartmental structure taking into account the specific behaviour of the different groups in the population. It is formulated as a system of ODEs. The theoretical analysis of the model yields threshold values for the dosage of the pheromone above which extinction of the population is ensured.

The practical relevance of the results obtained in this thesis shows that mathematical modelling is an essential supplement to experiments in optimizing control strategies.

Key words: Dynamical Systems; Insect Trapping Models; Advection-Diffusion-Reaction Equation; Threshold Analysis; Parameter Identification; Pest management; Vector control

Acknowledgements

Firstly, I would like to express my sincere appreciation and thanks to my two amazing supervisors, Professor Roumen Anguelov and Doctor Hdr Yves Dumont. They ensured the smooth proceedings of this collaborative research between the University of Pretoria and CIRAD. Thank you both for your continuous support and constant encouragements during my PhD journey. I am very grateful for the excellence of your knowledge and your teachings, I couldn't have been in better hands. Further, Yves, I truly admire your energy and your contagious conviction in the practical applications of mathematical modelling. At times, these came in handy. Thank you for all the very motivating discussions which always helped me to connect the research to the real life problems and move forward. Roumen, thank you for your rigour, your high expectations and your endless patience in making me understand important concepts. Thank you also for always making me see how much progress I have done when everything seemed to stagnate.

I would also like to thank my collaborator Doctor Chris Weldon from the Department of Zoology and Entomology of the University of Pretoria. Thank you for you valuable expertise on fruit flies and for organising a "field trip" to show mathematicians how trapping experiments are carried out.

Further, I would like to thank the Department of Mathematics and Applied Mathematics of the University of Pretoria for awarding me a three-years Pilot bursary and providing me with a comfortable working environment. I would also like to acknowledge the Center of Excellence in Mathematical Sciences (CoE-MaSS) for its support

towards this research which allowed me to complete my work in excellent conditions. I would also like to acknowledge the support of the South African National Research Foundation and the French Ministry of Foreign Affairs and International Development in the framework of the PHC PROTEA 2015 call. Thanks also to the CIRAD UMR AMAP for hosting me during several enjoyable and always productive stays in Montpellier (France).

Special thanks also to the SARChI Chair in Mathematical Models and Methods in Bioengineering and Biosciences (M^3B^2) and in particular to its successive representatives , Professor Jean Lubuma, Doctor Michael Chapwanya and Professor Jacek Banasiak, for giving me the great opportunity to organise our weekly Biomath Coffee meetings. I addition to learning how to make coffee, it was an enriching experience which exposed me to a wide range of stimulating topics.

I would like to express my sincere gratitude to all the administrative staff and colleagues form the Department of Mathematics and Applied Mathematics in UP for their availability and their contribution to ease all the paperwork twists. Special thanks to Yvonne McDermot, Alta van der Merwe, Ronél Oosthuizen, Rachel Combrink and Lorelle Bizaaré. Many thanks also to Nathalie Hodebert and Nora Bakker from the Cirad in France.

I would also like to thank my friends and postgraduate office mates. Ania, I thank you warmly for welcoming me to your house during my very first stay in Pretoria and making me feel instantaneously comfortable in South Africa. I truly miss our ritual weekly brunch! Shanthi, thank you for spreading so much good... I will always remember the day you came to see me with a cup cake to cheer me up. Christine, always in a good mood. Thank you for helping me stay fit by taking me along some of your Husky walks. Wha-Suck, thanks for believing in me and for your spiritual support. Tesfalem, Hagos, Abey, Ocean, Gediyon,... thank you for giving me the chance to get a taste of the Ethiopian culture. Ahmesugenalew. Cheerful Usman, thank you for keeping me updated on the French football team. Basit, Koffi,... All the best to those of you still busy with the completion of your degree.

Finally, a special thanks to my fiancé Thierry. Thank you for your precious advices and for putting up with me throughout the stressful final steps of the writing of the thesis. Last but definitely not least, I would like to thank my family: my

parents, Anne and Jean-Claude, my brothers, Frédéric and Julien, and their families for always being supportive in my life choices. You gave me the emotional support and strength to go through the challenges and complete this PhD. You made me feel close to you despite the distance. For everything, I thank you.

Contents

List of Figures

Chapter 1

Introduction

1.1 General context

Pest insects represent a major threat to public health, food security as well as economy. As reported by the World Health Organization (WHO), today, over 17% of all infectious diseases are vector-borne diseases and are accountable for more than a million deaths each year. Pest insects, for their part, represent a major threat for food production due to there destructive impact on agriculture. In unprotected crops, damages levels can reach 100%. As a consequence, pest insects may have disastrous economical impact. While, the abundant presence of insect-vectors in tourist areas forces to reduce outdoor activities, due to their nuisance and potential health risks [88], the damages caused by agricultural pests not only account for direct crop losses, but also limit exportation and require costly quarantine measures. Billions of US dollars are spent each year on insect pest management in crops to prevent agricultural losses and ensure food production [46]. Thus, the development of efficient control strategies against pest insects to reduce their adverse impact is a challenge of utmost importance.

In order to control pest populations, particular attention is given to Integrated Pest Management (IPM) programs, also known as Integrated Pest Control (IPC) [9]. The aim of such programs is to maintain the pest at a level where they do not represent a risk (economical or epidemiological), while satisfying ecological and toxicological environmentally respectful requirements. Chemical control can be used in IPM, on condition that it does no exceed some low-threshold concentration which ensures no risk for human health. Trapping is often used in IPM programs to monitor pest population indicating their presence and abundance and/or to reduce the size of the population. Biological control methods, which use another

living organism to control a pest (i.e. pest-specific predator), are also often considered for IPM. However, the success of IPM requires a full understanding of the biology of the pest and its ecology [56, 227, 250]. In particular, the knowledge of the pest population size and spatial distribution, as well as other parameters of biological/ecological importance (e.g. lifespan, dispersal rate, etc.) is essential to plan efficient control strategies.

In the prospect of optimizing control strategies, it is necessary to study the dynamics of the population in time and in space. To address this issue, several approaches can be considered. The increase or decline of population abundance can be assessed by direct observations in the field. However, to get a better understanding on the underlying processes that drive the dynamics of a population over a certain period of time, modelling is a useful tool. Indeed, mathematical models consist in describing a process, such as the dynamics of a population, based on knowledge about this process and assumptions. These models can be used to test new hypotheses on the biological mechanisms which govern the dynamics of an insect population, and thereby sharpen or guide the study on its biology and ecology. In addition, analysis of the model and/or simulations allow to test numerous scenarios which is often impractical by field experiments, as they would be too costly and time consuming. Thus, mathematical modelling is an essential supplement to experiments in designing and optimizing pest control strategies.

1.2 Some insect species of interest

We focus our attention on three species of pest-insects that represent a major economical and health concerns in South Africa, namely, the Oriental Fruit Fly *Bactrocera dorsalis*, the False Codling Moth *Thaumatotibia leucotreta*, and the Asian Tiger Mosquito *Aedes albopictus*. These three species have a certain number of similarities in terms of structure within the population as well as ecological behaviour which constitute the biological models considered in this thesis. In particular, these species are small and abundant with a similar life cycle made of four stages where eggs develop into larvae, which then evolve in pupae before emerging as flying-insect adults.

Firstly, particular attention is given to *Bactrocera dorsalis* (Figure 1.2), commonly called the Oriental Fruit Fly, due to its invasive potential [145] and wide diversity of fruit range [211]. It was recorded in the Northern part of the Limpopo province in South Africa in 2010 [167], initially under the identification of *Bactrocera invadens* Drew, Tsuruta & White (Diptera: Tephritidae) [164, 78] which turned out to be the same species as *B. dorsalis* [216, 215]. *B. dorsalis* represents a major threat for fruit industries in South Africa. The life cycle of a fruit fly is represented in Figure 1.1. There are four main stages in the life of a fruit fly: eggs, larvae, pupae and adults. A female lays its eggs just underneath the skin of the host-fruit.

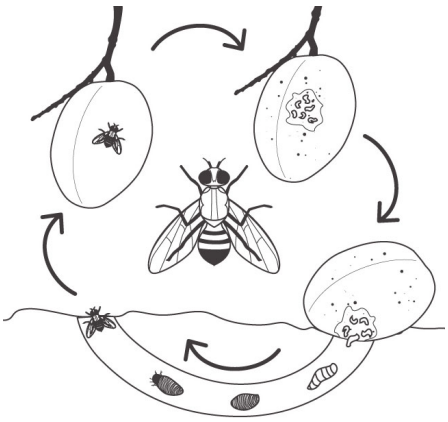

Figure 1.1: Life cycle of fruit fly. (http://preventfruitfly.com.au/about-fruit-fly/life-cycle/)

The larvae develop inside the fruit, digging galleries in the flesh of the fruit which accelerates its maturation causing it to fall from the tree. An example of citrus fruit damaged by fruit fly is shown in Figure 1.4. Once on the ground, the larvae come out from the fruit and bury themselves up to 20 cm deep in the soil. Larvae develop into pupae, before emerging as young adults (immature adults). Following emergence, young adults immediately seek for food (fruit juice, nectar, plant sap, etc. [22]) in order to initiate its reproduction cycle.

Fruit flies are rarely found in very dry areas due to limitations on the host distribution and abundance. Rainy season favours fruit growth and thus leads to expansion of the population, while during dry seasons, when fruits are not available, the population contracts [186, 22]. More information specific to *B. dorsalis* are provided in Focus 1.

Figure 1.2: Fruit fly *Bactrocera dorsalis*. (Source: http://www.kenyabiologics.com/)

Focus 1 (The Oriental Fruit Fly)**.**

Name: *Bactrocera dorsalis*
Origin and distribution: Asia. Today it is distributed all over the world and labelled as invasive species in most areas.
Main impact: (http://www.cabi.org/)

- Economical: high crop loss, cost of quarantine measures
- Environmental: competition for food with other species leads to displacement of endemic non-invasive species.

Biological and ecological facts:

- Life stages duration:
  eggs: 1.2-3 days [89, 191]
  larvae: 5-15 days [89, 191]
  pupae: 8-13 days [89, 191]
  adults: several months depending on environmental conditions [89, 191]
- Mating: occurs on the host-fruit when females come for oviposition. Females detect suitable hosts for laying their eggs using both visual and olfactory mechanisms. Indeed, fruit flies are attracted to the yellow colour, and hydrolyzed proteins. Once the host is identified, females fly around the fruit to choose the spot where to deposit her eggs [22, 191].
- Temperature: between 10° and 30°, however, at lower temperature, pupae can enter dormancy until temperatures get sufficiently warm for emergence. This is how fruit flies overwinter. In autumn, larvae enter in the soil, pupate within a few days and remain dormant until the next warm season [191].

Common control: cultural (fruit bagging, early harvesting, removal and destruction of fallen fruits), chemical (spray of insecticides mixed with a protein bait), sterile insect technique, male annihilation technique.

Secondly, special interest is given to *Thaumatotibia leucotreta*, commonly known as the False Codling Moth (FCM) (Figure 1.3). The FCM is a highly invasive pest, indigenous to southern Africa and Ethiopia [30] and is a key pest for citrus industry in South-Africa. The life cycle of the FCM is similar to the life cycle of *B. dorsalis* with four stages: eggs, larvae, pupae and adult. A female deposits eggs on the surface of a host fruit. Then, follows the larval stage with five instars. Along their development, larvae progress inside the host feeding on the pulp. Upon maturity the larvae exit the fruit and drop to the ground where they spin a cocoon and enter the pupal state. Although the cocoons lie at the surface of the ground, they are difficult to find due to their soil-like colour. Finally adults emerge with a ratio of females to males of 1:2 [71, 60]. Focus 2, page 15 provides more specific information

on the duration of each stage.

Figure 1.3: Adult False codling moth *Thaumatotibia leucotreta*. (Source: http://idtools.org/)

Focus 2 (The False Codling Moth).

Name: *Thaumatotibia leucotreta*
Origin: Southern Africa and Ethiopia [30].
Main impact:

- Economical: crop losses, large range of hosts (citrus, apples, mango, litchi, cotton, coffee, ...)

Biological and ecological facts:

- Life stages duration:
  eggs: 6-12 days [217, 69]
  larvae: 25-67 days [231, 70]
  pupae: 21-80 days depending on the season [68]
  adults: 1-3 weeks in the field [126]
- Mating: occurs shortly after emergence of females, within 2-3 days, and lay eggs at 3-5 days of age. However, these periods can be considerably longer at low temperature. At 10°C, the pre-oviposition period can last up to 22 days followed by a oviposition a period which can last up to 23 days [71]. In the field, the life span of adults lasts from 1 to 3 weeks [126]. Adult moth typically fly during the night and female usually lay their eggs at sunset [67].

Common control: biological (parasitoids, pathogenes), chemical, mating disruption using pheromones.

A similarity between *B. dorsalis* and the FCM is that females lay their eggs in fruits in which they develop into larvae. These larvae feed themselves digging galleries in the flesh of the fruit which accelerates its maturation causing it to fall from the tree. An example of citrus fruit damaged by fruit flies is shown in Figure 1.4.

Thirdly, mosquitoes represent a major threat to human health as they are responsible for the transmission of diseases such as Chikungunya [196], Dengue [114], West Nile

a)  b) 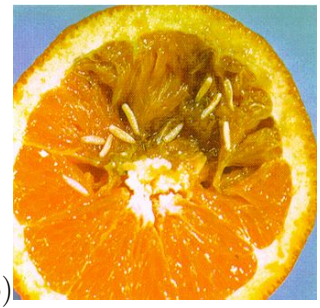

Figure 1.4: Damages on a) the exterior and b) the interior of a citrus caused by *B. dorsalis*.

virus [45], Zika virus [110], etc [176, 139, 31, 100]. A special focus is made on *Aedes albopictus* mosquitoes (Figure 1.6). Similarly to the fruit flies, there are four main stages in the life cycle of a mosquito: eggs, larvae, pupae and adult. The egg, larvae and pupae stages are aquatic, while the adult stage is aerial (Figure 1.5). A female mosquito lays its eggs directly on a water surface or on humid substrates, i.e. breeding sites. Eggs hatch into larvae which undergoes four sloughing. After emergence, adult males and females mate. Then, females disperse seeking for a host to have a blood meal which is necessary for egg maturation. Specific data relative to *Aedes albopictus* mosquitoes are given in Focus 3.

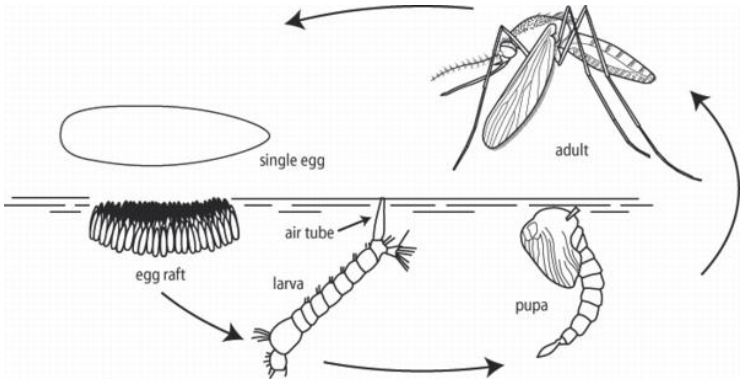

Figure 1.5: Life cycle of moquito. (http://www.tmjv.ca/project-showcase/environmental/mosquito-control-at-tsawwassen-first-nation/)

,

Figure 1.6: Adult mosquito *Aedes albopictus*. (Source: https://en.wikipedia.org)

Focus 3 (The Asian Tiger Mosquito)**.**

Name: *Aedes albopictus*
Origin: originally fund in tropical and subtropical zones, however, according to cabi (http://www.cabi.org/), today they are present in most parts of the world over all continents.
Main impact:

- Health: responsible for the transmission of several diseases among which Yellow fever, Chikungunya, West Nile fever, Dengue, or Zika virus.
- Economical: affects tourism and outdoor activities.

Biological and ecological facts:

- Life stages duration [51, 76]:
  eggs: 3-7 days
  larvae: 7-26 days
  pupae: 2-9 days
  adults: 15-39 days
- Mating: males seek for females near the breeding sites from which they will emerge. Females can lay between 50 and 500 eggs [51, 57].

Common control: chemical (DDT, BTI), trapping (BG-sentinelTM, collapsible mosquito trap with attractant like CO_2), mechanical (destruction of breeding sites), physical (mosquito nets and repellents), biological (*Metarhizium anisopliae*).

1.3 Control methods

In order to manage pest insects and prevent the damage they cause, several control methods are commonly used. Chemical control has been widely used in the past due to its efficiency in reducing pest abundance. However, chemical control has harmful side effects which encourages the use of other methods. Alternative methods consist of modifying the environment to prevent damages of the pests. These damages can also be avoided by setting physical barriers to put the hosts out of reach of the pest. However, these methods may be difficult to implement on a large scale. Biological control, behaviour disruption and mass trapping are interesting alternatives to control insect pest populations meeting the requirements of IPM. Each method has its advantages and disadvantages. Efficient control is usually done via an appropriate combination of methods.

1.3.1 Chemical control

Chemical control consists in massive spraying of insecticides which include ovicides and larvicides to kill eggs and larvae. For instance, *dichlorodiphenyltrichloroethane*, also known as DDT which has been widely used to kill adult mosquitoes [143], while another product, *bacillus thuringiensis israelensis*, more commonly known as BTI, is usually poured into their breeding sites to destroy the larvae [23]. For the control of fruit flies, Dimethoate, Malathion or Methidathion are often used [183]. Benzyl-urea is another commonly used pesticide used for the control of the false codling moth *Thaumatotibia leucotreta* [232].

Despite the efficiency of chemical control in reducing the pest population, this method also has substantial adverse effects on human health, livestock and/or environment [240, 103, 224]. The use of insecticides is detrimental to the environment and can disturb the entire ecosystem. Indeed, the chemical may be dangerous for other species among which possible natural predators of the pest. The use of chemicals also contributes to pollution of the soil and underground water [177]. In addition, these products are also dangerous for the producer, who is exposed to it when spraying, as well as for the consumer since residuals of the chemical can be found in the fruits or vegetables treated. In addition, there is a high risk that insects develop resistance to the chemical leading to the use of stronger products [132, 202, 165]. All these drawbacks make chemical control a non-sustainable method as part of IPM.

1.3.2 Environmental management

Environmental management includes a wide range of interventions to reduce the abundance of pest-insects populations. A way to reduce the damages of a pest is by transforming the pest's habitat through environmental modifications to produce unfavourable conditions for its establishment. In the case of fruit flies or moths, removing and destroying the fallen fruits and/or mummies allow to interrupt the development and growth of the eggs and larvae and limit the number of new emerging adults susceptible to cause damage [106, 232]. Mosquitoes are highly abundant in urban areas due to the availability of hosts for blood meals, and the wide range of potential breeding sites. Mosquito breeding sites are typically small and shallow with stagnant water which offer a wide range of potential breeding sites sometime difficult to find. Breeding sites can be natural (leafs retaining water, puddles, etc.) as well as domestic (plant saucers, tires, ornamental bird baths , buckets, clogged gutters, any objects susceptible of retaining water)(Figure 1.7) [122]. Measures consisting in reducing the number of breeding site have been recommended at least since the 1910's in order to prevent transmission of Malaria [249, 210]. However, such a method cannot be effective without the awareness and help of the local population to clean there own habitat. Thus, environmental

Figure 1.7: Examples of breeding sites for mosquitoes.

management has the advantage of being environmentally friendly as it only affects the pest itself, with no risk for the producers and consumers. However, modifying the environment is often difficult to put into practice as it requires a considerable manpower. In addition, to obtain significant results, a good understanding on the ecology of the pest is essential, in particular its distribution and seasonal variations.

1.3.3 Physical control

Physical control aims at limiting contacts between the pest and its host. For example, mosquito nets can be set to prevent people from being bitten. To prevent fruit fly damages in crops, fruits can be bagged (Figure 1.8) to prevent females from accessing the hosts to lay eggs. Another way to reduce contact between the host and the pest is to adapt agricultural

Figure 1.8: Mango fruit bagging.

practices. For instance, early harvesting of the fruits can also prevent fruit fly damages, as for the olive fruit fly [208]. Although physical control presents no risks for the environment, its implementation is difficult on a large scale due to its local action and no direct reduction in the pest population abundance.

1.3.4 Biological control

Biological control consists in involving other living organisms such as natural predators, parasites, or parasitoids to maintain the abundance of the pest population below acceptable (health and economical) level. Parasitoids are organisms that "live" on another one taking resources from a single host. While parasitoids usually kill there host, it is not necessarily the case for parasites [107]. For instance, weaver ants (*Oecophylla longinoda*) have been used in controlling mango fruit fly in Benin [243]. As for the control of the false codling moth, there are 25 known natural enemies present in Southern Africa [232]. Particular attention has been given to the egg parasitoid *Trichogrammatoidea cryptophlebia* for commercial biological control [232]. Concerning the biological control of mosquitoes, predation on the aquatic stage is usually more effective than on the adult stage due to its limited spatial displacements. The most important predators for aquatic mosquitoes are species of fish, such as the *Gambusia affinis* fish or the *Poecilia reticulata* fish, respectively native from Central America and

South America. These have been used for decades for mosquito biological control [154]. To a smaller extent, some birds species use mosquito larvae as a source of food such as the *Anas platyrhynchos* duck. Few birds actually feed on mosquitoes as they are usually day-light hunters, thus their hunting periods typically do not coincide with mosquitoes activities. On the other hand, bat are night-hunters and represent a higher predation risk for mosquitoes. Species of amphibians, like newts and their larvae are also considered as important predators for immature mosquitoes. Other predators can be mentioned, like the flatworm *Turbellaria*, some spices of spiders and mites or crustaceans, some insects (dragonflies, heteroptera, trichoptera, diptera etc.) and parasites (nematodes). Although macro organisms, like fish or nematodes, have been widely used for mosquito control, they are often difficult to rear and can only survive in specific ecological environments which makes their use in biological control programs difficult and expensive. Further, a wide variety of pathogens have been discovered over the past decades which represent important risk for the mosquito population. For more extensive details on the predators of mosquitoes, the reader shall refer to the book of Becker. [24, Chapter 16].

As part of biological control, one can mention the replacement of dengue-vector *Aedes* mosquito population by a population of mosquitoes unable to transmit the disease using the intracellular bacterium *Wolbachia* which interferes with the transmission of the disease pathogen. Alternatively, *Wolbachia* can also be used to control a population via Cytoplasmic Incompatibility (IC). In this case, males infected with *Wolbachia* become unable to reproduce successfully with uninfected females or with females infected with another strain of *Wolbachia* [251]. The method consists in releasing large amounts of mosquitoes infected by *Wolbachia* which contaminate wild mosquitoes leading to a decline of the abundance of mosquitoes able to transmit the disease [129, 130]. Further, mathematical modelling approaches have shown to provide encouraging results for the successful control of a vector population using *Wolbachia* (see [97, 151, 29, 213] and references therein).

1.3.5 The sterile insect technique

Another branch of control goes back from the 1950's with the work of Knipling [146, 148] as he discovered that the abundance of mosquitoes could be reduced if females mate with sterile males. In this context, the sterile insect technique (SIT) is a promising control method for pest-insect populations. SIT consists in releasing a large number of reared sterilized males to compete with wild males for female insemination. Females inseminated by sterile males produce non-viable offspring, leading to the reduction of the mosquito population [147, 155]. SIT is of great interest as it targets exclusively the insect to control and has no detrimental effect on the surrounding environment. SIT has shown to be a successful method in various

cases [148], for example, in the control of the mosquito *Aedes albopictus* in Italy [25]. SIT has also been considered for the control of the false codling moth in South Africa [131], or for the control of *Bactrocera dorsalis* fruit fly [92]. SIT is a promising alternative as it enables producers to meet the strict sanitary international exportation requirements (no pesticides residues on fruits). However, to be successful, SIT requires an acute understanding on the insect ecology and biology.

1.3.6 Genetic control

Using a similar approach as for SIT control, genetic pest management is based on the release genetically modified (GM) insects [109, 2]. In the Release of Insects carrying a Dominant Lethals (RIDL) method [234], the GM insects carry a lethal gene in their genome which causes death of there offspring at early stages of development. In turns, this reduces the abundance of the insect population. Promising attempts of RIDL have been made by the company Oxitec on *Aedes aegypti* in Malaysia and in Brazil [104].

Alternatively, instead of carrying a lethal gene, GM insects can carry a disease-refractory gene. Following the same releasing process, the GM insects produce offspring that cannot transmit the disease, reducing progressively the proportion of insects active in the disease transmission process. Eventually, this leads to a replacement of the insect population by a disease-refractory population. An advantage of population replacement is that the insect species is not eliminated and can still play its role its ecosystem. This method has been considered, for instance, to control *Aedes aegypti* mosquito by genetically altering it capacity to support the yellow fever virus replication [50].

However, a limitation in genetic control is that it relies on the parent-to-offspring transmission of the novel traits. Thus, the success of the method relies on the mating of genetically modified insects with wild insects of the same species. This means that a specific transgenic strain is required for each species. This can make genetic control impracticable when several species of the same *group* (i.e. several mosquito species) are responsible for the transmission of the same disease. To overcome this limit, a recent study proposes a *para-transgenic* approach [255].

A major advantage of biological, SIT or genetic control, is its species-specific nature. With such methods, the target-pest is control without affecting other species or the surrounding environment. Further, the involvement of living organisms allow to reach areas that other cannot be controlled using other methods due to physical barriers or lack on the ecological knowledge of the pest (i.e. its interactions with the environment, its shelters, etc.). Moreover, there are no health concerns for producers and consumer due to chemical residues meeting

the requirements of IPM. Despite its environmentally friendly aspects biological control can be difficult to implement. Indeed, the natural predators are usually expensive and sometimes difficult to rear in large abundance. In addition, evaluating the establishment of the predator in a new environment is difficult (Can the predator represent a risk of invasion? Can it survive in the new environment?). Further, a good understanding on the pest biology and its interactions with the environment is essential for its success. In particular, for efficient control strategy, one should address the following questions:

- When and where should the modified insects be released?
- Which quantity of modified insects should be introduced to ensure efficient control?
- At what frequency should the releases occur?

Planning efficient biological control is not straightforward. To optimize such strategies, mathematical models can provide a useful tool to study the system and simulate various scenarios.

1.3.7 Behaviour disruption

Another control method which is fully part of IPM consists in modifying the behaviour of insects. This can be done by attracting them away from the host they represent a risk for and/or possibly towards a trap where they get killed, or by disturbing their life cycle using lures of the natural attractants that condition the behaviour of the insects, such as food, pheromones, CO_2, or specific colours or shapes [93].

Poison baits methods are today's most common control techniques used to control fruit flies. These methods consist of food attractant mixed with an insecticide (such as malathion or GF-120), usually applied on a part of an orchard or a tree, on which adult flies feed and get poisoned [167, 168]. This method has shown efficient results in the control of *B. dorsalis* and *C. cosyra* in Benin [244].

In a similar manner, in male annihilation technique (MAT), a sex attractant is used together with insecticide to attract and poison male fruit flies [135, 256]. In particular, this method has been used for the control of *B. dorsalis* (Focus 1, page 14) in South Africa [167] and in French Polynesia [158]. MAT has also been widely used on various types of crops against the False Codling Moths (Focus 2, page 15) [21, 48]. Early success of MAT for eradication of *B. dorsalis* in the Okinawa Islands has been show in 1984 [152]. More recently, the method has been successfully used in Italian greenhouses to protect tomato crops from the damages of *Tuta absoluta* [58]. Supports, like coconut husks, can be used to soak the

male attractant with the insecticide (Figure 1.9). Such methods are typically used in traps in order to monitor the presence and abundance of flies. These traps are containers in which the attractant and insecticide can be placed, with holes, usually in funnel shape to facilitate the entrance. In addition the attractiveness of the traps can also depend on visual cues, such as the size, shape, colour or placement of the traps [59, 207, 206]. The Mcphail trap, shown in Figure 1.10, is commonly used [229, 3].

Figure 1.9: Blocks of coconut husks, soaked in a mixture of sex-attractant methyl eugenol and insecticide Malathion, to be nailed on trees used in French Polynesia to attract and kill male Oriental fruit flies. (photo: L. Leblanc)

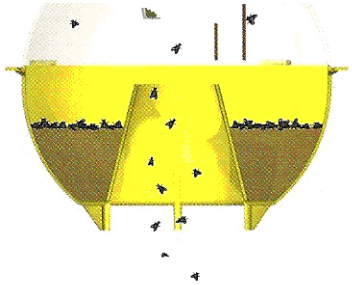

Figure 1.10: Mcphail trap.

1.4 Modelling population dynamics

Population dynamics is the study of the variations in a population size, its structure and/or its distribution with respect to changes in various factors such as time, space, temperature and other environmental factors. The aim of population dynamics is to identify the factors responsible for the growth or decline of a population. Further, it provides a better understanding of the underlying processes that explain how a population interacts with its surrounding environment, for instance, how individuals react to different stimuli. The study of population dynamics has a wide range of useful applications. Studying the spread of a disease, for instance, helps to identify the best periods of intervention to reduce epidemiological risks [34, 172]. In pest management, the understanding of the pest population dynamics allows to develop appropriate control methods to maintain the population at a low risk level [163]. Population dynamics is also a powerful tool to predict biological invasions [113], by modelling its spreading for instance, and evaluate ecological risks.

Population dynamics can be studied following empirical or theoretical approaches. On the one hand, empirical study of population dynamics is based on observation data obtained via experimentation. A descriptive analysis can be carried out to describe the variations observed in a population in the setting of the experiment. Observation data are useful to establish the behaviour of the population, however, it is typically inherent to the experimental setting and provides very limited information on the general dynamics of a population. On the other hand, theoretical study of population dynamics allows to test various biological hypothesis difficult to assess with direct observations, in particular concerning interactions between the population and its environment, through methods of analysis such as statistical or mathematical modelling.

A **model** is a process through which given specific inputs (e.g. time, spatial location or temperature), and specific parameters (e.g. growth rate or dispersal rate), provides of an output which is an approximation of a variable of interest such as the population size. To study the evolution of a biological process, the input variables can be discrete or continuous. In the discrete framework, the output of the model is computed at values of the variable occurring at distinct points, while in the continuous setting, the values of the variable are defined on a real interval.

A model is built on biologically/ecologically relevant hypothesis and assumptions to provide an approximation of the population variable of interest, such as the population size, given specific inputs and parameter values. Statistical models are constructed using a specific set of observation data from which the parameter values of the model are estimated in such a way that the output of the model fits as well as possible to the data. Thus, statistical

models often provide a good match to the data, but the results are limited by the fact that they are constructed and valid only for the specific setting of the experiment for which the observation data were obtained. Such a model can be used to identify correlations between different variables. However, it does not give information on *why* such correlations exist. Mathematical models on the other hand, are built on biological and ecological knowledge of the population dynamics, independently from specific observation data. Although the output of mathematical models is not as good in fitting observation data, they offer the possibility to change the settings and simulate various scenarios. This process allows to gain understanding on the underlying mechanisms that govern the dynamics of the population.

Modelling is a useful tool to improve our understanding on the interactions between the population and its environment. Through simulations, modelling enables to vary the parameters and identify the factors of importance in the variation of a population. In the following, we discuss how heterogeneity in a population can be handled considering structured population models. Then, we give an overview on models incorporating the space and time variables, which represent the major interest in this thesis.

1.4.1 Structured population models

Individuals of a population can contribute significantly differently to the dynamics of the population depending on different aspects, such as their age, stage of development, epidemiological state, spatial position, etc. In the following we will refer to such aspects as *structuring variables*. In order to obtain a meaningful model, we structure the population to take into account the heterogeneity of the individual with respect to the mentioned-above aspects.

If the structuring variable is discrete assuming a finite number of distinct states, then the model is formulated via a system of equations for which each equation accounts for the dynamics of the population in each state of the structuring variable. Typically the different distinct states are referred to *compartments*, and the resulting model is called a *compartmental model*. For example, insects have distinct stages of development, eggs, larvae, pupae and adults, with specific duration, survival rates, exposure to predation, behaviour, displacement ranges, etc.

A compartmental model can be discrete or continuous with respect to the time variable. In the discrete case, the state of the population is approximated at specific times $t_0, t_1, \ldots, t_K$, using a relation of the form

$$\mathbf{N}_{k+1} = \mathbf{f}(\mathbf{N}_k), \quad k \in \{0, 1, \ldots, K\}, \tag{1.1}$$

where $\mathbf{N}_k$ is the vector of each compartments of the population at time t_k, and $\mathbf{f}$ is a vector of

functions which describes the dynamics of each compartment (i.e. demography, interactions between the compartments, etc.). One of the most well-known models of this type, is the Leslie matrix model [161] where the population (usually, only the females are taken into account) is divided into a finite number of age classes (or stages of development [160]) to account for age-specific behaviour. If N_i denotes the number of individuals in age class (or life stage) $i \in \{0, 1, \ldots, n-1\}$, s_i the fraction of individuals that survived from class i to class $i+1$, and g_i the per capita number of offspring supplying the compartment N_0 with a mother in class N_i, the Leslie model is formulated as

$$\begin{pmatrix} N_0 \\ N_1 \\ N_2 \\ \vdots \\ N_{n-1} \end{pmatrix}_{t+\Delta t} = \begin{pmatrix} g_0 & g_1 & \ldots & g_{n-1} & g_n \\ s_0 & 0 & \ldots & 0 & 0 \\ 0 & s_1 & \ldots & 0 & 0 \\ \vdots & \vdots & \ddots & \vdots & \vdots \\ 0 & 0 & \ldots & s_{n-2} & 0 \end{pmatrix} \begin{pmatrix} N_0 \\ N_1 \\ N_2 \\ \vdots \\ N_{n-1} \end{pmatrix}_t \tag{1.2}$$

or

$$\mathbf{N}_{t+\Delta t} = L\mathbf{N}_t, \tag{1.3}$$

where L is the Leslie transition matrix, and Δt denotes the time step between two consecutive computations. Asymptotic behaviour of the solution of the Leslie model can be done by studying its eigen values. In particular, if λ denotes the dominant real eigen value of the Leslie matrix L (existence of λ is due to the Perron-Frobenius theorem [49]), then, the age structure of the population converges to the eigen vector associated to λ, N^*. Further, if $\lambda > 1$, the total population grows exponentially, if $\lambda < 1$, the total population decreases exponentially, and if $\lambda = 1$, the total population remains constant. Among other applications, this approached has been used for instance to study the dynamics of aphids insects [187] or the beetle *Lasioderma searaicoarn* [160].

When the time-variable is continuous, then the state of the population at time t is approximated by a continuous and differentiable vector function $\mathbf{N}(t) \in \mathbb{R}^n$. The resulting model is a system of ODEs formulated as follows

$$\frac{d\mathbf{N}(t)}{dt} = \boldsymbol{\phi}(\mathbf{N}(t)) \tag{1.4}$$

or equivalently

$$\begin{cases} \dfrac{dN_1}{dt} &= \phi_1(t, N_1, \ldots, N_n) \\ \vdots & \\ \dfrac{dN_n}{dt} &= \phi_n(t, N_1, \ldots, N_n) \end{cases} \tag{1.5}$$

where $\boldsymbol{\phi}$ is a continuous vector function. Each differential equation of (1.5) describes the temporal growth of a specific (homogeneous) compartment and can be modelled using standard temporal population models (exponential, logistic, etc.) and functional and numerical responses (e.g. Holling type responses [133]).

The model presented in chapter 5 is of the form of (1.5) and aims to study the impact of mating disruption, using female pheromones, and trapping control on a pest-insect population. There, the population according to its stage of development and to specific behavioural aspects of importance in the mating disruption and trapping process. More precisely, since the control targets the adult stage, we consider on the one hand an aquatic stage which gathers eggs, larvae and pupae. Further, since the control affects the behaviour of the males, they have their own compartment. Finally, since the population of males affects the fertilisation of females, the latter are compartmented in "females available for mating" and "fertilised females". This leads to a 4-compartment model formulated as a system of 4 ODEs. The mathematical background used to study theoretically such models is provided in chapter 2, section 2.4.

An alternative to the discrete case is the situation when the structuring variable is continuous. Age, or position can be continuous structuring variables. In this case, a single equation can account for the population dynamics with respect to the time variable as well as the structuring variable formulated by a partial differential equation (PDE). If the structuring variable x is defined in an open domain of $\mathbb{R}^p$, then a PDE of order m can be written in the following generic form.

$$\frac{\partial N(t,x)}{\partial t} = F\left(t, N(t,x), \dots, D_x^{\alpha} N(t,x), \dots\right), \quad \alpha \in \mathbb{R}^p, |\alpha| < m \tag{1.6}$$

As an example, to study the spread of infectious diseases through a population structured continuously in age McKendrick and Kermack [181, 144] were the fist to introduce a PDE model. In this model $N(t,x)$ denotes the density of the population of age x at time t and $\mu(x)$ is an age-dependent mortality function. Further, $b(x)$ represents the fecundity function which determines the recruitment into the population at age $x = 0$. The *McKendrick - von Foerster* equation [246] is then formulated as

$$\frac{\partial N(t,x)}{\partial t} + \frac{\partial N(t,x)}{\partial x} = -\mu(x) N(t,x), \tag{1.7}$$

with boundary condition

$$N(t,0) = \int_0^{\infty} b(x) N(t,x) dx. \tag{1.8}$$

In chapters 3 and 4, the models are structured in space. The aim of the models is to simulate trapping data in order to estimate parameters by using different trap configurations. Hence, in these models, the localisation in space is considered an important factor affecting the dynamics of the population. In the section below, we present some commonly used models which account for spatial heterogeneity.

1.4.2 Spatio-temporal models

The growth of a population is strongly correlated to its geographic distribution range [162]. A spatio-temporal population model is a structured population model that governs the dynamics a population with respect to changes in time and space. Adding the spatial component allows to model population dynamics with more realism taking into account interactions between a species and its habitat. Adding spatial information however adds complexity to the model making it more difficult to study and simulations more computationally intensive. Therefore a trade-off between the realism of the model and the question it is aimed to answer must be kept in mind for its conception.

1.4.2.1 Characteristics of spatio-temporal models

Different aspects can be considered to categorize spatio-temporal models [44, 112]. We follow here the characterisation given by [44]. The first characteristics that can be mentioned is on whether the space component is taken into account implicitly in the model, or explicitly [66, 112]. In **implicit** spatial models the population is assumed to be spatially structured, however the model does not incorporate topographic localisations. These models are relatively simple but do not allow to study the effect of the structure of the environment on the dynamics of the population. On the other hand, in **explicit** models the individuals of the population are allocated a topographic localisation. This allows to combine the dynamics of the population to geographic data, such as maps of the habitat. Therefore, explicit models allow to account for the complexity of the environment and obtain a better understanding on the ecology of a population.

Such models can simulate the trajectories of the individuals in a population. These are **Individual-Based Models** (IBM). The trajectory of each individual is governed by specific rules to take into account the variability of the individuals interactions with other members and the environment. An extensive review of applications of IBM models can be found in [75]. In particular, it has been used to model the dynamics of the Large Blue Butterfly, *Maculinea arion* in the framework of species conservation [111]. IBMs can be very useful to

model complex processes. It has been used and analysed for instance to investigate dynamics of a prey-predator system of populations structured in age and space [174]. However some disadvantages of such models are that they are computationally intensive and that it is necessary to have a very acute understanding and knowledge of the insect's behaviour to program and simulate the individual dynamics. Indeed, not only they require specific instructions for each individuals, but a large number of individual trajectories need to be simulated to obtain information at the population level [26].

Alternatively, models can account for the whole population assuming homogeneity among individuals using **population models**, also known as **mass-interaction models**. Population models are analytical and do not account for variability among individuals. It can be assumed, for example, that all individuals are identical [26]. Thus, population models are suitable for the study of an averaged behaviour of the population. Such models can be useful to study interactions between populations or within a population [66, 237]. This approach is particularly suitable for the modelling of abundant populations, such as insects [83]. Models discussed below in sections 1.4.2.2 and 1.4.2.4 are examples of population models.

Further, models can be categorised as deterministic or stochastic. **Deterministic** models simulate the average behaviour of the population without taking into account variability in the parameters or in the functions describing the model. Such an approach is particularly suitable to model the dynamics at a population level. On the opposite, **stochastic** models the dynamics are governed by probability function to account for variability which makes them more appropriate to model dynamics of small populations [85]. Although stochastic models are more realistic, they are also more difficult to study theoretically.

Another distinction that can be made among these models is on the discrete or continuous nature of the space variable. In **discrete-space models**, the space is divided in separate areas with an index referring to its position [84], while **continuous-space models** use the spatial coordinates of each location [66].

Considering the possible combinations of the characteristics presented above gives rise to a wide variety of models. The choice of the model depends on the population as well as on the aim of the model. We now give some examples of commonly used models with applications.

1.4.2.2 Metapopulation models

When the space variable is taken into account implicitly, temporal models at specific locations can be constructed with location-specific parameters and interactions between them, while in the explicit case, the model incorporates a space variable. This is the case of

metapopulation models, first formulated by R. Levin in 1969, where the space is discretized in distinct patches with their own specificities on which temporal dynamics are described [117, 118]. The spatio-temporal model is then a coupling of the temporal models on each of the patches with interactions between them. Metapopulation models can be formulated mathematically by ODE or Difference Equations. Metapopulation models have been used, for example, to study host-parasit interactions in patchy environments [120]. In particular it has been used to describe the spatio temporal dynamics of the pathogen *Wolbachia* (used for the control of *Aedes* mosquitoes) in a age-structured host population [116]. Metapopulation models have also been used to study the spread of Malaria in a vector-host population structured according to its infectious state [11, 10]. Another example of application of metapopuation model is to model the adaptation of fruit flies in a patchy environment [221].

1.4.2.3 Cellular-automata models

In cellular automata models the space explicit and discretized in a regular grid of cells. Each cell is attributed a state chosen among a fine set of states which is defined as a function of the states of a finite number of neighbouring cells. Cellular automata models can be seen as an extension of the metapopulation model proposed by Levin where the cells are patches with topographic locations [237]. A cellular automata is suitable for IBM representation where a cell may contain at most a single organism and the model can simulate local dispersal to the neighbouring cells emitted from a specific release cell. The rules which define the state of each cell may be stochastic or not. FlySim is a cellular automata program developed to simulate life cycles of the olive fruit fly [199]. In [223], a cellular automata model is used for the control of Chagas disease by modelling the dynamics of its insects vector.

1.4.2.4 Advection-Diffusion-Reaction

In the prospect of modelling pest-insect population dynamics, a particular attention is given to **Advection-Diffusion-Reaction** (ADR) models governed by PDEs. These are deterministic mass-interaction models continuous in time and space, thus they account for an average behaviour of the population. In ADR models, the diffusion process accounts for the random dispersal of the individuals of the population, without considering any sort of stimulus to direct their movements [74, 190]. The advection process accounts for directional displacements due to a flow, like wind transport, or attractiveness to a point (food, breading site, attractive traps...). Finally the reaction process governs the demography. In addition, in order to account for some heterogeneity within the population, the individuals can be

grouped according to their age class or development stage. In this case the models becomes a system of coupled ADR equations where the reaction process also accounts for interactions between the different compartments.

ADR models are continuous in space (x) and time (t) and are formulated in terms of partial differential equations [112]. The general form of a ADR equation is given as follows:

$$\frac{\partial u(t,x)}{\partial t} = a\frac{\partial u(t,x)}{\partial x}) + D\frac{\partial^2 u(t,x)}{\partial x^2} + f(t,x), \tag{1.9}$$

where $u(t,x)$ represents the population density at time t and position x, the parameters D and a are respectively the diffusion rate and the advection force, and the function f is the reaction term.

The population ADR models can be derived from random walk processes at the individual level using Taylor's expansions. This derivation is detailed in several publications [27, 188, 238]. Alternatively, it is worth mentioning that the diffusion processes can also be derived using flux considerations instead of random walk processes [87, 238]. In the latter case, the derivation is based on the physics conservation law and the Fick's law of diffusion which connects fluxes of particles to their gradient [61]. The derivation of models from individual level to the population level is a challenge of its own as the dynamics of the individuals are typically more complicated than a simple non-isotropic random walk. For example, in [200], a chemotaxis population model is derived from individual behaviours, for two interacting populations where one is a stimulus of the other.

These models are particularly useful to study insect dispersal [16, 121, 238] and biological invasion processes [220]. For example, in [209] a reaction-diffusion is constructed to predict the expansion of the invasive chalcid *Megastigmus schimitscheki* in plantations of cedars. Further, the knowledge of the spatio-temporal distribution of an organism is a crucial information for species conservation or, on the opposite, for control plans. ADR models have been used for instance to evaluate the effect of SIT control. In [241] a diffusion-reaction model is used to describe the spread of the sterile male codling moths, *Cydia pomonella*. In [80] an ADR model is formulated to investigate the impact of environmental factors (spatial heterogeneity and temperature) on an *Aedes* mosquito population and to test various SIT-control strategies. In addition, dispersal abilities of insects is an essential information to plan efficient control of pest insects and/or prevent biological invasions [220, 238]. A diffusion-based model has been used to study, for example, the dispersal of the sterile Mediterranean fruit fly *Ceratis capitata* from a release point [197].

ADR models can be studied analytically to obtain biologically relevant results. For instance, in some cases, we can obtain *equilibrium solutions* that describe the spatial distribution of the organism as time approaches infinity. Such results are very useful to under-

stand the interaction between spatial heterogeneity and movement, and/or to determine areas where the organisms are most likely to establish. Some theoretical background useful for the mathematical study of ADR models is provided in chapter 2 section 2.3.

1.5 Estimating insect population size

The population size is an essential information to plan appropriate management. The most accurate method to determine the size of a population is via **direct observation**. This method consists in counting all the individuals of the population in the area considered. Despite the reliability of the method, it is not practical for insect populations. Indeed, insects are numerous and sometimes difficult to find as they can easily hide under leafs, or be visible only at specific times of the day, thus counting all the insects in an area would be labour intensive and time consuming. Therefore, **estimation methods** are usually used to measure insect population size. Several approaches can be considered to estimate the size of a population [218] such as **sampling**, **Mark-Release-Recapture (MRR)** or **model fitting**.

1.5.1 Sampling

When the population is abundant, as for insects, it is not possible to count all the individuals in a large area. In such cases the abundance of a population can be estimated by counting individuals on samples. The sampling strategy must account for the population biology, ecology, behaviour and distribution in order to define an appropriate sampling unit. The counts obtained on the sample units allow the computation of the total count over the study area.

For insect populations, a common sampling unit is the **quadrat**. Sampling on quadrats consists in selecting randomly small areas on the domain, for example squares of a $1m^2$, on which all the individuals are counted. This information is than used to infer the size of the population over the whole domain. Quadrats are however not natural sampling units and require to choose relevant size and shape. Further, quadrats require that the population remain immobile during the counting period.

Alternatively, population abundance can be estimated from **line transects** [38]. This method consists in defining a transect line in the study area where each individual seen within a particular width is recorded with its perpendicular distance to the line and position on the line. The abundance of the population is determined by means of an estimation method among which the Hayne estimator, Fourier series or Shape-restricted estimator [153].

Another strategy is **distance sampling** [38]. This method consists in choosing a point randomly on the study area and measure the distance from the point to the nearest individual. Distance sampling has been used for example to estimate abundance of the invasive ant *Solenopsis invicta* [142] and butterflies [137].

An advantage of line transect and distance sampling is that it allows to determine if the spatial distribution of the population if random, aggregated or uniform [115, 142]. However, counting individuals on samples, in particular for abundant population of small organisms are usually labour intensive and require a good knowledge on the ecology of the population.

1.5.2 Mark-Release-Recapture

The principle of MRR was first used by Graunt in 1662 to estimate the human population of London. The method was extended to ecological problems with the works of Peterson on Danish fisheries in 1896, and it is in 1933 that MRR was first used in entomology by Jackson to estimate insect population abundance.

MRR consists in capturing a sample of the population, marking the individuals, typically with a coloured marker that does not affect their biology and behaviour. They are then released in such a way that they intermingle with the rest of the population before recapturing is carried out. The ratio between the marked and released insects and the total recaptured is analysed.

MRR is a powerful method which can provide information on the demography, movements or abundance of a population [153]. In a work of 1962, MRR provided a more accurate estimate than sampling for the shield bug *Eurygaster integriceps* [13]. However, a certain number of assumptions must be taken into account to carry the appropriate experiment and analysis to obtain reliable estimations.

1.5.2.1 Assumptions

In order to exploit the results of MRR experiments, assumptions are made [226]. First, the marking of individuals does not affect their behaviour and life expectancy. In addition, the marks are not lost during the study period. Then it is assumed that the released individuals mix completely in the population and that marked individuals have the same chance to be caught than any other member of the population. Moreover, the collect of the recaptures must be done at discrete times, and the collect process must be done over a short time compared to the overall time of the experiment.

Further, the method must be adapted depending on if the population is assumed to be *open* or *closed*. A population is closed if its size remains unchanged over the period of the experiment. This assumes that there is no growth or decline of the population due to demography or migration. Such an assumption can hold for short-time studies, and in this

case the Lincoln-Petersen method or the Schnabel method are commonly used. The Petersen-Lincoln and the Schnabel methods are quite restrictive by their assumptions. In particular, the closed population assumption is not realistic. Alternatively, for open populations the Jolly-Seber method is more appropriate as it takes into account changing population [198].

1.5.2.2 Some common methods

The **Lincoln-Petersen method** [86, 173] is the simplest method to obtain an estimate of a population size using MRR. In this method the population is assumed to be closed, thus during the period between the release and the recapture of individuals, there is no death, no birth, no immigration and no emigration. Further, it does not account for possible errors in the experiment such as loss of marks, mistakes in the recording process, etc. The estimator of the population size is derived under the additional assumption that all individuals have the same probability of being captured, thus the ratio of marked recaptured, m, over the total number of marked, M, should be equal to the ratio of the total number of captured (marked and not marked), n, over the total population, N:

$$\frac{m}{M} = \frac{n}{N}. \tag{1.10}$$

Thus, an estimator, $\hat{N}$ of the population size is

$$\hat{N} = M\frac{n}{m},$$

with the associate standard error

$$SE = \sqrt{\frac{M^2 n(n-m)}{m^2(m+1)}}.$$

However, (1.5.2.2) tends to overestimate the total population size, particularly when the sample of marked individuals is small. Thus, it is recommended to use one of the two the modified estimators [86]

$$\hat{N} = \frac{(M+1)(n+1)}{(m+1)} - 1,$$

with the associated standard error

$$SE = \sqrt{\frac{M^2(n+1)(n-m)}{(m+1)^2(m+2)}}.$$

The estimator and its standard error can be used to compute a 95% confidence interval for the population size as follows

$$CI = [\hat{N} - 1.96 \times SE; \hat{N} + 1.96 \times SE]$$

In other words, there is a 95% probability that the population size N belongs to the interval CI.

The **Schnabel method** is an extension Lincoln-Petersen method, for closed population based on the same assumptions. The Schnabel method consists of a time-series of capture-recapture experiments using a single type of mark. Thus at time t, the *marked* insects, M_t, are the insects captured in one or several prior captures. The multiple MRR experiments are than processed as series of Lincoln-Petersen samples, that is, this estimation of the population size is

$$\hat{N} = \frac{\sum_t n_t M_t}{\sum_t m_t} \tag{1.11}$$

where n_t is the total number of captured individuals(marked and not marked) at time t and m_t is the number of marked insects captured at time t.

The main advantage of the Schnabel method is that it can identify violation to the assumption under which all individual have equal chances to be caught. Indeed, if the assumption is verified, the proportion of the marked individuals on the number of previously marked individuals should fit a straight line. Otherwise, the assumption is violated.

The **Jolly-Seber method** has been developed for open populations which is a biologically more realistic assumption as it takes into account changing population in time through births, deaths, migration, etc. [198]. In the Jolly-Seber methods, MRR samples are collected at several times, but unlike for the Scnabel method, the marks specific to each capture time. This allows to determine when a marked individual was last captured. In this method, the sampling of the individuals must be done randomly and over a short period of time compared to the duration of the study. Since this method is designed for open populations, it is possible to carry MRR experiments over long time periods (several weeks/months/years).

Detailed study of MRR experiments using these methods can be found in [153]. In particular, methods to find the confidence intervals for each of these estimators are given, providing essential information on the reliability of the estimates. Further, numerous computer software are available to estimate population size using MRR data [226], such as MARK [253], NORMARK [252], CAPTURE [204], or E-SURGE [52].

1.5.3 Trapping model approach

Mathematical modelling allows to test different trapping strategies and help to optimize field experiments to collect the useful information. Petrovski et al. [195] estimate insect population density based on two modelling approaches for the dynamics of the population. First, they use a two-dimensional IBM model to simulate trajectories of insects which are

captured as they cross the boundary of a trap represented by a circle. Then they consider a population model based on a diffusion process, assuming a uniform distribution of the population, where the trapping is modelled by setting the population density to 0 inside the area of trap. The number of captured insects is estimated by computing the total diffusive flux of the population through the boundary of the trap over a specific period of time. In the work of Petrovskaya et al. [194], the approach is different as the abundance of the population is estimated by interpolation on a domain discretized in such a way that the nodes of the grid correspond to trap locations. In particular, the authors estimate the abundance of the population over the whole domain based on a sparse trap network. In the works of Banks et al. [14, 15], however, a transport equation models the flux of a population with a PDE, and the estimation of parameters of the model, among which the initial population abundance is based on cubic spline approximation.

In the models presented in chapters 3 and 4, the population size and distribution correspond to the initial condition of the population dynamics model. The estimation of the population abundance and other parameters (diffusion rate, attractiveness of the traps, etc.) is obtained using a least square approach. While in chapter 3, the distribution of the initial population is assumed homogeneous, in chapter 4 we estimate population parameters considering various spatial distributions of the population.

1.6 Modelling trapping

In order to analyse population dynamics, to monitor the evolution of the population, estimate the population size or reduce populations, a typical approach is to use trapping data. Taking into account trapping in mathematical models is a challenge of its own and several approaches can be considered. Trapping can be modelled in a spatially explicit way where each trap has a localisation and the dynamics of the population depend on the distance to the trap. This is the approach of the models we are considering in chapters 3 and 4 in a two-dimensional domain. Alternatively, trapping can be modelled implicitly, via a removal process which does not account for any spatial structure of the population. This is the process modelled in chapter 5. In the following we give an overview of the modelling of the trapping process in spatial and non-spatial settings.

1.6.1 Spatially explicit trapping

From the modelling perspective, a trap can be seen as a bounded area of the spatial domain, typically small. Individual entering this area have a certain probability to be captured. The capture process can be modelled by removing the individuals from the system, using an excess death rate for instance, or they can stay in the trap area with no possibility to come out. This modelling choice can be important depending on whether the effect of the capture impacts or not the dynamics of the *free* individuals. For example, an accumulation of individuals at a particular location may favour or not the trapping of neighbouring individuals.

Two trapping approaches can be considered: **passive trapping** and **active trapping**. The major difference between the two approaches depends on the *effect* of the traps on the dynamics of the free-individuals, outside the area of the trap. Indeed, in the case of active trapping, typically the trap releases an attractant which influences the directional movements of individuals in the vicinity of the trap and this influence is all the more important as individuals get closer to the trap. On the other hand, in the case of passive trapping, the trap itself does not impact the dynamics of the free population, at most the captured individuals, such as accumulation phenomenon, may possibly affect the chances of capture in the vicinity of the trap. It is worth mentioning that although we only considered the case of chemical attractants in this thesis, visual cues can also influence the movements of insects. In [195], the authors modelled a passive trap as a circular area which terminate the path of any insect crossing its boundary while the movements of the individuals is random modelled at the scale of individuals via a random walk process. They also modelled the movements at the population level via a diffusion process and two shapes of traps: circular and square,

where the capture process is modelled by setting a zero-density condition at the boundary of the trap. Another approach to model passive traps was considered in [194], where the space is discretized by a grid whose nodes correspond to trap positions. We now describe the modelling of active trapping.

Often, in order to maximize the chances to capture insects, attractive traps are used. Those traps release a chemical attractant (food, pheromone, CO_2, etc.) that diffuses in the environment which guides the individuals towards the trap. The diffusion of a chemical in air is a complex process which can exhibit random meandering patterns generated by turbulences in the environment [188]. Thus the concentration of the chemical fluctuates randomly with a tendency to be higher closer to its source forming a filamentary plume.

The plume formation is a very complex phenomenon and it can be approximated by simpler shapes such as an ellipse [80, 82]. Indeed, it can be assumed that in a still environment, such chemical spreads according to Fick's law via a diffusion process for which the contour concentration levels are circles. In the presence of wind, we can assume that these circles are deformed into ellipses taking into account the wind direction and speed by varying its orientation and its stretching. The area within the plume where the concentration of the chemical is above a threshold that can be detected by insect and influence their behaviour is referred to the **active space** of the trap [41]. In a plume, the concentration of the chemical is higher closer to the release point and lower further from the release point affecting the force of attraction and therefore the probability of capture. This assumption has been supported by MRR experiments assessing that the probability of capture increases with a decreasing distance to attractive traps [189, 259]

A common way to model insect trapping is by considering the **effective attractive radius** (EAR) of the attractive trap. The EAR is an imaginary spherical area around the trap needed to catch as many insects as a passive trap [43]. The EAR is not a representation of the chemical plume as it does not correspond to the actual area of the trap. In [33] the authors studies the response of insects to the dosage of pheromone traps by means of probability of capture using the attraction range [247].

The capture of individuals can occur anywhere on the domain where a probability of capture is defined spatially, with increasing value when getting closer to the location of the trap. In [166], a computer model is developed to study the sensitivity of an active-trapping network on capture probability. In this work, three modelling approaches are considered to assess the efficiency of the trap setting. One relates capture probability to the ratio of the capture areas of a trap setting to the total area. However, a drawback of this approach is that the probability of capture of an individual, given its distance to a trap is either 0 or 1. The next approach considers a capture probability model where the probability of capture

is a function of the distance to the trap and can vary between 0 and 1. Then, instantaneous capture probability is considered and represents the average probability of being captured in a given area at a specific time. Finally a probability of capture over time is described through a diffusion process which gives to the distribution of a population at a particular time, given an initial distribution of the population.

In the setting of ADR models, the response of individuals to the trap is determined by the force of attraction in the advection process guiding the individuals towards the trap. It is a function of the distance to the trap, with high values close to the trap, and decreasing as the with increasing distance. In this approach, the capture of individuals occurs inside the area of the trap. In the model presented in chapter 3 , the dynamics of insects is governed by an ADR process where the advection term accounts for the attractiveness of traps. In this work, the traps are represented as small circles in which insects have a maximum probability of capture. The force of attraction of the traps is constant in time and occurs in a ring around the trap, being at its maximum attractiveness at the boundary of the trap and decreases to 0 in the ring.

For more realism, the diffusion process of the chemical attractant can also be modelled via an ADR process of its own. This can be particularly useful when counting of captured insects starts simultaneously with the setting of the traps, that is when the traps start diffusing the chemical. This leads to a chemotaxis model [141, 127] where the attraction of the insects to the traps is a function of the chemical concentration at any position and any time. In [64] a spatio-temporal model is developed to simulate the host-seeking behaviour of mosquitoes. In this model, the hosts release CO_2 which is traced back by mosquitoes. The dynamics of the mosquitoes represented in this work are similar to those of insects responding to an attractant released from a trap. In this approach, the release of the CO_2 has been modelled using a ADR model, while the trajectories of the responding mosquitoes were governed by an IBM based on a random walk process.

The model represented in chapter 4 is a chemotaxis model consisting in the coupling of an ADR model governing the spread of the chemical attractant released from the traps with the ADR model governing the dynamics of the insects where the advection coefficient in the insect's equation is a function of the chemical concentration. In this model, the traps in which the capture occurs are represented as small circles, while the active space around the trap is defined by a threshold concentration of the chemical attractant which can be detected by the insects.

1.6.2 Spatially implicit trapping

When the model does not account for the spatial variations of the population dynamics, the trapping can be taking into account implicitly by adding a removal rate of individuals. Omitting the space variable in trapping models assumes that the individuals all have the same chance of being captured regardless of their position. In order to account for additional characteristics of the trap, such as its effectiveness only on a specific class of the population, the model can be structured accordingly.

The model developed in chapter 5 aims to investigate the effect of MAT and trapping on an insect population. In order to analyse the model theoretically, we omitted the space structure and rather focused on the structure within the population. This model is based on the approach proposed Barclay and Van den Driessche [18] where they developed temporal models to simulate pheromone trapping of insects. In these models, we assume that only males are attracted to a chemical female-sex-pheromone released from a trap. Not only the males get distracted by the chemical disrupting the mating, but the proportion males who got distracted have a high risk of being captured. To take into account these two aspects, the population is divided in four compartments based on the biological knowledge and behavioural knowledge: immature, adult males, adult females available for mating and adult females ready to lay their eggs supplying the immature compartment. The transition from females available for mating, to females ready to lay eggs depends on the number of males available, and therefore we model this transition as a function of the proportion of males that have not be disrupted by the pheromone released from the traps. Then, the capture only occurs on the proportion of males that have been disrupted via an additional mortality term in the equation modelling the dynamics of the adult males.

1.7 Aim and objectives of this thesis

This thesis aims to provide a mathematical framework for the development and/or improvement of pest-insect control strategies satisfying the requirements of IPM programs. This mathematical framework comprises mathematical models accompanied by appropriate theoretical analysis and thresholding, by adequate schemes for numerical solutions as well as efficient and reliable procedures for parameter identification. It is developed in order to address challenges related to what, when and how questions regarding control interventions. The first objective of the thesis is to develop mathematical methods and practically applicable protocols to estimate the insect population size and distribution, using trap data, which is an essential information for planning effective control measures. The second objective is to predict the impact of a specific control strategy on a pest population, and identify how to drive a pest population to extinction.

To address the first objective, we develop a generic two-dimensional spatio-temporal Trap-Insect Model (TIM) model based on biological and ecological knowledge of the species. Attractive traps are placed on the domain at an initial time for which the population has a specific size and distribution. The spatio-temporal dynamics of the insects responding to attractive traps is driven by (i) a diffusion process that accounts for the dispersal capacity of the insects; (ii) an advection process that accounts for the attractiveness of the traps, and (iii) a reaction process that accounts for demographics and trapping. Thus, the model is formulated by an ADR equation. Usually, the dispersal capacity of the insects, as well as the value of the parameters related to the traps are unknown and need to be estimated together with the initial population size and distribution. This task is further challenging as these parameters depend on environmental changes (temperature, humidity, wind, etc.) which vary in time. A major outcome of this thesis is a protocol to identify a set of parameters using trap data collected over a short period of time during which the parameters can be assumed constant. This objective is addressed in chapters 3 and 4 of this thesis.

The second objective of this thesis is addressed by constructing a model for the control of crop-pests via mating disruption, using a female pheromone, and trapping. In this setting, males are diverted from females compromising their insemination. To account for specific behaviours within the population induced by the choice of the control method, the population is divided in appropriate compartments. The dynamics of the insect population is described by a temporal compartmental model governed by a system of ODEs. The effect of the dosage of the pheromones has been studied theoretically and allowed identify values of practical interest, such as a threshold value above which extinction of the population is ensured. This work is presented in chapter 5.

This thesis is organised as follows.

In chapter 2, we recall some basic mathematical principles used for the analysis of the models presented thereafter.

Chapter 3, deals with the two-dimensional spatio temporal modelling of insect trapping in the prospect of parameter estimation. In this chapter the active area of the trap is modelled by a circle around each trap where the attractiveness of the trap is static and is defined by a function which is null outside this area and increases to a maximum value with decreasing distance to the trap. The distribution in time and space of the population is computed numerically on a spatial domain discretized by a regular grid via a finite difference method. The model presented in this chapter allowed to test different settings of interfering traps to estimate parameter values of the model using a uniform initial distribution of the population.

The model presented in chapter 4 governs the dynamics of insects coupled with a model governing the spread of the chemical attractant released from traps. This model is formulated via system of ADR equations. Here, the active space around each trap is determined by a threshold value of the concentration of the chemical above which the behaviour of insects is affected. The advection process in the equation modelling the insects dynamics is a function of the concentration of the chemical. This model is studied theoretically and the solution is computed numerically on an unstructured mesh using the method of finite elements. The model is then used to propose a protocol for parameter estimation, using data simulated with various settings of traps and initial distributions.

In chapter 5, we present a model to simulate the control of insects via mating disruption and trapping using pheromone-baited traps. Considering the specifics of the control method, the population is divided into several compartments and modelled as a system of ODEs. The effect of the dosage of the pheromone on the persistence of the population is studied mathematically using the theory of monotone dynamical systems.

Finally, chapter 6 concludes on the work of the thesis and provides perspectives and open questions for future studies.

Chapter 2

Mathematical models and methods

2.1 Introduction

The models presented in chapters 3 and 4 describe the trapping of insects using attractive traps on a spatio-temporal scale. These models are defined via PDEs describing advection-diffusion-reaction processes. Numerical simulations of trapping data are used to estimate insect population abundance and distribution as well as other unknown parameters of the models related to the traps. These models allow to test various trapping scenarios and help optimizing field protocols for data collection. The methods used for parameter identification are presented in the respective chapters.

The model described in chapter 5 models the response of a pest-insect population to mating disruption and trapping control on a temporal scale. This model is described via a system of ODEs and aims to simulate the impact of the control. Its theoretical study allows to identify thresholds of biological importance for the management of the pest population. More precisely, the study of this model allows to identify a threshold for the mating disruption effort required to ensure extinction of the pest population.

In chapters 3, 4 and 5 the models define dynamical systems. These systems cannot be solved explicitly. Chapter 2 provides an introduction to the numerical methods used in computing approximate solutions. The related theory regarding the well-posedness of the problems and the quality of approximations is also provided. It includes, on the one hand, analysis and convergence properties, but on the other hand, also analysis on replicating essential biologically relevant properties of the solutions, i.e. positivity, boundedness.

This chapter is organised as follows. In section 2.2 we present the general setting of dy-

namical systems to which the models of this thesis belong to. Section 2.3 is devoted to the theoretical study of dynamical systems defined via advection-diffusion-reaction equations, using the theory of Lions, based on the variational formulation of the problem. Complementary studies of models described in chapters 3 and 4 are given in this section as application of this theory. Section 2.4 deals with the theoretical study of dynamical systems defined via ODEs. In particular, special attention is given to monotone dynamical systems used in the study of the model of chapter 5. Finally, in section 2.5 we briefly present the numerical methods used to compute the solutions of the advection-diffusion-reaction equations arising from the models of chapters 3 and 4. More specifically, we present the method of lines which consists in discretizing the PDE problem first with respect to the space variable to obtain a system of ODEs. Here we only focus on the space discretization using the finite difference approach, as in chapter 3, and the finite elements approach, as in chapter 4.

2.2 General setting for the models

The models presented in chapter 3, 4 and 5 are dynamical systems. A dynamical system describes the evolution in time of the different states of a system. The set of states is often referred to as the *phase space* and it can be of different nature depending on the formulation of the problem. For instance, the phase space of a dynamical system defined via an ODE representing the evolution of a population size can be a subset of $\mathbb{R}$. When the population is divided into compartments, then its dynamics are governed by a system of ODEs, and then, the states of its dynamical system are vectors of $\mathbb{R}^n$ giving the size of each compartment. The states of a dynamical system can also be functions or vector of functions. When we deal with spatio-temporal trapping models governed by PDEs (resp. systems of PDEs), then the phase space of the corresponding dynamical system becomes the space of $\mathbb{R}$-valued functions (resp. $\mathbb{R}^n$-valued functions).

Dynamical systems can be categorized according to the nature of its parameter (time), its phase space and its evolution rule. The time as well as the phase space can be continuous or discrete. Further, the evolution rule can be deterministic or stochastic. When the evolution rule is deterministic, it takes each state of the system to a unique subsequent state, which is not the case when the evolution rule is stochastic. The models presented in chapters 3, 4 and 5 describe continuous deterministic dynamical systems, thus we only focus on this case. The set of states is a topological space denoted by $\mathcal{D}$. In more precise terms the definition of dynamical system is given as follows [128]:

Definition 2.2.1. *Let $\mathcal{D}$ be a topological space. A dynamical system is a $\mathcal{C}^1$ map $\varphi : \mathbb{R}^+ \times \mathcal{D} \to \mathcal{D}$ such that $\varphi_t \equiv \varphi(t, \cdot) : \mathcal{D} \to \mathcal{D}$ satisfies the following properties:*

(i) $\varphi_0 = Id$, *and*

(ii) $\varphi_{t+s} = \varphi_t \circ \varphi_s$, $\forall t, s \geq 0$.

The operator φ is called a *semigroup operator*, since it follows from (i) and (ii) that $\{\varphi_t, t \geq 0\}$ is a semigroup with respect to composition. The operator φ is also called a *semiflow*.

The models presented in chapters 3 and 4 are formulated via PDEs and the model of chapter 5 is a system of ODEs. In all cases, the model can be formulated in the following operator form

$$\frac{du(t)}{dt} = Au(t) + f; \quad u(0) = u_0 \tag{2.1}$$

where $u(t) \in \mathbb{R}^n$ when the model is given as a system of ODEs and where u is a mapping

$$\begin{aligned} u: \quad [0,\infty] &\longrightarrow V \\ t &\longmapsto u(t) \equiv u(t,\cdot) \end{aligned} \tag{2.2}$$

V being a functional space, when the model is formulated by PDEs. Then, we have that

$$u(t) = \varphi_t(u_0)$$

is a solution of the IVP (2.1).

In many cases, it is not possible to find an explicit formulation for a solution to such problems. In order to study PDE or ODE problems, we typically investigate the *well-posedness* of the problem. A problem is said to be well-posed (in the sense of Hadamard) when it satisfies the following conditions:

there exists a solution to the problem; (2.3)

this solution is unique; (2.4)

the solution depends continuously on the data of the problem. (2.5)

In sections 2.3 and 2.4, we give some mathematical background in the appropriate settings to show that the problems describe well-posed dynamical systems. For the advection-diffusion models presented in chapters 3 and 4 formulated by PDEs, we consider the problem in its weak form. For the model of chapter 5, however, we consider the setting of monotone dynamical systems.

2.3 Advection-Diffusion-Reaction models

In the models of chapters 3 and 4, we consider the spatio-temporal variations of a concentration or abundance of insects governed by ADR equations. This concentration is denoted $u(t,x)$ and defined on a time-space domain $\Omega_T = [0,T]\times\Omega$, where $T \in \mathbb{R}^+$ and Ω is a domain in $\mathbb{R}^2$ with a piecewise smooth boundary $\Gamma = \partial\Omega$. The ADR equation can be written in the general form:

$$\frac{\partial u}{\partial t} + Lu = f, \quad \text{in } \Omega_T, \quad u(0,x) = u_0, \tag{2.6}$$

with

$$Lu = -\sum_{i,j=1}^{2} \frac{\partial}{\partial x_j}\left(d^{i,j}(t,x)\frac{\partial u}{\partial x_i}\right) + \sum_{i=1}^{2} a^i(t,x)\frac{\partial u}{\partial x_i} + c(t,x)u. \tag{2.7}$$

Further, to complete the formulation of the problem, we provide information on the dynamics at the boundary, Γ, of the domain. We can distinguish two main types of boundary conditions:

- Dirichlet: $u(t,x) = \alpha(t,x), \quad x \in \Gamma$. Here the value is defined on the boundary. Example of application: if we consider a domain out of which individuals cannot survive, than we take $\alpha(t,x) = 0$.
- Neumann: $\frac{\partial}{\partial n}u(t,x) = g(t,x), \quad x \in \Gamma$, where n denotes the outward normal vector to Γ. Here the flux in and out of the domain is determined. For example, if we consider an isolated domain with no movement of individuals in and out of the domain, than we take $g(t,x) = 0$.

However, other boundary conditions can be formulated. For instance the Robin boundary condition is a combination of Dirichlet and Neumann, where the flux at the boundary depends on the density of u at the boundary. It is also possible to consider different types of boundary conditions on different parts of Γ.

In this thesis, we consider only homogeneous Dirichlet conditions

$$u(t,x) = 0, \quad x \in \Gamma, \quad \forall t \in (0,T], \tag{2.8}$$

or homogeneous Neumann conditions

$$\frac{\partial u(t,x)}{\partial n} = 0, \quad x \in \Gamma, \quad \forall t \in (0,T]. \tag{2.9}$$

Given problem (2.6), a solution is expected to lie in the space of real-valued functions of class $\mathcal{C}^1$ with respect to t and $\mathcal{C}^2$ with respect to x and it is referred to as a *classical solution*.

However, except in some particular cases, finding a classical solution of (2.6) with boundary conditions (2.8) or (2.9) which satisfies properties (2.3)-(2.5) is usually not possible. Thus, typically, the well-posedness of a problem is rather studied on a wider class of solutions which require weaker smoothness conditions, referred to as *weak solutions*.

2.3.1 Preliminaries

In order to study the weak solutions, and given the boundary conditions (2.8) or (2.9), we introduce the following functional spaces:

$$
\begin{aligned}
L^2(\Omega) &= \left\{ f : \Omega \to \mathbb{R}; f \text{ is measurable and } |f|^2 \text{ is measurable and integrable} \right\}, \\
H^1(\Omega) &= \left\{ w \in L^2(\Omega) : \frac{\partial w}{\partial x_i} \in L^2(\Omega), 1 \leq i \leq 2 \right\}, \\
H_0^1(\Omega) &= \left\{ w \in H^1(\Omega) : w|_\Gamma = 0 \right\}.
\end{aligned}
$$

For $w \in H^1(\Omega)$, we define the weak partial derivatives $g_i = \frac{\partial w}{\partial x_i}$, for $1 \leq i \leq 2$, as

$$
\int_\Omega w \frac{\partial \varphi}{\partial x_i} = -\int_\Omega g_i \varphi, \quad \forall \varphi \in \mathcal{C}_c^\infty(\Omega),
$$

where $\mathcal{C}_c^\infty$ is the set of infinitely differentiable functions with compact support. Note that the space $L^2(\Omega)$ is a Hilbert space with a scalar product

$$
(v, w)_{L^2} = \int_\Omega vw, \tag{2.10}
$$

and its associated norm is

$$
\|v\|_{L^2(\Omega)}^2 = \left(\int_\Omega |v|^2 \right)^{\frac{1}{2}}. \tag{2.11}
$$

Further, the space $H^1(\Omega)$ is a Hilbert space with a scalar product

$$
(v, w)_{H^1} = \int_\Omega vw + \int_\Omega \nabla v \nabla w, \tag{2.12}
$$

and its associated norm is

$$
\|v\|_{H^1(\Omega)}^2 = \|v\|_{L^2(\Omega)}^2 + \|\nabla v\|_{L^2(\Omega)}^2. \tag{2.13}
$$

In the following, we use the notation

$$\begin{aligned} V &= H^1(\Omega) \quad \text{for the boundary condition (2.9), and} \\ V &= H_0^1(\Omega) \quad \text{for the boundary condition (2.8) .} \end{aligned}$$

We denote V' the dual space of V, that is

$$V' = H^{-1}(\Omega).$$

Moreover, since V is dense in $L^2(\Omega)$ such that $V \subset L^2(\Omega)$ with continuous embedding, and since there is a natural isometry between the space $L^2(\Omega)$ and its dual space, then it follows from the Riesz Representation Theorem [36, Theorem 4.11] that $L^2(\Omega)$ can be identified with its dual space.

Let us recall some commonly used notations. The duality pairing between two elements of the spaces V' and V can be seen as an extension of the scalar product in $L^2(\Omega)$ defined in (2.10),

$$< v, w >_{V',V} = \int_\Omega vw, \quad v \in V', w \in V. \tag{2.14}$$

For $j > 0$,

$$\mathcal{C}^j([0,T], V) = \left\{ \text{ V-valued functions that are of class } \mathcal{C}^j \text{ with respect to t } \right\}.$$

Let $d_t u$ denote the derivative of u with respect to t, and $d_t^l u$ the derivative of order l. Then $\mathcal{C}^j([0,T], V)$ is a Banach space with a norm

$$\|u\|_{\mathcal{C}^j([0,T],V)} = \sup_{t\in[0,T]} \sum_{l=0}^{j} \|d_t^l u\|_V.$$

For $0 < p < \infty$,

$$L^p(0,T,V) = \{ \text{ V-valued functions whose norm in V is in } L^p(]0,T[)\}.$$

Then $L^p(0,T,V)$ is a Banach space with respect to the norm

$$\|u\|_{L^p(]0,T[,V)} = \begin{cases} \left(\int_0^T \|u(t)\|_V^p\right)^{\frac{1}{p}}, & \text{if } 1 \le p < +\infty \\ ess \sup\limits_{t\in[0,T]} \|u\|_V, & \text{if } p = +\infty. \end{cases}$$

Let $B_0 \subset B_1$ be two reflexive Banach spaces with continuous embeddings. Then the space

$$\mathcal{W}(B_0, B_1) = \{v \in L^2(0,T; B_0) : d_t v \in L^2(0,T; B_1)\}$$

equipped with norm $\|u\|_{\mathcal{W}(B_0,B_1)} = \|u\|_{L^2(0,T;B_0)} + \|u\|_{L^2(0,T;B_1)}$, is a Banach space.

Lemma 2.3.1 (Integration by parts). *For all $u, v \in \mathcal{W}(V, V')$, we have:*

$$\int_0^T < \frac{\partial u}{\partial t}, v >_{V',V} dt = (u(T), v(T))_L - (u(0), v(0))_L - \int_0^T < \frac{\partial v}{\partial t}, u >_{V',V} dt \tag{2.15}$$

Lemma 2.3.2 (Green's formula). *Let $\sigma \in [L^\infty(\Omega)]^{n\times n}$.*

$$\int_\Omega \nabla \cdot (\sigma \cdot \nabla u)v = \int_\Gamma \frac{\partial u}{\partial \vec{n}} v - \int_\Omega \sigma \nabla u \cdot \cdot \nabla v, \quad \forall u \in \mathcal{C}^2(\bar{\Omega}), \quad \forall v \in \mathcal{C}^1(\bar{\Omega}), \tag{2.16}$$

where $\vec{n}$ is the outward normal vector to Γ [94, Corollary B.59].

Lemma 2.3.3 (Holder's inequality). *Let $f \in L^p(\Omega)$ and $g \in L^q(\Omega)$ with $1 \le p \le +\infty$ and $\frac{1}{p} + \frac{1}{q} = 1$, then $fg \in L^1(\Omega)$ and*

$$\int_\Omega |fg| \le \|f\|_{L^p(\Omega)} \|g\|_{L^q(\Omega)}.$$

Lemma 2.3.4 (Gronwall's [94]). *Let $\beta \in \mathbb{R}$, $\varphi \in \mathcal{C}^1(0, T; \mathbb{R})$ such that*

$$\frac{d\varphi}{dt} \le \beta\varphi + f.$$

Then,

$$\forall t \in [0, T], \quad \varphi(t) \le e^{\beta t}\varphi(0) + \int_0^T e^{\beta(t-\tau)} f(t) d\tau.$$

2.3.2 Variational formulation

Here, we assume that

$$d^{i,j}, a^i, c \in L^\infty([0, T] \times \Omega), \tag{2.17}$$

$$f \in L^2(\Omega), \tag{2.18}$$

$$u_0 \in L^2(\Omega). \tag{2.19}$$

In chapter 4 the state of the dynamical system defined via (2.6) at time t is the distribution of insects over the spatial domain Ω given an initial distribution, $u(0, x) = u_0$. Equation (2.6) is extended to $\mathcal{C}([0, T], V)$ in the form of problem (2.1) where the operator A is defined on V as follows. We say that

$$w = Au \quad \text{if } \int_\Omega wv = -\int_\Omega \left(\sum_{i,j=1}^2 d^{i,j}(t, \cdot) \frac{\partial u}{\partial x_i} \frac{\partial v}{\partial x_j} + \sum_{i=1}^2 a^i(t, \cdot) \frac{\partial u}{\partial x_i} v + c(t, \cdot)uv \right), \quad \forall v \in V. \tag{2.20}$$

In fact by multiplying equation (2.6) by $v \in V$ and integrating by parts, we derive the *weak formulation* of problem (2.6) which is equivalent to the problem in the form (2.1) with A as defined in (2.20):

$$\begin{cases} \text{Find } u \in \mathcal{W}(V, V') \text{ such that:} \\ \\ < \frac{d\mathbf{u}(t)}{dt}, v >_{V',V} + B(t; \mathbf{u}(t), v) =< f, v >_{V',V}, \quad \text{a.e. } t \in]0, T[, \forall v \in V, \\ \\ \mathbf{u}(0) = u_0, \end{cases} \tag{2.21}$$

where the mapping $B : [0,T] \times V \times V \longrightarrow \mathbb{R}$ is such that $B(t; \cdot, \cdot)$ is the bilinear form on $[0,T]$ defined for $u, v \in V$ as

$$B(t; u, v) = \int_\Omega \left(\sum_{i,j=1}^{2} d^{i,j}(t, \cdot) \frac{\partial u}{\partial x_i} \frac{\partial v}{\partial x_j} + \sum_{i=1}^{2} a^i(t, \cdot) \frac{\partial u}{\partial x_i} v + c(t, \cdot) uv \right) dx. \tag{2.22}$$

2.3.3 Existence and uniqueness

We assume that B satisfies the following properties:

(P1) The function $t \longmapsto B(t; u, v)$ is measurable $\forall u, v \in V$.

(P2) There is a constant M such that $|B(t; u, v)| \leq M \|u\|_V \|v\|_V$ for a.e. $t \in [0,T]$ and $\forall u, v \in V$.

(P3) There is $\alpha > 0$ and $\gamma > 0$ such that $B(t; u, u) \geq \alpha \|u\|_V^2 - \gamma \|u\|_{L^2}^2$ for a.e. $t \in [0,T]$ and $\forall u \in V$. (L^2-coercivity condition)

Definition 2.3.1. *Equation (2.21) defines a parabolic problem whenever the properties (P1)-(P3) are satisfied.*

The existence and uniqueness of solutions to problem (2.21) comes from the theorem of J.L. Lions [94]:

Theorem 2.3.1 (Lions' theorem as given in Brezis Thm. 10.9 [36])**.**
Given $f \in L^2(0,T; V')$ and $u_0 \in L$, there exist a unique function u satisfying

$$u \in L^2(0,T; V) \cap \mathcal{C}([0,T]; L), \quad \frac{du}{dt} \in L^2(0,T; V')$$

$$< \frac{du(t)}{dt}, v >_{V',V} + B(t; u(t), v) =< f, v >_{V',V}, \quad \textit{for a.e. } t \in (0,T), \quad \forall v \in V,$$

and

$$u(0) = u_0.$$

Corollary 2.3.1. *Under hypothesis (P1)-(P3), the problem (2.21) has a unique solution.*

2.3.4 Regularity of the weak solution

Given [36, Theorem 9.25, Theorem 9.26 and Remark 24] we can show that the weak solution of (2.21) lies in fact in the space $H^2(\Omega)$ provided some regularity on the coefficients:
Theorem 2.3.2 (Regularity of the second order elliptic problem [96])**.**
Let Ω be an open set of class $\mathcal{C}^2$ with Γ bounded. Let $f \in L^2(\Omega)$, $d^{i,j} \in \mathcal{C}^1(\bar{\Omega})$, $a^i \in \mathcal{C}^1(\Omega)$ and let $u \in H_0^1(\Omega)$ (resp. $H^1(\Omega)$) satisfy

$$\int_\Omega \left(\sum_{i,j=1}^{2} d^{i,j} \frac{\partial u}{\partial x_i} \frac{\partial v}{\partial x_j} + \sum_{i=1}^{2} a^i \frac{\partial u}{\partial x_i} v + cuv \right) = \int_\Omega fv, \forall v \in H_0^1(\Omega) \text{ (resp. } H^1(\Omega)) \tag{2.23}$$

Then $u \in H^2(\Omega)$ and $\|u\|_{H^2(\Omega)} \leq C\|f\|_{L^2}$, where C is a constant depending only on Ω.
Theorem 2.3.3. *Let $u_0 \in H_0^1(\Omega)$, $f \in L^2(0,T;L^2(\Omega))$. Suppose that $u \in L^2(0,T;H_0^1(\Omega))$, with $u' \in L^2(0,T;H^{-1}(\Omega))$ is the weak solution of*

$$u_t + Lu = f \qquad \text{in } [0,T] \times \Omega \tag{2.24}$$
$$u = 0 \qquad \text{on } \Gamma \times [0,T] \tag{2.25}$$
$$u = u_0 \qquad \text{on } \Omega \times \{t = 0\} \tag{2.26}$$

Then, in fact

$$u \in L^2(0,T;H^2(\Omega)) \cap L^\infty(0,T;H_0^1(\Omega)), \quad u' \in L^2(0,T;L^2(\Omega)), \tag{2.27}$$

and we have

$$ess \sup_{0 \leq t \leq T} \|u(t)\|_{H_0^1(\Omega)} + \|u\|_{L^2(0,T;H_0^1(\Omega))} + \|u'\|_{L^2(0,T;L^2(\Omega))} \leq C \left(\|f\|_{L^2(0,T;L^2(\Omega))} + \|u_0\|_{H_0^1(\Omega)} \right), \tag{2.28}$$

where C is a constant which depends on Ω, T and the coefficients of L.

If in addition, $u_0 \in H^2(\Omega)$ and $f' \in L^2(0,T;L^(\Omega))$, then

$$u \in L^\infty(0,T;H^2(\Omega)), \tag{2.29}$$
$$u' \in L^\infty(0,T;L^2(\Omega)) \cap L^2(0,T;H_0^1(\Omega)), \tag{2.30}$$
$$u'' \in L^2(0,T;H^{-1}(\Omega)), \tag{2.31}$$

with

$$ess \sup_{0\le t\le T} \left(\|u(t)\|_{H^2(\Omega)} + \|u'\|_{L^2(\Omega)}\right) + \|u'\|_{L^2(0,T;H_0^1(\Omega))} + \|u''\|_{L^2(0,T;H^{-1}(\Omega))} \le C\left(\|f\|_{H^1(0,T;L^2(\Omega))} + \|u_0\|_{H^2(\Omega)}\right), \tag{2.32}$$

Theorem 2.3.4 (Regularity: Friedman Corollary of Theorem 10.2 [102]). *Let L be uniformly parabolic in $\bar{\Omega}_T$ and assume that the coefficients $d^{i,j}$, a^i and c belong to $\mathcal{C}^k(\bar{\Omega}_T)$ and $f \in H^{k-i+2m(i+1)}(\bar{\Omega}_T)$, where $i = 1 + [p + n/2 + 1)/2m]$, $k = 2m + p + i + [(n+1)/2]$ and p is a non-negative integer. Assume that Γ is of class $\mathcal{C}^{2m(i+1)}$.*
Then $u \in \mathcal{C}^{2m+p}(\bar{\Omega} \times [\varepsilon, T]), \forall \varepsilon > 0$.

2.3.5 The maximum principle

The maximum principle is a useful tool to study properties of elliptic and parabolic equations [201, 96]. This principle states that the maximum of a solution is achieved on the boundary of the domain where it is defined. Assume that the operator L has the non-divergent form:

$$Lu = -\sum_{i,j=1}^{2} d^{i,j} \frac{\partial^2 u}{\partial x_i x_j} + \sum_{i=1}^{2} a^i \frac{\partial u}{\partial x_i} + cu. \tag{2.33}$$

where the coefficients $d^{i,j}$, a^i and c are continuous. We also assume that $d^{i,j} = d^{j,i}$. Denote $\Omega_T = [0,T] \times \Omega$ and $\bar{\Omega}_T$ its closure and $\Gamma_T = \bar{\Omega}_T - \Omega_T$ the parabolic boundary of Ω_T.

Denote

$$u^+ = \begin{cases} u & \text{if } u > 0 \\ 0 & \text{if } u \le 0 \end{cases} \quad \text{and } u^- = \begin{cases} -u & \text{if } u < 0 \\ 0 & \text{if } u \ge 0. \end{cases} \tag{2.34}$$

Then, we have $u = u^+ - u^-$.

Theorem 2.3.5 (Weak maximum principle for $c \ge 0$). *Assume that $u \in \mathcal{C}^2(\Omega_T) \cap \mathcal{C}(\bar{\Omega}_T)$ and $c \ge 0$ in $\bar{\Omega}_T$.*

(i) If

$$u_t + Lu \le 0 \quad \text{in } \bar{\Omega}_T, \tag{2.35}$$

then u satisfies

$$\max_{\bar{\Omega}_T} u = \max_{\Gamma_T} u^+. \tag{2.36}$$

(ii) If

$$u_t + Lu \ge 0 \quad \text{in } \bar{\Omega}_T, \tag{2.37}$$

then u satisfies

$$\min_{\bar{\Omega}_T} u = -\max_{\Gamma_T} u^-. \tag{2.38}$$

[96, Theorem 9, section 7.1]

2.3.6 Properties of the weak solution

To obtain positivity or, in general, bounds to the solution, we usually use the Maximum Principle. As seen in Section 2.3.5, the Maximum Principle requires higher regularity of the weak solution then the one given by Theorem 2.3.1. More precisely, the weak solution has to be a classical solution. As one can see from Theorem 2.3.4, such regularity requires substantially higher regularity of the data functions. An alternative approach is to use positivity results for the weak solutions.

Positivity results appear in a number of publications [73, Chap. XVIII, §4, Theorem 2], [94, Chap 6, Prop 6.11], [108]. However, we did not find one that can be directly applied to problem (2.21). Hence we state more general results with detailed proofs. These can be considered as extensions of [94, Chap 6, Proposition 6.11].

Before proceeding with the theorems we consider some auxiliary properties of $H^1(\Omega)$ and $H_0^1(\Omega)$. For $w \in V$, where $V = H^1(\Omega)$ or $= H_0^1(\Omega)$ we define the functions

$$w^+(x) = \begin{cases} w(x) & \text{if} \quad w(x) > 0 \\ 0 & \text{if} \quad w(x) \le 0 \end{cases} \tag{2.39}$$

$$w^-(x) = \begin{cases} 0 & \text{if} \quad w(x) \ge 0 \\ -w(x) & \text{if} \quad w(x) < 0. \end{cases} \tag{2.40}$$

Hence $w = w^+ - w^-$. It was shown in [72, Chap IV, §7, Proposition 6] that if $w \in H^1(\Omega)$ then $w^+, w^- \in H^1(\Omega)$. As an easy consequence one can see that if $w \in H_0^1(\Omega)$ then $w^+, w^- \in H_0^1(\Omega)$ so that in terms of the notation here we have $w^+, w^- \in V$ whenever $w \in V$. It follows further from the proof of [72, Chap IV, §7, Proposition 6] that for any $j = 1, 2$

$$\frac{\partial}{\partial x_j} w^+(x) = \begin{cases} \frac{\partial}{\partial x_j} w(x) & \text{if} \quad w(x) > 0 \\ 0 & \text{if} \quad w(x) \le 0 \end{cases}$$

and

$$\frac{\partial}{\partial x_j} w^-(x) = \begin{cases} 0 & \text{if} \quad w(x) \ge 0 \\ -\frac{\partial}{\partial x_j} w(x) & \text{if} \quad w(x) < 0. \end{cases}$$

Then it follows from the general form (2.22) of $B(t;\cdot,\cdot)$ that

$$B(t;w^+,w^-)=0. \tag{2.41}$$

Theorem 2.3.6. *Let the bilinear form $B(t,u,v)$ be L^2-coercive on $H_0^1(\Omega)$ (see P3). If $u\in\mathcal{W}(H^1(\Omega),H^{-1}(\Omega))$ is such that*

$$< \frac{du(t)}{dt}, v >_{H^{-1},H_0^1} + B(t;,u(t),v)\geq 0, \quad \forall t\in(0,T], \forall v\in H_0^1(\Omega), \text{ and } v\geq 0, \tag{2.42}$$

$$u(t)|_\Gamma \geq 0, \tag{2.43}$$

$$u(0)\geq 0, \tag{2.44}$$

then $u(t,x)\geq 0$ a.e. in Ω.

Proof. Let $u\in\mathcal{W}(H^1(\Omega),H^{-1}(\Omega))$ satisfy (2.42)-(2.44). For every $t\in[0,T]$, $u(t)=u^+(t)-u^-(t)$ where $u^+(t),u^-(t)\in H^1(\Omega)$ and are defined as in (2.39) and (2.40). The condition $u|_\Gamma\geq 0$ implies that $u^-|_\Gamma=0$, so that $u^-(t)\in H_0^1(\Omega)$. Clearly, we also have $u^-\geq 0$. Then setting $v=u^-(t)$ in (2.42) we obtain

$$< \frac{d}{dt}(u^+-u^-), u^- >_{H^{-1}(\Omega),H_0^1(\Omega)} + B(t;u^+-u^-,u^-)\geq 0.$$

Using that $< \frac{d}{dt}u^+, u^- >_{H^{-1}(\Omega),H_0^1(\Omega)}=0$, and (2.41), the inequality simplifies to

$$\frac{1}{2}\frac{d}{dt}\|u^-\|_{L^2}^2 + B(t;u^-,u^-)\leq 0.$$

Then it follows from the L^2-coercivity of $B(t;\cdot,\cdot)$ that

$$\frac{1}{2}\frac{d}{dt}\|u^-\|_{L^2}^2 \leq -\alpha\|u^-\|_{H_0^1(\Omega)}^2 + \gamma\|u^-\|_{L^2}^2 \leq \gamma\|u^-\|_{L^2}^2.$$

From the Gronwall's inequality

$$\|u^-\|_{L^2}^2 \leq \|u_0^-\|^2 e^{2\gamma t}.$$

Since $u_0^-=0$ a.e. in Ω, we have $\|u_0^-\|=0$ and therefore $\forall t\in[0,T]$, $u(t,x)=u^+(t,x)\geq 0$ a.e. in Ω. □

Theorem 2.3.7. *Let the bilinear form $B(t,u,v)$ be L^2-coercive on $H^1(\Omega)$. If $u\in\mathcal{W}(H^1(\Omega),H^{-1}(\Omega))$ is such that*

$$< \frac{du(t)}{dt}, v >_{H^{-1},H^1} + B(t;,u(t),v)\geq 0, \quad \forall t\in(0,T], \forall v\in H^1(\Omega), \text{ and } v\geq 0, \tag{2.45}$$

$$u(0)\geq 0, \tag{2.46}$$

then $u(t,x)\geq 0$ a.e. in Ω.

Proof. Let $u \in \mathcal{W}(H^1(\Omega), H^{-1}(\Omega))$ satisfies (2.45)-(2.46). For every $t \in [0,T]$, $u(t) = u^+(t) - u^-(t)$ where $u^+(t), u^-(t) \in H^1(\Omega)$ and are defined as in (2.39) and (2.40). Clearly, we also have $u^- \geq 0$. Then setting $v = u^-(t)$ in (2.45) we obtain

$$< \frac{d}{dt}(u^+ - u^-), u^- >_{H^{-1}(\Omega),H^1(\Omega)} + B(t; u^+ - u^-, u^-) \geq 0.$$

Using that $< \frac{d}{dt}u^+, u^- >_{H^{-1}(\Omega),H^1(\Omega)} = 0$, and (2.41), the inequality simplifies to

$$\frac{1}{2}\frac{d}{dt}\|u^-\|^2_{L^2} + B(t; u^-, u^-) \leq 0.$$

Then it follows from the L^2-coercivity of $B(t; \cdot, \cdot)$ that

$$\frac{1}{2}\frac{d}{dt}\|u^-\|^2_{L^2} \leq -\alpha\|u^-\|^2_{H^1(\Omega)} + \gamma\|u^-\|^2_{L^2} \leq \gamma\|u^-\|^2_{L^2}.$$

From the Gronwall's inequality

$$\|u^-\|^2_{L^2} \leq \|u_0^-\|^2 e^{2\gamma t}.$$

Since $u_0^- = 0$ a.e. in Ω, we have $\|u_0^-\| = 0$ and therefore $\forall t \in [0,T]$, $u(t,x) = u^+(t,x) \geq 0$ a.e. in Ω. □

2.3.7 Asymptotic behaviour

In section 2.3.3, the existence and uniqueness of the weak solution to problem (2.6) with boundary conditions (2.8) or (2.9) has been established. Here, we investigate the behaviour of the solution as t approaches $+\infty$. In particular we seek for time-independent solutions, that is, *steady states* of the system, also called *equilibrium solutions*. Steady state solutions may be constant in space, in which case they are called *spatially homogeneous*, or they may depend explicitly on the spatial variable in which case they are called *spatially heterogeneous* [170].

Definition 2.3.2. *A steady state solution of problem (2.6) is a solution $u \in \Omega$ which satisfies the elliptic problem*

$$Lu = f, \quad \forall x \in \Omega \tag{2.47}$$

with boundary conditions (2.8) or (2.9).

Below, we first recall existence and uniqueness results for steady state solutions. Then we give a brief overview of the main types of steady states as well as their stability properties.

2.3.7.1 Existence and uniqueness

Following the same approach as in section 2.3.2, we consider the stationary problem in its variational form, and we seek $u \in V$ such that

$$B(u, v) = f(v) \tag{2.48}$$

where $B : V \times V \longrightarrow \mathbb{R}$ is the bilinear form defined for $u, v \in V$ as

$$B(u, v) = \int_{\Omega} \left(\sum_{i,j=1}^{2} d^{i,j} \frac{\partial u}{\partial x_i} \frac{\partial v}{\partial x_j} + \sum_{i=1}^{2} a^i \frac{\partial u}{\partial x_i} v + cuv \right) dx. \tag{2.49}$$

Lemma 2.3.5 (Lax-Milgram [94])**.** *Let V be a Hilbert space, let $B \in \mathcal{L}(V \times V; \mathbb{R})$, and let $f \in V'$. Assume that the bilinear form is coercive. i.e.*

$$\exists \alpha > 0, \forall u \in V, \quad B(u, u) \geq \alpha \|u\|_V^2. \tag{2.50}$$

Then the problem of finding $u \in V$ such that

$$B(u, v) =< f, v >_{V',V}, \quad \forall, v \in V \tag{2.51}$$

is well-posed with a priori estimate

$$\forall f \in V', \quad \|u\|_V \leq \frac{1}{\alpha} \|f\|_V. \tag{2.52}$$

2.3.7.2 Steady state solutions

Consider the classical problem (2.6) with boundary condition (2.9) and the corresponding ODE problem defined by

$$\frac{du(t)}{dt} = f. \tag{2.53}$$

Assume that u^* is a stationary solution of (2.53).

Definition 2.3.3. *A solution problem (2.6), $u(\cdot, x) = u^*, \quad \forall x \in \Omega$ is called a spatially homogeneous steady state [170].*

Denote $\tilde{u}^*$ the steady state of problem (2.6), corresponding to the stationary solution u^*. Practical study of the local stability of homogeneous steady state solutions can be found in [245, 170]. In particular, it can be shown that if u^* is unstable, then $\tilde{u}^*$ is also unstable, however the asymptotic stability of u^* does not guaranty the asymptotic stability of $\tilde{u}^*$. When u^* is stable but $\tilde{u}^*$ is unstable, then we obtain a so-called a *Turing instability* [239]. Indeed, in some cases, adding a diffusion operator may have a destabilizing effect. In other cases, it

may give rise to the formation of patterns which constitute a stable spatially heterogeneous solution. The study of Turing instabilities can be found in [245, 170].

In chapter 3, we model the diffusion of the concentration of a chemical attractant released from traps which determines the attraction of the insects towards them. We show that as time approaches $+\infty$, the concentration converges to a spatially heterogeneous steady state solution. Assume that the rate at which the chemical attractant diffuses is significantly higher than the rate at which insects spread, we solve numerically the insect population dynamics problem by considering the steady state concentration of the chemical attractant.

2.3.8 Application to single PDE model of Chapter 3

In chapter 3 we model the spatio-temporal dynamics of insects via an advection-diffusion process on a domain Ω. The abundance of insects at time $t \in [0, T]$, $T > 0$, and position $x \in \Omega$ is denoted by $u(t, x)$. We consider homogeneous Neumann conditions on the boundary, $\Gamma = \partial\Omega$, and we assume that we are given $u_0 \geq 0$ such that $u(0, \cdot) = u_0$ on Ω. The model is formulated as follows:

$$\begin{cases} \frac{\partial u}{\partial t} - \nabla(s(x)\nabla u) + \nabla(a(x)u) = 0, \\ \frac{\partial u}{\partial n}|_{\Gamma} = 0, \\ u|_{t=0} = u_0. \end{cases} \tag{2.54}$$

The reader is invited to refer to chapter 3 for explicit formulations of the functions $s(x)$ and $a(x)$ as well as for the description of the process. In particular, s and a are continuous and differentiable functions of the space variable x such that $0 < \varepsilon \leq s(x) \leq \sigma, \forall x \in \Omega$ and $0 \leq a(x) \leq a_{max}, \forall x \in \Omega$. In the following, we carry out a theoretical analysis of model (2.54) using the variational approach.

2.3.8.1 Variational formulation

Consider u as a mapping of t into $H^1(\Omega)$ satisfying a homogeneous Neumann boundary condition.

$$\mathbf{u} : [0, T] \longrightarrow H^1(\Omega), \tag{2.55}$$

and we seek for a solution

$$\mathbf{u} \in \mathcal{W}(H^1(\Omega), H^{-1}(\Omega)). \tag{2.56}$$

We multiply each term of (2.54) by a test function $v \in H^1(\Omega)$ and integrate over Ω, then, for $t > 0$ and $v \in H^1(\Omega)$, we have

$$\int_{\Omega} \left(\frac{\partial \mathbf{u}(t)}{\partial t} v - \nabla \cdot (s(x)\nabla \mathbf{u}(t))v + \nabla(a(x)\mathbf{u}(t))v \right) = 0. \tag{2.57}$$

Using Green's theorem, we have

$$\int_\Omega \frac{\partial \mathbf{u}(t)}{\partial t} v(x) + \int_\Omega \left(s(x)\nabla \mathbf{u}(t)\cdot\nabla v - a(x)\nabla \mathbf{u}(t)\cdot\nabla v\right) = 0. \tag{2.58}$$

Denoting

$$B(u,v) = \int_\Omega \left(s(x)\nabla u\cdot\nabla v - a(x)\nabla u\cdot\nabla v\right), \tag{2.59}$$

we obtain that the weak formulation of problem (2.54) as

$$\begin{cases} \text{Find } \mathbf{u}\in \mathcal{W}(H^1(\Omega), H^{-1}(\Omega)), \text{ such that:} \\ \\ < \frac{\partial \mathbf{u}(t)}{\partial t}, v >_{H^{-1}(\Omega),H^1(\Omega)} + B(\mathbf{u}(t), v) = 0, \\ \\ \mathbf{u}(0) = u_0. \end{cases} \tag{2.60}$$

Note that this problem is of the form (2.21) where the right hand side is zero. Further the bilinear form (2.22) is given by (2.59) and it is actually independent of t.

2.3.8.2 Existence and uniqueness

Proposition 2.3.1. *Problem (2.54) admits a unique weak solution.*

Proof. We verify that the bilinear form verifies the hypothesis of Lions theorem (P1-P3). Note that $0 < \epsilon \leq s(x) \leq \sigma$, and $a(x) < a_{max}$. $\forall u, v \in H^1(\Omega)$,

$$\begin{aligned} |B(u,v)| &= |\int_\Omega s(x)\nabla u\nabla v - \int_\Omega a(x)u\nabla v| \\ &\leq \sigma \int_\Omega |\nabla u \nabla v| \\ &\leq \sigma \|\nabla u\|_{L^2(\Omega)} \|\nabla v\|_{L^2(\Omega)} \\ &\leq \sigma \left(\|\nabla u\|_{L^2(\Omega)}\|\nabla v\|_{L^2(\Omega)} + \|u\|_{L^2(\Omega)}\|v\|_{L^2(\Omega)}\right) \\ &\leq \sigma \|u\|_{H^1(\Omega)}\|v\|_{H^1(\Omega)} \end{aligned}$$

Thus (P2) is satisfied with $M = \sigma$. Moreover, the bilinear form B is coercive: $\forall u \in H^1(\Omega)$,

$$\begin{aligned} B(u,u) &= \int_\Omega s(x)(\nabla u)^2 - \int_\Omega a(x)u\nabla u \\ &\geq \epsilon\|\nabla u\|^2_{L^2(\Omega)} - a_{max}\int_\Omega |u||\nabla u| \\ &\geq \epsilon\|\nabla u\|^2_{L^2(\Omega)} - a_{max}\|u\|_{L^2(\Omega)}\|\nabla u\|_{L^2(\Omega)} \\ &\geq \epsilon\|\nabla u\|^2_{L^2(\Omega)} - \frac{\epsilon}{2}\|\nabla u\|^2_{L^2(\Omega)} - \frac{a^2_{max}}{2\epsilon}\|u\|^2_{L^2(\Omega)} \\ &= \epsilon\|\nabla u\|^2_{L^2(\Omega)} + \frac{\epsilon}{2}\|u\|^2_{L^2(\Omega)} - \frac{\epsilon}{2}\|u\|^2_{L^2(\Omega)} - \frac{\epsilon}{2}\|\nabla u\|^2_{L^2(\Omega)} - \frac{a^2_{max}}{2\epsilon}\|u\|^2_{L^2(\Omega)} \\ &= \frac{\epsilon}{2}\|u\|^2_{H^1(\Omega)} - (\frac{\epsilon}{2} + \frac{a^2_{max}}{2\epsilon})\|u\|^2_{L^2(\Omega)} \end{aligned} \tag{2.61}$$

Thus (P3) is satisfied, with $\alpha = \frac{\epsilon}{2}$ and $\gamma = \frac{\epsilon}{2} + \frac{a^2_{max}}{2\epsilon}$. □

Proposition 2.3.2 (A priori estimates)**.** *Considering problem (2.60), for any fixed $t > 0$, we have*

$$\|u\|^2_{L^2} \leq e^{\frac{a^2_{max}}{\epsilon}t}\|u_0\|^2_{L^2} \tag{2.62}$$

Furthermore, if

$$\|u\|^2_{L^2([0,T],L^2(\Omega))} \geq -\frac{a^2_{max}}{\varepsilon}\|u_0\|^2_{L^2([0,T],L^2(\Omega))} \tag{2.63}$$

Proof. Let $v = u$ in problem (2.60), for $t > 0$:

$$\begin{aligned} &(\frac{\partial u}{\partial t}, u) + B(u,u;t) = 0 \\ \therefore\quad &\frac{1}{2}\frac{d}{dt}\|u\|^2_{L^2} + B(u,u;t) = 0 \end{aligned}$$

Using the L^2-coercivity of B, using the notation $\alpha = \frac{\epsilon^u}{2}$ and $\gamma = \frac{\epsilon^u}{2} + \frac{a^2_{max}}{2\epsilon^u}$, we have

$$\frac{1}{2}\frac{d}{dt}\|u\|^2_{L^2} + \alpha\|u\|^2_{H^1} - \gamma\|u\|^2_{L^2} \quad \leq \quad 0 \tag{2.64}$$

Since $\|u\|^2_{H^1} = \|u\|^2_{L^2} + \|\nabla u\|^2_{L^2} \geq \|u\|^2_{L^2}$,

$$\begin{aligned} &\tfrac{1}{2}\tfrac{d}{dt}\|u\|^2_{L^2} + \alpha\|u\|^2_{L^2} - \gamma\|u\|^2_{L^2} \leq 0 \\ \therefore\quad &\tfrac{1}{2}\tfrac{d}{dt}\|u\|^2_{L^2} \leq (\gamma - \alpha)\|u\|^2_{L^2} \\ \therefore\quad &\tfrac{d}{dt}\|u\|^2_{L^2} \leq 2(\gamma - \alpha)\|u\|^2_{L^2} \end{aligned} \tag{2.65}$$

Applying Gronwall inequality with $\beta = (\gamma - \alpha)$ and $f = 0$, yields:

$$\|u\|_{L^2}^2 \leq e^{2(\gamma-\alpha)t}\|u_0\|_{L^2}^2. \tag{2.66}$$

Further, from (2.65), integration by parts over the interval $[0, T]$ leads to the second estimate in the $L^2([0, T], L^2(\Omega))$-norm:

$$\|u(T)\|_{L^2}^2 - \|u_0\|_{L^2}^2 + 2(\alpha - \gamma)\int_0^T \|u\|_{L^2}^2 dt \quad \leq \quad 0.$$

Finally, by adding both sides of the inequality by $\|u_0\|_{L^2}^2$, dividing by $2(\alpha - \gamma) = -\frac{a_{max}^2}{\varepsilon}$ and omitting the term $\|u(T)\|_{L^2}^2$ yields to the estimate:

$$\|u\|_{L^2([0,T],L^2(\Omega))}^2 \quad \geq \quad -\frac{a_{max}^2}{\varepsilon}\|u_0\|_{L^2([0,T],L^2(\Omega))}^2.$$

□

2.3.8.3 Positivity of the solution

Proposition 2.3.3. *The weak solution of problem (2.54) is essentially non-negative, i.e.*

$$\forall t \in [0, T], \quad u(t, x) \geq 0 \text{ a.e. in } \Omega.$$

Proof. Consider $u \in \mathcal{W}(H^1(\Omega), H^{-1}(\Omega))$ the solution of problem (2.60). As shown in the proof of Proposition 2.3.1, the bilinear form $B(t; \cdot, \cdot)$ is L^2-coercive on $H^1(\Omega)$. Therefore the positivity of u is a straightforward consequence of Theorem 2.3.7.

□

2.3.9 Application to the system of PDEs of Chapter 4

In chapter 4 we consider a chemotaxis model governed by three equations. It is assumed that a chemical attractant is released in traps to which the insects respond. Here $c(t, x)$ represents the concentration of the chemical attractant at time $t \in [0, T]$, and position $x \in \Omega \subset \mathbb{R}^2$. The abundance of insects at time $t \in [0, T]$ and position $x \in \Omega$ are divided in

two compartments: the *free* insects $u_f(t,x)$, and the *captured* insects $u_c(t,x)$. The model is formulated via the system of PDEs as follows.

$$\frac{\partial c(t,x)}{\partial t} - \epsilon^c \Delta c(t,x) + \lambda(x)(c(t,x) - c_{sat}) = -\mu_c c(t,x) \tag{2.67}$$

$$\frac{\partial u_f(t,x)}{\partial t} - \epsilon^u \Delta u_f(t,x) + \nabla \cdot (\chi(c)\nabla c(t,x) u_f(t,x)) = -f(x)u_f(t,x) \tag{2.68}$$

$$\frac{\partial u_c(t,x)}{\partial t} = f(x)u_f(t,x), \quad x \in \Gamma, t > 0 \tag{2.69}$$

$$c(t,x) = 0, \quad x \in \Gamma, t > 0 \tag{2.70}$$

$$\nabla u_f \cdot \vec{n} = 0, \quad \text{on } \Gamma \tag{2.71}$$

$$\nabla u_c \cdot \vec{n} = 0, \quad \text{on } \Gamma \tag{2.72}$$

$$c(0,x) = 0, \quad x \in \Omega \tag{2.73}$$

$$u_f(0,x) = u_0(x), \quad x \in \Omega \tag{2.74}$$

$$u_c(0,x) = 0, \quad x \in \Omega \tag{2.75}$$

where $\vec{n}$ denotes the outward normal vector on Γ, the boundary of the domain Ω.

Here, ϵ^c, ϵ^u, c_{sat} and μ_c are positive constants and $\lambda(x)$, $\chi(c)$ and $f(x)$ are positive and bounded smooth function with

$$\begin{aligned} &0 \leq \lambda(x) \leq \lambda_{max}, \\ &0 \leq \chi(c) \leq \alpha, \\ &0 \leq f(x) \leq c_{sat}\lambda_{max}. \end{aligned}$$

Further, we have

$$u_0(x) \geq 0, \quad \forall x \in \Omega.$$

The reader is invited to refer the to chapter 4 for a detailed description of the model.

One can note that the problem for c, (2.67), (2.70), (2.73), can be solved independently. Hence, in the following, we first carry out the theoretical analysis of problem (2.67), (2.70), (2.73), and afterwards we study the problem (2.68), (2.71), (2.74) assuming that c is a data function. Similarly, problem (2.68), (2.71), (2.74) can be solved independently from (2.69), (2.72), (2.75). In the following, we first formulate problem (2.67)-(2.75) in variational form. Then, we provide complementary results to those presented in chapter 4 or similar results using an alternative approach to those of chapter 4.

2.3.9.1 Variational formulation

To apply the theory of weak solutions, we consider c, u_f and u_c not as functions of t and x, but as mappings of t into functional spaces on Ω. Thus, the weak problem is

$$\begin{cases} \text{Find } \mathbf{c} \in \mathcal{W}(H_0^1(\Omega), H^{-1}(\Omega)), \quad \mathbf{u}_f \in \mathcal{W}(H^1(\Omega), H^{-1}(\Omega)), \\ \text{and } \mathbf{u}_c \in \mathcal{W}(H^1(\Omega), H^{-1}(\Omega)), \quad \text{such that:} \\ \\ < \frac{d\mathbf{c}(t)}{dt}, w >_{H^{-1},H_0^1} + a(\mathbf{c}(t), w) =< c_{sat}\lambda, w >_{H^{-1},H_0^1}, \quad \forall w \in H_0^1(\Omega) \\ \\ < \frac{d\mathbf{u}_f(t)}{dt}, v >_{H^{-1},H^1} + b(\mathbf{u}_f(t), v) = 0, \quad \forall v \in H^1(\Omega), \\ \\ < \frac{d\mathbf{u}_c(t)}{dt}, v >_{H^{-1},H^1} = \int\limits_\Omega f(x)\mathbf{u}_f(t)v, \quad \forall v \in H^1(\Omega) \\ \\ \mathbf{c}(0) = 0, \quad \mathbf{u}_f(0) = u_0, \quad \text{and } \mathbf{u}_c(0) = 0. \end{cases} \tag{2.76}$$

where a and b are the bilinear forms: $\forall c, w \in H_0^1(\Omega), \forall t \in [0, T]$,

$$a(c, w) = \int\limits_\Omega \left(\epsilon^c \nabla c \cdot \nabla w + (\lambda(x) + \mu)cw\right), \tag{2.77}$$

and $\forall u_f, v \in H^1(\Omega) \forall t \in [0, T]$,

$$b(t; u_f, v) = \int\limits_\Omega \left(\epsilon^u \nabla u_f \cdot \nabla v - (\chi(c)\nabla c(t, x)u_f) \cdot \nabla v + f(x)u_f v\right). \tag{2.78}$$

A detailed derivation of the variational formulation (2.76) can be found in Chapter 4.

2.3.9.2 Study of c: the stationary problem

The equation governing the dynamics of c is independent from the rest of the model, and it can therefore be studied independently. We consider the diffusion-reaction problem formulated by (2.67), (2.70) and (2.73).

Prior to the theoretical analysis of the model (2.67), (2.70) and (2.73) governing the spread of the attractant released from the traps which is done in (2.3.9.2), a particular attention is given to the associated stationary problem, that is, when $\frac{\partial c(t,x)}{\partial t} = 0$. In this case, the weak formulation of the stationary problem consists of finding $c \in H_0^1(\Omega)$ such that the bilinear form a is independent of t and defined as

$$a(c, w) =< c_{sat}\lambda, w >_{H^{-1},H_0^1}, \quad \forall w \in H_0^1(\Omega). \tag{2.79}$$

Proposition 2.3.4 (Existence and uniqueness)**.** *Problem (2.79) admits a unique solution.*

Proof. We prove the existence and uniqueness of the solution of problem (2.79) using the Lax-Milgram lemma ([94], lemma 2.2). Note that $0 < \mu \leq \lambda(x) + \mu \leq \lambda_{max} + \mu$, and $\epsilon^c > 0$. $\forall c, w \in H_0^1$,

$$\begin{aligned}
|a(c,w)| &= |\int_\Omega \epsilon^c \nabla c \nabla w dx + \int_\Omega (\lambda(x)+\mu) cw dx| \\
&\leq \epsilon^c \int_\Omega |\nabla c \nabla w| dx + (\lambda(x)+\mu) \int_\Omega |cw| dx \\
&\leq \epsilon^c \|\nabla c\|_{L^2} \|\nabla w\|_{L^2} + (\lambda_{max}+\mu)\|c\|_{L^2}\|w\|_{L^2} \quad \text{(by Hölder's inequality)} \\
&\leq M(\|\nabla c\|_{L^2}\|\nabla w\|_{L^2} + \|c\|_{L^2}\|w\|_{L^2}) \quad (M = \max\{\epsilon^c, \lambda_{max}+\mu\}) \\
&\leq M\|c\|_{H_0^1}\|w\|_{H_0^1}.
\end{aligned}$$

Moreover, the bilinear form a is coercive: $\forall c \in H_0^1$,

$$\begin{aligned}
a(c,c) &= \int_\Omega \epsilon^c (\nabla c)^2 dx + \int_\Omega (\lambda(x)+\mu) c^2 dx \\
&\geq \epsilon^c \|\nabla c\|_{L^2}^2 + \mu \|c\|_{L^2}^2 \\
&\geq k\left(\|\nabla c\|_{L^2}^2 + \|c\|_{L^2}^2\right) \quad (k = \min\{\epsilon^c, \mu\}) \\
&= k\|c\|_{H_0^1}^2.
\end{aligned}$$

Further, since the functional f is bounded, $(0 \leq f(x) \leq c_{sat}\lambda_{max}, \forall x \in \Omega)$, the hypothesis of the Lax-Milgram lemma are satisfied, thus problem (2.79) admits a unique solution. □

Now, we make sure that the problem is well posed by showing that the norm of the solution is bounded.

Proposition 2.3.5 (A priori estimate)**.** *Considering problem (2.79), if $k = \min\{\epsilon^c, \mu\}$, we have the following a priori estimates:*

$$\|c\|_{L^2}^2 \leq \frac{1}{k^2}\|f\|_{L^2}^2. \tag{2.80}$$

Proof. Choose $w = c$ as a test function in (2.79)

$$\begin{aligned}
a(c,c) &= \int_\Omega f c dx \\
&\leq \|f\|_{L^2}\|c\|_{L^2} \quad \text{(by Hölder's inequality)} \\
&\leq \frac{1}{2k}\|f\|_{L^2}^2 + \frac{k}{2}\|c\|_{L^2}^2 \quad \text{(by Peter-Paul inequality)}
\end{aligned} \tag{2.81}$$

By the coercivity of a,

$$a(c,c) > k\|c\|^2_{H^1_0} = k\left(\|c\|^2_{L^2} + \|\nabla c\|^2_{L^2}\right) \geq k\|c\|^2_{L^2},$$

therefore,

$$\begin{aligned} k\|c\|^2_{L^2} &\leq \frac{1}{2k}\|f\|^2_{L^2} + \frac{k}{2}\|c\|^2_{L^2}, \\ \therefore \quad \frac{k}{2}\|c\|^2_{L^2} &\leq \frac{1}{2k}\|f\|^2_{L^2}, \\ \therefore \quad \|c\|^2_{L^2} &\leq \frac{1}{k^2}\|f\|^2_{L^2}. \end{aligned}$$

□

2.3.9.3 Study of c: the evolution problem

Consider the parabolic problem

$$\begin{cases} \text{Find } \mathbf{c} \in \mathcal{W}(H^1_0, H^{-1}), \text{ such that:} \\ \\ < \frac{d\mathbf{c}(t)}{dt}, w >_{H^{-1}(\Omega), H^1_0(\Omega)} + a(\mathbf{c}(t), w) =< c_{sat}\lambda, w >_{H^{-1}, H^1_0}, \quad \forall w \in H^1_0(\Omega), \\ \\ \mathbf{c}(0) = 0. \end{cases} \tag{2.82}$$

Proposition 2.3.6 (Existence and uniqueness)**.** *Problem (2.82) admits a unique solution.*

Proof. Note that the bilinear form of the stationary problem (2.79) has the same properties of the bilinear form of the evolution problem (2.82) for a fixed $t \in [0,T]$. Hence the proof is the same as for Theorem 2.3.4, i.e. show that the properties of the bilinear form satisfies the properties (P1)-(P3) to apply Lions theorem. □

We now investigate a priori estimates on the solution to problem (2.82) to ensures its continuous dependence on the known data.

Proposition 2.3.7 (A priori estimate)**.** *Considering problem (2.82), for any fixed $t > 0$, if $k = \min\{\epsilon^c, \mu\}$, we have the following a priori estimates:*

$$\|c\|^2_{L^2} \leq e^{-kt}\|c_0\|^2_{L^2} + \frac{1}{k^2}\|\lambda_{max} c_{sat}\|^2_{L^2}. \tag{2.83}$$

Furthermore,

$$\|c\|^2_{L^2([0,T],L^2(\Omega))} \leq \frac{1}{k^2}\|\lambda_{max} c_{sat}\|^2_{L^2([0,T],L^2(\Omega))} + \frac{1}{k}\|c_0\|^2_{L^2}. \tag{2.84}$$

Proof. Choose $w = c$ as a test function in (2.82). For the sake of simplifying the notation, in this proof we denote $f(x) = \lambda(x)c_{sat}$. Let $t \in]0, T[$

$$\int_\Omega \frac{\partial c}{\partial t} c dx + a(c, c) = \int_\Omega f c dx.$$

We have

$$\begin{aligned} \int_\Omega f c dx &\leq \|f\|_{L^2}\|c\|_{L^2} \quad \text{(by Hölder's inequality)} \\ &\leq \frac{1}{2k}\|f\|^2_{L^2} + \frac{k}{2}\|c\|^2_{L^2} \quad \text{(by Peter-Paul inequality).} \end{aligned}$$

By the coercivity of a,

$$a(c, c) > k\|c\|^2_{H^1_0} = k\left(\|c\|^2_{L^2} + |c|^2_1\right) \geq k\|c\|^2_{L^2},$$

also, provided that $c(x, t)$ is differentiable with respect to $t \in]0, T[$,

$$\int_\Omega \frac{\partial c}{\partial t} c dx = \frac{1}{2}\int_\Omega \frac{\partial}{\partial t}(c^2) dx = \frac{1}{2}\frac{d}{dt}\|c\|^2_{L^2}.$$

Altogether, we obtain

$$\frac{1}{2}\frac{d}{dt}\|c\|^2_{L^2} + k\|c\|^2_{L^2} \leq \frac{1}{2k}\|f\|^2_{L^2} + \frac{k}{2}\|c\|^2_{L^2}.$$

Gathering the terms in $\|c\|^2_{L^2}$ and diving by $\frac{1}{2}$ yields:

$$\frac{d}{dt}\|c\|^2_{L^2} + k\|c\|^2_{L^2} \leq \frac{1}{k}\|f\|^2_{L^2}. \tag{2.85}$$

Owing to Gronwall's lemma ([94], lemma 6.9),

$$\|c\|^2_{L^2} \leq e^{-kt}\|c_0\| + \frac{1}{k}\int_0^t e^{-k(t-\tau)}\|f\|^2_{L^2} d\tau = e^{-kt}\|c_0\| + \frac{1}{k^2}\|f\|^2_{L^2}\left(1 - e^{-kt}\right).$$

Since $t > 0$ and $k > 0$, $\left(1 - e^{-kt}\right) \leq 1$, therefore,

$$\|c\|^2_{L^2} \leq e^{-kt}\|c_0\| + \frac{1}{k^2}\|f\|^2_{L^2}.$$

Further, from (2.85), integration by parts over the interval $[0, T]$ leads to the second estimate in the $L^2([0, T], L^2(\Omega))$-norm:

$$\|c(T)\|^2_{L^2} - \|c_0\|^2_{L^2} + k\int_0^T \|c\|^2_{L^2} dt \leq \frac{1}{k}\int_0^T \|f\|^2_{L^2} dt.$$

Finally, by adding both sides of the inequality by $\|c_0\|^2_{L^2}$, dividing by k and omitting the term $\|c(T)\|^2_{L^2}$ yields to the estimate:

$$\|c\|^2_{L^2([0,T],L^2(\Omega))} \leq \frac{1}{k^2}\|f\|^2_{L^2([0,T],L^2(\Omega))} + \frac{1}{k}\|c_0\|^2_{L^2([0,T],L^2(\Omega))}.$$

□

We now show that the solution of the evolution problem (2.82) tends to a stationary solution as $t \to \infty$ which is the solution of the stationary problem (2.79).

Proposition 2.3.8 (Convergence to the stationary solution)**.** *The solution $c(t,x), \forall (t,x) \in \mathbb{R}^+ \times \Omega$ of (2.82), converges to the solution c_{stat} of the stationary problem (2.79) as t approaches infinity.*

$$\lim_{t\to\infty} c(t,x) = c_{stat}. \tag{2.86}$$

Proof. The proof can be found in Chapter 4. □

In chapter 4, the positivity and boundedness of the solution is shown using the Maximum Principle. Thus the existence of the solution of the classical solution was assumed, i.e. solution of (2.67),(2.70),(2.73). Here, we use Theorem 2.3.6 and Theorem 2.3.7 to show the positivity and boundedness of the weak solution of (2.67),(2.70),(2.73).

Proposition 2.3.9 (Boundedness of c)**.** *The weak solution c of (2.67),(2.70),(2.73) satisfies*

$$0 \leq c(t,x) \leq c_{stat}, \quad a.e \text{ in } \Omega, \forall t \in (0,T]. \tag{2.87}$$

Proof. Consider $c \in \mathcal{W}(H^1_0(\Omega), H^{-1}(\Omega))$ the weak solution of problem (2.67),(2.70),(2.73), c is the solution of the variational problem (2.82). As shown in the proof of Proposition 2.3.6, the bilinear form $a(t;\cdot,\cdot)$ is L^2-coercive on $H^1_0(\Omega)$. Then using that $\lambda(x)c_{sat} \geq 0, x \in \Omega$, the positivity of c is a straightforward consequence of Theorem 2.3.6.

Consider $\tilde{c} = c_{sat} - c$. Then $\tilde{c}(t) \in H^1(\Omega)$ satisfies

$$\begin{aligned}
&< \frac{d\tilde{c}(t)}{dt}, w >_{H^{-1},H^1_0} + a(\tilde{c}(t), w) =< \mu_c c_{sat}\lambda, w >_{H^{-1}(\Omega),H^1_0(\Omega)}, \quad \forall w \in H^1_0(\Omega),\\
&\tilde{c}(t)|_\Gamma = c_{sat} > 0,\\
&\tilde{c}(0) = c_{sat} > 0.
\end{aligned}$$

Since $\mu_c c_{sat}\lambda(x) \geq 0, x \in \Omega$, Theorem 2.3.7 yields $\tilde{c} \geq 0$, that is, $c \leq c_{sat}$.

□

2.3.9.4 Study of u_f

Consider the problem

$$\begin{cases} \text{Find } \mathbf{u}_f \in \mathcal{W}(H^1(\Omega), H^{-1}(\Omega)), \text{ such that:} \\ \\ < \frac{d\mathbf{u}_f(t)}{dt}, v >_{H^{-1}(\Omega), H_0^1(\Omega)} + b(\mathbf{u}_f(t), v) = 0, \quad \forall v \in H^1(\Omega), \\ \\ \mathbf{u}_f(0) = u_0. \end{cases} \tag{2.88}$$

Proposition 2.3.10. *Problem (2.68),(2.71),(2.74) admits a unique weak solution.*

Proof. We show that problem (2.88) satisfies the hypothesis of Lions' theorem. Let $t \in [0, T]$. For any u, v in H^1 we have:

$$|b(t; u_f, v)| = |\int_\Omega \epsilon^u \nabla u_f \cdot \nabla v dx - \int_\Omega \chi(c) u_f \nabla c \nabla v dx + \int_\Omega f(x) u_f v dx|$$

We have that $\int_\Omega \chi(c) u_f \nabla c \nabla v dx \geq 0$, and since $f(x)$ bounded, $\exists M_f > 0$ such that $f(x) \geq M_f$, therefore

$$|b(t; u_f, v)| \leq \epsilon^u \int_\Omega |\nabla u_f \cdot \nabla v| dx + M_f \int_\Omega |u_f v| dx \tag{2.89}$$

By Holder's inequality, we have

$$|b(t; u_f, v)| \leq \epsilon^u \|\nabla u_f\|_{L^2} \|\nabla v\|_{L^2} + M_f \|u_f\|_{L^2} \|v\|_{L^2}$$

Let $M = \max(\epsilon^u, M_f)$,

$$\begin{aligned} |b(t; u_f, v)| &\leq M_f \left(\|\nabla u_f\|_{L^2} \|\nabla v\|_{L^2} + \|u_f\|_{L^2} \|v\|_{L^2} \right) \\ &\leq M_f \|u_f\|_{H^1} \|v\|_{H^1} \end{aligned}$$

Therefore (P2) is satisfied.

Let $v = u_f$.

$$b(t; u_f, u_f) = \int_\Omega \epsilon^u \nabla u_f \cdot \nabla u_f dx - \int_\Omega \chi(c) u_f \nabla c \nabla u_f dx + \int_\Omega f(x) u_f u_f dx$$

Since c is a smooth function, $c \in \mathcal{C}^1(\Omega)$, thus since $\chi(c)$ is bounded and ∇c is continuous and bounded, $\exists A > 0$ such that $\int_\Omega |\chi(c) u_f \nabla c \nabla u_f| dx \leq A \int_\Omega |u_f| . |\nabla u_f| dx$. Therefore, using

Holder's inequality followed by Peter-Paul inequality, we obtain

$$\begin{aligned}\int_\Omega \chi(c)u_f\nabla c\nabla u_f dx &\leq A\int_\Omega |u_f|.|\nabla u_f|dx\\ &\leq A\|u_f\|_{L^2}\|\nabla u_f\|_{L^2}\\ &\leq \frac{\epsilon^u}{2}\|\nabla u_f\|_{L^2}^2+\frac{A^2}{2\epsilon^u}\|u_f\|_{L^2}^2\end{aligned}$$

Moreover, $0\leq f(x)\leq M_f$, therefore

$$\begin{aligned}b(t;u_f,u_f) &\geq \epsilon^u\|\nabla u_f\|_{L^2}^2-\left(\frac{\epsilon^u}{2}\|\nabla u_f\|_{L^2}^2+\frac{A^2}{2\epsilon^u}\|u_f\|_{L^2}^2\right)\\ &= \frac{\epsilon^u}{2}\|\nabla u_f\|_{L^2}^2-\frac{A^2}{2\epsilon^u}\|u_f\|_{L^2}^2\\ &= \frac{\epsilon^u}{2}\|\nabla u_f\|_{L^2}^2+\frac{\epsilon^u}{2}\|u_f\|_{L^2}^2-\frac{\epsilon^u}{2}\|u_f\|_{L^2}^2-\frac{A^2}{2\epsilon^u}\|u_f\|_{L^2}^2\\ &= \frac{\epsilon^u}{2}\|u_f\|_{H^1}^2-\frac{\epsilon^u}{2}\|u_f\|_{L^2}^2-\frac{A^2}{2\epsilon^u}\|u_f\|_{L^2}^2\\ &= \frac{\epsilon^u}{2}\|u_f\|_{H^1}^2-(\frac{\epsilon^u}{2}+\frac{N^2}{2\epsilon^u})\|u_f\|_{L^2}^2\end{aligned}$$

Therefore, b is L^2-coercive in the sense of property (P3) where $\alpha=\frac{\epsilon^u}{2}$ and $\gamma=\frac{\epsilon^u}{2}+\frac{A^2}{2\epsilon^u}$. Since the properties (P1), (P2) and (P3) are satisfied, the theorem of Lions (Corollary 2.3.1) ensures the existence and uniqueness of the solution.

□

Proposition 2.3.11 (A priori estimates)**.** *Considering problem (2.88), for any fixed $t>0$, we have*

$$\|u\|_{L^2}^2\leq e^{\frac{A^2}{2\epsilon^u}t}\|u_0\|_{L^2}^2 \tag{2.90}$$

Proof. Let $v=u$ in problem (2.88), for $t>0$:

$$\begin{aligned}&(\frac{\partial u}{\partial t},u)+a(t,u,u)=0\\ \therefore\quad &\frac{1}{2}\frac{d}{dt}\|u\|_{L^2}^2+a(t,u,u)=0\end{aligned}$$

Using the L^2-coercivity of a, using the notation $\alpha=\frac{\epsilon^u}{2}$ and $\gamma=\frac{\epsilon^u}{2}+\frac{A^2}{2\epsilon^u}$, we have

$$\frac{1}{2}\frac{d}{dt}\|u\|_{L^2}^2+\alpha\|u\|_{H^1}^2-\gamma\|u\|_{L^2}^2 \leq 0 \tag{2.91}$$

Since $\|u\|_{H^1}^2 = \|u\|_{L^2}^2 + \|\nabla u\|_{L^2}^2 \geq \|u\|_{L^2}^2$,

$$\begin{aligned} & \tfrac{1}{2}\tfrac{d}{dt}\|u\|_{L^2}^2 + \alpha\|u\|_{L^2}^2 - \gamma\|u\|_{L^2}^2 \leq 0 \\ \therefore \quad & \tfrac{1}{2}\tfrac{d}{dt}\|u\|_{L^2}^2 \leq (\gamma - \alpha)\|u\|_{L^2}^2 \end{aligned}$$

Applying Gronwall inequality with $\beta = (\gamma - \alpha)$ and $f = 0$, yields:

$$\|u\|_{L^2}^2 \leq e^{(\gamma-\alpha)t}\|u_0\|_{L^2}^2 \tag{2.92}$$

□

Proposition 2.3.12. *The weak solution of problem (2.68),(2.71),(2.74) is essentially non-negative, i.e.*

$$\forall t \in [0, T], \quad u_f(t, x) \geq 0 \text{ a.e. in } \Omega.$$

Proof. Consider $u_f \in \mathcal{W}(H^1(\Omega), H^{-1}(\Omega))$ the weak solution of problem (2.68),(2.71),(2.74). u_f is the solution of the variational problem (2.88). As shown in the proof of Proposition 2.3.10, the bilinear form $b(t; \cdot, \cdot)$ is L^2-coercive on $H^1(\Omega)$. Therefore the positivity of u_f is a straightforward consequence of Theorem 2.3.7.

□

2.4 Dynamical systems defined by a system of ODEs

In chapter 5, the models are temporal and governed by systems of ODEs representing the evolution in time of a compartmented insect population. Thus, the state of the system at time t is a real vector $x(t)$ representing the population densities in the respective compartments at time t. Hence, we consider a dynamical system defined via a system of ODEs on a subset of $\mathbb{R}^n$ as discussed below.

Let $\mathcal{D} \subset \mathbb{R}^n$. We consider the autonomous system of ODEs

$$\frac{dx}{dt} = f(x) \tag{2.93}$$

where $f : \mathcal{D} \longrightarrow \mathbb{R}^n$, with an initial condition

$$x(0) = x_0 \in \mathcal{D}. \tag{2.94}$$

We recall here some of the fundamental theory following mostly [128].

Theorem 2.4.1 (Local existence and uniqueness)**.** *Let $\mathcal{D}$ be an open subset of $\mathbb{R}^n$, $f : \mathcal{D} \longrightarrow \mathbb{R}^n$ a $\mathcal{C}^1$ map, and $x_0 \in \mathbb{R}^n$. Then there is some $a > 0$ and a unique solution*

$$x : [-a, a] \longrightarrow \mathcal{D}$$

of the differential equation (2.93) satisfying the initial condition (2.94). [128, Theorem 1, Section 2, Chap. 8]

Theorem 2.4.2. *Let $\mathcal{D}$ be an open subset of $\mathbb{R}^n$, and $f : \mathcal{D} \longrightarrow \mathbb{R}^n$ a $\mathcal{C}^1$ map. Let $x(t)$ be a solution on a maximal open interval $J = (\alpha, \beta)$, with $\beta < \infty$. Then given any compact set $K \subset \mathcal{D}$, there is some $t \in (\alpha, \beta)$ such that $x(t) \notin K$. [128, Theorem, Section 5, Chapter 8]*

In other words, Theorem 2.4.2 says that if $x(t)$ cannot be extended to a larger interval than (α, β), then it leaves any compact set. As a consequence, as t tends to β, $x(t)$ either tends to the boundary of $\mathcal{D}$ or $|x(t)|$ tends to ∞.

If for every $x_0 \in \mathcal{D}$ the system (2.93)-(2.94) has a unique solution $x(t)$ on $[0, +\infty)$, then (2.93) defines a dynamical system on $\mathcal{D}$ in terms of Definition 2.2.1. In this case the operator φ_t is given by

$$\varphi_t(x_0) = x(t), \quad t \geq 0.$$

Then, f defines a *vector field* satisfying

$$f(x) = \frac{d}{dt}\varphi_t(x)|_{t=0}.$$

The continuity of φ_t on x_0 is shown in [128, Theorem 2, Section 7, Chapter 8]. The global existence required above is obtained typically by using the concept of invariant set.

Definition 2.4.1 (Invariant set)**.** *A subset W of $\mathcal{D}$ is called (positively) invariant set of (2.93) if for every $x_0 \in W$ any solution of (2.93)-(2.94) of the form*

$$x : [0, \beta] \longrightarrow \mathcal{D}$$

is such that $x(t) \in W, t \in [0, \beta]$.

Proposition 2.4.1 (Global existence)**.** *Let A be a compact invariant subset of the system and let f be $\mathcal{C}^1$ on $\mathcal{D}$. Then for every $y_0 \in A$, there exists a unique solution*

$$y : [0, \infty) \longrightarrow \mathcal{D}, \quad y(0) = y_0,$$

and

$$y(t) \in A, \quad \forall t \geq 0.$$

[128, Proposition, Section 5, Chapter 8]

2.4.1 Asymptotic properties

The asymptotic properties describe the behaviour of a dynamical system as time goes to infinity. We denote by $\mathcal{O}_x^+, x \in \mathcal{D}$, the *forward orbits* or *trajectories* of the dynamical system on $\mathcal{D}$ described by the semiflow φ, i.e. the set of states that followed from an initial given state x,

$$\mathcal{O}_x^+ \equiv \{\varphi_t(x) : t \geq 0\}. \tag{2.95}$$

A point $x \in \mathcal{D}$ such that $\mathcal{O}_x^+ = \{x\}$ is called an *equilibrium*. We denote by E the set of all equilibria of the system. If there is a $T > 0$ such that $\varphi_{t+T}(x) = \varphi_t(x)$, $\forall t \geq 0$, then $\mathcal{O}_x^+ = \{\varphi_t(x) : 0 \leq t \leq T\}$ and $\varphi_t(x)$ is called a *T-periodic solution*.

We define the *ω-limit set* of $x \in \mathcal{D}$ by

$$\omega(x) = \cap_{t \geq 0} \overline{\cup_{s \geq t} \varphi_s(x)}. \tag{2.96}$$

For a dynamical system defined via (2.93), a point x^* is an equilibrium if and only if $f(x^*) = 0$.

Definition 2.4.2. *An equilibrium x^* of a semiflow φ is stable, if for every neighbourhood N of x^*, there is a neighbourhood $M \subset N$ such that if $x \in M$, then $\varphi_t(x) \in N, \forall t \geq 0$.*

Definition 2.4.3. *An equilibrium x^* of a semiflow φ is asymptotically stable if it is stable and there is neighbourhood N of x^*, such that every point in N approaches x^* as $t \to \infty$.*

In other words, an equilibrium is stable the orbits that start "near" an equilibrium stay "nearby". More strongly, an equilibrium is asymptotically stable if in addition the orbits that start "near" an equilibrium converge to the equilibrium.

To obtain stability properties of an equilibrium, we use the Jacobian matrix $Df(x^*)$ of the vector field f at x^*. Indeed, by the well-known theorem of Hartman and Grobman theorem [254, Theorem 19.12.6], the solutions of (2.93) in a neighbourhood of an equilibrium x^* behave topologically equivalently to the solutions of the linear system

$$\frac{dy}{dt} = Df(x^*)y \tag{2.97}$$

around 0. Techniques for solving linear systems can be applied to solve (2.97). In particular, properties of the equilibrium x^* are obtain by investigating the sign of the real parts of the eigenvalues of the matrix $Df(x^*)$.

Definition 2.4.4. *A equilibrium x^* of a $\mathcal{C}^1$ vector field f is hyperbolic if none of the eigen values of $Df(x^*)$ have zero real parts.*

Assume that x^* is a hyperbolic equilibrium, we have the following properties:

Proposition 2.4.2.

- *If all the eigenvalues of $Df(x^*)$ have negative real parts, then, x^* is stable.*
- *If some of the eigenvalues of $Df(x^*)$ have positive real parts, then, x^* is unstable.*

Definition 2.4.5. *Let x^* be an asymptotically stable equilibrium. The basin of attraction of x^* is the union of all the solution curves of (2.93) that tend towards x^* as $t \longrightarrow +\infty$.*

A common method to study the global stability of dynamical systems is to show the existence of a Lyapunov function:

Definition 2.4.6. *Let x^* be an equilibrium of the dynamical system defined via (2.93)on $\mathcal{D}$. If there is a neighbourhood U of x^* and a function $L \in \mathcal{C}^1(U, \mathbb{R})$*

(i) $L(x^*) = 0$

(ii) $L(x) > 0$, *for* $x \neq x^*$

(iii) $\nabla L(x) \cdot f(x) \leq 0, \quad x \in U$

then L is called a Lyapunov function. Further, if $\nabla L(x) \cdot f(x) < 0, \quad x \in U \backslash \{x^*\}$, then L is called a strict Lyapunov function for x^*.

The expression in (iii) is often called the Lyapunov derivative since for every solution $x(t)$ of (2.93) we have

$$\begin{aligned} \frac{dL(x(t))}{dt} &= \nabla L(x(t)) \cdot \frac{dx(t)}{dt} \\ &= \nabla L(x(t)) \cdot f(x(t)) \end{aligned}$$

Theorem 2.4.3. *Let x^* be an equilibrium of a dynamical system defined via (2.93).*

(i) If there exists a Lyapunov function in a neighbourhood U of x^*, then x^* is stable.

(ii) If there exists a strict Lyapunov function in a neighbourhood U of x^*, then x^* is asymptotically stable with basin of attraction containing U.

2.4.2 Monotone dynamical systems

> "A monotone dynamical system is just a dynamical system on an ordered metric space which has the property that ordered initial states lead to ordered subsequent states." [225].

A particularity of monotone dynamical systems is that they behave in a very "orderly" way. We explain below in more precise terms the meaning of this statement. A semiflow φ is said to be *monotone* if it satisfies

$$\varphi_t(x) \leq \varphi_t(y), \text{ whenever } x \leq y \text{ and } t \geq 0. \tag{2.98}$$

Further, φ is said to be *strongly order preserving* (SOP) if it is monotone and whenever $x < y$ there exist open subsets U, V of $\mathcal{D}$, with $x \in U$, $y \in V$ and $t_0 > 0$ such that

$$\varphi_{t_0}(\tilde{x}) \leq \varphi_{t_0}(\tilde{y}), \quad \forall \tilde{x} \in U, \forall \tilde{y} \in V.$$

In particular, the monotonicity of φ then implies that

$$\varphi_t U \leq \varphi_t V, \quad \forall t \geq t_0.$$

We introduce the notion of quasiconvergence which gives an essential property of monotone dynamical systems. A point $x \in \mathcal{D}$ is *quasiconvergent* if $\omega(x) \subset E$. We denote by Q the set of all quasiconvergent points. A point $x \in \mathcal{D}$ is convergent if $\omega(x)$ consists of a single point of E. We denote by C the set of all convergent points. In other words,

$$x \in Q \iff \omega(x) \subset E,$$

$$x \in C \iff \omega(x) = x^* \in E.$$

If E consists of disjoint equilibria, then $Q = C$.

Theorem 2.4.4 (Convergence criterion)**.** *Let $\varphi_T(x) \geq x$ for some $T \geq 0$. Then $\omega(x)$ is a T-periodic orbit.*
If $\varphi_t(x) \geq x$ for t belonging to a non-empty open subset of $\mathbb{R}^+ \backslash \{0\}$ then $\varphi_t(x) \to p \in E$ as $t \longrightarrow \infty$. In particular, if φ is SOP and $\varphi_T(x) > x$ for some $T > 0$ then $\varphi_t(x) \longrightarrow p \in E$ as $t \longrightarrow \infty$.

Proof. [225, Theorem 2.1, Section 2, Chapter 1]. □

As a consequence of Theorem 2.4.4, a monotone dynamical system cannot have an attracting periodic orbit. (A periodic orbit, $\mathcal{O}$, is attractive if there is an open set U containing $\mathcal{O}$ such that $\omega(x) = \mathcal{O}, \forall x \in U$.)

If $x \in \mathcal{D}$, we say that x can be *approximated from below (resp. above)* in $\mathcal{D}$ if there is a sequence $\{x_n\}$ in $\mathcal{D}$ such that $x_n < x_{n+1} < x$ (resp. $x_n > x_{n+1} > x$) for $n \geq 1$ and $x_n \longrightarrow x$ as $n \longrightarrow \infty$.

Theorem 2.4.5. *Suppose that each point of $\mathcal{D}$ can be approximated either from above or from below in $\mathcal{D}$. If φ is SOP then*

$$\mathcal{D} = \mathrm{Int}Q \cup \overline{\mathrm{Int}C}.$$

In particular Int$Q$ *is dense in $\mathcal{D}$. [225, Theorem 4.3, Section 4, Chapter 1]*

Theorem (2.4.5) shows that the property of quasi-convergence is generic for SOP dynamical systems in the sense that the set Q of all quasi-convergent points contains an open and dense subset of $\mathcal{D}$. The power of this property is further demonstrated in the particular case of E being a singleton as stated in the next theorem.

Theorem 2.4.6 (Global Asymptotic Stability)**.** *Suppose that $\mathcal{D}$ contains exactly one equilibrium, x^*, and that every point of $\mathcal{D}\backslash\{x^*\}$ can be approximated from above and from below in $\mathcal{D}$. Then,*

$$\omega(x) = x^*, \quad \forall x \in \mathcal{D}.$$

[225, Theorem 3.1, Section 2, Chapter 2]

Let (2.93) define a dynamical system on $\mathcal{D} \subset \mathbb{R}^n$. We consider the usual *partial order* on $\mathbb{R}^n$, that is, for $x, y \in \mathbb{R}^n$, we have $x \leq y$ if $y - x \in \mathbb{R}^n_+$, or equivalently

$$x \leq y \iff x_i \leq y_i, \quad \forall i = 1, \ldots, n.$$

It is common that the systems describing population dynamics are coupled via feedbacks between the compartments. For instance, for a system of the type (2.93), for $i, j = 1, \ldots, n$,

- if f_i is increasing with respect to x_j for $i \neq j$, then x_j is said to have has a positive feedback on x_i, while
- if f_i is decreasing with respect to x_j for $i \neq j$, then x_j is said to have has a negative feedback on x_i.

Definition 2.4.7. *System (2.93) is said to be cooperative if for every $i = 1, ..., n$, x_j has a positive feedback on x_i, $j = 1, ..., n$, $j \neq i$.*

Theorem 2.4.7. *If f is differentiable on D then the system (2.93) is cooperative if and only if*

$$\frac{\partial f_i}{\partial x_j}(x) \geq 0, \quad i \neq j, \quad x \in D. \tag{2.99}$$

Then the dynamical system (2.93) is monotone if and only if it is cooperative. More precisely, we have the following theorems.

Theorem 2.4.8. *Let (2.93) be a cooperative system and let $x(x_0, t)$ be a solution of (2.93)-(2.94) on $[0, T)$. If $y(t)$ is a differentiable function on $[0, T)$ satisfying*

$$\frac{dy}{dt} \leq f(y), \quad y(0) \leq x_0,$$

then

$$y(t) \leq x(x_0, t), \quad t \in [0, T).$$

[248, Theorem II, 12, II]

Theorem 2.4.9. *Let (2.93) be a cooperative system, and $a, b \in \mathcal{D}$. If $a \leq b$ and if for $t > 0$, $x(a, t)$ and $x(b, t)$ are defined, then $x(a, t) \leq x(b, t)$, $t > 0$.*

[225, Proposition 1.1, Section 1, Chapter 3]

In chapter 5 we use the monotonicity of a dynamical system to show the global asymptotic stability of the equilibria using Theorems 5.5.3 ([225, Prop. 1.1 p32]), 5.5.4 ([225, Thm. 3.1 p18], [6, Thm. 6]) and 5.5.5, which are consequences from Theorems 2.4.5, 2.4.8 and 2.4.9.

2.5 Numerical methods for differential equations

2.5.1 Introduction

In this section we first discuss the numerical methods used to approximate the solutions of the models formulated in chapters 3, 4 and 5 on a discrete domain. In chapters 3 and 4, the models are defined via PDEs, and the solutions are approximated via the Method of Lines. That is, the problem is first discretized with respect to the space variable which reduces the problem to a system of ODEs. This system can then be solved at discrete time steps using standard methods for ODEs. In particular, the model of chapter 3 consists of a singe equation. The space is discretized using the finite difference approach. We approximated the classical solution of the problem and this requires approximations of the first and second derivatives of the solution with respect to the space variable. Those approximations are derived using Taylor's expansion. In chapter 4, the model consists of a system of PDEs. The space is discretized via the finite element approach. Thus we consider the variational formulation of the problem and approximate the weak solution of the problem. Each equation of the system is approximated and solved independently one after the other at each time step. Once discretized with respect to the space variable, the models of chapters 3 and 4 are reduced to systems of ODEs.

Systems of ODEs can then be solved using a standard method, such as a θ-scheme (chapter 3 and 4) or trapezoidal rule and second order backward differences (chapter 5) [136], a non-standard scheme (chapter 4) [179], or considering an operator splitting approach (chapter 4) [136] to use the most appropriate method to solve specific parts of the system.

The numerical computations carried in chapters 3 and 4 are used to identify parameter values from simulated trapping data. This process consists in defining an objective function to minimize. The objective functions of chapters 3 and 4 are minimized using respectively the Gauss-Newton line search algorithm, performed with the Matlab built-in function **fminunc**, and the Levenberg-Marquardt algorithm performed using the Matlab built-in function **lsqr-solve**. Details on the parameter identification processes are not details in this section. The reader is invited to refer to the chapters in question for details on the parameter estimation processes.

In the following we first introduce the method of lines with some basic requirements on numerical schemes. Then, we present the finite difference method as well as the finite element method used for the space discretization of the models of chapters 3 and 4, respectively.

2.5.2 The Method of Lines and basic concepts

It is usually not possible to find an explicit formulation for the solution of continuous problems formulated by PDEs. In such cases, we approximate the continuous problem by a discrete problem for which the solution can be computed numerically. In other words, if $u(t,x), t \in [0,T], x \in \Omega \subset \mathbb{R}^n$ is the solution of a PDE problem, we compute approximations of $u(t,x)$ at specific values of $t \in \{t_0, t_1, \ldots, t_K\} \subset [0,T]$ and $x \in \{x_0, x_2, \ldots, x_{N+1}\} \subset \Omega$. Here we consider the method of lines (MOL) approach which consists in discretizing the problem first with respect to the space variable in order to reduce the problem to a system of ODEs continuous in time.

Consider a general parabolic problem of the form

$$\mathcal{P}(u) := \frac{\partial u}{\partial t}(t,x) - \mathcal{L}u(t,x) - f(x) = 0, \quad t \in [0,T], x \in \mathbb{R}^n, \tag{2.100}$$

where $\mathcal{L}$ is a differential operator in x defined as

$$\mathcal{L}u = d(x)\nabla^2 u(t,x) + a(x)\nabla(t,x) + c(x)u(t,x). \tag{2.101}$$

After discretising the spatial derivative in (2.100) we obtain a system of ODEs of the form

$$P(\mathbf{u}) := \frac{d\mathbf{u}}{dt} - \mathbf{L}\mathbf{u} - \mathbf{f} = 0 \tag{2.102}$$

where $\mathbf{u}(t) \in \mathbb{R}^{N+2}$ and $\mathbf{L}$ is a $(N+2) \times (N+2)$ matrix. Then an approximation in time of the solution to system (2.102) can be constructed using the method of approximation of ODEs of our choice.

Let us recall some important properties required for numerical methods to approximate the solutions of differential equations. The first requirement is that the method must be *consistent* (Focus 4). The consistency is related to the quality of the numerical method regardless on the choice of the discretisation on the values of the independent variables.

Focus 4 (Consistency).

Let Φ be the exact solution to (2.100), i.e. $\mathcal{P}(\Phi) = 0$, and let ϕ be the exact solution to (2.102), i.e. $P(\phi) = 0$. Let ψ be any continuous function of (t, x) with a sufficient number of contious derivatives such that $\mathcal{L}(\psi)$ can be evaluated at the points $(t_k, x_i)_{k=0,\dots,K, i=0,\dots,N+1}$. The *truncation error* at the grid point $\psi_{k,i} = \psi(t_k, x_i)$ is defined by

$$T_{k,i}(\psi) = P(\psi_{i,k}) - \mathcal{P}(\psi_{i,k}). \tag{2.103}$$

If we set $\psi = \Phi$, then

$$\tau_{k,i} := T_{k,i}(\Phi) = P(\Phi_{i,k}) \tag{2.104}$$

is called the *local truncation error* at the point (t_k, x_i). If

$$T_{k,i}(\psi) \longrightarrow 0 \quad \text{as } \Delta t \to 0 \text{ and } h \to 0$$

then the numerical method is said to be *consistent* with the differential equation $\mathcal{P}(\Phi) = 0$ [95].

Further, the method must be *convergent* (Focus 5). That is, as the step size of the discretized values of the independent variables approach 0, then the solution of the numerical scheme must converge to the solution of the differential equation.

Focus 5 (Convergence).

Let Φ be the exact solution of (2.100) with independent variables t and x, and let ϕ be the exact solution of (2.102). Denote $\boldsymbol{\phi}_k$ the the component of $\phi_{k,i}$ at a particular time step t_k. Define the discretisation error as

$$\mathbf{e}_k = \boldsymbol{\phi}_k - \boldsymbol{\Phi}_k \tag{2.105}$$

The numerical method P is said to be convergent when

$$\lim_{h \to 0} \left(\max_{k=0,\dots,K} \|\mathbf{e}_k\|_h \right) = 0, \tag{2.106}$$

where the norm $\|\cdot\|_h$ is defined as $\|u\|_h = \left(h \sum_{k=0}^{K} |u_k|^2 \right)^{1/2}$ [95].

Finally, the method must be *stable* (Focus 6). Stability is typically defined in terms of

boundedness of the numerical solution as $T \to \infty$ and prevents propagation of errors or blow up of the solution, due to rounding errors on the data [95].

Focus 6 (Stability)**.**

Let $\boldsymbol{\phi}_k$ as defined in Focus 5. A method is stable if for any $T > 0$, there exist a constant which depends on T, $C_T > 0$, such that

$$\|\boldsymbol{\phi}_k\|_h \leq C_T, \quad k = 0, \ldots, K, \quad \text{and} \quad h \to 0, \quad \Delta t \to 0.$$

$$\boldsymbol{\phi}_{k+1} = A\boldsymbol{\phi}_k + \mathbf{d}.$$

Lax defines the difference scheme as stable if there exist a positive constant M such that

$$\|A^k\| \leq M, \quad k = 0, \ldots, K. \tag{2.107}$$

Condition (2.107) is satisfied as long as $\|A\| \leq 1$. Then if we denote the spectral radius of A by $\rho(A)$, it follows that $\rho(A) \leq 1$.

If the numerical method is consistent, then the convergence can be obtained via the Lax equivalence theorem also referred to as the Lax-Richtmeyer theorem [95, 205, 235].

Theorem 2.5.1 (Lax equivalence theorem)**.** *If a linear finite difference equation is consistent with a properly posed linear initial-values problem then stability is necessary and sufficient for convergence of ϕ to Φ as the mesh size lengths tend to zero [95, 235].*

For the discretization in space, two approaches are considered here: the finite difference method and the finite element method, discussed below.

2.5.3 Finite difference method

The principle of the finite difference method is to approximate the the differential operator $\mathcal{L}$ in (2.100) by replacing its derivatives using differential quotients. Here we assume that the space is discretized in a regular grid with constant step size Δx. The PDEs model presented in Chapters 3 involves the differential operators ∇u and $\nabla^2 u$ where $u = u(t, x, y)$ with $t \in [0, T]$, and $(x, y) \in \mathbb{R}^2$. Recall that

$$\nabla u(t, x, y) = \frac{\partial u}{\partial x} + \frac{\partial u}{\partial y}, \quad \text{and} \quad \nabla^2 u(t, x, y) = \frac{\partial^2 u}{\partial x^2} + \frac{\partial^2 u}{\partial y^2}.$$

The finite difference method aims to find an approximated solution to the classical PDE problem. By construction, the PDE problem is reduced to a linear system of the form (2.102)

easier to solve. In order to obtain approximations, we use Taylor series expansions. The FD method is relatively simple to implement which is one of its main advantages, however, it is limited to simple geometries.

2.5.3.1 Approximation of the 1st and 2nd space derivatives

Let $u(t,x)$ be a function of time and space. Let Δx be the space step size. We have

$$\frac{\partial u}{\partial x} = \lim_{\Delta x \to 0} \frac{u(t,x+\Delta x) - u(t,x)}{\Delta x}.$$

For small Δx, a Taylor's expansion in the neighbourhood of x is defined as

$$u(t,x+\Delta x) = \sum_{k=0}^{\infty} \frac{\Delta x^k}{k!} \frac{\partial^k u}{\partial x^k}$$

By truncating the series at order n yields

$$u(t,x+\Delta x) = u(t,x) + \Delta x \frac{\partial u}{\partial x} + \frac{\Delta x^2}{2} \frac{\partial^2 u}{\partial x^2} + ... + \frac{\Delta x^n}{n!} \frac{\partial^n u}{\partial x^n} + \mathcal{O}(\Delta x^{n+1}) \tag{2.108}$$

where $\mathcal{O}(\Delta x^{n+1})$ is the *truncation error* and $n+1$ is the order of the method.

Given the Taylor series at order n, a *forward difference* approximation of the 1st derivative $\frac{\partial u}{\partial x}$ can be obtain using (2.108) for $n = 1$:

$$u(t,x+\Delta x) = u(t,x) + \Delta x \frac{\partial u}{\partial x} + \mathcal{O}(\Delta x^2) \tag{2.109}$$

where $\mathcal{O}(\Delta x^2)$ indicates that the error of the approximation is proportional to Δx^2 with

$$\frac{\partial u}{\partial x} \approx \frac{u(t,x+\Delta x) - u(t,x)}{\Delta x}. \tag{2.110}$$

Further, there exist a constant $C > 0$, such that for $\Delta x > 0$ sufficiently small we have

$$\left| \frac{u(t,x+\Delta x) - u(t,x)}{\Delta x} - \frac{\partial u}{\partial x} \right| \leq C \Delta x; \quad C = \sup_{y \in [x, x+\Delta x]} \frac{\left| \frac{\partial^2 u}{\partial x^2} \right|}{2}. \tag{2.111}$$

replacing $\frac{\partial u}{\partial x}$ by $\frac{u(t,x+\Delta x)-u(t,x)}{\Delta x}$ yields an error of order Δx and it is said that the approximation is consistent at the 1st order.

Similarly, a *backward difference* approximation can be obtained by considering

$$u(t,x-\Delta x) = u(t,x) - \Delta x \frac{\partial u}{\partial x} + \mathcal{O}(\Delta x^2). \tag{2.112}$$

To improve the approximation, other schemes can be considered. For instance, we can obtain a second order consistent approximation with the *central difference* scheme which considers both (2.109) and (2.109). By substracting these two expression we obtain

$$\frac{\partial u}{\partial x} \approx \frac{u(t, x + \Delta x) - u(t, x - \Delta x)}{2\Delta x} \tag{2.113}$$

To obtain an approximation of the 2nd order derivative, we consider the forward and backward difference approximations using Taylor's expansion up to the fourth order. We obtain

$$u(t, x + \Delta x) = u(t, x) + \Delta x \frac{\partial u}{\partial x} + \frac{\Delta x^2}{2}\frac{\partial^2 u}{\partial x^2} + \frac{\Delta x^3}{6}\frac{\partial^3 u}{\partial x^3} + \mathcal{O}(\Delta x^4) \tag{2.114}$$

$$u(t, x - \Delta x) = u(t, x) - \Delta x \frac{\partial u}{\partial x} + \frac{\Delta x^2}{2}\frac{\partial^2 u}{\partial x^2} - \frac{\Delta x^3}{6}\frac{\partial^3 u}{\partial x^3} + \mathcal{O}(\Delta x^4). \tag{2.115}$$

Adding the two approximations yields

$$\frac{\partial^2 u}{\partial x^2} \approx \frac{u(t, x + \Delta x) - 2u(t, x) + u(t, x - \Delta x)}{\Delta x^2}. \tag{2.116}$$

Lemma 2.5.1. *Suppose u is a $\mathcal{C}^4$ continuous function on an interval $[x - h_0, x + h_0]$, $h_0 > 0$. Then there is a constant $C > 0$ such that $\forall h \in]0, h_0[$ we have:*

$$\left| \frac{u(t, x + h) - 2u(t, x) + u(t, x - h)}{h^2} - \frac{\partial^2 u}{\partial x^2} \right| < Ch^2, \quad C = \sup_{y \in [x - h_0, x + h_0]} \frac{\left| \frac{\partial^4 u(y)}{\partial x^4} \right|}{12} \tag{2.117}$$

The differential quotient

$$\frac{u(t, x + h) - 2u(t, x) + u(t, x - h)}{h^2}$$

is a consistent second-order approximation of the second derivative of u at the point x.

2.5.3.2 The finite difference scheme

For sake of simplicity we consider a square domain $\Omega = [\alpha, \beta] \times [\alpha, \beta]$ with boundary Γ. We also assume that $\Delta x = \Delta y = h = 1/(n + 1)$ and we set

$$\begin{array}{llllll} x_0 = \alpha, & x_1 = x_0 + h, & \ldots & x_i = x_{i-1} + h, & \ldots & x_{n+1} = x_n + h = \beta \\ y_0 = \alpha, & y_1 = y_0 + h, & \ldots & y_j = y_{j-1} + h, & \ldots & y_{n+1} = y_n + h = \beta \end{array}$$

for $i, j = 0, 1, \ldots, n, n + 1$. This yields a total of $(n + 2) \times (n + 2)$ grid points at which we want to approximate the solution of (2.100).

Let $u_{i,j} = u(\cdot, x_i, y_j)$ for $i, j = 0, 1, \ldots, n, n+1$.We have

$$\nabla u(\cdot, x_i, y_j) \approx \frac{u_{i+1,j} - u_{i-1,j}}{2h} + \frac{u_{i,j+1} - u_{i,j-1}}{2h} \tag{2.118}$$

$$\nabla^2 u(\cdot, x_i, y_j) \approx \frac{u_{i-1,j} - 2u_{i,j} + u_{i+1,j}}{h^2} + \frac{u_{i,j-1} - 2u_{i,j} + u_{i,j+1}}{h^2} \tag{2.119}$$

The differential operator $\mathcal{L}$ at a generic point (x_i, y_j), $i, j = 1, \ldots, n$, in the interior of the domain Ω is written as

$$\begin{aligned} \mathcal{L}u(x_i, y_i) \approx\ & d(x_i, y_j)\left(\frac{u_{i-1,j} - 2u_{i,j} + u_{i+1,j}}{h^2} + \frac{u_{i,j-1} - 2u_{i,j} + u_{i,j+1}}{h^2}\right) \\ & + a(x_i, y_j)\left(\frac{u_{i+1,j} - u_{i-1,j}}{2h} + \frac{u_{i,j+1} - u_{i,j-1}}{2h}\right) \qquad (2.120) \\ & + c(x_i, y_j)u_{i,j} \end{aligned}$$

(2.121)

Rearranging the terms, we have

$$\begin{aligned} \mathcal{L}u(x_i, y_i) \approx\ & u_{i-1,j}\left(\frac{d_{i,j}}{h^2} - \frac{a_{i,j}}{2h}\right) + u_{i,j-1}\left(\frac{d_{i,j}}{h^2} - \frac{a_{i,j}}{2h}\right) + u_{i,j}\left(c_{i,j} - 4\frac{d_{i,j}}{h^2}\right) \\ & + u_{i+1,j}\left(\frac{d_{i,j}}{h^2} + \frac{a_{i,j}}{2h}\right) + u_{i,j+1}\left(\frac{d_{i,j}}{h^2} + \frac{a_{i,j}}{2h}\right). \end{aligned}$$

On the boundary, the homogeneous Neumann condition yields:

$$\begin{aligned} \text{for } i = 0, j = 0, \ldots, n+1, \quad \vec{\nabla} u(x_0, y_j) \cdot \vec{n} &= \left(\frac{u_{1,j} - u_{-1,j}}{2h}; \frac{u_{0,j+1} - u_{0,j-1}}{2h}\right) \cdot (-1; 0)^t \\ &= -\frac{u_{1,j} - u_{-1,j}}{2h} \\ &= 0 \end{aligned}$$

therefore, the term $u_{-1,j}$ can be substituted by $2h + u_{1,j}$.

Similarly,

for $i = n+1, j = 0, \ldots, n+1$, the term $u_{n-2,j}$ can be substituted by $2h + u_{n,j}$

for $i = 0, \ldots, n+1, j = 0$, the term $u_{i,-1}$ can be substituted by $2h + u_{i,1}$

for $i = 0, \ldots, n+1, j =, n+1$, the term $u_{i,n-2}$ can be substituted by $2h + u_{i,n}$

Therefore,

$$\mathcal{L}u + f \approx \mathbf{Lu} + \mathbf{f} \tag{2.122}$$

where $\mathbf{L}$ is a $(n+2)^2 \times (n+2)^2$ block tridiagonal real matrix, and $\mathbf{u}$ and $\mathbf{f}$ are $(n+2)^2 \times 1$ real vectors:

$$\mathbf{u} = \begin{bmatrix} u_{0,0} \\ u_{2,0} \\ \vdots \\ u_{n+1,0} \\ u_{0,1} \\ u_{1,1} \\ \vdots \\ u_{n+1,1} \\ \vdots \\ u_{n+1,n+1} \end{bmatrix}, \quad \text{and} \quad \mathbf{f} = \begin{bmatrix} f(x_0, y_0) \\ f(x_2, y_0) \\ \vdots \\ f(x_{n+1}, y_0) \\ f(x_0, y_1) \\ f(x_1, y_1) \\ \vdots \\ f(x_{n+1}, y_1) \\ \vdots \\ f(x_{n+1}, y_{n+1}) \end{bmatrix}$$

Thus, we approximate problem (2.100) by problem (2.102).

Note that in the case of Dirichlet boundary conditions, the values of u on the boundary is known, therefore it needs not be approximated. In this case, problem (2.102) can be considered only on the interior points of the domain, that is, on $n \times n$ grid points. Then, whenever a value of the boundary is involved in the discretisation schemes, it can be substituted by the value imposed by the Dirichlet condition.

Once the space-discretization done via the finite difference method, the problem is reduced to the following initial value ODEs system:

$$\frac{d\mathbf{u}}{dt} = \mathbf{L}\mathbf{u} + \mathbf{f} \tag{2.123}$$

2.5.4 Finite element method

The FEM finds its first applications in the field of mechanics in the 1950's as it allows to work with complex geometries of the domain. The method consists in approximating a problem in its variational form defined on an infinite space by a problem defined on a finite sub-space. The solution of the continuous problem is approximated by a function determined by a finite number of parameters such as the value of the solution at specific points on the mesh. More precisely, the domain is discretized in elements that can be more or less refined depending on the complexity of the domain and the expected stiffness of the solution. The solution is approximated element-wise and then assembled to produce an approximation over the whole domain. Further, the FEM facilitates the implementation of the boundary conditions as they are taken into account in the spaces of approximation of the solution.

However, computing element-wise solutions require to compute integrals over each element which makes the implementation of the FEM complex and computationally intensive. We recall here some of the essential theory needed for the application of the FEM discussed in chapter 4. We follow mainly [96, 35, 94].

2.5.4.1 The Galerkin method

The Galerkin method consists in converting a continuous operator problem into a discrete problem. To do so, we consider the problem in its weak form. The aim is to build a weak solution by constructing solutions on a finite-dimentional space and then passing to limits. The functional space V denotes either the space $H^1(\Omega)$ if Neumann boundary conditions are considered or $H_0^1(\Omega)$ if homogeneous boundary conditions are considered.

The problem in its variational form consists of seeking $\mathbf{u} \in \mathcal{W}(V, V')$, such that

$$\left(\frac{d\mathbf{u}}{dt}, v\right) + B(\mathbf{u}, v, t) = (\mathbf{f}, v)\,; \quad \mathbf{u}(0) = u_0, \tag{2.124}$$

for all $v \in V$, where $(\cdot, \cdot)$ denotes the scalar product in $L^2(\Omega)$.

A discrete problem is constructed by replacing the space V by a finite dimensional space $V_m = \{V_1, V_2, \dots V_m\}$ Then we seek solutions $\mathbf{u}_m : [0, T] \to V$ of the form

$$\mathbf{u}_m(t) = \sum_{k=1}^{m} \alpha_m^k(t) v_k \tag{2.125}$$

where the coefficient $\alpha_m^k(t)$ are such that

$$\alpha_m^k(0) = (u_0, v_k)\,, \quad k = 1, \dots, m \tag{2.126}$$

and

$$\left(\frac{d\mathbf{u}_m}{dt}, v_k\right) + B(\mathbf{u}_m, v_k, t) = (\mathbf{f}, v_k) \tag{2.127}$$

Problem (2.127) is in fact the projection of problem (2.124) onto the finite-dimensional V_m.

The existence of $\mathbf{u}_m$, solution of (2.126)-(2.127) is ensured by the following theorem.

Theorem 2.5.2 (Existence and uniqueness of an approximate solution)**.** *For each $m = 1, 2, \dots,$ there exist a unique function $\boldsymbol{u}_m$ of the form*

$$\boldsymbol{u}_m(t) = \sum_{k=1}^{m} \alpha_m^k(t) v_k, \tag{2.128}$$

which satisfies (2.126) and (2.127) [96].

The following energy estimate holds for the approximation of the solution u_m.

Theorem 2.5.3. *There is a constant C depending on the domain Ω, T and the coefficients of the linear operator L such that*

$$\max_{0\leq t\leq T}\|\boldsymbol{u}_m(t)\|_{L^2(\Omega)}+\|\boldsymbol{u}_m\|_{L^2(0,T;V)}+\|\frac{d\boldsymbol{u}_m}{dt}\|_{L^2(0,T;V^{-1})}\leq C\left(\|\boldsymbol{f}\|_{L^2(0,T;L^2(\Omega))}+\|u_0\|_{L^2(\Omega)}\right). \tag{2.129}$$

Using the estimate in Theorem 2.5.3 one can show that the sequence $(\mathbf{u}_m)$ has a convergent subsequence with limit satisfying (2.127). This is an alternative to the method of Lions presented in Section 2.3.3 to show existence and uniqueness of the weak solution of problem (2.127) [96, Theorems 3 and 4, Section 7.1].

2.5.4.2 The Finite Elements

We now define a finite element following the definition of Ciarlet [55, 35].

Definition 2.5.1. *Let*

*(i) $K\subseteq\mathbb{R}^n$ be a bounded closed set with nonempty interior and piecewise smooth boundary (the **element domain**),*

*(ii) $\mathcal{P}$ be a finite-dimensional space of functions on K (the space of **shape functions**) and*

*(iii) $\mathcal{N}=\{N_1,N_2,\ldots,N_k\}$ be a basis for $\mathcal{P}'$ (the set of **nodal variables**).*

*Then, $(K,\mathcal{P},\mathcal{N})$ is called a **finite element**.*

Definition 2.5.2. *Let $(K,\mathcal{P},\mathcal{N})$ be a finite element. The basis $\{\phi_1,\phi_2,\ldots,\phi_k\}$ of $\mathcal{P}$ dual to $\mathcal{N}$ (i.e. $n_i(\phi_j)=\delta_{i,j}$) is called the **nodal basis** of mathcal$P$.*

Consider the approximate problem

$$\begin{cases}\text{Seek } u_h\in\mathcal{C}^1([0,T];V_h) \text{ such that}\\[2ex] (\frac{d}{dt}u_h,v)_{L^2(\Omega)}+B(t,u_h,v_h)=(f,v_h)_{L^2(\Omega)},\quad \forall t\in[0,T],\forall v_h\in V_h,\\[2ex] u_h(0)=u_{0h},\end{cases} \tag{2.130}$$

where $u_{0h}\in V_h$ is an approximation of u_0. Problem (2.130) defines a system of coupled ODEs for which existence and uniqueness of the solution is guaranteed by the Cauchy-Lipschitz Theorem.

We introduce the operator $P_{ht} \in \mathcal{L}(V, V_h)$ defined for $t \in [0,T]$ and such that, for all $w \in V$, $P_{ht}(w)$ is a solution to

$$\forall v_h \in V_h, \quad B(t, P_{ht}(w), v_h) = B(t, w, v_h). \tag{2.131}$$

The operator P_{ht} is a projection. Moreover, when the bilinear form B is the Laplace operator, then P_{ht} is called the elliptic projector. We make the following hypothesis:

$$(EP) \begin{cases} \text{There is } c > 0 \text{ such that, for all } w \in \mathcal{C}^1([0,T];W), \text{ and } \forall j \in \{0,1\}, \\ \\ \|w - P_{ht}(w)\|_{\mathcal{C}^j([0,T],L^2(\Omega))} + h\|w - P_{ht}(w)\|_{\mathcal{C}^j([0,T],V)} \leq ch^{k+1}\|w\|_{\mathcal{C}^1([0,T],W)} \end{cases}$$

Theorem 2.5.4. *Assume that (EP) holds and that $u \in \mathcal{C}^1([0,T],W)$. Then for all h,*

$$\frac{1}{\sqrt{T}}\|u-u_h\|_{L^2([0,T];V)} \leq \frac{1}{\sqrt{\alpha T}}\|u_0-u_{0h}\|_{L^2(\Omega)}+c\left(1+\frac{1}{\sqrt{T}}+\frac{1}{\alpha\sqrt{c_P}}\right)h^k\|u\|_{\mathcal{C}^1([0,T];W)} \tag{2.132}$$

2.5.4.3 Application to the problem of Chapter 4

In chapter 4, we consider triangular elements. More precisely, the domain Ω is subdivided in triangles such that no vertex of any triangle lies in the interior of an edge of another triangle, and such that the collection of triangles $\{K_i\} \in \mathbb{R}^2$ satisfy

$$\text{int}K_i \cap \text{int}K_j = \emptyset, \text{ if } i \neq j, \quad \text{and} \quad \bar{\Omega} = \bigcup_{K_i \in \mathcal{T}} K_i.$$

Such subdivision is called a *triangulation*. We denote by $\mathcal{T}(\Omega)$ such a triangulation on Ω. We do not extend on construction of the triangulation here, however it is worth mentioning software such as GMSH [105] or Freefem [124] can be used to generate such mesh satisfying specific geometrical specifications (number of vertices, size of the elements, etc.).

Further, here we consider linear Lagrange elements. More precisely, we have the space of shape functions $\mathcal{P}_1$, the set of all polynomial of degree ≤ 1,

$$\mathcal{P} = \mathcal{P}_1 = \{v \in \mathcal{C}^0(\Omega) : v|_K \in \mathbb{P}_1, K \in \mathcal{T}(\Omega)\}, \tag{2.133}$$

and the set of nodal variables $\mathcal{N}_1 = \{N_1, N_2, N_3\}$. Here, the nodal variables are evaluated at the vertices of the K. We denote bu N_v the total number of nodes of $\mathcal{T}(\Omega)$. Further, we consider ψ_i, $i = 1, \ldots, N_v$, piecewise linear functions of order, equal to 1 at the node i and 0 at all other nodes. A representation of the function ψ_i is given in Figure 2.1. For $i = 1, \ldots, N_v$, the functions ψ_i are linearly independent and form a basis for the space of continuous piecewise linear functions Ω: where $\mathbb{P}_1$ denotes the set of linear polynomials. In

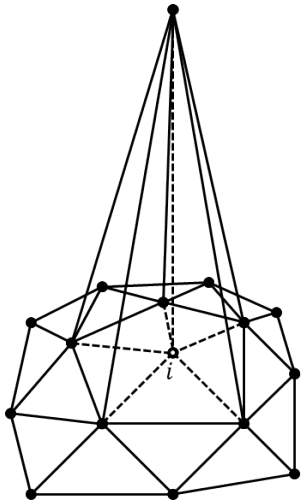

Figure 2.1: Representation of the piecewise linear function ψ_i.

particular, in the case of homogeneous Dirichlet conditions on the boundary of the domain Γ, we define the space of shape functions

$$\mathcal{P}_{1,0} = \{v \in P_1 : v|_\Gamma = 0\}. \tag{2.134}$$

We seek for an approximation $\tilde{u} \in \mathcal{P}_1$ (or $\tilde{u} \in \mathcal{P}_{1,0}$ depending on the boundary conditions) of the solution of problem (2.124), u, in the form

$$\tilde{u} = \sum_{i=1}^{N_v} u_i \psi_i(x) \tag{2.135}$$

where u_i is the value of u at the position of the node i. In terms of the notations of Theorem 2.132, we have $k = 1$. We take u_{0h} to be the interpolant of u_0. Then it follows from Theorem 2.132 that the L^2-error of the approximated solution is $\mathcal{O}(h)$. The functions ψ_i, $i + 1, \ldots, N_v$ are called *global shape functions*. In terms of implementation of the finite element method a system to compute an approximation of the solution of problem (2.124) on each element is build. The element-wise systems are then assembled to built the system over the whole domain. We denote by $\tilde{u}_K$ the restriction of $\tilde{u}$ to the element $K \in \mathcal{T}(\Omega)$.

$$\tilde{u}_K = \tilde{u}|_K = \sum_{i=1}^{3} u_i|_K \phi_i^K(x) \tag{2.136}$$

where, for $i = 1, 2, 3$, the functions $\phi_i^K(x)$ are linearly independent linear polynomials equal to 1 at the node i, and 0 at the two other nodes. Substituting in (2.124), yields a linear elementary system,

$$\boldsymbol{M}_K \dot{U}_K + \boldsymbol{A}_K U_K = F_K. \tag{2.137}$$

where $U_K = (u_1|_K, u_2|_K, u_3|_K)^T$, $\dot{U}_K = (\dot{u}_1|_K, \dot{u}_2|_K, \dot{u}_3|_K)^T$, with $\dot{u}_{K_j} = \dfrac{\partial u}{\partial t}|_K$.

To carry the computations, we consider a *reference element*, $\hat{K}$, on which *local shape functions* are defined. This implies that a linear transformation to pass from any element K to the reference element $\hat{K}$ needs to be defined. For more details on this step, the reader may refer to Focus 7. Also note that to compute the coefficients of the matrices $\mathbf{M}_K$, $\mathbf{A}_K$ and vector F_K, numerical integration methods are required. For the application of Chapter 4, numerical integration is done using Hammer weighted quadrature rule of the third degree of precision [101, Apendix C].

Focus 7.

Denote by $\boldsymbol{x}_1^K = (x_1^K, y_1^K)$, $\boldsymbol{x}_2^K = (x_2^K, y_2^K)$ and $\boldsymbol{x}_3^K = (x_3^K, y_3^K)$ the coordinates of the nodes of element K. Assume that the reference element $\hat{K}$ is defined in the system of coordinates $\boldsymbol{\xi} = (\xi, \eta)$. Then for each node $\boldsymbol{x}_i^K$ of K, there is a corresponding node $\boldsymbol{\xi}_i^k$ of $\hat{K}$. We denote by T^K the transformation from $\hat{K}$ to K which satisfies

$$T^K(\boldsymbol{\xi}_i^K) = \boldsymbol{x}_i^K, \quad i = 1, 2, 3, \tag{2.138}$$

or inversely

$$(T^K)^{-1}(\boldsymbol{x}_i^K) = \boldsymbol{\xi}_i^K, \quad i = 1, 2, 3, \tag{2.139}$$

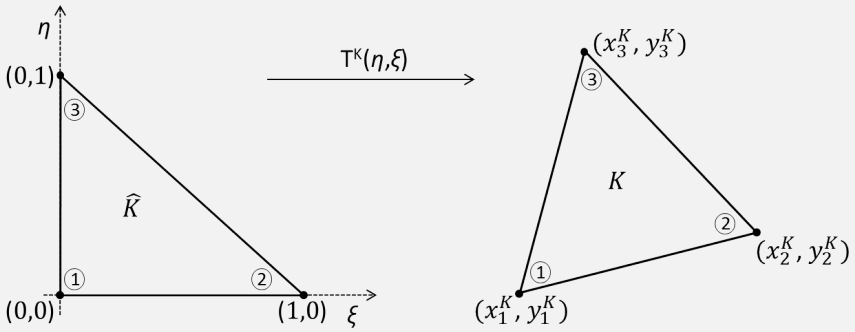

Linear transformation on a triangular element.

We define the linear local shape functions on $\hat{K}$ as follows:

$$\hat{\phi}_1(\boldsymbol{\xi}) = 1 - \xi - \eta, \quad \hat{\phi}_2(\boldsymbol{\xi}) = \xi, \quad \hat{\phi}_3(\boldsymbol{\xi}) = \eta. \tag{2.140}$$

Thus, for $i, j = 1, 2, 3$, $\hat{\phi}_i(\boldsymbol{\xi}_j)$ satisfies

$$\hat{\phi}_i(\boldsymbol{\xi}_j) = \delta_i^j = \begin{cases} 1 & \text{if } i = j, \\ 0 & \text{otherwise.} \end{cases} \tag{2.141}$$

The transformation $T^K : \hat{K} \longrightarrow K$ can be written is the form:

$$\begin{bmatrix} x, y \end{bmatrix} = T^k(\boldsymbol{\xi}) = \sum_{i=1}^{3} \hat{\phi}_i(\boldsymbol{\xi}) \begin{bmatrix} x_i^k \\ y_i^k \end{bmatrix} = \begin{bmatrix} (1-\xi-\eta)x_1^K + \xi x_2^K + \eta x_3^K \\ (1-\xi-\eta)y_1^K + \xi y_2^K + \eta y_3^K \end{bmatrix} \tag{2.142}$$

Once the elementary systems are defined, they are assembled to form a linear system on the entire discretized domain $\mathcal{T}(\Omega)$. This leads to a sparse system of equations of the form

$$\boldsymbol{M}\dot{U} + \boldsymbol{A}U = F, \tag{2.143}$$

where U, $\dot{U}$ and F are real column vectors of size N_v and where $\boldsymbol{M}$ and $\boldsymbol{A}$ are real $(N_v \times N_v)$ matrices. System (2.143) can be solved using ODE solvers.

2.6 The time discretization

Several approaches can be considered to approximate the solution of the problem in time. Here we briefly introduce the methods used in chapters 3, 4 and 5 of this thesis. Once the space-discretization is done via the finite difference method, the problem is reduced to the following initial value ODEs system:

$$\frac{d\mathbf{u}}{dt} = F(t, \mathbf{u}); \quad \mathbf{u}(0) = \mathbf{u}_0. \tag{2.144}$$

We compute approximations of the solution $\mathbf{u}(t), t \in [0, T]$, at discrete time steps $\{t_0, t_1, \ldots, t_K\} \in [0, T]$ with the time step $\Delta t > 0$ such that for all $k + 0, \ldots, K$, $t_k = k\Delta t$. Denote $\mathbf{u}^k$ the approximation of the solution $\mathbf{u}(t_k)$. A standard way to approximate $\frac{d\mathbf{u}}{dt}$ is using finite differences at each time step:

$$\frac{du}{dt} \approx \frac{u^{k+1} - u^k}{\Delta t}. \tag{2.145}$$

However, other approximations can be considered as for the non-standard methods as shown below. The Foci 8 to 11 provide a brief description of the methods used in the different chapters of this thesis.

Focus 8 (The θ-method)**.**

The θ-method is written as:

$$\mathbf{u}^{k+1} = \mathbf{u}^k + \Delta t \left(\theta F(t^k, \mathbf{u}^k) + (1 - \theta) F(t^{k+1}, \mathbf{u}^{k+1})\right), \tag{2.146}$$

where θ is a parameter with values in the interval $[0, 1]$. The θ-method is a one-step method which is implicit whenever $\theta \in [0, 1)$, and explicit when $\theta = 1$.

- When $\theta = 1$, (2.146) is the Euler's method and it is 1^{st} order in time.
- When $\theta = 0$, (2.146) is the Backward Euler's method and it is 1^{st} order in time.
- When $\theta = 1/2$, (2.146) is the Crank-Nicolson method or Trapezoidal Rule (TR), and it is 2^{nd} order in time.

Focus 9 (The TR-BDF2 method)**.**

The Trapezoidal Rule and second-order Backward Finite Difference (TR-BDF2) method [12, 134] is a composite method using the trapezoidal rule (Focus 8) followed by the second-order backward difference method.
Fist, the trapezoidal rule is applied on some interval to obtain an approximation of the solution at some intermediate time step $t^{k+\tau} = t^k + \tau\Delta t \in [t^k, t^{k+1}]$. Thus we compute $\mathbf{u}^{k+\tau}$ as follows:

$$\mathbf{u}^{k+\tau} = \mathbf{u}^k + \tau\frac{\Delta t}{2}\left(F(t^k, \mathbf{u}^k) + F(t^{k+\tau}, \mathbf{u}^{k+\tau})\right).$$

Then the second-order backward finite difference scheme is used to compute $\mathbf{u}^{k+1}$:

$$\mathbf{u}^{k+1} = \frac{1}{\tau(2-\tau)}\mathbf{u}^{k+\tau} - \frac{(1-\tau)^2}{\tau(2-\tau)}\mathbf{u}^k + \frac{1-\tau}{2-\tau}\Delta t F(t^{k+1}, \mathbf{u}^{k+1}).$$

The TR-BDF2 method is a one-step method of the 2^{nd} order in time.

Focus 10 (The Non-Standard method)**.**

The Non-Standard (NS) method [179, 180] aims to construct an exact numerical scheme to approximate the solution of an initial value problem formulated with differential equations. More precisely, the numerical approximation of the solution at the time step t^k is exactly the solution of the problem at the same time step:

$$\mathbf{u}^k = \mathbf{u}(t^k).$$

In the NS method the denominator Δt of the discrete time derivative is replace by a non-negative function $\Phi(\Delta t)$ such that $\Phi(\Delta t) = \Delta t + O(\Delta t^2)$ as Δt converges to 0. The choice of the function Φ is not unique and depends on the original problem. In particular, for the decay problem

$$\frac{du}{dt} = -\lambda u; \quad u(0) = u_0, \tag{2.147}$$

a NS scheme can written as

$$\frac{u^{k+1} - u^k}{\Phi(\Delta t)} = -\lambda u^k, \quad \text{with } \Phi(\Delta t) = \frac{1 - e^{-\lambda\Delta t}}{\lambda}. \tag{2.148}$$

Focus 11 (Splitting approach for an ADR problem)**.**

A semi-decretized ADR problem can be formulated as follows:

$$\frac{du}{dt} = \mathcal{A}(u) + \mathcal{D}(u) + \mathcal{R}(u),$$

where $\mathcal{A}$, $\mathcal{D}$ and $\mathcal{R}$ represent respectively the advection terms, the diffusion terms and the reaction terms. A basic splitting approach consists in solving successively each terms using the numerical method of our choice [136, 80]. For a time step $\Delta t > 0$, the splitting approach leads to the following algorithm:

1. solve $\frac{du_{\mathcal{A}}}{dt} = \mathcal{A}(u_{\mathcal{A}})$ with $u_{\mathcal{A}}(0) = u^k$ on $[0, \Delta t]$,
2. solve $\frac{du_{\mathcal{D}}}{dt} = \mathcal{D}(u_{\mathcal{D}})$ with $u_{\mathcal{D}}(0) = u_{\mathcal{A}}(\Delta t)$ on $[0, \Delta t]$,
3. solve $\frac{du_{\mathcal{R}}}{dt} = \mathcal{R}(u_{\mathcal{R}})$ with $u_{\mathcal{R}}(0) = u_{\mathcal{D}}(\Delta t)$,
4. set $u^{k+1} = u_{\mathcal{R}}(\Delta t)$.

Detailed description of the method and its analysis can be found in [156, 136].

While the ODE system of chapter 3 is solved via a standard method, using a Crank-Nicolson scheme (Focus 8 with $\theta = 1/2$), in chapter 4 we consider a splitting approach (Focus 11) where the advection and diffusion parts are solved simultaneously using a Crank-Nicolson scheme and the reaction is solved using a Non-Standard scheme (Focus 10). As for the model of chapter 5, it is defined via a system of ODEs solved using the built-in routine **ode23tb** of Matlab which solves systems of stiff ODEs using a TR-BDF2 scheme (Focus 9).

Chapter 3

Parameter identification in population models for insects using trap data

This work has appeared in

Claire Dufourd, Christopher Weldon, Roumen Anguelov, Yves Dumont, Parameter Identification in Population Models for Insects Using Trap Data, Biomath 2 (2013), 1312061, http://dx.doi.org/10.11145/j.biomath.2013.12.061

3.1 Abstract

Traps are used commonly to establish the presence and population density of pest insects. Deriving estimates of population density from trap data typically requires knowledge of the properties of the trap (e.g. active area, strength of attraction) as well as some properties of the population (e.g. diffusion rate). These parameters are seldom exactly known, and also tend to vary in time, (e.g. as a result of changing weather conditions, insect physiological condition). We propose using a set of traps in such a configuration that they trap insects at different rates. The properties of the traps and the characteristics of the population, including its density, are simultaneously estimated from the insects captured in these traps. The basic model is an advection-diffusion equation where the traps are represented via a suitable advection term defined by the active area of the traps. The values of the unknown parameters of the model are derived by solving an optimization problem. Numerical simulations demonstrate the accuracy and the robustness of this method of parameter identification.

3.2 Introduction

This work is motivated by the need to develop a reliable and efficient method for detecting the presence and estimating population density of the invasive fruit fly, *Bactrocera invadens* Drew, Tsuruta & White (Diptera: Tephritidae) in South Africa. *Bactrocera invadens* is a fruit fly species introduced from Asia to Africa where it was first described and recorded in Kenya in 2003 [78, 164]. In 2010, *B. invadens* was detected in the northern part of the Limpopo province in South Africa [167]. Its capacity for rapid population growth, high invasive potential [145], and wide range of fruit hosts [211] represents a major threat for all fruit industries in South Africa.

Fruit flies are a perennial problem in South Africa because in addition to *B. invadens* there are three endemic species that already represent economic pests. Fruit flies have historically been controlled in South Africa by the application of insecticide cover sprays. Current practice, however, involves the use of alternative control strategies due to regulation- and consumer-driven requirements for fruit to be free of insecticide residues. The primary techniques used in fruit fly control are the application of bait sprays [167], M3 bait stations [168], or the 'male annihilation technique' [167]. All three techniques work on the same principal: a food or sex attractant, which is fed on by adult flies, is mixed with an insecticide such as malathion or GF120. With regard to *B. invadens*, male annihilation technique has been applied to control incursions in South Africa [167]. Another control strategy for this pest may include mass-trapping, which uses male attractants to capture and kill males of a population, leading to reduced female mating and possibly causing local extinction of the population [90]. Alternatively, the Sterile Insect Technique (SIT) may represent a useful approach to control incursions of *B. invadens*. SIT involves the release of large numbers of sterilized males that compete with wild males for female fertilization, which leads to no production of viable offspring [155] and its success can be measured using the ratio of sterile: wild insects captured in and array of surveillance traps [146].

Regardless of the alternative control strategy used, their successful application requires a good knowledge of the distribution of the pest, and their dispersal capacity and density. The density of an insect population, however, is a parameter that cannot easily be obtained by direct field observations because traps usually sample only a small proportion of all individuals. To overcome this problem, it is often the case that captures of insects in traps are compared to simulated data [119]. An advection-diffusion equation is considered for modelling the dynamics of fruit flies, where density is the initial value of the model. Such a model requires knowledge of the properties of the trap such as the active area [41] and the strength of attraction, as well as some properties of the population, like its diffusion rate [195]. These parameters are seldom exactly known, and also tend to vary with changing weather [184] and

landscape heterogeneity [80],[79].

Determining the values of these parameters is actually an inverse problem, that is, given the solution of the model, or at least part of it, one or more of the model parameters can be identified. The parameter identification problem consists of finding a unique and robust estimation for the parameter values. This problem leads to solving a global optimization problem in order to find the set of parameters that minimizes an objective function. Mathematically, the existence and uniqueness of this global minimum relies on the well-posedness of the inverse problem, while its robustness relies on its well-conditionedness. However, inverse problems are typically ill-posed or conditioned, [157, 63, 193]. In this paper, we show that by using different settings of interfering traps we obtain a parameter identification problem which can be solved numerically in a reliable way. It is essential in this approach that interfering traps generate different incoming streams of insects. Thus, more information about the characteristics of the insect population is provided. Indeed, as the relationship between the setting and the traps is highly non linear and not well understood, several settings of traps are considered and the robustness of the estimates are compared. We demonstrate empirically that using this approach, the problem of simultaneously identifying a set of unknown parameters is well-posed and well-conditioned. The numerical procedure falls under the well-known trial-and-error method of regularization theory [236].

3.3 The Insect Trapping Model: The Direct Problem

The model is formulated on a domain $\Omega \subset \mathbb{R}^2$ which is assumed to be isolated, i.e. there is no immigration and no emigration of insects. It is also assumed that when there is no stimulus, the insects individually follow a random walk. Because insects are often in large abundance, we can apply a diffusion equation to model the dispersal of insects at population level [238]. The traps set on Ω are attractive. Thus, the active area of the trap [41] is the area where the concentration of the attractant is above the threshold of concentration at which the fruit flies can detect it. Therefore, in this area the insects will be influenced to move in a prefered direction towards the trap. This can be modelled using an advection equation [16]. Finally, we assume that our experiments take place over a short period of time, thus we may omit reaction terms.

Using the above assumptions, the insect dynamics can be modelled via an advection-diffusion.

$$\begin{aligned} &\tfrac{\partial u}{\partial t} - \nabla(s(x)\nabla u) + \nabla(a(x)u) = 0, \\ &\tfrac{\partial u}{\partial n}|_{\partial\Omega} = 0, \\ &u|_{t=0} = u_0. \end{aligned} \tag{3.1}$$

$u(t,x)$ denotes the population density at time t and at the point $x=(x_1,x_2)\in\Omega$.

The advection function $a(x)$ is space-dependent and determines the attractiveness of the trap with respect to the distance to the center of the trap. The traps are circular of radius R_{trap}. Assume that the active area of a trap is defined by a disk of radius R_{max} from the center of the trap. Then the insects that are beyond this disk are not subjected to advection and we assume that their dynamics are only governed by the diffusion term. As the insect gets closer to the trap, the force of attraction increases and reaches its maximum at a distance R_{min} from the center of the trap. If N is the number of traps distributed on the domain, then:

$$\begin{aligned} a(x) &= \sum_{T=1}^{N} a_T(x), \\ a_T(x) &= a_{max}\alpha(||x_T-x||)\tfrac{x_T-x}{||x_T-x||}, \end{aligned} \tag{3.2}$$

where x_T is the coordinate of trap T, and the function $\alpha(d)$ is defined for $d\in[0,+\infty)$, as follows.

$$\alpha(d)= \begin{cases} \sin\left(\frac{\pi d}{2R_{trap}}\right), & \text{if } d<R_{trap} \\ 1, & \text{if } R_{trap}\le d<R_{min} \\ \frac{1}{2}\left(\cos\left(\pi\frac{d-R_{min}}{R_{max}-R_{min}}\right)+1\right), & \text{if } R_{min}\le d<R_{max} \\ 0 & \text{if } R_{max}\le d \end{cases} \tag{3.3}$$

The function $\alpha(d)$ is represented in Fig. 3.1. Note that the value of the advection inside the trap does not really matter, and we make $\alpha(d)$ decrease to 0 from the distance R_{trap} to ensure the continuity of $a(x)$.

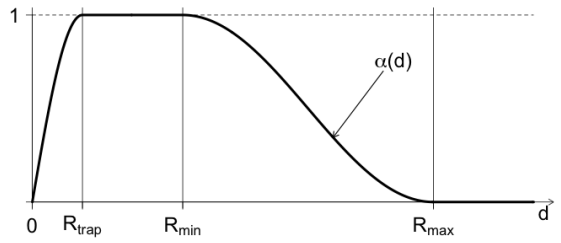

Figure 3.1: Graph of the function $\alpha(d)$

The diffusion coefficient $s(x)$ is also space-dependent. It is assumed to be constant, $s(x)=\sigma$, outside the active areas of the traps. Since the insects do not escape from the traps there should be no diffusion across the trap boundary. In order to ensure the existence and uniqueness of the (weak) solution of (3.1) we assume that inside a trap the function $s(x)$ has a positive value ε which is so small that the implied diffusion effect in the time interval of

observation can be neglected. In order to further ensure continuity of s we take

$$\begin{aligned} &s(x) = \sigma - \sum_{T=1}^{N} s_T(||x_T - x||), \\ &s_T(d) = \\ &\begin{cases} \sigma - \varepsilon, & \text{if } d \leq R_{trap} \\ (\sigma-\varepsilon)\Big(1 - \frac{d-R_{trap}}{R_{min}-R_{trap}}\Big)+\varepsilon, & \text{if } R_{trap}<d \leq R_{min} \\ 0, & \text{if } R_{min} < d. \end{cases} \end{aligned} \tag{3.4}$$

3.4 The Parameter Identification Problem

The trap parameters, R_{min}, R_{max} and a_{max}, as well as the diffusion parameter σ are seldom know. Therefore, although our main goal is to estimate the initial population density u_0, these other parameters are also needed. For simplicity, we assume that the initial population density is a constant, that is, $u_0(x) = u_0 \in \mathbb{R}, \forall x \in \Omega$. Denote $p = (u_0, \sigma, R_{min}, R_{max}, a_{max})$ the vector of the parameters to identify. Let $\mathcal{P}$ be a compact subset of $\mathbb{R}^5$ to which p belongs. When solving the direct problem (3.1), we are given p and we find a function u satisfying the differential equation in (3.1) and the respective boundary and initial conditions. This way, we define a mapping ϕ from the domain $\mathcal{P}$ of parameters to the space of solutions:

$$u = \phi(p) \tag{3.5}$$

It is well-know that the solution operator ϕ is continuous and injective. Therefore, using the compactness of $\mathcal{P}$ we obtain that the operator $\phi^{-1} : \phi(\mathcal{P}) \longrightarrow \mathcal{P}$ is continuous ([236], p.29). Thus, the inverse problem to (3.1) is well-posed. Then if a solution u of (3.1) is given, the value of $p = \phi^{-1}(u)$ can be determined by well-known methods, e.g. minimizing a norm of $u - \phi(p)$. However, in practice u is commonly not known, at least not on the whole domain $\Omega \times [0, +\infty)$ [193]. What is usually available is a function $B(u)$ referred to as *observation operator* [39].

Therefore the parameter identification problem is stated as follows: Given an observation ψ, find p such that

$$(B \circ \phi)(p) = \psi. \tag{3.6}$$

In the setting of problem (3.1) the observation operator consists of the insect count in traps at given times $t_1, t_2, ..., t_K$. More precisely, we have

$$B(u) = \begin{pmatrix} B_1(u, t_1) & \dots & B_1(u, t_K) \\ \vdots & & \vdots \\ B_N(u, t_1) & \dots & B_N(u, t_K) \end{pmatrix},$$

where $B_T(u, t_k)$ is the total number of insects captured in trap T until time t_k, $T = 1, ..., N$, $k = 1, ..., K$. Hence the observation ψ in (3.6) is an $N \times K$ real matrix

$$\psi = \begin{pmatrix} \psi_{1,t_1} & \dots & \psi_{1,t_K} \\ \vdots & & \vdots \\ \psi_{N,t_1} & \dots & \psi_{N,t_K} \end{pmatrix}.$$

Note that B is an array of numbers representing averaged values of u on particular areas of the domain at finite number of points in time. Hence, the injectivity of $B \circ \phi$ is problematic. Furthermore, the observation ψ contains both model and measurement error which further complicates the well-posedness of equation (3.6). In particular, ψ is not necessarily an element of $(B \circ \phi)(\mathcal{P})$. As usual for such situations, p is obtained as a solution of (3.6) in a least square sense, that is, p is a solution of the optimization problem,

$$\Phi(p) = \|(B \circ \phi)(p) - \psi\|_F^2 \longrightarrow \min, \tag{3.7}$$

where $\|A\|_F = \left(\sum_{i=1}^{m} \sum_{j=1}^{n} |a_{i,j}|^2 \right)^{1/2}$.

Let p^* be the minimizer of Φ, that is

$$p^* = \arg\min_{p \in \mathcal{P}} \Phi(p) \tag{3.8}$$

In the setting of the current model, both the observation operator and the model (3.1) depend on the distribution of the traps. Our aim is to find trap configurations for which the minimizer of Φ is unique and can be reliably determined by a numerical procedure. In order to investigate the properties of (3.7), equivalently (3.8), we solve the optimization problem iteratively using a random multistart approach [260] over a set of initial values of $p \in \mathcal{P}$. For each randomly selected starting value of p, a local minimum of Φ is found using the Gauss-Newton line search algorithm. The solution of (3.7) is identified as the estimated parameter values of the minimum of the local minima. Thus, increasing the number of starting values increases the chances of finding the global minimum of the objective function. Furthermore, for each trap setting, we consider how well the global minimum can be discriminated from the other local minima. This gives an important indication on how well the parameter values can be identified in the presence of noise and we refer to it as robustness. Here we investigate the influence of the choice of the settings of traps on the accuracy and robustness of the method.

In general, one can expect that increasing N and K leads to a more regular problem. However, as shown in [15], an incoming stream can be quite accurately identified by using relatively small number of observations. Furthermore, if the traps are far enough from each

other, the rows of $B(u)$ are the same. Therefore, in the considered setting, just increasing the size of the matrix $B(u)$ would not improve substantially the regularity of the problem. Our approach is to have some of the traps close enough so that due to interferences, they produce different streams of trapped insects. This will increase the rank of the matrix B which can be reasonably expected to improve the regularity of the problem. Empirical evidence supporting this conjecture is provided in the next section, where the effect of different configuration is examined.

3.5 Description of the experiments

We consider four trap settings:

- (A) single trap,
- (B) nine traps in a square formation,
- (C) five traps in a Z-formation,
- (D) five traps in a kite formation.

These four setting are shown on Fig. 3.2. Note that in all cases the traps are sufficiently far from the boundary of the domain Ω so that in the considered period of observation the boundary condition in (3.1) remains reasonable. Fig. 3.3 represents the population distribution after 15 time units using setting (D). The interference between the traps can be observed in Fig. 3.4, which is a zoom in of Fig. 3.3. Note that in these experiments, because of the symmetry of the trap distribution, identical trap counts are observed in several traps. In Fig. 3.2, the traps identified with the same symbols have identical incoming streams. Therefore, by using the nine traps of setting (B) for instance, we multiply the amount of information by three compared to the one-trap setting (A). In settings (C) and (D), five traps are used. Due to their configuration, setting (C) produces three distinct incoming streams, whereas setting (D) produces four distinct incoming streams. The distinct incoming streams obtained in each setting are represented in Fig. 3.5.

Considering the different settings of traps we run numerical simulations in order to estimate, one, two, three, and finally four parameters simultaneously using the cummulative trap counts over 15 time units ($K = 15$). Since the parameter of main interest to identify here is the initial population density u_0, it is always among the parameters to estimate. The diffusivity of the insects σ, is the second parameter of main interest when dealing with insect dispersal. The choice of the remaining parameters to estimate is based on a sensitivity analysis. We selected in priority parameters on which the model has the highest sensitivity.

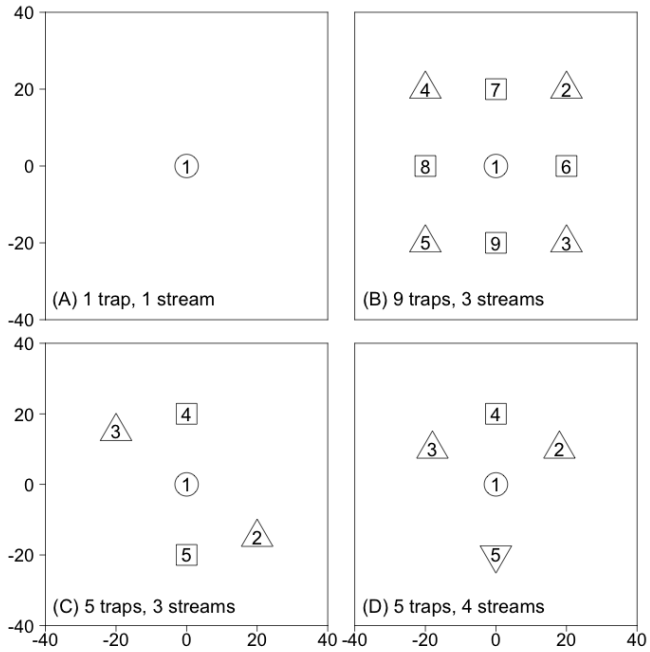

Figure 3.2: Distribution of the traps on Ω for each setting. The symbols identify the traps that produce identical incoming streams within each setting.

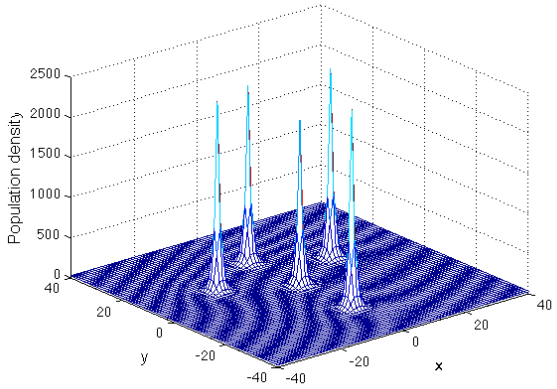

Figure 3.3: Insect distribution after 15 time units using setting (D).

Indeed, when solving the inverse problem, the more sensitive the original problem on a parameter is, the more accurate the parameter identification is. The sensitivity of a parameter is a measure of the change in the output of the model caused by a change in this parameter value. However, since the parameters under consideration have different order of magnitude, it is more appropriate to measure their elasticity index, i.e. the proportional change in the

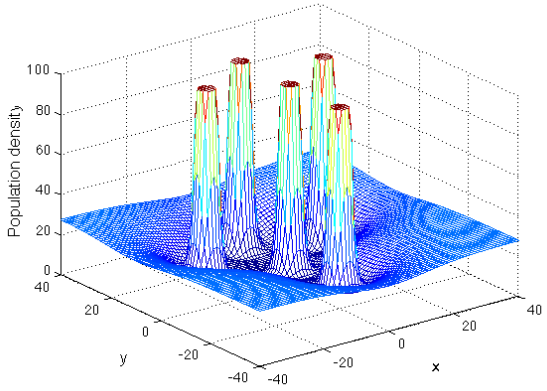

Figure 3.4: Interference between the traps using setting (D). Zoom in of Fig. 3.3.

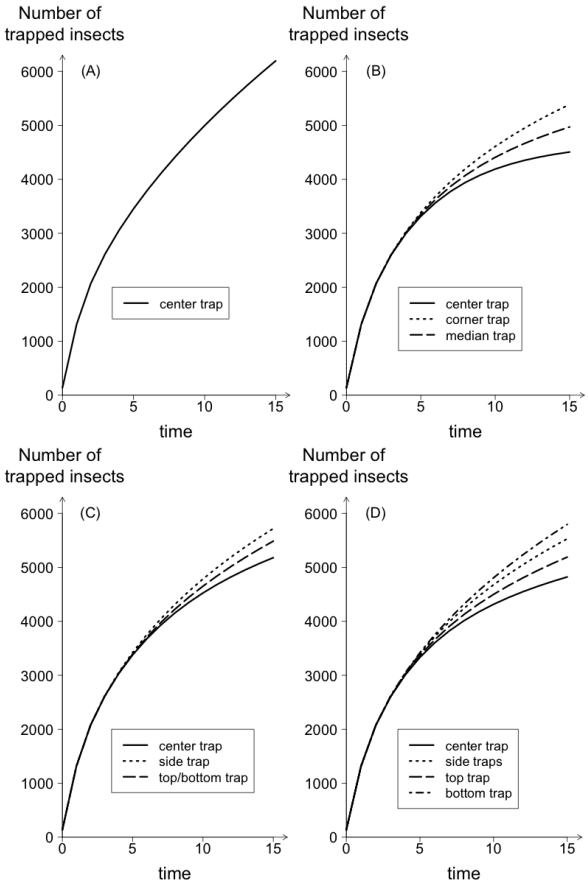

Figure 3.5: Cumulative number of captured insects in each trap, using the trap settings (A), (B), (C) and (D) of Fig. 3.2.

output of the model caused by a change in the value of the parameter. The elasticity indices of each parameter with respect to each setting of traps is given in Table 3.2. Note that the output of the model is the most sensitive to a change in the parameter for which the elasticity index is the greatest. Therefore, in order the output of the model is more sensitive to changes of values of a_{max} than of R_{max} for which the model is more sensitive to changes of R_{min}. Therefore, we proceeded to the parameter identification of $p_1 = (u_0)$, $p_2 = (u_0, \sigma)$, $p_3 = (u_0, \sigma, a_{max})$ and $p_4 = (u_0, \sigma, a_{max}, R_{max})$. Our aim is to find p^*_κ that satisfies (3.8), where κ denotes the number of parameters to be estimated ($\kappa = \{1; 2; 3; 4\}$). We limited our numerical simulations to the simultaneous estimation of 4 parameters due to limitations in computational capacity. Indeed, when solving the inverse problem, each evaluation of the objective function requires solving problem (3.1).

Table 3.1: Values of the parameters used to simulate the field data

parameter	unit	value
u_0	insects/unit area	27.5
σ	m^2/time unit	5.23
a_{max}	m/time unit	5.75
R_{max}	m	8
R_{min}	m	2

Table 3.2: Elasticity of the parameters with respect to the incoming streams of insects. Let ν denote a parameter, and $z(\nu)$ the incoming stream of insects with respect to ν, then, the elasticity index of parameter ν is $E_\nu = \nu\|z(\nu) - z(\nu + \Delta\nu)\|_2 / (\|z(\nu)\|_2 \Delta\nu)$

Setting	Trap	u_0	σ	a_{max}	R_{max}	R_{min}
(A)		1.00	0.92	1.42	1.26	0.60
(B)	Center	1.00	1.02	1.26	0.83	0.54
	Corner	1.00	0.96	1.35	1.06	0.57
	Median	1.00	0.98	1.31	0.95	0.55
(C)	Center	1.00	0.98	1.33	1.01	0.56
	Side	1.00	0.95	1.38	1.15	0.59
	Top/Bottom	1.00	0.95	1.36	1.08	0.58
(D)	Center	1.00	0.98	1.29	0.90	0.55
	Side	1.00	0.95	1.36	1.10	0.58
	Top	1.00	0.97	1.33	1.01	0.56
	Bottom	1.00	0.94	1.39	1.17	0.59

Since we do not have real field data, we simulated the data over a period of 15 time units with the values of parameters given in Table 3.1. Assuming that the period between two

consecutive collects of data is equal to one time unit, we extract from the simulated data only those that correspond the collect time. A noise of 5% is added to the simulated data, and this gives $\psi = (\psi_{i,t_1} \dots \psi_{i,t_K})_{i=1..N}$, where N is the number of traps. The use of simulated data also allows us to compare the estimation with the real values of the parameters.

The numerical solution of the initial value boundary problem (3.1) is obtained by using the Crank-Nicolson scheme [62, 233]. The optimisation problem (3.8) is solved by using the matlab function **fminunc** which performs the Gauss-Newton line search algorithm [99]. Since this function finds only a local minimum, we run it with many randomly selected initial points in order to have a reasonable certainty that the global minimum is among the local minima found. Here we choose $u_0^{(0)} \in [5; 45]$, $\sigma^{(0)} \in [4; 6]$, $a_{max}^{(0)} \in [2; 8]$, $R_{max}^{(0)} \in [3; 10]$ as ranges of the initial parameter values.

3.6 Results and Discussion

The results of the experiments described above are presented in Table 3.3. The values of the local minima of Φ, and the respective estimated values of the parameter vectors $\tilde{p}_\kappa$, with $\kappa = \{1; 2; 3; 4\}$, are given according to the trap setting. According to our method, when several local minima of Φ are found, the identified set of parameter values corresponds to the global minimizer of Φ, that is, the minimizer of the smallest local minimum. The $*$ on the right of the table indicates the values of the parameters identified as global minimizers of Φ. In these experiments, we investigate the accuracy and the robustness of the identified parameter values. The accuracy of p_κ^* is measured by calculating the relative error to the exact solution $\bar{p}_\kappa$ (Table 3.1) i.e. $E_{rel}{=}\|\bar{p}_\kappa - p_\kappa^*\|/\|\bar{p}_\kappa\|$. In this setting the concept of robustness of the method represents how well the global minimum value of Φ is discriminated against the values of Φ of other minima.

As a preliminary experiment, Table 3.4 presents the identified values and relative errors of p when a single parameter value is unknown. $p = (u_0)$, $p = (\sigma)$, $p = (a_{max})$ and $p = (R_{max})$ are successively identified using each setting of traps. These results are in agreement with the sensitivity analysis provided in Table 3.2, i.e. the more sensitive the output of the model to a certain parameter, the more accurate its estimation.

Table 3.3: Local mimima of the objective function Φ, with the four settings of traps with respect to the number of parameters estimated simultaneously. TS stands for the trap setting used (Fig. 3.2). The * indicates the set of parameters identified as the global minimizer of Φ.

p	TS	Φ	$\tilde{u_0}$	$\tilde{\sigma}$	$\tilde{a}_{max}$	$\tilde{R}_{max}$	E_{rel}
$p_1 = (u_0)$	(A)	240004	27.63	–	–	–	0.5% *
	(B)	259813	27.43	–	–	–	0.3% *
	(C)	572150	27.45	–	–	–	0.2% *
	(D)	620115	27.31	–	–	–	0.7% *
$p_2 = (u_0, \sigma)$	(A)	219149	21.49	3.31	–	–	22.5% *
		222543	25.43	4.73	–	–	
	(B)	256632	27.01	5.15	–	–	1.8% *
	(C)	572066	27.52	5.24	–	–	0.1% *
		826874	19.69	2.45	–	–	
	(D)	619615	27.46	5.26	–	–	0.2% *
$p_3 = (u_0, \sigma, a_{max})$	(A)	204279	17.79	4.30	7.89	–	34.9% *
		214067	21.14	6.44	7.90	–	
	(B)	256473	26.70	5.16	5.81	–	2.8% *
		297564	18.37	4.48	7.65	–	
	(C)	572055	27.61	5.23	5.73	–	0.4% *
		636640	17.35	4.18	8.07	–	
	(D)	598689	25.17	5.48	6.31	–	8.4% *
		647548	17.43	4.45	8.14	–	
$p_4 = (u_0, \sigma, a_{max}, R_{max})$	(A)	210462	33.31	3.25	5.07	5.83	22.1% *
		210466	34.38	3.08	4.90	5.71	
		210471	32.75	3.35	5.17	5.89	
		210503	32.02	3.47	5.30	5.98	
		210533	31.53	3.56	5.39	6.03	
		210679	30.22	3.81	5.65	6.20	
	(B)	255885	26.93	5.09	5.64	8.15	2.1% *
		277462	18.24	4.00	6.80	8.56	
	(C)	571732	27.51	5.28	5.85	7.88	0.6% *
		609828	17.47	3.84	7.05	8.61	
	(D)	597514	25.40	5.37	6.07	8.18	7.2% *
		615604	17.66	4.06	7.08	8.61	

Table 3.4: Identified values of the single value parameter p and its relative error with respect to the trap setting, TS. The values of the estimates are rounded to two digits after the decimal point.

TS	p	$\tilde{u_0}$	$\tilde{\sigma}$	$\tilde{a}_{max}$	$\tilde{R}_{max}$	$\tilde{R}_{min}$	E_{rel}
(A)	$p=(u_0)$	27.63	–	–	–	–	0.48%
	$p=(\sigma)$	–	5.20	–	–	–	0.60%
	$p=(a_{max})$	–	–	5.77	–	–	0.37%
	$p=(R_{max})$	–	–	–	8.03	–	0.41%
	$p=(R_{min})$	–	–	–	–	2.02	0.81%
(B)	$p=(u_0)$	27.43	–	–	–	–	0.24%
	$p=(\sigma)$	–	5.24	–	–	–	0.21%
	$p=(a_{max})$	–	–	5.74	–	–	0.17%
	$p=(R_{max})$	–	–	–	7.98	–	0.24%
	$p=(R_{min})$	–	–	–	–	1.99	0.64%
(C)	$p=(u_0)$	27.45	–	–	–	–	0.19%
	$p=(\sigma)$	–	5.24	–	–	–	0.19%
	$p=(a_{max})$	–	–	5.74	–	–	0.13%
	$p=(R_{max})$	–	–	–	7.99	–	0.17%
	$p=(R_{max})$	–	–	–	–	1.99	0.05%
(D)	$p=(u_0)$	27.31	–	–	–	–	0.69%
	$p=(\sigma)$	–	5.27	–	–	–	0.71%
	$p=(a_{max})$	–	–	5.72	–	–	0.49%
	$p=(R_{max})$	–	–	–	7.95	–	0.60%
	$p=(R_{min})$	–	–	–	–	1.96	1.76%

3.6.1 Do interfering trap-settings provide better results than non-interfering trap settings?

From Table 3.3 we can see that, using setting (A) i.e. without trap interference, the number local minima found increases, as the number of parameters to identify simultaneously increases. Conversely, using the setting with trap interferences, a maximum of two minima were found.

Moreover, the minima found using one trap are in a maximum range of 5% of the optimal value of ϕ and within this range, the norms of the different minima can differ by 15%. More precisely, for $p = p_2$ (resp. $p = p_3$), the minima are found withing a range of 2% (resp. 15%) of the optimal value of ϕ. In particular, when $p = p_4$, 6 minima are found within a range of 0.1% of the optimal value of ϕ where the norm of the minima can differ by 10.6%. This shows

that, without interferences, as the number of parameters to identify increases, the reliability of the estimates decreases.

Furthermore, we can see from Table 3.3, that the one-trap setting provides a poor accuracy of the estimates when several parameter values are identified simultaneously, compared to the other setting. In fact, using one trap, the relative error of the estimates is above 22% when two or more parameter values are estimated, whereas, using the other settings, the relative error is always below 8.4%. Therefore, when two or more parameters are to be identified, we may conclude that interfering trap settings provide estimates with better accuracy than non-interfering trap settings. However, from Table 3.3, note that if a single parameter needs to be identified, setting (A), using only one trap, would provide a sufficiently accurate and reliable estimate. In this case, adding more traps is not really helpful. This suggests that one must choose an appropiate setting depending on the parameters that need to be identified.

By investigating further on the results, when $p = p_3$ using one trap, we simulated the incoming streams using the global minimizer of Φ ($p_3 = p_3^*$), (Table 3.3). The curve obtained with the latter simulation as well as the curve representing the incoming stream simulated using the real value of p , given in Table 3.1 ($p_3 = \bar{p}_3$), are represented in Fig. 3.6. As we can see, the two curves are hardly distinguishable, meaning that two different sets of parameters can lead to very similar incoming streams. This illustrates the ill-conditionedness of the problem where two very similar streams of trapped insects are produced using two very different sets of parameters ($E_{rel} = 34.9\%$, Table 3.3).

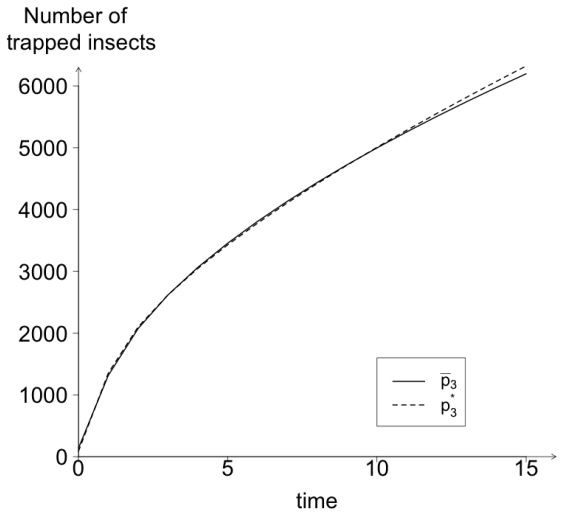

Figure 3.6: Simulated cumulative number of captures when estimating three parameters with setting (A), using the real values, $\bar{p}_3$, and the identified values, p_3^*.

3.6.2 Interfering trap-setting strategies

We have shown above that using a setting of traps that are interfering provide better results for parameter identification in terms of robustness and accuracy when several parameters are identified simultaneously. However, little is known on the actual role of the interferences between the traps and their effect on the regularity of the problem. In order to understand the effect of these interactions, several interfering trap settings are compared.

We study the results obtained using the nine-trap setting (B) and the setting (D) of five traps. One could expect better accuracy and robustness of the estimates using setting (D) since in this setting four distinct incoming streams are produced whereas only three are produced using setting (B). However, apart from the case $p = p_1$, the relative error of the estimate using setting (D) is always lower than using setting (B). Considering the fact that the noisy data are averaged over the traps producing the same streams, in setting (B), the corner and median noisy data are averaged over three traps, whereas only the noisy data of the two side traps are averaged using setting (D). Therefore, the data used to identify the parameters using setting (B) are smoother than those used with setting (D). This reduces the effect of the noise and may explain why more accurate and robust estimations are obtained using nine traps.

In setting (C), five traps are used producing three distinct incoming streams as for the nine-trap setting (B). The estimates obtained using setting (C) are the most accurate compared to all the other experiments that were carried out ($E_{rel} = 6\%$ for $p = p_4$). The robustness, however, is not as good as for the nine trap setting. For instance, when $p = p_3$, two local minima of ϕ are found within 10% (resp. 14%) of its optimal value for setting (C) (resp. setting (B)). Despite this, the global minimum of ϕ is clearly identified. This counter intuitive result shows that the interference phenomenon is not trivial. In particular, we can see in Fig. 3.5 that the 3 incoming streams produced by the nine trap setting are more distinct than those obtained using the five-trap setting. A possible explanation may relate to the sensitivity of the parameters. Indeed, the parameters a_{max} and R_{max} are more sensitive using setting (C) than when using setting (B) (Table 3.2). Such a result suggest that there must be an optimal setting which would allow to obtain robust and accurate parameter estimation using as few traps as possible.

These results show that trap interference can be used to make the problem more regular, however, the relationship between the regularity of the problem and the interference between the traps is highly nonlinear and therefore difficult to analyse.

3.7 Conclusion

Parameter Identification is challenging, in particular when the direct problem is defined by PDEs, since it often leads to solving inverse problems that are ill-posed or ill-conditioned. We demonstrate numerically that the interferences between traps can be used to make the problem well-posed and well-conditioned using a trial-and-error approach. This method enables the identification of parameter values that describe population characteristics, i.e the population density, its diffusion rate, attractiveness of the traps and their maximum radius of attraction. By choosing biologically realistic ranges of parameter values to estimate, the parameters are identified as the global minimizer of function Φ using starting values over these ranges. We show numerically that trap interferences can be used not only to increase the accuracy of the estimates, but also to find a global minimum which can be well discriminated from the other local minima. The trial-and-error method over the choice of the trap setting, followed with the multistart approach to solve the optimization method increases the chances of succeeding in solving the parameter identification problem. For each trap setting trial, we found numerically the global minimum of the objective function and we measured how well it is discriminated from the other minima. The setting where the global minimum can be the best discriminated from the other minima provides an inverse problem that is well-conditioned and thus provides the most robust solution to the parameter identification problem. Note that, once a "good" setting of trap is identified, other methods, such as random search methods, could be interesting alternatives to finding the global minimum of the objective function [260, 53, 1].

Furthermore this work investigates how experiments using traps should be conducted in the field so that sufficient information is recorded, using as few traps as possible. Indeed, the optimal setting of traps depends on the parameters that need to be identified. For instance, we showed that a setting using only one trap would be sufficient to identify a single parameter. However when several parameters are unknown, interfering traps provide more accurate and more reliable estimates. In particular, setting (C) stands out from the other settings. Due to a highly nonlinear relationship between the trap interferences and the regularity of the problem, it is challenging to find an optimal setting of traps providing highly accurate and robust estimates. A global sensitivity of the model to the parameters will be considered in a future work to give more insight into this relationship. This is a promising method, not only from the numerical and theoretical perspective for parameter identification, but may also prove to be of practical importance for the determination of insect population density in the field with the use of traps.

Acknowlegment

The support of the National Research Foundation of South Africa and Citrus Research International Ltd. (Project: 1075) is acknowledged. Y. Dumont would also like to thank the support of the "SIT feasibility program" in Reunion, jointly funded by the French Ministry of Health and the European Regional Development Fund (ERDF).

Chapter 4

Simulations and parameter estimation of a trap-insect model using a finite element approach

This work has appeared in

R. Anguelov, C. Dufourd ans Y. Dumont, Simulations and parameter estimation of a trap-insect model using a finite element approach, Math. Comput. Simulation 133:47-75 (2015), http://dx.doi.org/10.1016/j.matcom.2015.06.014

4.1 Abstract

Estimating pest population size is of utmost importance in biological control. However field experiments can be difficult and expensive to conduct, with no guarantee that usable results will be produced. In this context, the development of mathematical models and numerical tools is crucial to improve the field experiments by suggesting relevant data which can be used to estimate parameters related to the pest's biology and to the traps (e.g. duration of the experiments, distance of the releases, etc.). Here we develop a trap-insect model (TIM), based on coupled partial differential equations. The model is studied theoretically and a finite element algorithm is developed and implemented. A protocol for parameter estimation is also proposed and tested, with various data. Among other results, we show that entomological knowledge is absolutely necessary for efficient estimation of parameters,

in particular population size.

4.2 Introduction

In the context of pest control and management, the success of any strategy requires a good understanding of the insect's biology as well as knowledge on its spatial distribution, dispersal capacity, density, etc. Typically the only data available is obtained using traps. Estimating population densities is complicated when little is known on the behaviour of the insects interacting with the traps as well as with the environment. Mark-release-recapture (MRR) experiments are often used to estimate some biological and ecological population parameters, e.g. size, dispersal, survival, etc. Models and estimation methods exist to quantify the size of the population (see [54] for an overview). Programs, like E-SURGE [52], and MARK [253] are also available. They are based on statistical analysis and fitting, and provide estimations of some population parameters using recapture data from particular field experiments (individual tracking). However, with these tools, testing different strategies is costly and time consuming as it requires many field experiments to get results.

Beyond estimation of population size, optimizing trapping strategies is fundamental in pest control programs (see for instance [9, 108]), and trap network is a component of crucial practical importance in terms of capture probabilities [166]. Many studies address this problem by relating the distance to a trap and capture probabilities using statistical distributions such as exponential [65, 197] or Cauchy [175] distributions, or empirical logistic equation [33]. More recently, Manoukis et al. [166] used the hyperbolic secant function to model the probability of capture of attracting traps depending on the distance to the trap. In a previous work [81], we addressed the question of trapping networks as we developed a mathematical model for estimating insect population parameters using trap data in various configurations. The dynamics of the insects responding to attractive traps were modelled via an advection-diffusion-reaction equation, where the direction and force of attraction were defined by an analytical function of the space variable. This approach enables the estimation of model parameters and population characteristics using various settings of traps, and comparison of their efficacy via numerical simulations.

In this paper we develop a trap-insect model (TIM), which consists of a chemotaxis model that simulates the spread of a chemical attractant released by traps, coupled with an insect spreading model, in which the insects' response to the attractant is modelled. In [64], the authors developed a mosquito-host model where the spread of the CO_2 released by the hosts is described via an advection-diffusion-reaction, while the response of the mosquitoes is modelled via an individual based random walk process. Here we propose to model simultaneously the spread of the chemical attractant and the dynamics of flying insects, like fruit flies or mosquitoes, using a system of advection-diffusion-reaction equations.

In [81], the solution of the insect model was approximated using a finite difference approach. Here, the solution of the model is approximated using the finite element method [94]. In the finite element method, the domain is subdivided into elementary sub-domains (like triangles in 2D or tetrahedra in 3D) where the approximated solution is piecewise polynomial on the whole domain. Further, this method offers the possibility to refine the mesh around the traps and take into account local dynamics. Numerical approximations of the trap counts are obtained by simulation and used to estimate some parameters of the insects' dynamics.

The paper is structured as follows. We first describe the coupled chemotaxis model. Then, in sections 3 and 4, we write the problem in variational form and we give some qualitative properties of the solutions. Next, the numerical scheme implementing the finite element method is described in section 5, followed by some numerical simulations in section 6. Finally, in section 4.8, we consider applications to parameter identification, and specifically the estimation of the size of the insect population. We implement and test a feasible experimental protocol chain, and we discuss the results.

4.3 The model

It is commonly assumed that insects such as mosquitoes or fruit flies, move according to an isotropic random walk when they are not influenced by any stimulus in a homogeneous wind-free environment. Under such conditions, the movement of the insect population is governed by a simple diffusion equation [222]. Thus, when passive traps are used, insects are neither attracted to nor repulsed from the traps, and move according to a random walk until they "accidentally" get trapped [37]. Yet, the survival of the insect population depends on its ability to locate food and breeding sites, and therefore insects adapt their displacements accordingly [138]. This suggests that insects rather follow a correlated random walk allowing a bias in the insects' movement direction [140, 230]. In the deterministic model, the average biased behaviour of the population is modelled via an advection term [188].

To increase the chance of capturing insects, attractive traps are often used. The latter release a chemical attractant (CO_2, pheromone, odour) which spreads. In a 2-dimensional domain, $\Omega \subset \mathbb{R}^2$, the active space of such traps is defined as the area where the concentration of the attractant is above a minimum threshold concentration level which can be detected by the targeted insects [214, 185]. In other words, the active space of a trap is the area where its attraction takes place.

Modelling the spread of a chemical attractant in air is a challenge on its own. When it is assumed that the chemical is released at a constant rate, in a homogeneous environment with

still air, the active space is a disc centred at the trap [79] and its radius defines the attraction range (i.e. the maximum distance from the trap to which attraction takes place) [214]. However, in the presence of wind, or if the environment is not homogeneous, the spread of the chemical is subjected to turbulences, and in such cases, the active space of the attractant is often described as a 'plume' [91]. To circumvent this difficulty, homogeneous spread [188, 32] is often assumed when introducing wind in models. In [80], for instance, areas of attraction were defined as circular areas deformed into ellipses to take into account the wind's direction and speed.

To model the capture of insects, it is necessary to define how the attraction towards the source takes place. In many studies, empirical functions relate the distance to the trap to a certain probability of capture [175, 197, 166]. In previous work [79], we adopted this approach, as the attraction was taking place within a radius R_{max} from the centre of the trap, and the force of attraction was defined as function which increases as the distance to the trap decreases. Here, we model the force of attraction using the gradient of the concentration of the chemical.

The model developed here aims to describe simultaneously the spread of the chemical attractant and the dynamics of the insects responding to it. While the spread of the chemical can be modelled independently, the movement of the insects is biased by the concentration of the chemical and its gradient. More precisely, we assume that the insects detect the chemical above certain concentration and respond by moving in the direction of the gradient. It is assumed that this movement is more persistent when the gradient is steeper. Further a chemotactic sensitivity function, $\chi(c)$ is introduced to model the sensitivity of the insects to the chemical attractant. Mathematically this is modelled via an advection term in the model of the dynamics of the insects, where the advection's direction and strength is governed by the gradient of the concentration of its chemical attractant and the function χ. Further, in order to avoid accumulation of insects inside the traps we adopt a compartmental approach and distinguish the free insects, u_f, from the captured insects, u_c. The dynamics of the free insects is governed by an advection-diffusion equation to account for their response to the attractive traps while the change in the captured insects results from the removal due to the reaction term in the equation modelling the free insects.

In terms of mathematical modelling, a trap T is a circular area of the domain Ω with a centre x_T and a radius R_T. Outside this area, no transition occurs from the free compartment to the captured compartment. Inside the trap, transition occurs and its capture rate increases as the insects get closer to the centre of the trap. This capture rate is represented in Figure 4.1. Once captured, the free insects pass into the captured compartment from which they cannot escape.

4.3.1 Modelling the spread of the chemical attractant

The spread of the chemical is governed by the Fick's law of fluid dynamics, where the particles of a fluid move from area of high concentration to area of low concentration. This is modelled via a diffusion term, $\epsilon^c \Delta c(t,x)$, where $c(t,x)$ is the concentration of the chemical at time t and position x, and ϵ^c is the diffusivity of the chemical. The emission of the chemical takes place within a circular area of radius $R_e < R_T$ around the centre of the trap. For each trap, this release is modelled using a circularly symmetric smooth function, which is 0 outside the area defined by R_e and reaches its maximum at the centre. Further, we assume that the release of c is regulated by a saturation level c_{sat}, which represents the maximum concentration of c in the air. Then, the rate of release of the attractant c over Ω is the sum of the disjoint rates of release in all traps. Under the above assumptions this rate of release of c at a time $t > 0$ and point $x \in \Omega$ is given by $\lambda(x)(c_{sat} - c(t,x))$, where

$$\lambda(x) = \sum_{T=1}^{N_{trap}} \Lambda(||x - x_T||) \tag{4.1}$$

with Λ a decreasing smooth function on $[0, +\infty)$ such that $\Lambda'(0) = 0$ and $\Lambda(z) = 0$ for $z \geq R_e$. An explicit formulation of Λ used to perform numerical experiments is given in section 4.7.

Finally it is reasonable to assume that the chemical vanishes in time. This is modelled by a reaction term on the right-hand side of the equation, $-\mu_c c(t,x)$, where $\mu_c > 0$ represents the vanishing rate. This yields a diffusion-reaction equation with a forcing term, given in (4.2).

4.3.2 Modelling the insects' dynamics

Insects' dynamics are modelled via an advection-diffusion-reaction equation. Unlike the equation for the chemical, the diffusion is derived from the assumption that the motion of the individual members of the population is governed by an isotropic random walk [228, 222, 37] if they are not submitted to any stimulus.

The diffusion of the insects is modelled by the term $\epsilon^u \Delta u(t,x)$, where $u(t,x)$ is the density of insects at time t and position x, and ϵ^u is the diffusion coefficient of the insects. Here we assume that ϵ^u is constant over the domain. However, ϵ^u may depend on x in order to account for a heterogeneous environment. Further it may be also function of t as it depends on weather related factors, e.g. temperature or rainfall.

In [81], we consider a space-dependent diffusion coefficient to account for the fact that once the insects are trapped they remain in the trap and cannot escape. Thus, in order to avoid

insects "escaping" the trap by diffusivity due to accumulation inside the traps, the diffusion coefficient was set to a negligible value inside the traps. Here, the trapped insects are removed from the free-insect compartment, and transferred to the captured compartment. Therefore, the diffusion coefficient for the insects is taken constant over the entire domain. A similar compartmental approach for mosquito population was used in [80, 79] to model different dynamics depending on the stage of development of mosquitoes or on their behavioural characteristics.

The transfer from the free compartment to the captured compartment (i.e. the capture rate) is modelled using the smooth transition function, $f(x), x \in \Omega$, which depends on the the distance to the centre of the trap. More precisely, it is assumed that outside the traps, no transfer occurs. As from the boundary of trap, the rate of capture of the trap increases up to its maximum capture rate r, which then remains constant inside the traps. Thus, as shown in Figure 4.1, the capture rate is equal to its maximum value, r, inside the traps, or more precisely in a radius of $R_T - \varepsilon$ around the centre of the trap, and zero outside the traps, i.e. when $z \geq R_T$.

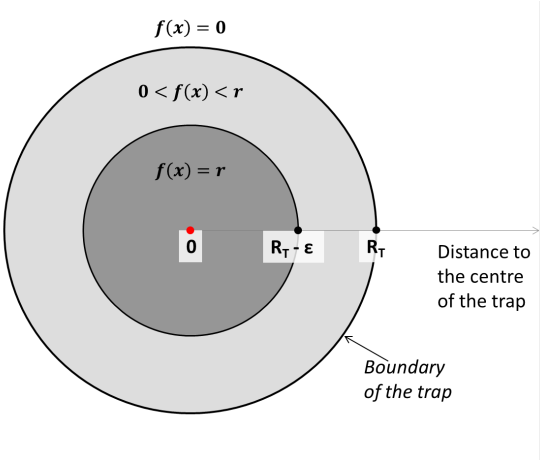

Figure 4.1: Representation of a trap of radius R_T. $f(x)$ is the value of the capture rate defined in (4.42)-(4.43)

However, in the presence of a stimulus, insects can be attracted to, or repelled from, the source of that stimulus. In this particular study, we consider the case where insects are attracted to a source located inside a trap. As mentioned earlier, the direction and speed of the motion of the insects are affected by the concentration and the gradient of the chemical when the concentration is above the threshold c_{min}. This is referred to as chemotaxis [141] and gives rise to an advection term, $\nabla \cdot (\chi(c)\nabla c(t,x)u_f(t,x))$, where the advection coefficient is the product of the gradient of the concentration of the chemical by a sensitivity coefficient [188], $\chi(c)$. The latter enables us to define the relationship between the

steepness of the gradient of the concentration of the chemical and the strength of attraction of the insects towards the source, that is, towards the trap. Note that this advection occurs only in areas where the concentration of the chemical is above the threshold c_{min}, i.e. in the active space of the traps [42]. Thus, $\chi(c)$ is an increasing smooth function of the concentration of the chemical attractant c which is null whenever $c < c_{min}$, and bounded above by a certain value which can be interpreted as the maximum possible response of the insects to the gradient of c. In section 4.7, we define an explicit formulation of $\chi(c)$ used for the numerical experiments.

Finally, we could add a reaction term for the insects to account for the natural growth of the population, (birth and death), and for possible excess mortality. Here, we will omit this term as the experiments take place over a short period of time, such that the demography and other parameters related to the environment can be assumed to remain constant.

4.3.3 The coupled model

We consider the concentration of the chemical attractant c, the free-insect density u_f, and the captured-insect density u_c, as functions on the spatio-temporal domain $[0, T] \times \Omega$, where $T \in \mathbb{R}^+$, and Ω is a domain in $\mathbb{R}^2$ with piecewise smooth boundary. At $t = 0$, we assume that the traps are placed in the domain where all insects are free with a distribution u_0. Under these assumptions, we have that $c(0, x)$ is equal to zero everywhere on Ω, $u_f(0, x)$ is equal to the distribution $u_0(x), x \in \Omega$ and $u_c(0, x) = 0, x \in \Omega$.

Let $\Gamma = \partial\Omega$ denote the boundary of Ω. We assume that the domain Ω is large enough and that the traps are sufficiently far from the boundary Γ so that the concentration c is negligible on Γ. Then we consider homogeneous Dirichlet boundary conditions on Γ, i.e. $c|_\Gamma = 0$. Further, we assume that there is no immigration and emigration in and out of the domain (or that immigration and emigration compensate), so that homogeneous Neumann boundary conditions can be applied for u_f and u_c. Under these assumptions, the model is

formulated as follows:

$$\frac{\partial c(t,x)}{\partial t} - \epsilon^c \Delta c(t,x) + \lambda(x)(c(t,x) - c_{sat}) = -\mu_c c(t,x) \tag{4.2}$$

$$\frac{\partial u_f(t,x)}{\partial t} - \epsilon^u \Delta u_f(t,x) + \nabla \cdot (\chi(c)\nabla c(t,x) u_f(t,x)) = -f(x) u_f(t,x) \tag{4.3}$$

$$\frac{\partial u_c(t,x)}{\partial t} = f(x) u_f(t,x), \quad x \in \Gamma, t > 0 \tag{4.4}$$

$$c(t,x) = 0, \quad x \in \Gamma, t > 0 \tag{4.5}$$

$$\nabla u_f \cdot \vec{n} = 0, \quad \text{on } \Gamma \tag{4.6}$$

$$\nabla u_c \cdot \vec{n} = 0, \quad \text{on } \Gamma \tag{4.7}$$

$$c(0,x) = 0, \quad x \in \Omega \tag{4.8}$$

$$u_f(0,x) = u_0(x), \quad x \in \Omega \tag{4.9}$$

$$u_c(0,x) = 0, \quad x \in \Omega \tag{4.10}$$

where $\vec{n}$ denotes the outward normal vector on Γ.

4.4 The variational formulation of the problem

The general existence and uniqueness theory of initial-boundary value problems for parabolic systems of the form (4.2)-(4.10) is typically given in terms of weak solutions, that is, the solutions of an associated variational problem. Since, in addition, the numerical simulations are computed by the finite element method, we give explicitly the variational formulation of the problem. As usual we use the notation

$$H^1(\Omega) = \{w \in L^2(\Omega) \colon \frac{\partial w}{\partial x_i} \in L^2(\Omega), 1 \leq i \leq 2\},$$
$$H_0^1(\Omega) = \{w = H^1(\Omega) \colon w|_\Gamma = 0\}.$$

To apply the theory of weak solutions, we consider c, u_f and u_c not as functions of t and x, but as mappings of t into spaces on Ω. In particular, taking into account the boundary conditions (4.5), (4.6) and (4.7), we consider

$$\begin{aligned} c &: [0,T] \longrightarrow H_0^1(\Omega), \\ u_f &: [0,T] \longrightarrow H^1(\Omega), \\ u_c &: [0,T] \longrightarrow H^1(\Omega). \end{aligned}$$

Therefore, we seek

$$\begin{aligned} c &\in L^2\left(0,T;H_0^1(\Omega)\right), \quad \text{with } \frac{dc}{dt} \in L^2\left(0,T;H^{-1}(\Omega)\right), \\ u_f &\in L^2\left(0,T;H^1(\Omega)\right), \quad \text{with } \frac{du_f}{dt} \in L^2\left(0,T;H^{-1}(\Omega)\right), \\ u_c &\in L^2\left(0,T;H^1(\Omega)\right), \quad \text{with } \frac{du_c}{dt} \in L^2\left(0,T;H^{-1}(\Omega)\right), \end{aligned}$$

where $H^{-1}(\Omega)$ is the dual space of $H^1(\Omega)$.

If we multiply each term of the equation (4.2) by a test function $w \in H_0^1$ and integrate over Ω, then, for $t > 0$ and $w \in H_0^1(\Omega)$, we obtain

$$\int_\Omega \left(\frac{\partial c(t,x)}{\partial t} w(x) - \epsilon^c \Delta c(t,x) w(x) + (\lambda(x)+\mu) c(t,x) w(x) \right) dx = \int_\Omega c_{sat} \lambda(x) w(x) dx. \tag{4.11}$$

Using that $w|_\Gamma = 0$, the divergence theorem yields

$$-\int_\Omega \epsilon^c \Delta c(t,x) w(x) dx = \int_\Omega \epsilon^c \nabla c(t,x) \cdot \nabla w(x) dx + \int_\Gamma \frac{\partial c}{\partial n} w(x) dx. \tag{4.12}$$

Hence, equation (4.11) is reduced to

$$\begin{aligned} &\forall w \in H_0^1(\Omega), \\ &\int_\Omega \left(\frac{\partial c(t,x)}{\partial t} w(x) + \epsilon^c \nabla c(t,x) \cdot \nabla w(x) + (\lambda(x)+\mu) c(t,x) w(x) \right) dx \\ &= \int_\Omega c_{sat} \lambda(x) w(x) dx. \end{aligned} \tag{4.13}$$

In a similar way, the divergence theorem is applied to obtain a variational formulation of (4.3) with boundary condition (4.6). Here, in order to simplify the integral of the advection term, we use in addition the fact that $c|_\Gamma = 0$ and therefore $\chi(c)|_\Gamma = 0$. More precisely, we have

$$\int_\Gamma (\chi(c) \nabla c(t,x) u_f(t,x) v(x)) \cdot \vec{n} = 0. \tag{4.14}$$

Altogether, the variational formulation for the system (4.2)-(4.7) is as follows:

$$\begin{aligned}
&\forall w \in H_0^1(\Omega), \quad \forall v \in H^1(\Omega),\\
&\int_\Omega \frac{\partial c(t,x)}{\partial t} w(x)dx + \int_\Omega \left(\epsilon^c \nabla c(t,x)\cdot\nabla w(x) + (\lambda(x)+\mu)c(t,x)w(x)\right)dx\\
&= \int_\Omega c_{sat}\lambda(x)w(x)dx, \qquad (4.15)\\
&\int_\Omega \frac{\partial u_f(t,x)}{\partial t} v(x)dx + \int_\Omega \left(\epsilon^u \nabla u_f(t,x)\cdot\nabla v(x) - (\chi(c)\nabla c(t,x)u_f(t,x))\cdot\nabla v(x)\right)dx\\
&= -\int_\Omega f(x)u_f(t,x)v(x)dx, \qquad (4.16)\\
&\int_\Omega \frac{\partial u_c(t,x)}{\partial t} v(x) = \int_\Omega f(x)u_f(t,x)v(x)dx. \qquad (4.17)
\end{aligned}$$

Denote by a the bilinear form associated with the variational problem (4.15), defined as

$$a(c,w) = \int_\Omega \left(\epsilon^c \nabla c(t,x)\cdot\nabla w(x) + (\lambda(x)+\mu)c(t,x)w(x)\right)dx, \quad \forall c, w \in H_0^1(\Omega), \qquad (4.18)$$

and by b, the bilinear form associated with (4.16),

$$\begin{aligned}
b(u_f, v) = \int_\Omega &[\epsilon^u \nabla u_f(t,x)\cdot\nabla v(x) - (\chi(c)\nabla c(t,x)u_f(t,x))\cdot\nabla v(x)\\
&+ f(x)u_f(t,x)v(x)]dx, \quad \forall u_f, v \in H^1(\Omega). \qquad (4.19)
\end{aligned}$$

If we choose $w = c$ in $H_0^1(\Omega)$, we can show that a is coercive, i.e. there is a constant k_a such that

$$a(c,c) \geq k_a \|c\|_{H_0^1}^2. \qquad (4.20)$$

Similarly, if we choose $v = u_f$ in $H^1(\Omega)$, we can show that b is L^2-coercive, i.e. there are two constants k_b and γ_b such that

$$b(u_f, u_f) \geq k_b \|u_f\|_{H^1}^2 - \gamma_b \|u_f\|_{L^2}^2. \qquad (4.21)$$

Consequently, the existence and uniqueness of the solutions of the problems (4.15)-(4.17) with initial conditions (4.8)-(4.10) follows from Lions theorem [94, Thm. 6.6] or [36, Thm. 10.9]. Alternatively, existence and uniqueness can be derived from the general semi-group theory [192, Cor. 2.8].

4.5 Some qualitative properties

In this section we give some qualitative properties of the model (4.2)-(4.10) which are of biological significance, e.g. positivity and boundedness of all solutions. These properties are derived by using the maximum principle. Hence, we need to remark first that the weak solutions of the problem (4.2)-(4.10) are actually $\mathcal{C}^2$. This result follows from the standard regularity theory for the solutions of parabolic problems, e.g. see [36, Sec. 9.6].

Proposition 4.5.1. *For any solution $c(t,x)$ of (4.2), with $0 \leq c(0,x) \leq c_{sat}$, we have*

$$0 \leq c(t,x) \leq c_{sat}, \quad (t,x) \in [0,T] \times \Omega.$$

Proof. Using the notation $Lc = -\frac{\partial c}{\partial t}(t,x) + \epsilon^c \Delta c(t,x)$ and $hc = -(\lambda(x) + \mu_c)c(t,x)$, the governing equation for c can be written as

$$(L+h)c = -\lambda(x)c_{sat}. \tag{4.22}$$

Denote by λ_{max} the maximum of $\lambda(x)$, for $x \in \Omega$. Then, we have

$$\begin{array}{rrl} -\lambda_{max}c_{sat} \leq & -\lambda(x)c_{sat} & \leq 0 \quad \text{and,} \\ -(\lambda_{max}+\mu_c) \leq & -(\lambda(x)+\mu_c) & \leq 0. \end{array} \tag{4.23}$$

Let

$$m = \min_{(t,x)\in[0,T]\times\Omega} c(t,x).$$

Assume that $m < 0$. Since $(L+h)c \leq 0$, or equivalently $(L+h)[-c] \geq 0$, and $h \leq 0$, the maximum principle [201, Chapt. 3, Thm. 4] yields that there exists P on $[0,T]\times\Gamma \cup [0]\times\Omega$ such that $-c(P) = m < 0$. The contradiction with $c|_\Gamma = 0$ shows that $m \geq 0$ and therefore $c(t,x) \geq 0, t \geq 0, x \in \Omega$.

If we apply the maximum principle in a similar way to the function $c_{sat} - c$ we obtain $c_{sat} - c(t,x) \geq 0$ or equivalently, $c(t,x) \leq c_{sat}, t \geq 0, x \in \Omega$ □

Consider the stationary problem for c:

$$\begin{cases} \forall w \in H_0^1(\Omega), \\ a(c,w) = \int\limits_\Omega c_{sat}\lambda(x)w(x)dx, \\ c(0,x) = 0, \quad x \in \Omega. \end{cases} \tag{4.24}$$

Given the coercivity of the bilinear form associated with problem (4.24), existence and uniqueness of the weak solution follows from the Lax-Milgram theorem [36, Cor. 5.8]. We denote by $c_{stat} \in H_0^1(\Omega)$ the solution to problem (4.24). In the following proposition we show the convergence of the solution of the evolutionary problem to c_{stat} as time tends to infinity.

Proposition 4.5.2 (Convergence to the stationary solution)**.** *The solution c of problem (4.15), converges in $L^2(\Omega)$ to the solution c_{stat} of problem (4.24) as t goes to $+\infty$, i.e.*

$$\lim_{t\to\infty} \|c(t,\cdot) - c_{stat}\|_{L^2}^2 = 0. \tag{4.25}$$

Proof. Let $\tilde{c}(t,\cdot) = c(t,\cdot) - c_{stat}(x) \in H_0^1(\Omega)$. If we subtract (4.24) from (4.15), we obtain

$$\left(\frac{d}{dt}\tilde{c}, w\right) + a(\tilde{c}, w) = 0, \quad w \in H_0^1. \tag{4.26}$$

Choosing $w = \tilde{c}$, we obtain

$$\frac{1}{2}\frac{d}{dt}\|\tilde{c}\|_{L^2}^2 + a(\tilde{c}, \tilde{c}) = 0. \tag{4.27}$$

Using the coercivity (4.20) of the bilinear form a, we deduce

$$\frac{1}{2}\frac{d}{dt}\|\tilde{c}\|_{L^2}^2 + k_a\|\tilde{c}\|_{L^2}^2 \leq 0. \tag{4.28}$$

Thus, the Gronwal Lemma, yields the inequality

$$\|\tilde{c}\|_{L^2} \leq \|\tilde{c}(0)\|_{L^2} e^{-k_a t}, \quad \text{for all } t > 0,$$

which implies that

$$\lim_{t\to\infty} \|\tilde{c}\|_{L^2}^2 = 0.$$

□

Proposition 4.5.3. *For any solution $u_f(t,x)$ of (4.3), with $u_f(0,x) \geq 0$, we have*

$$0 \leq u_f(t,x) \quad (t,x) \in [0,T] \times \Omega.$$

Proof. Similar to (4.2), the governing equation (4.3) of u_f can be written in the form $(L + h)u_f = 0$ where L is a uniformly parabolic operator and function h is bounded on $[0,T] \times \Omega, T > 0$. Then the inequality $u_f(t,x) \geq 0, (t,x) \in [0,T] \times \Omega$, follows from the maximum principle with Neumann boundary conditions [201, Chapt.3, Thm.6 and Remark 2].

□

4.6 The numerical scheme

We use a finite element method to find continuous piecewise polynomial approximations of the solutions $c(t,x)$, $u_f(t,x)$ and $u_c(t,x)$. Denote by $\mathcal{T}(\Omega)$ a triangulation of Ω. A generic element of $\mathcal{T}(\Omega)$ is denoted by K so we have that

$$\Omega = \bigcup_{K\in\mathcal{T}(\Omega)} K.$$

Denote by N_v the number of vertices in $\mathcal{T}(\Omega)$. Let k_c (resp. k_u), be the order of the polynomial approximation of c (resp. u_f and u_c). Then, the approximation, c^h, of c belongs to the space

$$P^h_{k_c} = \{v \in \mathcal{C}^0(\Omega) : v|_K \in \mathbb{P}_{k_c}, K \in \mathcal{T}(\Omega)\},$$

where $\mathbb{P}_k$ denote the set the polynomials of degree k. More precisely, taking into account the homogeneous Dirichlet boundary condtions (4.5), we have that c^h belongs to the space

$$P^h_{k_c,0} = \{v \in P^h_{k_c} : v|_\Gamma = 0\}.$$

A basis for $P^h_{k_c}$ is given in terms of $k_c \times N_v$ linearly independent global shape functions $\psi_{c_i}, i = 1, ..., k_c N_v$, which equal one at node i and zero at all other nodes,

$$P^h_{k_c} = \text{span}\{\psi_{c_i} : i = 1, \ldots, k_c N_v\}.$$

Similarly, introducing $k_u \times N_v$ linearly independent shape functions $\psi_{u_i}, i = 1, ..., k_u N_v$, we define, u^h_f and u^h_c as approximations for u_f and u_c in the space

$$P^h_{k_u} = \{v \in \mathcal{C}^0(\Omega) : v|_K \in \mathbb{P}_{k_u}, K \in \mathcal{T}(\Omega)\} = \text{span}\{\psi_{u_i} : i = 1, \ldots, k_u N_v\}.$$

Then, we seek for approximations c^h, u^h_f, u^h_c of c, u_f, u_c in the form

$$\begin{aligned} c^h(t,x) &= \sum_{i=1}^{k_c N_v} c_i(t)\psi_{c_i}(x), \\ u^h_f(t,x) &= \sum_{i=1}^{k_u N_v} u_{f_i}(t)\psi_{u_i}(x), \\ u^h_c(t,x) &= \sum_{i=1}^{k_u N_v} u_{c_i}(t)\psi_{u_i}(x). \end{aligned} \tag{4.29}$$

In the following we formulate a semi-discrete approximation using the method of lines (MOL) to discretize first in space and then in time. The problem is then reduced to a system of ordinary differential equations in time [203]. Afterwards, different approaches are considered to discretize the problem in time for c, u_f and u_c.

4.6.1 The semi-discrete approximation

Consider the variational formulation (4.15)-(4.17) of the model on each element $K \in \mathcal{T}$. We use the simplified element-wise notations

$$\begin{aligned} c^h(t,x)|_K = c^K(t,x) &= \sum_{j=1}^{n_c^K} c_j^K(t)\phi_{c_j}^K(x), \\ u_f^h(t,x)|_K = u_f^K(t,x) &= \sum_{j=1}^{n_u^K} u_{f_j}^K(t)\phi_{u_j}^K(x), \\ u_c^h(t,x)|_K = u_c^K(t,x) &= \sum_{j=1}^{n_u^K} u_{c_j}^K(t)\phi_{u_j}^K(x), \end{aligned} \tag{4.30}$$

where $\phi_{c_j}^K$ and $\phi_{u_j}^K$ are the base functions on element K, and n_c^K, n_u^K, the number of such functions on K.

Substituting in (4.15)-(4.17) leads to

$$\left\{ \begin{array}{l} \forall w \in P_{k_c,0}^h, \forall v \in P_{k_u}^h, \\ \\ \sum_{j=1}^{n_c^K} \dot{c}_j^K(t) \int_K \phi_{c_j}^K(x) w(x) dx \\ + \sum_{j=1}^{n_c^K} c_j^K(t) \int_K \left(\epsilon^c \nabla \phi_{c_j}^K(x) \cdot \nabla w(x) + (\lambda(x) + \mu^c) \phi_{c_j}^K(x) w(x) \right) dx \\ = \int_K c_{sat} w(x) dx, \\ \\ \sum_{j=1}^{n_u^K} \dot{u_f}_j^K(t) \int_K \phi_{u_j}^K(x) v(x) dx \\ + \sum_{j=1}^{n_u^K} u_{f_j}^K(t) \int_K \left(\epsilon^u \nabla \phi_{u_j}^K(x) \cdot \nabla v(x) - \left(\chi(c) \nabla c(t,x) \phi_{u_j}^K(x) \right) \cdot \nabla v(x) \right) dx \\ = - \sum_{j=1}^{n_u^K} u_{f_j}^K(t) \int_K f(x) \phi_{u_j}^K v(x) dx, \\ \\ \sum_{j=1}^{n_u^K} \dot{u}_{c_j}^K(t) \int_K \phi_{u_j}^K(x) v(x) dx = \sum_{j=1}^{n_u^K} u_{f_j}^K(t) \int_K f(x) \phi_{u_j}^K v(x) dx, \end{array} \right. \tag{4.31}$$

where $\dot{c}_j^K = \frac{\partial c^h(t,x)}{\partial t}|_K, \dot{u}_{c_j}^K = \frac{\partial u_f^h(t,x)}{\partial t}|_K$, and $\dot{u}_{c_j}^K = \frac{\partial u_c^h(t,x)}{\partial t}|_K$.

In particular, (4.31) holds by taking $w(x) = \phi_{c_i}^K(x), i = 1, \ldots, n_c^K$ and $v(x) = \phi_{u_i}^K(x), i = 1, \ldots, n_u^K$, which leads to a linear system for the coefficients in (4.30). Denote by C^K, U_f^K

and U_c^K the vectors of these coefficients on element K, and $\dot{C}^K$, $\dot{U}_f^K$ and $\dot{U}_c^K$ the respective time derivatives. Then the linear system can be written in the form

$$\mathbf{M}_c^K \dot{C}^K + \mathbf{A}_c^K C^K = F_c^K \tag{4.32}$$
$$\mathbf{M}_u^K \dot{U}_f^K + \mathbf{A}_{u_f}^K U_f^K = -\mathbf{R}^K U_f^K \tag{4.33}$$
$$\mathbf{M}_u^K \dot{U}_c^K = \mathbf{R}^K U_f^K \tag{4.34}$$

where:

$$\begin{aligned}
m_{c_{i,j}}^K &= \int_K \phi_{c_j}^K(x)\phi_{c_i}^K(x)dx \\
a_{c_{i,j}}^K &= \int_K \epsilon^c \nabla\phi_{c_j}^K(x)\cdot\nabla\phi_{c_i}^K(x) + (\lambda(x)+\mu^c)\phi_{c_j}^K(x)\phi_{c_i}^K(x)dx \\
f_{c_i}^K &= \int_K c_{sat}\phi_{c_i}^K(x)dx \\
\\
m_{u_{i,j}}^K &= \int_K \phi_{u_j}^K(x)\phi_{u_i}^K(x)dx \\
a_{u_{f\,i,j}}^K &= \int_K \epsilon^u \nabla\phi_{u_j}^K(x)\cdot\nabla\phi_{u_i}^K(x) - \Big(\chi(c)\nabla c(t,x)\phi_{u_j}^K(x)\Big)\cdot\nabla\phi_{u_i}^K(x)dx \\
\\
r_{i,j}^K &= \int_K f(x)\phi_{u_j}^K(x)\phi_{u_i}^K(x)dx
\end{aligned} \tag{4.35}$$

4.6.2 The full discretization

In order to discretize the problem in time, a θ-scheme is considered to solve the equation for c. Concerning u_f, a splitting approach is considered where the diffusion and advection part is also solved using a θ-scheme, while the compartment transfer is solved using a non-standard approach. Since the trapping i.e. the transfer from u_f to u_c happens very fast, using the non-standard approach [179, 7], which replicates qualitatively correctly the dynamics of the equation, has an advantage as it allows to take large values for the trapping rate r.

To simplify the notations, we will omit the index K in the following, but it is assumed that we are dealing with the problem restricted to an element K. Assuming that C_n, U_{f_n} and U_{c_n} are known, we present below the algorithm to compute C_{n+1}, $U_{f_{n+1}}$ and $U_{c_{n+1}}$:

- C_{n+1} is computed using the θ-scheme, by solving

$$\mathbf{M}_c\dot{C}_n \approx \mathbf{M}_c\frac{C_{n+1}-C_n}{\Delta t} = F_c - \mathbf{A}_c\left(\theta C_{n+1} + (1-\theta)C_n\right) \tag{4.36}$$

  If $\theta = 0$, the scheme is fully explicit, while if $\theta = 1$, the scheme is fully implicit. The case $\theta = 1/2$ corresponds to the Crank-Nicolson scheme.

- $U_{f_{n+1}}$ is computed using a splitting approach as in [80]:
  - First we use the θ-scheme to solve the diffusion and the advection parts:

$$\mathbf{M}_u \dot{U}_{f_n} \approx \mathbf{M}_u \frac{U_{f_{n+1}} - U_{f_n}}{\Delta t} = \theta \mathbf{A}_{u_{c,n+1}} U_{f_{n+1}} - (1-\theta)\mathbf{A}_{u_{c,n}} U_{f_n} \tag{4.37}$$

    Denote $U_{f,1}$ the obtained solution.

  - We solve $\mathbf{M}_u \dot{U}_f = -\mathbf{R} U_{f,1}$ inside the traps with a non-standard scheme:

$$\begin{aligned} & \mathbf{M}_u \dot{U}_{f_n} \approx \mathbf{M}_u \frac{U_{f_{n+1}} - U_{f_n}}{\phi(\Delta t)} = -\mathbf{R} U_{f_n,1} \\ \Leftrightarrow \quad & \mathbf{M}_u U_{f_{n+1}} = \mathbf{M}_u U_{f_n} - \phi(\Delta t)\mathbf{R} U_{f_n,1} \end{aligned} \tag{4.38}$$

    with $\phi(\Delta t) = \frac{1-\exp(-Q\Delta t)}{Q}$, where $Q \geq max\{|\lambda|, \lambda \in sp(\mathbf{M}_u^{-1}\mathbf{R})\}$.

- $U_{c_{n+1}}$ is computed using the non-standard scheme:

$$\begin{aligned} & \mathbf{M}_u \dot{U}_{c_n} \approx \mathbf{M}_u \frac{U_{c_{n+1}} - U_{c_n}}{\phi(\Delta t)} = \mathbf{R} U_{f_n,1} \\ \Leftrightarrow \quad & \mathbf{M}_u U_{c_{n+1}} = \mathbf{M}_u U_{c_n} + \phi(\Delta t)\mathbf{R} U_{f_n,1}. \end{aligned} \tag{4.39}$$

  We can remark that the renormalization $\phi(\Delta t)$ of the denominator of the first differences in (4.38) and in (4.39) is such that in the case of one equation, the scheme is exact.

4.7 Numerical simulations

Software such as Freefem [123] are available for solving PDEs using the finite element methods, and offer a wide range of possibilities in terms of numerical integration methods, methods for solving linear systems, mesh generation, or choice for the space of approximation. However, such software may become difficult to use when dealing with parameter identification. Our code is implemented in Scilab [219] and parameter identification is performed by solving a minimization problem using the built-in function, **lsqrsolve** as described in the following section. The graphical representation, for its part, its done in Matlab [171], using the function **tricontour**, developed by D.C. Hanselman, which allows to represent the contours of a solution computed on a triangular mesh. The computations were done on a 64-bit operating system with a Intel core i7 processor and 48 gigabyte ram. In this section, we present numerical simulations obtained by solving problem (4.2)-(4.10) using the numerical method described in the previous section. We use a first order polynomial finite element approximation for c, u_f and u_c, and $\theta = 1/2$ in the θ-scheme.

4.7.1 Description of the experiments and mesh generation

Our experiments are done over a domain rescaled to $[-1,1]\times[-1,1]$. Software, like GMSH [105] or Freefem [123] are useful to perform triangulations of the domain and thus generate the (unstructured) mesh. In our experiments, the mesh is generated using Freefem as it allowed us to validate our Scilab code by comparing our solutions with the solutions generated by Freefem. In these simulations, we focus on the dynamics around the traps. For this reason, we use a non-uniform mesh which is refined around the traps. To do so using Freefem, the number of nodes on a closed curve around each trap is specified. For our experiments, we prescribed to have 40 vertices on a circle with a radius of 0.05 from the centre of the trap, while the radius of the trap is set to $R_T = 0.01$. The refinement of the mesh on the rest of the domain is done by defining the number of vertices wanted on the outer borders of the domain. Figure 4.2 shows the mesh generated by Freefem used in our numerical experiments considering one trap at the centre and $N_{borders} = 30$ vertices on the borders of the domain. The choice of the parameter values as well as the description of the parameters used in the following experiments are presented in Tables 4.1 (on page 131) and 4.2 (on page 133).

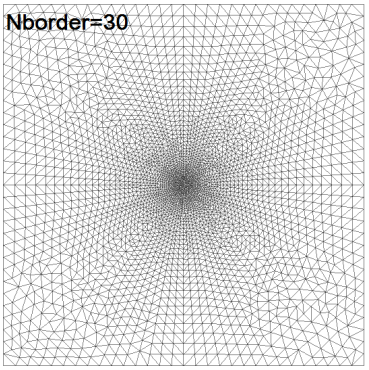

Figure 4.2: Mesh used in the simulation generated by Freefem using 30 nodes on the borders of the domain, and 40 nodes close to the trap. This mesh contains 3451 vertices with a maximum element size of 0.1029 (i.e. maximum distance between two vertices of a triangle).

4.7.2 Numerical simulation for the attractant

In this section, we present numerical simulations of the diffusion of the chemical attractant released at a constant rate from a source located inside the traps. The release rate is defined via (4.1), where Λ is given by (4.40),

$$\Lambda(z) = \begin{cases} (1+\cos(\pi\frac{z}{R_T}))\frac{\lambda_{max}}{2} & \text{if} \quad z < R_T, \\ 0 & \text{otherwise.} \end{cases} \tag{4.40}$$

with λ_{max} being the maximum of λ assumed at the centre of the traps. The values of the parameters used for the simulations are presented in Table 4.1.

Parameter	Value	Description
ϵ^c	0.003	diffusion coefficient of the chemical
μ_c	0.3	vanishing rate of the chemical
c_{sat}	1	saturation constant for the chemical
λ_{max}	1	maximum production of the chemical

Table 4.1: Description of the parameters and (personal) choice of values used in the simulations for the attractant.

Recall that in (4.2)-(4.10), the dynamics of the chemical are independent from the dynamics of the insects. Therefore, $c(t,x)$ can be solved independently, and the solution can be used at each time step to solve $u_f(t,x)$ and $u_c(t,x)$. We give a particular attention to the evolution of the area where the concentration of the chemical is above the threshold c_{min}, as this defines the area where the insects will be attracted to the centre of the trap, i.e. towards the source of the attractant. The evolution of the area of attraction in time is represented in Figure 4.3 for the first five days following the setting of the traps. Two configurations of traps are represented, a case with a single trap at the centre of the domain, and a case using five traps, in the configuration of setting C of [81]. The red line with the "Stat" label defines the area of attraction when $c(t,x)$ is at its stationary state c_{stat} defined in (4.24). We denote by c_{stat} the stationary solution, that is, when $\frac{\partial c}{\partial t} = 0$.

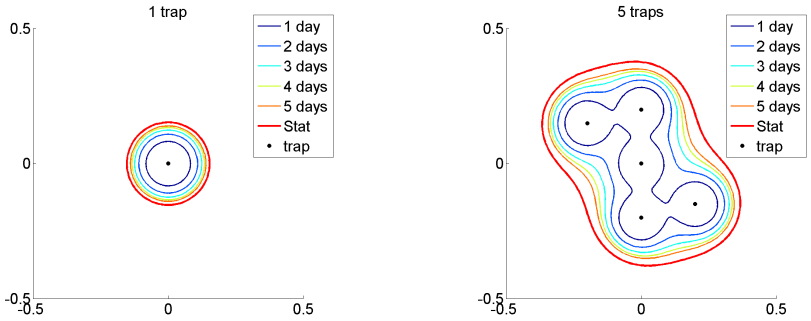

Figure 4.3: Evolution of the area of attraction in time, using one trap on the left, and five traps on the right.

Figure 4.4 represents the spatial distribution of the concentration of the chemical attractant at its stationary state. In particular, the level line corresponding to the threshold concentration c_{min} is highlighted in red to identify the area where the attraction takes place for the two trap settings.

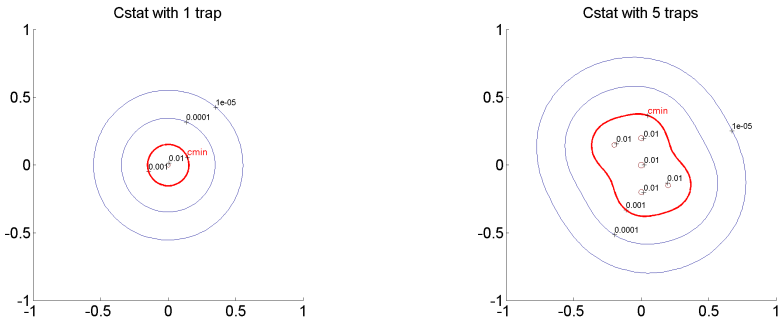

Figure 4.4: Level lines of the distribution of c_{stat}, using one trap on the left, and five traps on the right.

4.7.3 Numerical simulation for the insects

In order to carry out numerical simulations of the dynamics of the free insects $u_f(t,x)$, we first give explicit formulations of the chemotaxis function, χ, as well as the capture function, f, used in these simulations. We consider the function χ in the following form, which is consistent with its properties discussed in section 4.3.2:

$$\chi(c) = \begin{cases} 0 & \text{if} \quad c < c_{min} \\ \frac{\alpha}{\beta^2} \frac{\left(\frac{c-c_{min}}{\beta}\right)^2}{1+\left(\frac{c-c_{min}}{\beta}\right)^2} & \text{if} \quad c_{min} \leq c. \end{cases} \tag{4.41}$$

where α and β belong to $\mathbb{R}^+$. Here the parameter α gives the upper bound of $\chi(c)$, that is, the maximal possible response to the gradient of c, while β determines the speed of transition from no response ($\chi(c) = 0$) to near maximum response (e.g. $\chi(c) \geq 90\%$ of α). Similarly, taking into account its properties discussed in section 4.3.2, we consider the transfer rate f from the free compartment, u_f, to the captured compartment, u_c, as follows:

$$f(x) = r \sum_{T=1}^{N_{traps}} F(\|x - x_T\|_2), \tag{4.42}$$

with

$$F(z) = \begin{cases} 1 & 0 \leq z \leq R_T - \varepsilon \\ e^{1+\frac{\varepsilon^2}{(z-R_T+\varepsilon)^2-\varepsilon^2}} & R_T - \varepsilon < z < R_T \\ 0 & z \geq R_T, \end{cases} \tag{4.43}$$

Indeed, one can see from (4.42)-(4.43) that the transfer occurs only inside the traps, and the capture rate reaches its maximum value, r, in a radius of $R_T - \varepsilon$ around the centre of the traps. Between $R_T - \varepsilon$ and R_T, we observe that as z approaches $R_T - \varepsilon$, $F(z)$ approaches 1, and as z approaches R_T, $F(z)$ approaches 0.

We show numerical simulations assuming that the initial population is distributed homogeneously as well as heterogeneously (in patches). We consider both trap settings of the previous subsection. The values of the parameters related to the dynamics of the insects used in the simulations are presented in Table 4.2.

Parameter	Value	Description
ϵ^u	0.04	diffusion coefficient of the insect
c_{min}	10^{-3}	minimum concentration of the chemical that can be sent by the insects
α	20	chemotaxis coefficient
β	0.001	chemotaxis coefficient
r	1000	trapping rate

Table 4.2: Description of the parameters and (personal) choice of values used in the simulations for the insects.

4.7.3.1 Using u_0 homogeneous

Here, the initial population distribution $u_f(0, x)$ is assumed to be homogeneous over the domain. The evolution of the distribution of the free insects responding to the attractive traps, after one, three and 5 days are represented in Figure 4.5, together with the evolution of the area of attraction. Similarly, Figure 4.6, shows the dynamics of the insects when $c(t, x)$ is assumed to be at its stationary state. In these figures, the attraction of the insects towards the centre of the traps is clearly visible, as we can observe a "sink" effect where the traps are located.

4.7.3.2 Using a heterogeneous distribution for u_0

Assuming the initial insect population to be initially homogeneously distributed over the domain is not very realistic. In this section, we assume that at $t = 0$, the insects are distributed in patches. We consider two initial distributions, represented in Figure 4.7. The first initial distribution consists of two patches with different densities: we assume that the density in the top-left circle patch is three times higher than in the bottom-right square patch. The second one consists of five patches, with different densities. The relative densities between the patches are indicated in brackets.

The numerical simulations using the two trap settings are represented in Figures 4.8 to 4.11 together with the area where the attraction occurs. The CPU time, i.e. the amount of

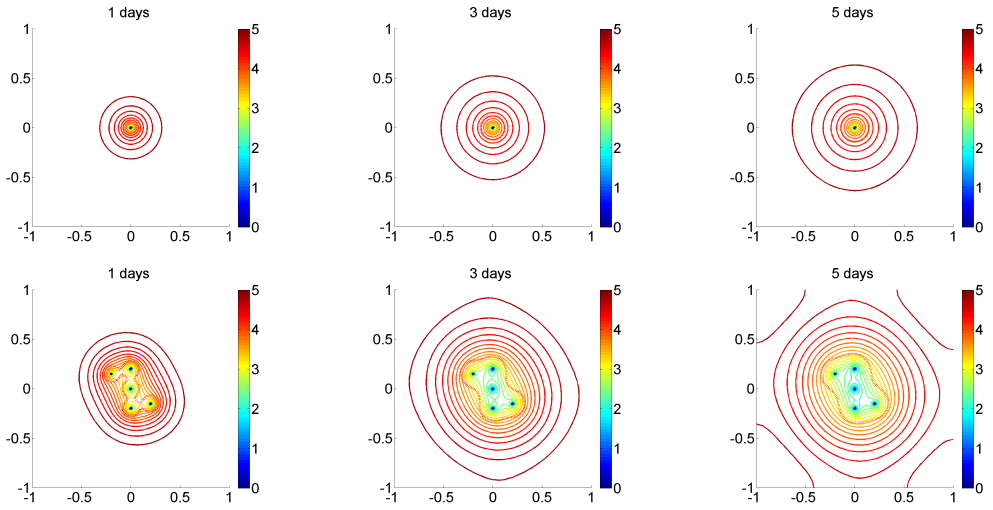

Figure 4.5: Evolution of the distribution of u_f using $c(t,x)$ non-stationary on a homogeneous initial distribution, using a single trap in the first row and five traps in the second row. The red dotted line delimits the attraction area where $c > c_{min}$.

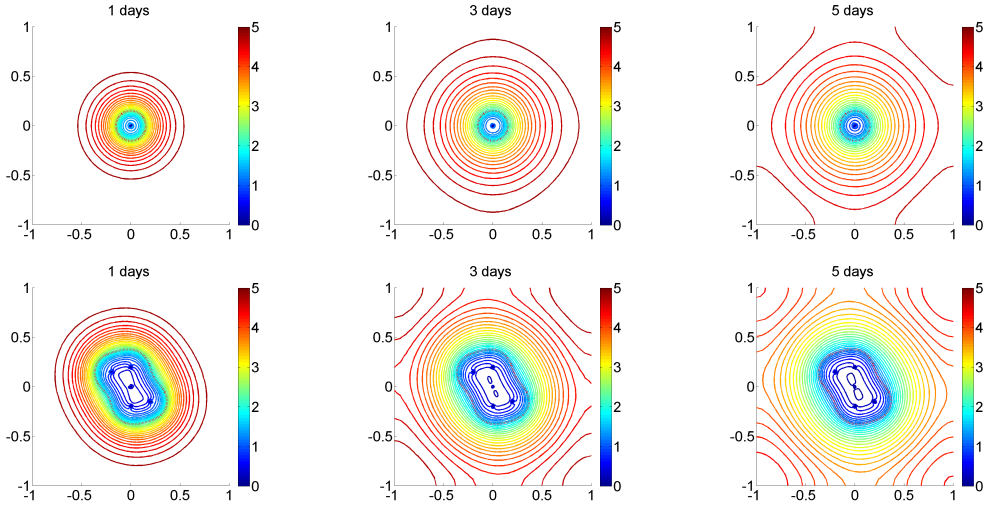

Figure 4.6: Evolution of the distribution of u_f using $c(t,x) = c_{stat}$ stationary on a homogeneous initial distribution, using a single trap in the first row and five traps in the second row. The red dotted line delimits the attraction area where $c_{stat} > c_{min}$.

time needed for the central processing unit to execute the instructions, allows to quantify the computational resources needed to solve the problem. Table 4.3 provides the CPU times required to perform the simulations of u_f over a period of 5 days, using an homogeneous initial distribution as well as the heterogeneous distributions represented in Figure 4.7, using 1 and 5 traps. In the upper part of the table, u_f was computed using the stationary solution,

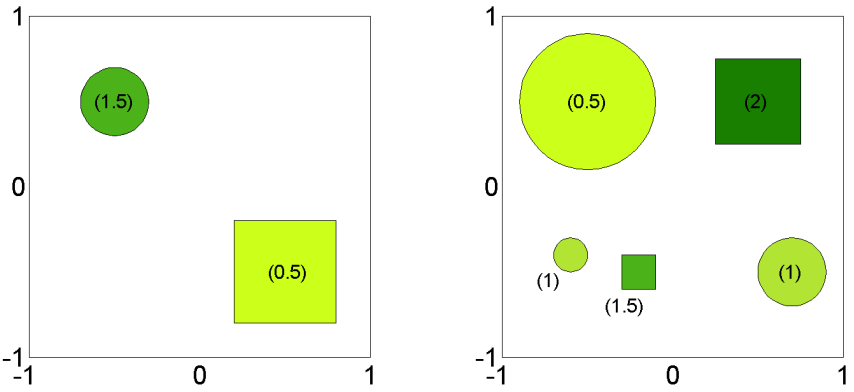

Figure 4.7: Heterogeneous initial distribution $u_f(0,x)$ distributed in two patches (left) and five patches (right). The numbers in brackets give the relative density of insects in each patch.

c_{stat}, of c, whereas in the bottom part, u_f was solved using the time-dependant solution for c. In fact, note that in practice, since c is independent from the insects, it is solved independently prior to the computation of u_f. The numerical results of c at each time step is saved and used accordingly in the computation of u_f. Thus, the results in the bottom section of Table 4.3, do not reflect the computational time required to solve c, but rather the time needed to update the advection part of the finite element matrix used to solve u_f at each time step. In Figures 4.8 and 4.9, the chemical attractant varies in time, whereas, in Figures 4.10 and 4.11, the simulations are done assuming that the chemical attractant is at its stationary state.

	u_0	1 Trap	5 Traps
CPU $u_f(t,x)$ using c_{stat}	homogeneous	45	96
	heterogeneous (2 patch)	44	97
	heterogeneous (5 patch)	45	109
CPU $u_f(t,x)$ using $c(t,x)$	homogeneous	2291	4369
	heterogeneous (2 patch)	2350	4505
	heterogeneous (5 patch)	2314	4536

Table 4.3: CPU times for the numerical simulations over 5 days with $dt = 0.1$, and the mesh with $N_{border} = 30$

.

Table 4.3 reveals that the initial distribution $u_f(0,x)$ has no significant effect on the computation time, however, the CPU time increases as the number of trap increases. Also, the CPU time is considerably increased (by a factor of 50), when u_f is solved coupled with

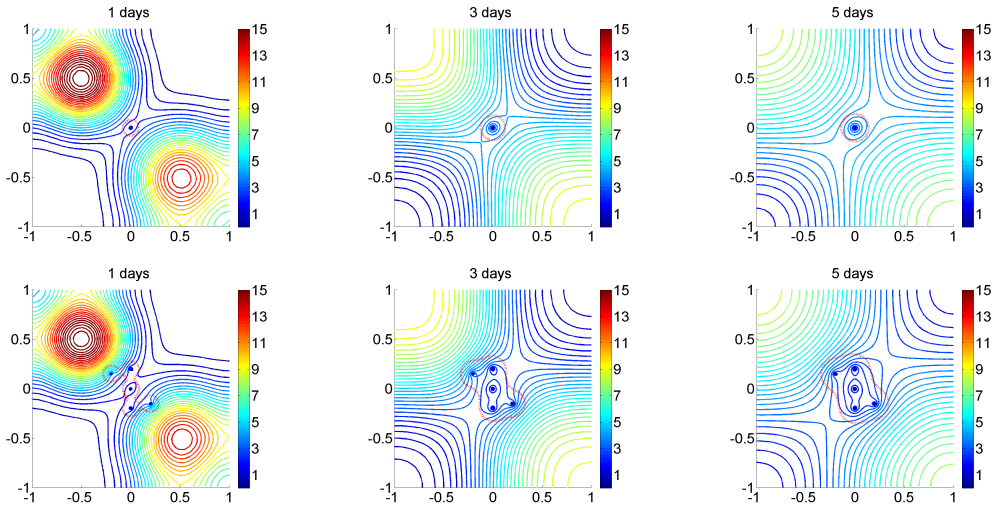

Figure 4.8: Evolution of the distribution of u_f using $c(t,x)$ non-stationary from a initial distribution in two patches, using a single trap in the first row and five traps in the second row. The red dotted line delimits the attraction area where $c > c_{min}$. ($N_{border} = 30$)

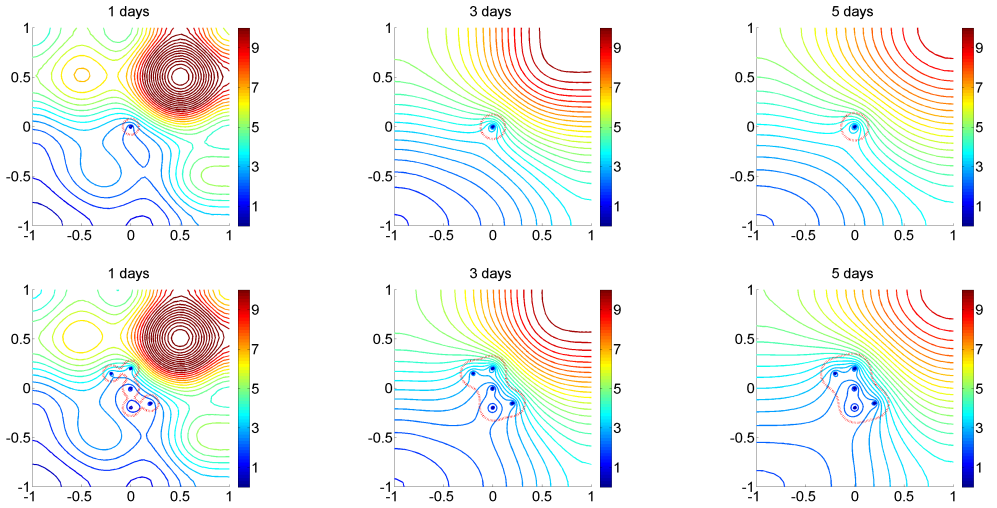

Figure 4.9: Evolution of the distribution of u_f using $c(t,x)$ non-stationary from a initial distribution in five patches, using a single trap in the first row and five traps in the second row. The red dotted line delimits the attraction area where $c > c_{min}$. ($N_{border} = 30$)

$c(t,x)$, instead of c_{stat} which is constant in time. This difference in CPU times is due to the fact that when u_f is solved with c_{stat}, the finite element matrix is constant in time, therefore it is constructed only once, whereas with $c(t,x)$, the advection part of the finite element matrix used to solve u_f has to be constructed at each time step. These results dealing

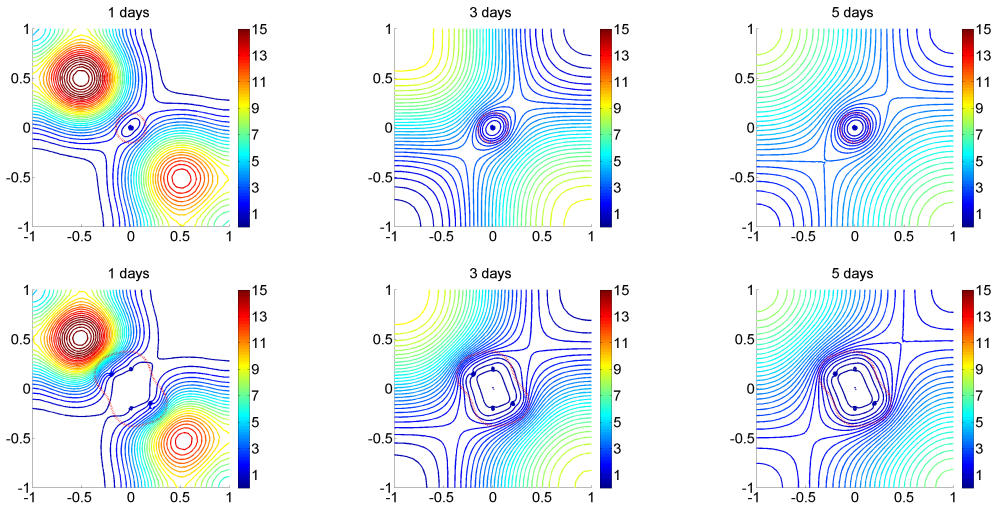

Figure 4.10: Evolution of the distribution of u_f using $c(t,x) = c_{stat}$ stationary from a initial distribution in two patches, using a single trap in the first row and five traps in the second row. The red dotted line delimits the attraction area where $c > c_{min}$. ($N_{border} = 30$)

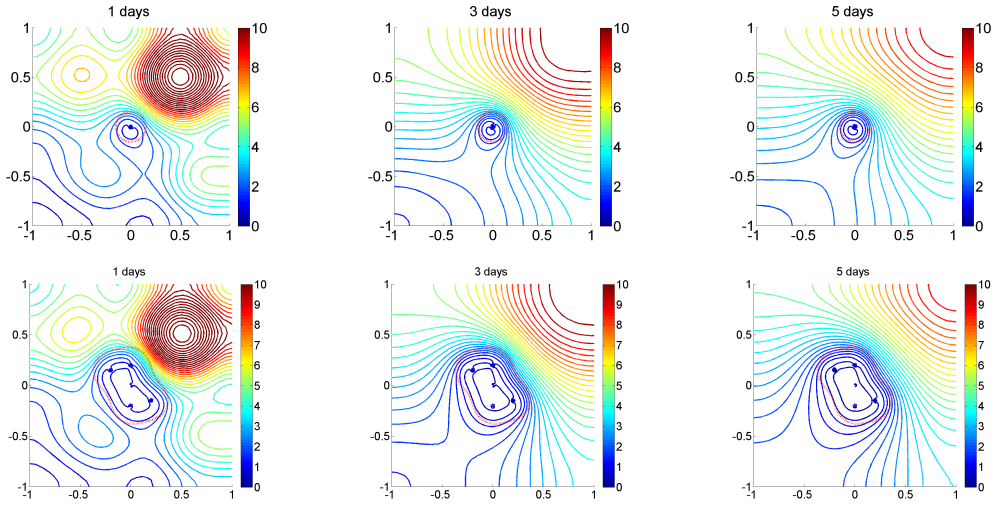

Figure 4.11: Evolution of the distribution of u_f using $c(t,x) = c_{stat}$ stationary from a initial distribution in five patches, using a single trap in the first row and five traps in the second row. The red dotted line delimits the attraction area where $c > c_{min}$. ($N_{border} = 30$)

with computational cost motivate our experiment protocol in the application of the following section when dealing with the estimation of the initial insect population density. Animated graphics are also available at http://linus.up.ac.za/academic/maths/PI/index.html.

4.8 Application to parameter identification

4.8.1 The parameter identification protocol

The objective of this mathematical model with respect to field experiments is to establish the presence of insect population and its density. In the setting of the model (4.2)-(4.10) this is u_0-the space distribution of insects at time $t = 0$ when the traps are put in place. In previous work, the initial population density of insects was estimated assuming that the population was homogeneously distributed [81]. Here, our goal is to estimate the size of the population $U_\Omega = \int\limits_\Omega u_f(0,x)dx$ as we consider a non-homogeneous distribution as well.

As usual for complex models as the model (4.2)-(4.10), in addition to the parameter of interest, that is u_0, there are other parameters with unknown values. Here we attempt to design a feasible protocol to estimate all unknown parameters including u_0. In doing so we need to note first that the solution of (4.2)-(4.10) is not observable in the field. The observable output is the set of the trap counts in all traps at any given time. More precisely, if the observation is at times $t_1, t_2, \ldots, t_K, \quad K \in \mathbb{N}$, the observed quantities are

$$\int\limits_{t=0}^{t_k} \int\limits_{T_j} u_c(t,x)dxdt, \quad j = 1, \ldots, N_{traps}, \quad k = 1, \ldots, K. \tag{4.44}$$

Let us assume that these numbers are arranged in a vector $\Psi = \big(\Psi_1, \ldots, \Psi_{N_{traps}\times K}\big)$. Naturally, with the traps $T_1, \ldots, T_{N_{traps}}$ and the observation times $t_1, t_2, \ldots, t_K$ being fixed, the value of Ψ depends on the value of the model parameters. Using $p = (p_1, \ldots, p_n)$ as a vector of unknown parameters (it can vary from one experiment to another) we have $\Psi = \Psi(p)$. Denote by $\hat{\Psi}$ the values of Ψ observed in a particular field experiment. Then the value of p is identified by solving the problem

$$\min_{p\in(P)} J(p) \tag{4.45}$$

where

$$J(p) = \|\Psi(p) - \hat{\Psi}\|_2^2 \tag{4.46}$$

and $\mathcal{P}$ is a compact subset of $\mathbb{R}^n$ to which p belongs.

While some of the parameters can be obtained with lab experiments, like the minimum threshold c_{min} which could be obtained with flight tunnels experiments, others are not available and need to be estimated together with U_Ω. Thus, here, besides U_Ω, we shall also estimate the diffusion capacity of the insects, ϵ^u, and the parameters of function χ, i.e. α

and β, related to the strength of the attraction of the traps. It is worth mentioning that, on the one hand, α and β are parameters describing the correlation between the attractive potential of the traps and the behaviour of the insects, thus we will refer to these parameters as the "trap-parameters". ϵ^u on the other hand is a specific characteristic of the insects and is not related to the traps. Therefore ϵ^u can be estimated independently from the trap parameters. We propose a chain of experiments which allows the successive estimation of the unknown parameters of the model in three steps (Figure 4.12).

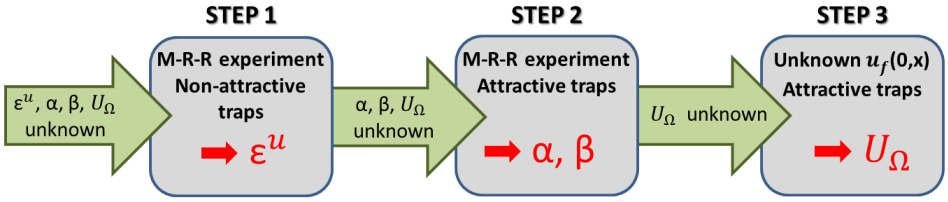

Figure 4.12: Steps of the experimental chain to estimate U_Ω

The first step consists in estimating ϵ^u, using MRR experiment [54] and non-attractive traps such that u_0 is known for all x in Ω and α and β are not needed. It is worth mentioning that if we assume that the traps are not attractive, the problem is reduced to a diffusion-reaction problem, and other approaches may be considered to identify the parameters of such problems. For instance, in [182] the authors reduce such a system of PDEs to a linear system of ODEs with respect to the parameters to identify, allowing parameter identification by means of linear least square procedure. The second step deals with the estimation of α and β. Again, we propose a MRR experiment with attractive traps, such that u_0 is known for all x in Ω. In this setting, we choose to release the marked insects after the installation of the traps, such that $c(t, x)$ is at its stationary state. Finally, U_Ω is estimated using the values of ϵ^u, α and β estimated in the previous steps. Since the dynamics of the insects change when the attractive traps are set, it is necessary to consider the insects' dynamics along with the spread and concentration of the chemical attractant in time.

4.8.2 Description of the numerical experiments and simulations

The global minimisation problem (4.45)-(4.46) is solved iteratively using a random multi-start approach [260] over a set of initial values of $p \in \mathcal{P}$. Function J in the global minimization problem is not available in explicit form. For any given value p of the parameters, $J(p)$ is computed as follows:

1. problem (4.2)-(4.10) is solved via the finite element method as presented in section 4.6 and section 4.7,
2. the integrals (4.44) which gives $\Psi(p)$ are evaluated,
3. the norm in (4.46) is computed.

In connection with part 2 above, we note that the area T_j of the j^{th} trap is not exactly represented in terms of the triangulation $\mathcal{T}(\Omega)$. We approximate the integral with the sum of integrals over all triangles intersecting T_j. This approach also preserves the property $\int_\Omega (u_f(t,x) + u_c(t,x))\,dx = \int_\Omega u_0(x)dx$, that is we have $\int_\Omega \left(u_f^h(t_n,x) + u_c^h(t_n,x)\right)dx = \int_\Omega u_0^h(x)dx$.

For each randomly selected starting value $p^0 \in \mathcal{P}$, a local minimum is found using the nonlinear least square Scilab solver **lsqrsolve** which performs the iterative Levenberg-Marquardt algorithm [169]. The solution of (4.45)-(4.46) is identified as the parameter value corresponding to the smallest local minimum. When several local minima are found, the difference between the values of the objective function of the global minimum and of the next smaller minimum, gives an indication on the robustness of the method and the reliability of the estimate.

We test the proposed protocol and its numerical implementation on simulated data, using a given parameter value $\bar{p} \in \mathcal{P}$ over a period of three or five days depending on the experiment. In the steps of identification of ϵ^u, α and β, random noise is added to the daily capture data, in order to take into account inaccuracy in the data. The noise is a random value selected from a uniform distribution over an interval $[-a, a], \quad a \in \mathbb{R}$. Here we choose $a = 5$. As for the estimation of U_Ω, the field data is simulated using particular distributions of u_0 (Figure 4.20), with $U_\Omega = 20,000$, but the estimations are computed using different distributions of u_0 (Figure 4.21), also with $U_\Omega = 20,000$. Thus, the data reflects the uncertainty in the initial distribution of the insects.

4.8.3 Results and discussion

4.8.3.1 STEP 1: Identification of ϵ^u

In order to estimate the diffusion coefficient of the insects, ϵ^u, we propose a MRR experiment using a non-attractive trap, e.g. a sticky trap. Therefore, the initial density and distribution, u_0, of insects released is known. Further, in the case of non attractive traps, $\chi = 0$ so that ϵ^u is the only unknown parameters. Here we consider releases of insects at

three distances from the trap, 10 meters, 30 meters and 50 meters, as presented in Figure 4.13.

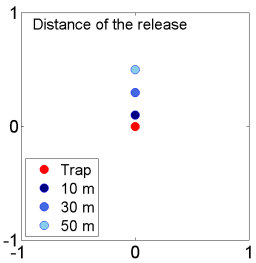

Figure 4.13: Position of the releases relatively to the position of the trap which is represented with a red dot.

Different size of releases, from 500 insects to 8000 insects and observation periods of three and five days were considered. The data is simulated by using random noise as described in section 4.8.2 replicated three or nine times. While solving the minimization problem, a single local minimum was found irrespectively of the starting value used for the algorithm, which suggests that the identifiability of the parameter is satisfied. In other words, there is uniqueness of the estimator of ϵ^u. The simulated cumulative and daily trap counts using a release of 1000 insects are represented in Figure 4.14 considering the different distances from the traps. Note that for other sizes of release similar curve profiles were obtained, differing only by the number of insects captured, thus they are not represented here. From this figure, we notice that the distance plays an important role in the capture dynamics of the insects. Indeed at 10 meters, a large number are captured after one day, while the amount of daily captures decreases afterwards. At 50 meters on the other hand, less insects are captured, and the maximum daily capture is observed after some time, two days here.

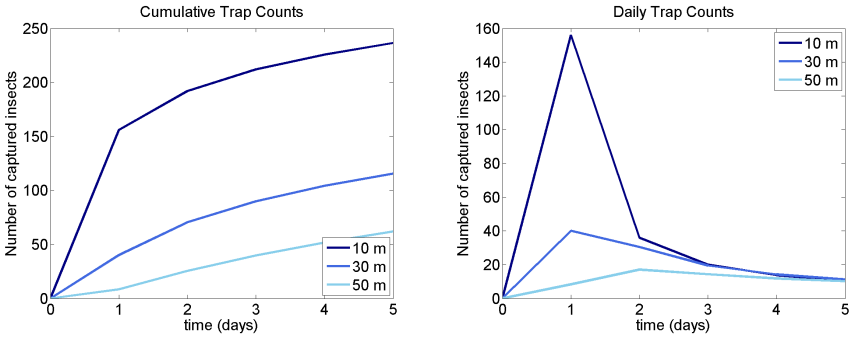

Figure 4.14: Cumulative (left) and daily (right) trap counts obtained for a release of 1000 insects at distances of 10, 30 and 50 meters from the centre of the trap, using non attractive traps.

Release size	Period	repli-cates	Distance to the trap		
			10 m	30 m	50 m
500	3 days	3	0.05043 (26.08%)	0.02553 (36.16%)	0.04801 (20.01%)
		9	0.03737 (6.57%)	0.03319 (17.02%)	0.03299 (17.52%)
	5 days	3	0.04382 (9.56%)	0.02290 (42.74%)	0.05174 (29.36%)
		9	0.03656 (8.59%)	0.03340 (16.49%)	0.03097 (22.57%)
1000	3 days	3	0.04061 (1.51%)	0.04060 (1.50%)	0.03443 (13.92%)
		9	0.04045 (1.11%)	0.03855 (3.62%)	0.04463 (11.57%)
	5 days	3	0.03950 (1.26%)	0.03995 (5.80%)	0.03499 (12.53%)
		9	0.04055 (1.37%)	0.03826 (4.35%)	0.04556 (13.90%)
2000	3 days	3	0.03956 (1.13%)	0.04552 (13.79%)	0.03884 (2.90%)
		9	0.04052 (1.29%)	0.04126 (3.16%)	0.04266 (6.62%)
	5 days	3	0.03957 (1.08%)	0.04212 (5.29%)	0.04015 (0.38%)
		9	0.04020 (0.50%)	0.04010 (0.22%)	0.04351 (8.78%)
4000	3 days	3	0.03984 (0.4%)	0.04023 (0.57%)	0.04020 (0.50%)
		9	0.04003 (0.08%)	0.03936 (1.60%)	0.04082 (2.05%)
	5 days	3	0.03982 (0.46%)	0.04007 (0.18%)	0.03947 (1.32%)
		9	0.04010 (0.25%)	0.03977 (0.57%)	0.04109 (2.73%)
8000	3 days	3	0.03981 (0.48%)	0.03901 (2.46%)	0.04019 (0.48%)
		9	0.04009 (0.22%)	0.04001 (0.03%)	0.04041 (1.02%)
	5 days	3	0.03977 (0.58%)	0.03902 (2.44%)	0.04002 (0.04%)
		9	0.04010 (0.25%)	0.04008 (0.20%)	0.04054 (1.35%)

Table 4.4: Estimate of ϵ^u along with its relative error for using one release of different size over 3-days and 5-days periods, using noisy data averaged over n replicates using a mesh with $N_{border} = 30$. (with cumulative counts).

The estimated values of ϵ^u, with their relative errors for the different combinations of size and position of the release, with period of observation and number of replicates, are presented in Table 4.4 and Figure 4.15. The results show that the size of the release has a significant effect on the accuracy of the estimation of ϵ^u. Indeed, Figure 4.15 shows that the relative error of the estimate decreases as the size of the release increases. For releases of 4000 and 8000 the relative error is below five percent. Moreover, the accuracy of the estimation is affected by the distance of the release to the trap, more precisely, farther releases generate higher relative error in the estimate of ϵ^u, particularly for small releases. For larger size of release, the distance is not a determining factor for accuracy of the estimate. Further, these results show that increasing the length of the observation period does not contribute to better accuracy, on the opposite, adding days of observation, from three days to five days,

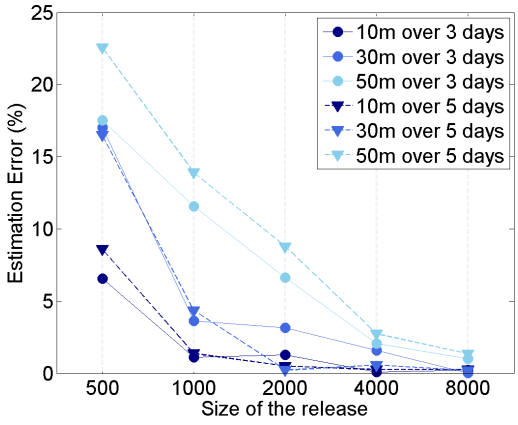

Figure 4.15: Relative error of the estimation of ϵ^u, Table 4.4 using $n = 9$ replicates

produce higher errors in general. Finally, Table 4.4 highlights the importance of replicates when doing the experiments. In particular, small insect populations are more sensitive to noise leading to a large uncertainty in the estimations, e.g. relative errors up to 36.16% are found when considering only three replicates with a population of only 500 insects.

4.8.3.2 STEP 2: Identification of α and β

In this step we proceed to the estimation of the trap parameters α and β which describe the attraction of the trap. As for step 1, MRR experiments are considered using attractive traps. Thus, u_0 is known and after step 1, so is an estimation of the value of ϵ^u. Following a similar protocol as in step 1, α and β are estimated using sizes of release varying from 500 to 8000 insects at distances of 10, 30 and 50 meters from the trap, over observation periods of three and five days. The positions of the releases are represented in Figure 4.16 together with the level lines of the distribution of the chemical attractant. In particular, the threshold level line c_{min} is represented by the red line. The data is simulated by using random noise as described in section 4.8.2 replicated nine times. Here we consider the estimation of parameters α and β estimated independently, as well as simultaneously.

The simulated cumulative and daily trap counts using a release of 1000 insects at distances of 10, 30 and 50 meters are represented in Figure 4.17. Note that similar curves were obtained for other sizes of release differing by the number of insects captured, and therefore are not represented here. We may note that the number of captured insects is substantially larger (here, roughly by a factor of 3), when using attractive traps (Figure 4.17), compared to non-attractive traps (Figure 4.14). Table 4.5 and Table 4.6 gather the results of the individual estimations of α and β, respectively, that is, assuming that the other parameter is known.

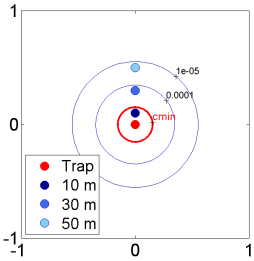

Figure 4.16: Representation of position of the releases relatively to the position of the trap which is represented with a red dot together with the level lines of the distribution of the chemical attractant. The level line c_{min} is represented by the red line.

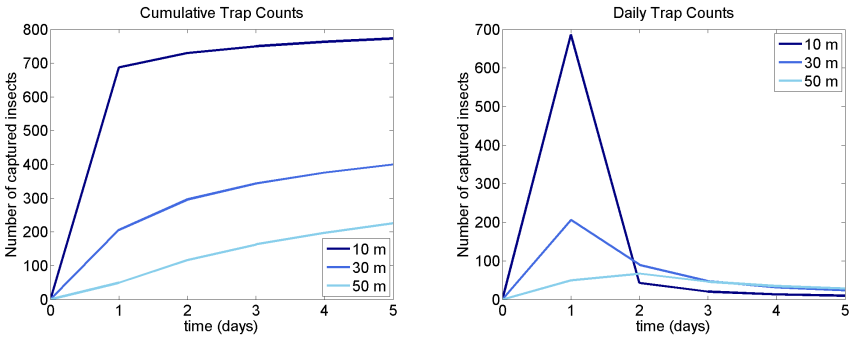

Figure 4.17: Cumulative (left) and daily (right) trap counts obtained for a release of 1000 insects at distances of 10, 30 and 50 meters from the centre of the trap, using $c = c_{stat}$.

The presented results are computed for varying size of the release, its distance to the trap as well as the period of collection of trap data. Graphical representation of the results in Table 4.5 and Table 4.6 is given in Figure 4.18.

The accuracy of the parameter estimation improves with the increase of size of the release and period of capture of data. One can further observe that the accuracy of the estimation is improved with proximity of the release to the trap which reflects the positive impact of the number of captured insects (see also Figure 4.14).

As expected, the errors of approximation are larger compared to the case of estimating single parameter at a time. The decreasing trend of the errors with respect to the size of the release is similarly well pronounced. One cannot observe a definite trend with respect to distance from the trap and period of observation indicating that the family of functions χ possibly should be parametrized in a different way. However, it is clear from Figure 4.19 that when α and β are simultaneously estimated (compared to their individual estimation), a larger release size is required for similar level of accuracy.

Release size	Period	Distance to the trap		
		10 m	30 m	50 m
500	3 days	20.0464 (0.23%)	20.1068 (0.53%)	20.2516 (1.25%)
	5 days	20.0030 (0.01%)	19.9976 (0.01%)	19.9688 (0.16%)
1000	3 days	20.0232 (0.12%)	20.0533 (0.27%)	20.1252 (0.63%)
	5 days	20.0015 ($< 10^{-2}$%)	19.9988 ($< 10^{-2}$%)	19.9844 (0.08%)
2000	3 days	20.0116 (0.06%)	20.0266 (0.13%)	20.0624 (0.31%)
	5 days	20.0007 ($< 10^{-2}$%)	19.9994 ($< 10^{-2}$%)	19.9922 (0.04%)
4000	3 days	20.0058 (0.03%)	20.0133 (0.07%)	20.0312 (0.16%)
	5 days	20.0004 ($< 10^{-2}$%)	19.9997 ($< 10^{-2}$%)	19.9961 (0.02%)
8000	3 days	20.0029 (0.01%)	20.0067 (0.03%)	20.0156 (0.08%)
	5 days	20.0002 ($< 10^{-2}$%)	19.9999 ($< 10^{-2}$%)	19.9981 ($< 10^{-2}$%)

Table 4.5: Identification of α. Average CPU time for the estimation of 1 local minimum, using 3 days: 370, using 5 days: 604.

Release size	Period	Distance to the trap		
		10 m	30 m	50 m
500	3 days	0.0009943 (0.57%)	0.0009872 (1.28%)	0.0009697 (3.03%)
	5 days	0.0009997 (0.03%)	0.0010005 (0.05%)	0.0010042 (0.42%)
1000	3 days	0.0009971 (0.29%)	0.0009360 (0.64%)	0.0009848 (1.52%)
	5 days	0.0009998 (0.02%)	0.0010002 (0.02%)	0.0010021 (0.21%)
2000	3 days	0.0009986 (0.14%)	0.0009968 (0.32%)	0.0009924 (0.76%)
	5 days	0.0009999 ($< 10^{-2}$%)	0.0010001 (0.01%)	0.0010011 (0.11%)
4000	3 days	0.0009993 (0.07%)	0.0009984 (0.16%)	0.0009962 (0.38%)
	5 days	0.0010000 ($< 10^{-2}$%)	0.0010001 ($< 10^{-2}$%)	0.0010005 (0.05%)
8000	3 days	0.0009996 (0.04%)	0.0009992 (0.08%)	0.0009981 (0.19%)
	5 days	0.0010000 ($< 10^{-2}$%)	0.0010000 ($< 10^{-2}$%)	0.0010003 (0.03%)

Table 4.6: Identification of β. Average CPU time for the estimation of 1 local minimum, using 3 days: 407, using 5 days: 619.

4.8.3.3 STEP 3: Identification of U_Ω

At this stage, U_Ω, the initial population size, is the only remaining parameter to be estimated since the estimations of ϵ^u, α and β are can be obtained from the previous steps. However, for the sake of testing the estimation of U_Ω and avoid bias from the errors of the previous estimates, we use the real values of ϵ^u, α and β (Table 4.2, page 133). The response of the insects to the spread of the chemical attractant is governed by the coupled model

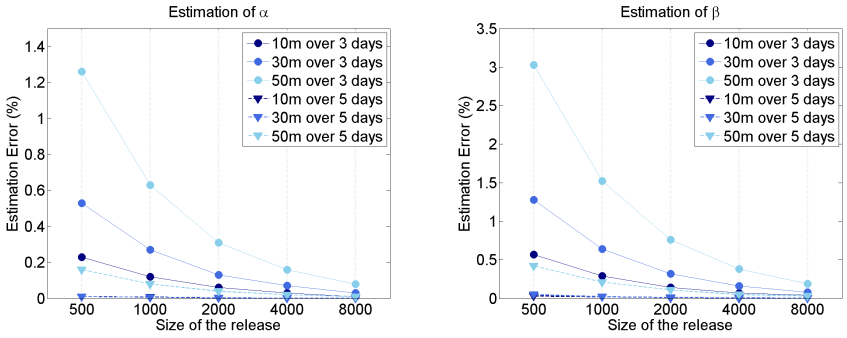

Figure 4.18: Relative error of the estimation of α (left) and β (right), when the two parameters are estimated independently.

Release size	Distance	$\tilde{\alpha}$	$\tilde{\beta}$
500	10 m	18.3877 (8.06%)	0.0007848 (21.52%)
	30 m	19.0532 (4.73%)	0.0008714 (12.86%)
	50 m	19.8727 (0.64%)	0.0009543 (4.57%)
1000	10 m	19.1151 (4.42%)	0.0008848 (11.52%)
	30 m	19.5047 (2.48%)	0.0009336 (6.64%)
	50 m	19.9358 (0.32%)	0.0009770 (2.30%)
2000	10 m	19.5348 (2.33%)	0.0009403 (5.97%)
	30 m	19.7465 (1.27%)	0.0009662 (3.38%)
	50 m	19.9677 (0.16%)	0.0009885 (1.15%)
4000	10 m	19.7613 (1.19%)	0.0009696 (3.04%)
	30 m	19.8717 (0.64%)	0.0009830 (1.70%)
	50 m	19.9838 (0.08%)	0.0009942 (0.58%)
8000	10 m	19.8791 (0.60%)	0.0009846 (1.54%)
	30 m	19.9355 (0.32%)	0.0009915 (0.85%)
	50 m	19.9919 (0.04%)	0.0009971 (0.29%)

Table 4.7: Estimations of α and β, when estimated simultaneously, for a period of 3 days. Average CPU time for the estimation of 1 local minimum: 8383.

(4.2)-(4.10). Naturally here, $c(t, x)$ is assumed non-stationary. In a previous work [81], the population was assumed to be homogeneously distributed over the domain while performing the parameter identification of the initial population density. Here, as mentioned in section 4.8.2, the field data is simulated using three particular distributions of u_0 (Figure 4.20): (1) a homogeneous distribution, (2) a "aligned orchard" distribution and (3) a "isolated trees" distribution.

Release size	Distance	$\tilde{\alpha}$	$\tilde{\beta}$
500	10 m	22.7231 (13.62%)	0.0013101 (31.01%)
	30 m	22.4039 (12.02%)	0.0012679 (26.79%)
	50 m	26.0284 (30.14%)	0.0016303 (63.03%)
1000	10 m	21.1884 (5.94%)	0.0011410 (14.10%)
	30 m	21.0901 (5.45%)	0.0011254 (12.54%)
	50 m	22.4223 (12.11%)	0.0012744 (27.44%)
2000	10 m	20.5588 (2.79%)	0.0010675 (6.75%)
	30 m	20.5211 (2.61%)	0.0010608 (6.08%)
	50 m	21.1059 (5.53%)	0.0011294 (12.94%)
4000	10 m	20.2714 (1.36%)	0.0010331 (3.31%)
	30 m	20.2549 (1.27%)	0.0013000 (3.00%)
	50 m	20.5302 (2.65%)	0.0010630 (6.30%)
8000	10 m	20.1338 (6.69%)	0.00101064 (1.64%)
	30 m	20.1261 (6.31%)	0.0010149 (1.49%)
	50 m	20.2587 (1.30%)	0.0010311 (3.11%)

Table 4.8: Identification of α and β simultaneously for a period of 5 days. Average CPU time for the estimation of 1 local minimum: 10808.

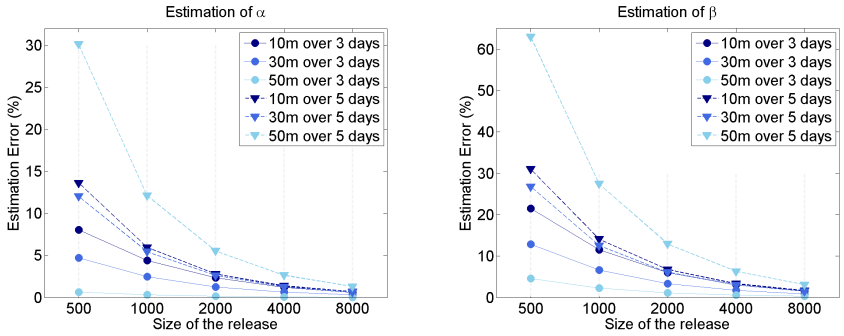

Figure 4.19: Relative error of the estimation of α and β, when the two parameters are estimated simultaneously.

However, the estimation of U_Ω is computed using different distributions of u_0, based on some ecological and entomological knowledge on the insects. These distributions are represented in Figure 4.21 and consist of a homogeneous distribution (A), a four-patch distribution (B), a sixteen-patch distribution (C) similar to (B) where each patch is subdivided into four patchs. Distributions (D1) and (D2) where insects are initially distributed in the four corners of the domain, and its complementary distribution where the insects are distributed in a cross-shape manner.

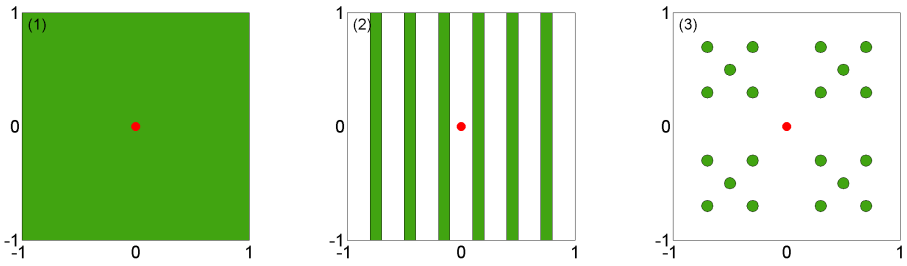

Figure 4.20: Population distribution used to generate trap data

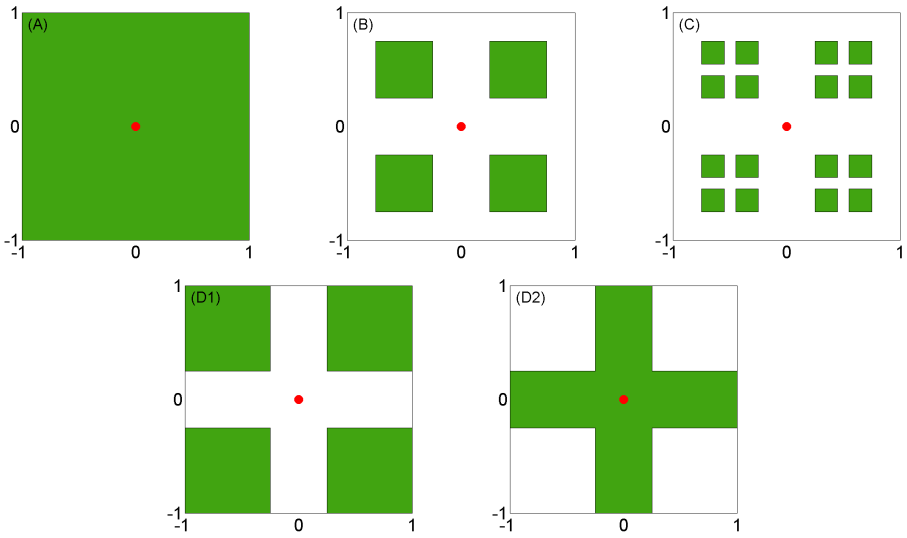

Figure 4.21: Initial population distributions used to identify U_Ω

The profile curves of the cumulative and daily trap counts are are represented in Figure 4.22, over a period of five days, and assuming that the initial population size is $U_\Omega = 20,000$ insects on the domain. The plain lines represent the field data generated using the distribution (1)-(3), while the trap counts using the initial distribution used for the estimations, (A)-(D2), are represented with the dotted lines. These graphs highlight the importance of heterogeneity of the distribution of the insects over the domain as different initial distributions exhibit different trap count profiles. Indeed, if the trap is located near an area where the abundance of the insects is high, such as for the case (D2), the traps have higher capture rates during the first days, whereas if the insects are initially far from the trap, like for (3),(A),(B),(C) and (D1), the capture rate is low at first, and increases progressively over the five days of capture.

The estimation of U_Ω is computed assuming that the real size of the population is $U_\Omega = 20,000$, and using three days of capture data, as well as five days. The results are recorded in Table 4.9 (resp. Table 4.10), for field data computed using the distributions (1) to (3) (Figure

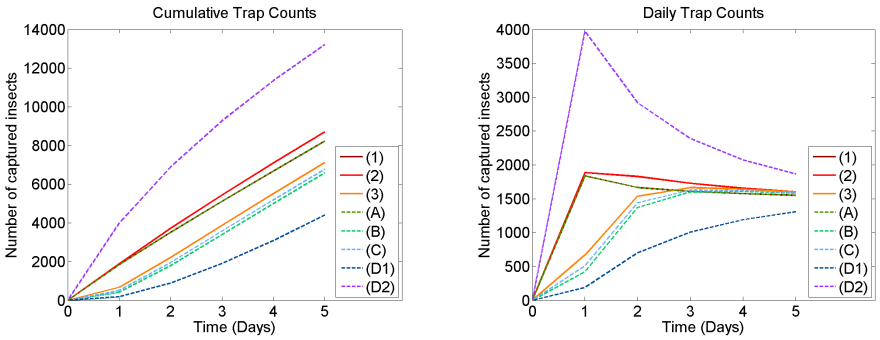

Figure 4.22: Cumulative and daily trap counts obtained with the initial distribution used to generate the data, (1)-(3) (represented by the plain lines), and with the initial distributions used to estimate the initial population size, (A)-(D1) (represented by the dotted lines), using $U_\Omega = 20,000$.

		Data distributions		
		(1)	(2)	(3)
Guessed distribution	(A)	20,000 (0%)	21,178 (5.89%)	16,109 (19.46%)
	(B)	26,914 (34.57%)	28,506 (42.53%)	22,058 (10.29%)
	(C)	25,962 (29.81%)	27,498 (37.49%)	21,244 (6.22%)
	(D1)	41,990 (109.9%)	44,466 (122.3%)	34,644 (73.22%)
	(D2)	11,639 (41.80%)	12,324 (38.38%)	9,296 (53.52%)

Table 4.9: Estimation of U_Ω using 3 days, with $\bar{U}_\Omega = 20,000$. The columns indicate the initial distribution of the insects used to generate the data, (1)-(3), while the lines correspond to the guessed initial distribution of the population used when performing the parameter identification of U_Ω. Average CPU time for the estimation of one local minimum: 27896.

		Data distributions		
		(1)	(2)	(3)
Guessed distribution	(A)	20,000 (0.00%)	21,575 (7.87%)	15,681 (21.60%)
	(B)	28,261 (41.31%)	30,487 (52.44%)	22,705 (13.52%)
	(C)	26,957 (34.78%)	29,080 (45.40%)	21,603 (8.02%)
	(D1)	49,655 (148.27%)	53,560 (167.80%)	40,141 (100.71%)
	(D2)	11,044 (44.78%)	11,913 (40.43%)	8,585 (57.07%)

Table 4.10: Estimation of U_Ω using 5 days, with $\bar{U}_\Omega = 20,000$. The columns indicate the initial distribution of the insects used to generate the data, (1)-(3), while the lines correspond to the guessed initial distribution of the population used when performing the parameter identification of U_Ω. Average CPU time for the estimation of one local minimum: 46767.

4.20), and estimating U_Ω the initial distributions (A) to (D2) (Figure 4.21) using a the three days (resp. five days). As expected, the estimation using experiment (1)-(A) produces the correct value of U_Ω. Then, we have that if the field data is generated using (2) the size of the population is better estimated using the homogeneous distribution (A) rather than any of the other distributions. As for field data generated using (3), the estimations are better as the initial distribution is closer to the real distribution. More precisely, the best distribution to estimate U_Ω when the field data is generated using (3) is distribution (C) which provides an estimate 6.22% relative error for five days of data. These estimations show clearly the influence of the initial distribution of the population in the global minimization searching algorithm. Indeed a bad choice for the distribution of u_0 leads to very inaccurate estimation of the population size. These results suggest that a reliable estimate the population size depends on the knowledge and understanding of the ecology of the insects. In other words, ecological knowledge, such as interactions between the insect and the vegetation, as well as entomological knowledge on the insect is crucial to obtain an accurate estimate of the population size.

Further, the results of Table 4.9 and Table 4.10 suggest that considering a period of five days produces more accurate estimations. However, if the initial distribution used for the estimation is close enough to the real distribution, a period of three days would allow accurate estimations while using less computational resources. We can remark that the average CPU time required to compute one estimation of U_Ω, using three days is 27896, while it increases to 46767 using five days of observation. As expected from the results on the computational costs in subsection 4.7.3.2, we note that the CPU times are considerably increased when c is used compared to c_{stat}. Indeed we mentioned that when the solution is computed with c, the finite element matrix used to solve u_f has to be computed at each time step. Since the parameter identification process consists of computing the solutions iteratively with many starting values, the estimation of parameters using c is considerably more computational intensive than when c_{stat} is used. The average CPU time for the computation of a single local minimum for the estimation of U_Ω using five days of data was 46767, while it was 604 (resp. 619) for the independent estimation of α (resp. β), that is more than 75 times more computational costly.

4.9 Conclusion

When dealing with pest or vector control, estimating the insect population density and distribution is one of the main concerns to plan efficient field intervention. Traps are usually used to collect information in order to estimate the population. The present work aims

to estimate insect population size using attractive traps. In that matter, we use a model of coupled partial differential equations which relate the spread of a chemical attractant released from the traps to the dynamics of the insects responding to it via a chemotaxis process. This model consists of a system of advection-diffusion-reaction equations whose solution is computed numerically using finite element approach. Hence, the problem is considered in its variational form. In this context, we ensure the well-posedness of the variational problem, and provide theoretical qualitative results on the solutions.

Numerical simulations are done on a domain discretized by triangular elements, refined around the traps, generated by the software Freefem [123]. Simulations of the spread of the chemical attractant allow us to follow the evolution of the active area of the trap, until $c(t, x)$ reached its stable stationary state c_{stat}. Then, the dynamics of insects are simulated using the non-stationary state of $c(t, x)$, as well as its stationary state, c_{stat}, on homogeneous and patchy initial distributions of the population u_0.

This model is applied to the problem of identifying parameter values of the model, among which the population size, U_Ω over the domain, but also the diffusion rate of the insects, ϵ^u, and trap-related parameters involved in the chemotaxis process. For this purpose, we proposed a protocol chain in three steps which enable the identification of each of these parameters using a single trap. First, ϵ^u is estimated using MRR experiments with non-attractive traps. Then, using the value of ϵ^u, attractive traps are used with MRR experiments to estimate the chemotaxis parameters. Note that in this paper, we considered a family of chemotaxis functions of two dependent variables, namely, α and β. Finally, U_Ω is identified using the estimated value of the other unknown parameters, considering different possible initial distribution of the insect population u_0. As a result we show the positive effect of longer period of data collection and of the size of the release on the quality of the estimation of ϵ^u, α and β as well as the positive effect of proximity of the release to the trap when the chemotaxis parameters are estimated one at a time. However, when α and β are estimated simultaneously, no definite trend could be establish relating the quality of the estimation to the period of data collection and distance of the release from the trap. Nevertheless, similar level of accuracy as for the estimation of one parameter at a time can be obtained by increasing the size of the release.

This work suggests an optimized field protocol to estimate insect population size, although several aspects are worth further investigation for more realistic results. For instance, the boundary conditions used here are quite restrictive as we assume no emigration and no immigration of the insects. More complex boundary conditions, involving flux at the boundary, such as Robin boundary conditions would be more realistic. Also, the compartmental approach for the free insects and the captured insects requires to define a transition process for insects to be captured. A more realistic way to model the trapping process could be to

consider a trap as hole in the domain. Then, appropriate boundary conditions at the border of the trap would allow to capture its properties.

Further, in this model, the parameters are taken constant in time and space. Under the condition that the experiments take place over a small period of time, during which the parameters do not experience much variations (related for instance to temperature, humidity, etc.), it is relevant to assume that the parameters are constant with respect to the time variable. However, some of the parameters such as the diffusion and the advection coefficients may vary in space if the landscape is heterogeneous. Thus, a step forward to be considered in this model, would be to enable links with GIS data. This would require to consider other programming language than Scilab, for faster computations, such as C++, Fortran, etc. Ultimately, validation of the model using real field data would assess the efficacy for the method.

Acknowledgement

The authors would like to thank the reviewers for their constructive comments. This work has been supported by the National Research Foundation, the French Ministry of National Education, Higher Education and Research, and the French Ministry of Foreign Affairs and International Development in the framework of the PHC PROTEA 2015 call. This work was also partly supported by the SIT phase 2 pilot program in Réunion, jointly funded by the French Ministry of Health and the European Regional Development Fund (ERDF) under the 2014-2020 Operational Programme.

Chapter 5

Mathematical model for pest-insect control using mating disruption and trapping

This work has been submitted to

R. Anguelov, C. Dufourd and Y. Dumont, Mathematical model for pest-insect control using mating disruption and trapping, Applied Mathematical Modelling

5.1 Abstract

Controlling pest insects is a challenge of main importance to preserve crop production. In the context of Integrated Pest Management (IPM) programs, we develop a generic model to study the impact of mating disruption control using an artificial female pheromone to confuse males and adversely affect their mating opportunities. Consequently the reproduction rate is diminished leading to a decline in the population size. For more efficient control, trapping is used to capture the males attracted to the artificial pheromone. The model, derived from biological and ecological assumptions, is governed by a system of ODEs. A theoretical analysis of the model without control is first carried out to establish the properties of the endemic equilibrium. Then, control is added and the theoretical analysis of the model enables to identify threshold values of pheromone which are practically interesting for field applications. In particular, we show that there is a threshold above which the global asymptotic stability of

the trivial equilibrium is ensured, i.e. the population goes to extinction. Finally we illustrate the theoretical results via numerical experiments.

5.2 Introduction

Pest insects are responsible for considerable damages on crops all over the world. Their presence can account for high production losses having repercussions on trading and exports as well on the sustainability of small farmers whose incomes entirely rely on their production. Exotic pests, can be particularly harmful as they can exhibit high invading potential due to the lack of natural enemies and their capacity to adapt to wide range of hosts and/or climate conditions. Therefore, pest management is essential to prevent devastating impact on economy, food security, social life, health and biodiversity.

Chemical pesticides have long been used to control pest populations. However, their extensive use can have undesired side effects on the surrounding environment, such as reduction of the pest's natural enemies and pollution. Further, the development of insect resistance to the chemical lead to the need of using stronger and more toxic pesticides to maintain their efficacy. Thus, extensive use of pesticides is not a sustainable solution for pest control. Constant efforts are being made to reduce the toxicity of the pesticides for applicators and consumers, and alternative methods are being developed or improved to satisfy the charter of Integrated Pest Management (IPM) programs [9]. IPM aims to maintain pest population at low economic and epidemiological risk while respecting specific ecological and toxicological environmentally friendly requirements.

The Sterile Insect Technique (SIT), Mass Annihilation Technique (MAT) or mating disruption are examples of methods part of IPM strategies. SIT consists in releasing large numbers of sterilised males to compete with wild males for female insemination, reducing the number of viable offspring, while MAT consists in reducing the number of one or both sexes by trapping using a species-specific attractant. Pheromones or para-pheromones are often used to manipulate the behaviour of a specific species [256, 135]. In this work, particular interest is given to mating disruption control which aims to obstruct the communication among sexual partners using lures to reduce the mating rate of the pest and thus lead to long-term reduction of the population [47].

Mating disruption using pheromones has been widely studied to control moth pests [21, 48] on various types of crops. An early demonstration of the applicability of MAT has been shown for the eradication of *Bactrocera doraslis* in the Okinawa Islands in 1984 [152]. More recently, the method has shown to be successful for the control of *Tuta absoluta* on tomato crops in Italian greenhouses [58]. Other successful cases are reported in [48], such as for the control of the pink bollworm *Pectinophora gossypiella* which attacks cotton, or the apple codling moth *Cydia pomonella*. However, mating disruption has sometimes been a failure as for the control of the coffee leaf miner *Leucoptera coffeela* [4] or for the control of the tomato pest

Tuta absoluta mentioned above in open field conditions [178] where mating disruption did not manage to reduce the pest population. According to [4, 178], the failure of the method may be attributed to composition and dosage of the pheromone and/or to a high abundance of insects. For mating disruption success, understanding the attraction mechanisms of the pest to the pheromone is important, like the minimum level response, the distance of attraction or the formulation of the pheromone used. Environmental constrains are also crucial factors to take into account. These include the climate, the wind, the crop's foliage, etc. Further, the population size must be accounted for in order to design appropriate control strategies. Thus, planning efficient and cost effective control is a real challenge which can explain the failure of the experiments mentioned above. Mathematical modelling can be very helpful to get a better understanding on the dynamics of the pest population, and various control strategies can be studied to optimise the control. Here we combine mating disruption using female-sex pheromones lures to attract males away from females in order to reduce the mating opportunities adversely affecting the rate reproduction. For more efficient control, lures can be placed in traps to reduce the male population. In 1955, Knipling proposed a numerical model to assess the effect of the release of sterile males on an insect population where the rate of fertilisation depends on the density of fertile males available for mating [146]. It is worth mentioning that in terms of modelling significant similarities can be found between MAT control and SIT control as the purpose of both methods is to affect the capacity of reproduction of the species. In the seminal works of Knipling et al. [150, 149], several approaches for the suppression of insect populations among which MAT and SIT. Further, an overview on the mathematical models for SIT control which of relevance to mating disruption control can be found in [86, Chapter 2.5].

In this paper we built a generic model for the control of a pest population using mating disruption and trapping to study the effort required to reduce the population size below harmful level. The model is derived using general knowledge or assumptions on insects' biology and ecology. We consider a compartmental approach based on the life cycle and mating behaviour to model the temporal dynamics of the population which is governed by a system of Ordinary Differential Equations (ODE). A theoretical analysis of the model is carried out to discuss the efficiency of the control using pheromone traps depending on the strength of the lure and the trapping efficacy. In particular we study the properties of the equilibria using the pheromone as a bifurcation parameter. We identify two threshold values of practical importance. One corresponds to the minimum amount of lure required to affect the female population equilibrium, while the second one is the threshold above which extinction of the population is achieved. We also show that on small enough populations, at invasion stage for instance, extinction may be achieved with a small amount of lure. We also show that combining mating disruption with trapping significantly reduces the amount of pheromone needed to obtain a full control of the population. The modelling approach

for mating disruption control considered in [18, 20, 98] where MAT control is modelled via discrete density-dependent models. In the later, the authors identified a threshold value for the amount of pheromones above which the control of an insect population is possible. Similar qualitative results may be found in [17] in the case of SIT control, however not presented as in such depth as in the present study.

In the first section, we give a description of the model without control and analyse it theoretically. In the following section we describe the model with control. To model the impact of the mating disruption, we use a similar approach as the one proposed by Barclay and Van den Driessche [18], where the amount of the artificial pheromone is given in terms of equivalent number of females. The model is studied theoretically, identifying threshold values which determine changes in the dynamics of the population. Finally, we perform numerical simulations to illustrate the theoretical results and we discuss their biological relevance.

5.3 The compartmental model for the dynamics of the insect

We consider a generic model to describe the dynamics of a pest insect population based on biological and behavioural assumptions. For many pest species, such as fruit flies or moths, two main development stages can be considered: the immature stage, denoted I, which gathers eggs, larvae and pupae, and the adult stage. Typically, the adult female is the one responsible for causing direct damage to the host when laying her eggs. We split the adult females in two compartments, the females available for mating denoted Y, and the fertilised females denoted F. We assume that a mating female needs to mate with a male in order to pass into the compartment of the fertilised females and be able to deposit her eggs. Therefore, we also add a male compartment, denoted M, to study how the abundance of males impacts the transfer rate from Y to F. We make the model sufficiently generic such that multiple mating can occur, which implies that fertilised females can become mating female again.

We denote r the proportion of females emerging from the immature stage and entering the mating females compartment. Thus a proportion of $(1-r)$ on the immature enter the male compartment after emergence. We assume that the time needed for an egg laid to emergence is $1/\nu_I$, thus the transfer rate from I to Y or M is ν_I. Then, when males are in sufficient abundance to ensure the fertilisation of all the females available for mating, the transfer rate from Y to F is ν_Y. However, if males are scarce, and if γ is the number of females that can be fertilised by a single male, then only a proportion $\frac{\gamma M}{Y}$ of Y-females can

pass into the F-females compartment. Therefore, the transfer rate from Y to F is modelled by the non-linear term $\nu_Y \min\{\frac{\gamma M}{Y}, 1\}$. Moreover, fertilised females go back to the mating females compartment with a rate of δ. Further, the fertilised females supply the immature compartment with a rate $b\left(1-\frac{I}{K}\right)$, where b is the intrinsic egg laying rate, while K is the carrying capacity of the hosts. Finally, parameters μ_I, μ_Y, μ_F are respectively the death rates of compartments I, Y, F and M. The flow diagram of the insects' dynamics is represented in Figure 5.1. The model is governed by the following system of ODEs:

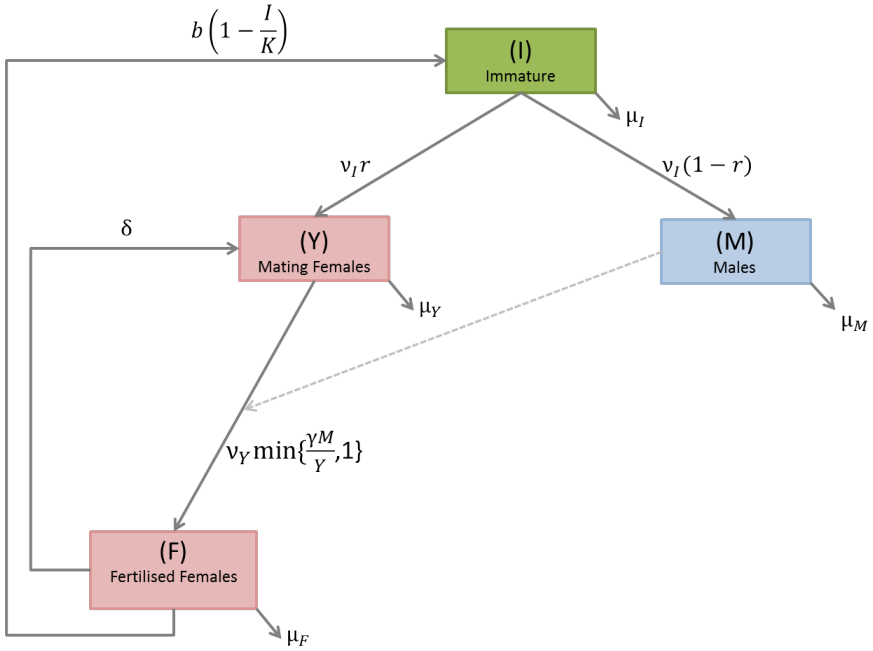

Figure 5.1: Life cycle of the insect.

$$\begin{cases} \frac{dI}{dt} &= b\left(1-\frac{I}{K}\right)F - (\nu_I + \mu_I)\, I, \\ \frac{dY}{dt} &= r\nu_I I - \nu_Y \min\{\frac{\gamma M}{Y}, 1\}Y + \delta F - \mu_Y Y, \\ \frac{dF}{dt} &= \nu_Y \min\{\frac{\gamma M}{Y}, 1\}Y - \delta F - \mu_F F, \\ \frac{dM}{dt} &= (1-r)\nu_I I - (\mu_M)M. \end{cases} \tag{5.1}$$

The list of the parameters used in the model are summarized in Table 5.1. They are taken from [89] in order to perform numerical experiments.

Parameter	Description	Unit	Value
b	Intrinsic egg laying rate	female^{-1}day^{-1}	9.272
r	Female to male ratio	-	0.57
K	Carrying capacity	-	1000
γ	Females fertilised by a single male	female	4
μ_I	Mortality rate in the I compartment	day^{-1}	1/15
μ_Y	Mortality rate in the Y compartment	day^{-1}	1/75.1
μ_F	Mortality rate in the F compartment	day^{-1}	1/75.1
μ_M	Mortality rate in the M compartment	day^{-1}	1/86.4
ν_I	Transfer rate from I to Y	day^{-1}	1/24.6
ν_Y	Transfer rate from Y to F	day^{-1}	0.5
δ	Transfer rate from F to Y	day^{-1}	0.1

Table 5.1: List of parameters and there values used in the numerical simulations.

5.3.1 Theoretical analysis of the model

The theoretical analysis of the model is carried out for the case of male abundance and the case of male scarcity. These two cases are separated by the hyperplane $Y = \gamma M$. The analysis of the two systems can be carried out independently on the orthant $\mathbb{R}^4_+$.

5.3.1.1 Case 1: Male abundance

In the case of male abundance, we recover the same model developed and studied in [82]. However, we follow another approach for the theoretical study. The system can be written in the vector form

$$\frac{dx}{dt} = f(x), \tag{5.2}$$

with $x = (I, Y, F, M)^T$, and

$$f(x) = \begin{pmatrix} b\left(1 - \frac{I}{K}\right) F - (\nu_I + \mu_I) I \\ r\nu_I I + \delta F - (\nu_Y + \mu_Y) Y \\ \nu_Y Y - (\delta + \mu_F) F \\ (1 - r)\nu_I I - \mu_M M \end{pmatrix}. \tag{5.3}$$

Note that the right hand side of system (5.2), $f(x)$, is continuous and locally Lipschitz, so uniqueness and local existence of the solution are guaranteed. In proving the global properties we will use the fact that the system is cooperative on $\mathbb{R}^4_+$, that is the growth in any compartment impacts positively on the growth of all other compartments. For completeness

of the exposition some basics of the theory of cooperative systems is given in Appendix C. Using Theorem 5.5.1, the system (5.2) is cooperative on $\Omega_K = \{x \in \mathbb{R}^4_+ : I \leq K\}$ because the non-diagonal entries of the Jacobian matrix of f

$$\mathcal{J}_f = \begin{pmatrix} -\left(\nu_I + \mu_I + b\frac{F}{K}\right) & 0 & b(1-\frac{I}{K}) & 0 \\ r\nu_I & -(\nu_Y + \mu_Y) & \delta & 0 \\ 0 & \nu_Y & -(\mu_F + \delta) & 0 \\ (1-r)\nu_I & 0 & 0 & -\mu_M \end{pmatrix}, \tag{5.4}$$

are non-negative on Ω_K.

The persistence of a population is typically linked to its Basic Offspring Number. For simple population models the basic offspring number is defined as the number of offspring produced by a single individual in their life time provided abundant resource is available. In general, the definition could be more complicated and its value is computed by using the next generation method. For the model in (5.2) the Basic Offspring Number is

$$\mathcal{N}_0 = \frac{br\nu_I\nu_Y}{(\mu_I + \nu_I)((\nu_Y + \mu_Y)(\delta + \mu_F) - \delta\nu_Y)}. \tag{5.5}$$

In this paper we will use $\mathcal{N}_0$ only as a threshold parameter. The persistence when $\mathcal{N}_0 > 1$ and the extinction when $\mathcal{N}_0 < 1$ are given direct proofs. Hence, we will not discuss the details on specific properties of the number. For completeness of the exposition the computation of (5.5) is given in Appendix A.

Theorem 5.3.1. *a) The system of ODE (5.2) defines a positive dynamical system on* $\mathbb{R}^4_+$.

b) If $\mathcal{N}_0 \leq 1$ *then* $TE = (0,0,0,0)^T$ *is a globally asymptotically stable (GAS) equilibrium.*

c) If $\mathcal{N}_0 > 1$ *then* TE *is an unstable equilibrium and the system admits a positive equilibrium* $EE^* = (I^*, Y^*, F^*, M^*)^T$, *where*

$$\begin{aligned} I^* &= \left(1 - \frac{1}{\mathcal{N}_0}\right) K, \\ Y^* &= \frac{r\nu_I(\delta + \mu_F)}{(\nu_Y + \mu_Y)(\delta + \mu_F) - \delta\nu_Y} \left(1 - \frac{1}{\mathcal{N}_0}\right) K, \\ F^* &= \frac{r\nu_I\nu_Y}{(\nu_Y + \mu_Y)(\delta + \mu_F) - \delta\nu_Y} \left(1 - \frac{1}{\mathcal{N}_0}\right) K, \\ M^* &= \frac{(1-r)\nu_I}{\mu_M} \left(1 - \frac{1}{\mathcal{N}_0}\right) K, \end{aligned}$$

which is a globally asymptotically stable (GAS) on $\mathbb{R}^4_+ \setminus \{x \in \mathbb{R}^4_+ : I = Y = F = 0\}$.

Proof. a) Let $q \in \mathbb{R}$, $q \geq K$. Denote

$$y_q = \begin{pmatrix} K \\ \frac{r\nu_I(\delta+\mu_F)}{(\nu_Y+\mu_Y)(\delta+\mu_F)-\delta\nu_Y} q \\ \frac{r\nu_I\nu_Y}{(\nu_Y+\mu_Y)(\delta+\mu_F)-\delta\nu_Y} q \\ \frac{(1-r)\nu_I}{\mu_M} q \end{pmatrix} \tag{5.6}$$

We have $f(\mathbf{0}) = \mathbf{0}$ and $f(y_q) \leq \mathbf{0}$. Then, from Theorem 5.5.4 it follows that (5.2) defines a positive dynamical system on $[\mathbf{0}, y_q]$. That is $\forall x \in [\mathbf{0}, y_q]$, the problem (5.2), given an initial condition $x(0) = x_0 \in [\mathbf{0}, y_q]$, admits a unique solution for all $t \in [0, \infty]$ in $[\mathbf{0}, y_q]$ [8]. Hence (5.2) defines a positive dynamical system on $\Omega_K = \cup_{q \geq K}[\mathbf{0}, y_q]$. Let now $x_0 \in \mathbb{R}^4_+ \setminus \Omega_K$. Using that the vector field defined by f points inwards on the boundary of $\mathbb{R}^4_+$ we deduce that the solution initiated at x_0 remains in $\mathbb{R}^4_+$. Then one can see from the first equation of (5.2) that $I(t)$ decreases until the solution is absorbed in Ω_K. Then (5.2) defines a dynamical system on $\mathbb{R}^4_+$ with Ω_K being an absorbing set.

b)Solving $f(x) = 0$ yields two solutions TE and EE^*. When $\mathcal{N}_0 \leq 1$ TE is the only equilibrium in $\mathbb{R}^4_+$. Then for any $q \geq K$ TE is the only equilibrium in $[\mathbf{0}, y_q]$. It follows from Theorem 5.5.4 that it is GAS on $[\mathbf{0}, y_q]$. Therefore, TE is GAS on Ω_K and further on $\mathbb{R}^4_+$ by using that Ω_K is an absorption set.

c) For $\varepsilon \in (0, I^*)$ we consider the vector

$$z_\varepsilon = \begin{pmatrix} \varepsilon \\ \frac{r\nu_I(\delta+\mu_F)}{(\nu_Y+\mu_Y)(\delta+\mu_F)-\delta\nu_Y} \varepsilon \\ \frac{r\nu_I\nu_Y}{(\nu_Y+\mu_Y)(\delta+\mu_F)-\delta\nu_Y} \varepsilon \\ \frac{(1-r)\nu_I}{\mu_M} \varepsilon \end{pmatrix}. \tag{5.7}$$

Straightforward computations show that $\frac{dY}{dt}(z_\varepsilon) = \frac{dF}{dt}(z_\varepsilon) = \frac{dM}{dt}(z_\varepsilon) = 0$, and that we have

$$\begin{aligned} \tfrac{dI}{dt}(z_\varepsilon) &= b\left(1 - \tfrac{\varepsilon}{K}\right) \tfrac{r\nu_I\nu_Y}{(\nu_Y+\mu_Y)(\delta+\mu_F)-\delta\nu_Y}\varepsilon - (\nu_I + \mu_I)\,\varepsilon, \\ &= \tfrac{br\nu_I\nu_Y}{(\nu_Y+\mu_Y)(\delta+\mu_F)-\delta\nu_Y}\varepsilon - \tfrac{br\nu_I\nu_Y}{(\nu_Y+\mu_Y)(\delta+\mu_F)-\delta\nu_Y}\tfrac{\varepsilon^2}{K} - (\nu_I + \mu_I)\,\varepsilon \\ &= (\nu_I + \mu_I)\mathcal{N}_0\varepsilon - (\nu_I + \mu_I)\mathcal{N}_0\tfrac{\varepsilon^2}{K} - (\nu_I + \mu_I)\,\varepsilon \\ &= (\nu_I + \mu_I)\left(\mathcal{N}_0(1 - \tfrac{\varepsilon}{K}) - 1\right)\varepsilon \\ &= (\nu_I + \mu_I)\tfrac{\mathcal{N}_0}{K}(I^* - \varepsilon)\varepsilon > 0. \end{aligned}$$

Thus, $f(x_\varepsilon) \geq \mathbf{0}$. For any $\varepsilon \in (0, I^*)$ and $q \in (\varepsilon, K]$ EE^* is a unique equilibrium in the interval $[z_\varepsilon, y_q]$ and hence, by Theorem 5.5.4, it is GAS on this interval. Therefore, EE^* is GAS also on $interior(\Omega_K)$. Using further that (i) if either $I(0)$ or $Y(0)$ or $F(0)$ is positive then $x(t) > 0$ for all $t > 0$ and that (ii) Ω_K is an absorbing set, we obtain that EE^* attracts all solution in $\mathbb{R}^4_+$ except the ones initiated on the M-axis. □

5.3.1.2 Case 2: Male scarcity

Next we consider the case when males are scarce, that is when $\gamma M < Y$. The system assumes the form

$$\begin{cases} \frac{dI}{dt} &= b\left(1-\frac{I}{K}\right)F-(\nu_I+\mu_I)\,I, \\ \frac{dY}{dt} &= r\nu_I I-\nu_Y\gamma M+\delta F-\mu_Y Y, \\ \frac{dF}{dt} &= \nu_Y\gamma M-(\delta+\mu_F)F, \\ \frac{dM}{dt} &= (1-r)\nu_I I-\mu_M M. \end{cases} \tag{5.8}$$

It is easy to see that the second equation can be decoupled. The system of the remaining 3 equations is of the form

$$\frac{du}{dt}=g(u), \tag{5.9}$$

where $u=\begin{pmatrix} I \\ F \\ M \end{pmatrix}$ and $g(u)=\begin{pmatrix} b\left(1-\frac{I}{K}\right)F-(\nu_I+\mu_I)\,I \\ \nu_Y\gamma M-(\delta+\mu_F)F \\ (1-r)\nu_I I-\mu_M M \end{pmatrix}$. The non-diagonal entries of the Jacobian of g,

$$\mathcal{J}_g=\begin{pmatrix} -(\nu_I+\mu_I+b\frac{F}{K}) & b\left(1-\frac{I}{K}\right) & 0 \\ 0 & -(\delta+\mu_F) & \nu_Y\gamma \\ (1-r)\nu_I & 0 & -\mu_M \end{pmatrix},$$

are non-negative. Hence the system (5.9) is cooperative. The Basic Offspring Number for system (5.9) is

$$\hat{\mathcal{N}_0}=\frac{b\gamma(1-r)\nu_I\nu_Y}{(\nu_I+\mu_I)(\delta+\mu_F)\mu_M}. \tag{5.10}$$

The following theorem describes the properties of system (5.9).

Theorem 5.3.2. *a) The system of ODE (5.9) defines a positive dynamical system on $\mathbb{R}^3_+$.*

b) If $\hat{\mathcal{N}_0}\leq 1$ then $TE=(0,0,0)^T$ is a globally asymptotically stable (GAS) equilibrium.

c) If $\hat{\mathcal{N}_0}>1$ then TE is an unstable equilibrium and the system admits a positive equilibrium $\hat{EE}=(\hat{I},\hat{F},\hat{M})$, where

$$\begin{aligned} \hat{I} &= \left(1-\frac{1}{\hat{\mathcal{N}_0}}\right)K, \\ \hat{F} &= \frac{\gamma(1-r)\nu_I\nu_Y}{(\delta+\mu_F)\mu_M}\left(1-\frac{1}{\hat{\mathcal{N}_0}}\right)K, \\ \hat{M} &= \frac{(1-r)\nu_I}{\mu_M}\left(1-\frac{1}{\hat{\mathcal{N}_0}}\right)K, \end{aligned}$$

which is a globally asymptotically stable (GAS) on $\mathbb{R}^3_+ \setminus \{x \in \mathbb{R}^3_+ : I = F = 0\}$.

Proof. a) Let $q \in \mathbb{R}$, $q \geq K$. Denote

$$\hat{y}_q = \begin{pmatrix} K \\ \frac{\gamma(1-r)\nu_I\nu_Y}{(\delta+\mu_F)\mu_M} q \\ \frac{(1-r)\nu_I}{\mu_M} q \end{pmatrix} \tag{5.11}$$

We have $g(\mathbf{0}) = \mathbf{0}$ and $g(\hat{y}_q) \leq \mathbf{0}$. Then, from Theorem 5.5.4 it follows that (5.9) defines a positive dynamical system on $[\mathbf{0}, \hat{y}_q]$. Hence it defines a positive dynamical system on $\hat{\Omega}_K = \cup_{q \geq K}[\mathbf{0}, \hat{y}_q]$. Let now $x_0 \in \mathbb{R}^3_+ \setminus \hat{\Omega}_K$. Using that the vector field defined by g points inwards on the boundary of $\mathbb{R}^3_+$ we deduce that the solution initiated at x_0 remains in $\mathbb{R}^3_+$. Then one can see from the first equation of (5.9) that $I(t)$ decreases until the solution is absorbed in $\hat{\Omega}_K$. Then (5.9) defines a dynamical system on $\mathbb{R}^3_+$ with $\hat{\Omega}_K$ being an absorbing set.

b)Solving $g(x) = 0$ yields two solutions TE and $\hat{EE}$. When $\hat{\mathcal{N}_0} \leq 1$, TE is the only equilibrium in $\mathbb{R}^3_+$. Then for any $q \geq K$ TE is the only equilibrium in $[\mathbf{0}, \hat{y}_q]$. It follows from Theorem 5.5.4 that it is GAS on $[\mathbf{0}, \hat{y}_q]$. Therefore, TE is GAS on $\hat{\Omega}_K$ and further on $\mathbb{R}^3_+$ by using that $\hat{\Omega}_K$ is an absorbing set.

c) For $\varepsilon \in (0, \hat{I})$ we consider the vector

$$\hat{z}_\varepsilon = \begin{pmatrix} \varepsilon \\ \frac{\gamma(1-r)\nu_I\nu_Y}{(\delta+\mu_F)\mu_M} \varepsilon \\ \frac{(1-r)\nu_I}{\mu_M} \varepsilon \end{pmatrix}. \tag{5.12}$$

Straightforward computations show that $\frac{dF}{dt}(\hat{z}_\varepsilon) = \frac{dM}{dt}(\hat{z}_\varepsilon) = 0$, and that we have

$$\begin{aligned} \tfrac{dI}{dt}(\hat{z}_\varepsilon) &= b\left(1 - \tfrac{\varepsilon}{K}\right) \tfrac{\gamma(1-r)\nu_I\nu_Y}{(\delta+\mu_F)\mu_M}\varepsilon - (\nu_I + \mu_I)\,\varepsilon \\ &= \tfrac{b\gamma(1-r)\nu_I\nu_Y}{(\delta+\mu_F)\mu_M}\varepsilon - \tfrac{b\gamma(1-r)\nu_I\nu_Y}{(\delta+\mu_F)\mu_M}\tfrac{\varepsilon^2}{K} - (\nu_I + \mu_I)\,\varepsilon \\ &= (\nu_I + \mu_I)\hat{\mathcal{N}_0}\varepsilon - (\nu_I + \mu_I)\hat{\mathcal{N}_0}\tfrac{\varepsilon^2}{K} - (\nu_I + \mu_I)\,\varepsilon \\ &= (\nu_I + \mu_I)\left(\hat{\mathcal{N}_0}(1 - \tfrac{\varepsilon}{K}) - 1\right)\varepsilon \\ &= (\nu_I + \mu_I)\tfrac{\hat{\mathcal{N}_0}}{K}(\hat{I} - \varepsilon)\varepsilon > 0. \end{aligned}$$

Thus, $g(x_\varepsilon) \geq \mathbf{0}$. For any $\varepsilon \in (0, \hat{I})$ and $q \in (\varepsilon, K]$ $\hat{EE}$ is a unique equilibrium in the interval $[z_\varepsilon, y_q]$ and hence, by Theorem 5.5.4, it is GAS on this interval. Therefore, $\hat{EE}$ is GAS also on $interior(\hat{\Omega}_K)$. Using further that (i) if either $I(0)$ or $F(0)$ is positive then $x(t) > 0$ for all $t > 0$ and that (ii) $\hat{\Omega}_K$ is an absorbing set, we obtain that $\hat{EE}$ attracts all solution in $\mathbb{R}^3_+$ except the ones initiated on the M-axis. □

It can be deduced from Theorem 5.3.2 that the non-trivial equilibrium value of Y is

$$\hat{Y} = \frac{r\nu_I(\delta+\mu_F)\mu_M - \nu_Y\gamma(1-r)\nu_I\mu_F}{\mu_Y(\delta+\mu_F)\mu_M}\left(1-\frac{1}{\hat{\mathcal{N}_0}}\right)K. \tag{5.13}$$

We note that the value of $\hat{Y}$ and in general the value of the variable Y can be negative. Hence, the system of ODE (5.8) defines a dynamical system on $\mathbb{R}_+ \times \mathbb{R} \times \mathbb{R}^2_+$.

5.3.1.3 Conclusions for model (5.1)

In what follows we assume that the population has an endemic equilibrium. Otherwise, no control would be necessary. Further, it is natural to assume that, at equilibrium, there is abundance of males. In terms of the parameters of the model these assumptions can be written as:

$$1.\quad \mathcal{N}_0 > 1, \tag{5.14}$$

$$2.\quad Y^* < \gamma M^*. \tag{5.15}$$

Under the assumptions (5.14) and (5.15) we have that $\hat{EE} > 0$ and $\hat{Y} < \gamma\hat{M}$. Indeed, when $\mathcal{N}_0 > 1$, the inequality

$$\frac{\hat{\mathcal{N}_0}}{\mathcal{N}_0} > 1$$

is equivalent to

$$\gamma > \frac{r(\delta+\mu_F)\mu_M}{(1-r)((\nu_Y+\mu_Y)(\delta+\mu_F)-\delta\nu_Y)},$$

which is ensured by (5.15). Therefore under assumptions (5.14) and (5.15) we have that $\hat{\mathcal{N}_0} > 1$, and by Theorem 5.3.2, we have that the system (5.8) has a non-trivial equilibrium, which is globally asymptotically stable on $\mathbb{R}_+ \times \mathbb{R} \times \mathbb{R}^2_+ \setminus \{(I,Y,F,M)^T : I = F = 0\}$.

Further, under (5.15), we have

$$\begin{aligned}
\hat{Y} - \gamma\hat{M} &= \hat{I}\left(\frac{r\nu_I(\delta+\mu_F)\mu_M - \nu_Y\gamma(1-r)\nu_I\mu_F}{\mu_Y(\delta+\mu_F)\mu_M} - \gamma\frac{(1-r)\nu_I}{\mu_M}\right)\\
&= \frac{\nu_I\hat{I}}{\mu_M}\left(\frac{r\mu_M}{\mu_Y} - \gamma(1-r)\frac{\nu_Y\mu_F+\mu_Y(\delta+\mu_F)}{\mu_Y(\mu_F+\delta)}\right)\\
&< \frac{\nu_I\hat{I}}{\mu_M}\left(\frac{r\mu_M}{\mu_Y} - \frac{r(\delta+\mu_F)\mu_M}{((\nu_Y+\mu_Y)(\delta+\mu_F)-\delta\nu_Y)}\frac{\nu_Y\mu_F+\mu_Y(\delta+\mu_F)}{\mu_Y(\delta+\mu_F)}\right)\\
&< \frac{\nu_I\hat{I}}{\mu_M}\left(\frac{r\mu_M}{\mu_Y} - \frac{r\mu_M}{\mu_Y}\right) = 0.
\end{aligned} \tag{5.16}$$

To summarize, under assumptions (5.14) and (5.15), the globally asymptotically stable equilibria of both (5.2) and (5.8) are in the male abundance region defined via $Y < \gamma M$. Hence the only non-trivial equilibrium of (5.1) is $EE^* = (I^*, Y^*, F^*, M^*)^T$. In this way we obtain the following result:

Theorem 5.3.3. *Given (5.14) and (5.15), the model (5.1) has two equilibria:*

a) TE which is unstable, and

b) EE^* which is asymptotically stable.

The equilibrium $EE*$ attracts solutions which are entirely in the male abundance region, excluding the M-axis. Solutions in the male scarcity region are attracted to $\hat{EE} = (\hat{I}, \hat{Y}, \hat{F}, \hat{M})^T$. Hence they leave the male scarcity region and enter the male abundance region. In the male abundance region they are governed by (5.2) and, therefore, attracted to EE^*. In general this reasoning does not exclude the possibility that a solution may leave the male abundance region, enter the male scarcity region and then leave it. However, our numerical simulations show that this happens only finite number of times, indicating that EE* is globally asymptotically stable on $\mathbb{R}^4_+ \setminus \{x \in \mathbb{R}^4_+ : I = F = 0\}$. Hence, eventually such solution stays in the male abundance region and therefore converges to EE^*.

5.4 Modelling mating disruption and trapping

5.4.1 Mating disruption and trapping

In order to maintain the pest population to a low level, we consider a control using female-pheromone-traps to disrupt male mating behaviour. More precisely, we take into account two aspects for the control. The first aspect consists of disturbing the mating between males and females to reduce the fertilisation opportunities, which in turn, reduces the number of offspring. This is done using traps that are releasing a female pheromone lure to which males are attracted. This leads to a reduction in the number of males available for mating near the females, and decreases the opportunity for fertilisation. The efficiency of mating disruption depends on the strength of the lure or on the number of traps in an area. The second aspect of the control is the trapping potential of the trap. We assume that the lure traps also contain an insecticide which can kill the captured insects.

5.4.2 The model

In order to take in account the effect of the lures, we consider the approach proposed by Barclay and Van den Driessche [18, 19]. That is, the strength of the lure is represented as the quantity of pheromones released by an equivalent number of wild females. Thus, in the model the effect of the lure corresponds to the attraction of Y_P additional females. In such a setting, the total number of "females" attracting males is $Y + Y_P$ [18]. In particular, this means that males have a probability of $\dfrac{Y}{Y+Y_P}$ to be attracted to wild females, and a probability of $\dfrac{Y_P}{Y+Y_P}$ to be attracted to the pheromone traps. Denote γ the number of females that can be inseminated by a single male. Then, the transfer rate from Y to F does not exceed $\nu_Y \dfrac{\gamma M}{Y+Y_P}$. When $\dfrac{\gamma M}{Y+Y_P} > 1$ the population is in a male abundance state and the transfer rate is ν_Y. However, when $\dfrac{\gamma M}{Y+Y_P} < 1$, then the population is in a male scarcity state and the transfer rate is $\nu_Y \dfrac{\gamma M}{Y+Y_P}$. Altogether, the transfer rate is $\nu_Y \min\{\frac{\gamma M}{Y+Y_P}, 1\}$.

The parameter α represents the death or capture rate for the fraction $\dfrac{Y_P}{Y+Y_P}$ of the males which are attracted by the lures. The flow diagram is represented in Figure 5.2 which yields the following system of ODEs:

$$\begin{cases} \frac{dI}{dt} &= b\left(1-\frac{I}{K}\right)F - (\nu_I + \mu_I)\, I, \\ \frac{dY}{dt} &= r\nu_I I - \nu_Y \min\{\frac{\gamma M}{Y+Y_P}, 1\}Y + \delta F - \mu_Y Y, \\ \frac{dF}{dt} &= \nu_Y \min\{\frac{\gamma M}{Y+Y_P}, 1\}Y - \delta F - \mu_F F, \\ \frac{dM}{dt} &= (1-r)\nu_I I - (\mu_M + \alpha\frac{Y_P}{Y+Y_P})M. \end{cases} \tag{5.17}$$

5.4.3 Theoretical analysis of the control model

The aim of this section is to investigate the existence of equilibria of model (5.17) and their asymptotic properties. First we consider the model in the male abundance state and in the male scarcity state independently. Then we draw conclusions for the general model.

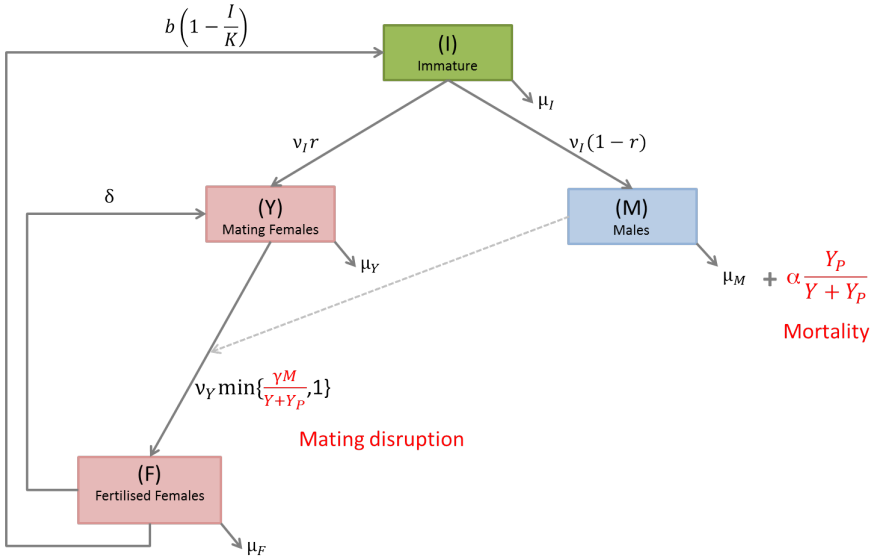

Figure 5.2: Control model using mating disruption and trapping.

5.4.3.1 Properties of the equilibria in the male abundance region ($\gamma M > Y + Y_P$)

The dynamics of the population in the male abundance region $Y + Y_P < \gamma M$ are governed by the following system of ODEs:

$$\begin{cases} \frac{dI}{dt} &= b\left(1-\frac{I}{K}\right)F - (\nu_I + \mu_I)\,I, \\ \frac{dY}{dt} &= r\nu_I I - \nu_Y Y + \delta F - \mu_Y Y, \\ \frac{dF}{dt} &= \nu_Y Y - (\delta + \mu_F)F, \\ \frac{dM}{dt} &= (1-r)\nu_I I - (\mu_M + \alpha\frac{Y_P}{Y+Y_P})M. \end{cases} \tag{5.18}$$

We note that the first three equations in (5.18) as in (5.2) are the same, while the fourth equation in both systems can be decoupled. Then, using exactly the same method as in Theorem 5.3.1 we obtain the following theorem.

Theorem 5.4.1. *a) The system of ODEs (5.18) defines a positive dynamical system on* $\mathbb{R}^4_+$.

b) Under assumptions (5.14) and (5.15), the system has a positive equilibrium $EE^{\#} = (I^*, Y^*, F^*, M^{\#}(Y_P))^T$, *where*

$$M^{\#}(Y_P) = \frac{(1-r)\nu_I(Y^*+Y_P)}{\mu_M(Y^*+Y_P)+\alpha Y_P} I^* = \frac{M^*}{1+\frac{\alpha Y_P}{\mu_M(Y^*+Y_P)}},$$

which is globally asymptotically stable on $\mathbb{R}^4_+ \setminus \{x \in \mathbb{R}^4_+ : I = Y = F = 0\}$.

The equilibrium $EE^{\#}$ is an equilibrium of (5.17) if and only if

$$Y^* + Y_P < \gamma M^{\#}(Y_P)$$

or, equivalently,

$$Y_P < Y_P^* := \frac{\gamma M^* - Y^*}{1 + \frac{\alpha}{\mu_M}} = \frac{1}{\mu_M + \alpha}\left(\gamma(1-r)\nu_I - \frac{r\nu_I(\delta+\mu_F)\mu_M}{(\nu_Y+\mu_Y)(\delta+\mu_F) - \delta\nu_Y}\right)\left(1 - \frac{1}{\mathcal{N}_0}\right)K. \tag{5.19}$$

The threshold value Y_P^* determines the minimal level of control below which the control has essentially no effect on an established pest population. More precisely, the effect is limited to reducing the number of males, while all other compartments remain in their natural equilibrium.

5.4.3.2 Properties of the equilibria in the male scarcity region ($\gamma M < Y + Y_P$)

In the region of male scarcity $\gamma M \leq Y + Y_P$ the dynamics of the population is governed by the system:

$$\begin{cases} \frac{dI}{dt} &= b\left(1 - \frac{I}{K}\right)F - (\nu_I + \mu_I)\,I, \\ \frac{dY}{dt} &= r\nu_I I - \nu_Y \frac{\gamma MY}{Y+Y_P} + \delta F - \mu_Y Y, \\ \frac{dF}{dt} &= \nu_Y \frac{\gamma MY}{Y+Y_P} - (\delta + \mu_F)F, \\ \frac{dM}{dt} &= (1-r)\nu_I I - (\mu_M + \alpha\frac{Y_P}{Y+Y_P})M. \end{cases} \tag{5.20}$$

The following theorem exhibits different behaviours of the model depending on the value of Y_P which can be interpreted as the effort of the mating disruption control.

Theorem 5.4.2. *a) The system of ODEs (5.20) defines a positive dynamical system on* $\mathbb{R}^4_+$.

b) TE is an asymptotically stable equilibrium of this system.

c) There exists a threshold value Y_P^{**} *of* Y_P *such that*

i) if $Y_P > Y_P^{**}$ *the only equilibrium of the system on* $\mathbb{R}^4_+$ *is TE;*

ii) if $0 < Y_P < Y_P^{**}$ *the system has three biologically relevant equilibria on* $\mathbb{R}^4_+$*, TE and two positive equilibria.*

Proof. a) The local existence of the solutions of (5.20) follows from the fact that the right hand side is Lipschitz continuous in $\mathbb{R}^4_+$. To obtain global existence it is enough to show that every solution is bounded. This can be proved directly, but it also follows from the upper approximation of the solutions discussed in the proof of Theorem 5.4.5. Hence, it is omitted here.

b) It is clear that $TE = (0,0,0,0)^T$ is an equilibrium. The Jacobian of the right hand side of system (5.20) is

$$\mathcal{J}_h(x) = \begin{pmatrix} -\left(\nu_I + \mu_I + b\frac{F}{K}\right) & 0 & b\left(1-\frac{I}{K}\right) & 0 \\ r\nu_I & -(\nu_Y\gamma M\frac{Y_P}{(Y+Y_P)^2} + \mu_Y) & \delta & -\nu_Y\gamma\frac{Y}{(Y+Y_P)} \\ 0 & \nu_Y\gamma M\frac{Y_P}{(Y+Y_P)^2} & -(\mu_F+\delta) & \nu_Y\gamma\frac{Y}{(Y+Y_P)} \\ (1-r)\nu_I & \frac{\alpha Y_P}{(Y+Y_P)^2}M & 0 & -(\mu_M + \alpha\frac{Y_P}{Y+Y_P}) \end{pmatrix}, \tag{5.21}$$

thus,

$$\mathcal{J}_h(TE) = \begin{pmatrix} -(\nu_I+\mu_I) & 0 & b & 0 \\ r\nu_I & -\mu_Y & \delta & 0 \\ 0 & 0 & -(\delta+\mu_F) & 0 \\ (1-r)\nu_I & 0 & 0 & -(\mu_M+\alpha) \end{pmatrix}. \tag{5.22}$$

Its eigenvalues are equal to its diagonal entries and are all negative real values. Hence TE is asymptotically stable.

c) Setting $\frac{dI}{dt} = 0$ in (5.20) yields

$$F = \frac{\nu_I + \mu_I}{b\left(1-\frac{I}{K}\right)} I.$$

Then, from $\frac{dM}{dt} = 0$, we have

$$M = \frac{(1-r)\nu_I}{\mu_M + \alpha\frac{Y_P}{Y+Y_P}} I.$$

Further, considering that $\frac{dY}{dt} + \frac{dF}{dt} = 0$, we deduce

$$Y = \frac{r\nu_I I - \mu_F F}{\mu_Y} = \left(\frac{r\nu_I}{\mu_Y} - \frac{\mu_F(\nu_I+\mu_I)}{\mu_Y b\left(1-\frac{I}{K}\right)}\right) I = \frac{\phi(I)}{\mu_Y b\left(1-\frac{I}{K}\right)} I.$$

with $\phi(I) = r\nu_I b(1-\frac{I}{K}) - \mu_F(\nu_I+\mu_I)$. Now, we use $\frac{dF}{dt} = 0$,

$$\frac{dF}{dt} = \frac{\nu_Y\gamma M}{Y+Y_P}Y - (\delta+\mu_F)F = \frac{\nu_Y\gamma(1-r)\nu_I I}{\mu_M(Y+Y_P)+\alpha Y_P}\frac{\phi(I)}{\mu_Y b\left(1-\frac{I}{K}\right)} I - (\delta+\mu_F)\frac{\nu_I+\mu_I}{b\left(1-\frac{I}{K}\right)} I = 0.$$

Thus by substituting the expressions of Y, F and M, we have

$$\frac{\nu_Y\gamma(1-r)\nu_I I}{\mu_M Y+(\mu_M+\alpha)Y_P}\frac{\phi(I)}{\mu_Y b\left(1-\frac{I}{K}\right)}I-(\delta+\mu_F)\frac{\nu_I+\mu_I}{b\left(1-\frac{I}{K}\right)}I=0$$

$$\Leftrightarrow \quad \left(\nu_Y\gamma(1-r)\nu_I\frac{\phi(I)}{\mu_Y b\left(1-\frac{I}{K}\right)}I\right)=\frac{(\delta+\mu_F)(\nu_I+\mu_I)}{b\left(1-\frac{I}{K}\right)}(\mu_M Y+(\mu_M+\alpha)Y_P)$$

$$\Leftrightarrow \quad \left(\nu_Y\gamma(1-r)\nu_I\frac{\phi(I)}{\mu_Y b\left(1-\frac{I}{K}\right)}I-\frac{(\delta+\mu_F)(\nu_I+\mu_I)(\mu_M)}{b\left(1-\frac{I}{K}\right)}\frac{\phi(I)}{\mu_Y b\left(1-\frac{I}{K}\right)}\right)=\frac{(\delta+\mu_F)(\nu_I+\mu_I)(\mu_M+\alpha)Y_P}{b\left(1-\frac{I}{K}\right)}.$$

Multiplying both side by $\mu_Y b^2(1-\frac{I}{K})^2$, we obtain an equation for I in the form

$$\psi(I):=I\xi(I)\phi(I)=\eta(Y_P,I), \tag{5.23}$$

where

$$\xi(I)=\nu_Y\gamma(1-r)\nu_I b\left(1-\frac{I}{K}\right)-(\delta+\mu_F)(\nu_I+\mu_I)\mu_M, \tag{5.24}$$

$$\phi(I)=r\nu_I b\left(1-\frac{I}{K}\right)-\mu_F(\nu_I+\mu_I), \tag{5.25}$$

and

$$\eta(Y_P,I)=\mu_Y(\delta+\mu_F)(\nu_I+\mu_I)(\mu_M+\alpha)b\left(1-\frac{I}{K}\right)Y_P. \tag{5.26}$$

Therefore, the non-trivial equilibria of (5.20) are of the form

$$Y_{MD} = \left(\frac{r\nu_I}{\mu_Y}-\frac{\mu_F(\nu_I+\mu_I)}{\mu_Y b\left(1-\frac{I_{MD}}{K}\right)}\right)I_{MD}, \tag{5.27}$$

$$F_{MD} = \frac{\nu_I+\mu_I}{b\left(1-\frac{I_{MD}}{K}\right)}I_{MD}, \tag{5.28}$$

$$M_{MD} = \frac{(1-r)\nu_I}{\mu_M+\alpha\frac{Y_P}{Y_{MD}+Y_P}}I_{MD}. \tag{5.29}$$

with I_{MD} a positive root of (5.23). Further, we note that to ensure $Y_{MD}>0$, it follows from (5.27) that I_{MD} must satisfy the condition

$$I_{MD}<K\left(1-\frac{\mu_F(\nu_I+\mu_I)}{r\nu_I b}\right). \tag{5.30}$$

Thus, to obtain biologically viable equilibria, I_{MD} must belong to the interval $\left[0,K\left(1-\frac{\mu_F(\nu_I+\mu_I)}{r\nu_I b}\right)\right]$.

The roots of (5.23) correspond to the values of I where the graph of the cubic polynomial ψ and the straight line $\eta(Y_P,\cdot)$ intersect. It is clear that, the straight line $\eta(Y_P,\cdot)$ intersects

the I-axis at $I = K$. From the factorization of $\psi(I)$ in (5.23), it is clear that the roots of ψ are

$$I_0 = 0, \quad I_1 = K\left(1 - \frac{(\delta + \mu_F)(\nu_I + \mu_I)\mu_M}{\nu_Y \gamma (1-r)\nu_I b}\right), \text{ and } I_2 = K\left(1 - \frac{\mu_F(\nu_I + \mu_I)}{r\nu_I b}\right). \tag{5.31}$$

Note that the the roots I_1 and respectively, I_2, are positive and smaller than K, i.e.

$$0 < I_1, I_2 < K,$$

provided

$$\frac{(\delta + \mu_F)(\nu_I + \mu_I)\mu_M}{\nu_Y \gamma (1-r)\nu_I b} < 1, \tag{5.32}$$

and respectively,

$$\frac{\mu_F(\nu_I + \mu_I)}{r\nu_I b} < 1. \tag{5.33}$$

Inequality (5.32) is satisfied under assumptions (5.15) and (5.14), and inequality (5.33) is equivalent to $\mathcal{N}_0 > 1$, that is, to (5.14). Therefore, under assumptions (5.14) and (5.15), we have that

$$I_1, I_2 \in [0, K].$$

Therefore, the graph of the cubic polynomial ψ is as given on Figure 5.3. Considering the

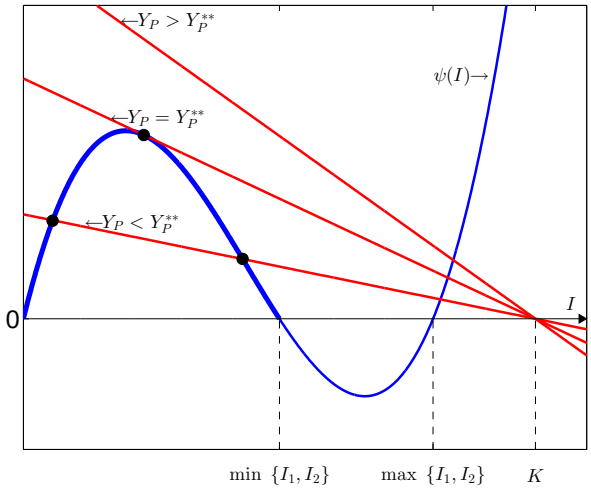

Figure 5.3: Intersections between the graphs of $\eta(Y_P, \cdot)$ (in red) and ψ (in blue) for different values of Y_P. The black dots represent the intersection points on the interval $[0, \min\{I_1, I_2\}]$.

inequality (5.30), only points of intersection of the straight line $\eta(Y_P, \cdot)$ with the section of the graph of ψ for $0 \leq I \leq \min\{I_1, I_2\}$, indicated by a thicker line on Figure 5.3, are of relevance to the equilibria of the model. Let us note that ψ is independent of Y_P while the

gradient of the line η is a multiple of Y_P. We denote by Y_P^{**} the value of Y_P such that the line $\eta(Y_P, \cdot)$ is tangent to the indicated section of the graph of ψ, see Figure 5.3. Then it is clear that for $Y_P > Y_P^{**}$ there is no intersection between $\eta(Y_P, \cdot)$ and ψ on $[0, \min\{I_1, I_2\}]$ while if $0 < Y_P < Y_P^{**}$ there are two such points of intersection. This proves items (i) and (ii) in c).

□

The next step in this analysis is to merge the results in Theorem 5.4.1 for system (5.18) and the results in Theorem 5.4.2 for the system (5.20) in order to obtain results for the model (5.17) which is actually our interest.

Let $I_{MD}^{(1)}$ and $I_{MD}^{(2)}$,$I_{MD}^{(1)} < I_{MD}^{(2)}$, be the roots of (5.23) when $0 < Y_P < Y_P^{**}$ and denote the respective equilibria by $EE_{MD}^{(1)}$ and $EE_{MD}^{(2)}$. First we show that $EE^{\#} = EE_{MD}^{(2)}$ when $Y_P = Y_P^*$. Indeed, Y_P^* is selected in such way that $\dfrac{\gamma M^*}{Y^* + Y_P^*} = 1$. Then, the right hand sides of (5.18) and (5.20) are the same at $EE^{\#}$. This implies that $EE^{\#}$ is an equilibrium of (5.20).

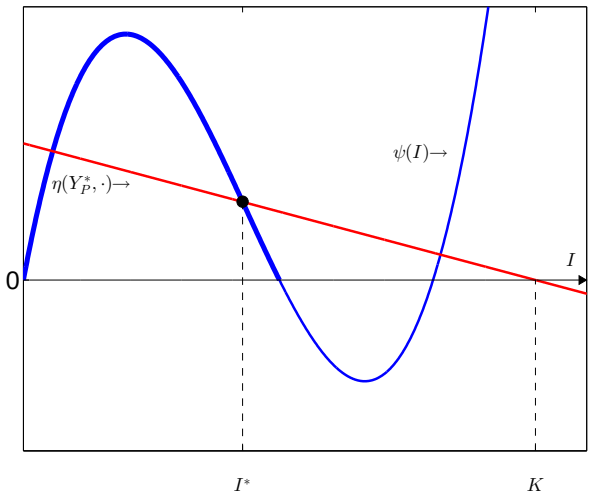

Figure 5.4: Intersections between the graphs of $\eta(Y_P^*, \cdot)$ (in red) and ψ (in blue). The black dot represent the intersection for $I = I^*$.

One can see from Figure 5.4 that for $0 < Y_P < Y_P^*$, we have

$$I_{MD}^{(1)} < I^* < I_{MD}^{(2)}, \tag{5.34}$$

and for $Y_P^* < Y_P < Y_P^{**}$, we have

$$I_{MD}^{(1)} < I_{MD}^{(2)} < I^*. \tag{5.35}$$

We investigate when the equilibria of (5.17) are biologically relevant, that is when they belong

to the male scarcity region. We have

$$\begin{aligned} & Y_{MD} + Y_P - \gamma M_{MD} \\ & = Y_{MD} + Y_P - \gamma \frac{(1-r)\nu_I}{\mu_M + \alpha \frac{Y_P}{Y_{MD}+Y_P}} I_{MD} \\ & = \frac{\mu_M Y_{MD} + \mu_Y Y_P + \alpha Y_P - \gamma(1-r)\nu_I}{\mu_M + \alpha \frac{Y_P}{Y_{MD}+Y_P}} I_{MD}. \\ & = \left(\frac{\mu_M}{\mu_M + \alpha \frac{Y_P}{Y_{MD}+Y_P}} \left(\frac{r\nu_I}{\mu_Y} - \frac{\mu_F(\nu_I+\mu_I)}{\mu_Y\left(1-\frac{I_{MD}}{K}\right)} \right) - \gamma(1-r)\nu_I \right) I_{MD} + (\mu_M + \alpha) Y_P. \end{aligned} \tag{5.36}$$

Let $Y_P^* < Y_P < Y_P^{**}$. Then using also (5.35) we have

$$\begin{aligned} & Y_{MD} + Y_P - \gamma M_{MD} \\ & \geq \frac{\mu_M}{\mu_M + \alpha \frac{Y_P}{Y_{MD}+Y_P}} \left(\frac{r\nu_I}{\mu_Y} - \frac{\mu_F(\nu_I+\mu_I)}{\mu_Y\left(1-\frac{I^*}{K}\right)} - \gamma(1-r)\nu_I \right) I_{MD} + (\mu_M + \alpha) Y_P \\ & = \left(\left(\mu_M \frac{r\nu_I(\delta+\mu_F)}{\nu_Y\mu_F + \mu_Y\mu_F + \delta\mu_Y} \right) - \gamma(1-r)\nu_I \right) I_{MD} + (\mu_M + \alpha) Y_P \quad \text{(using (5.19))} \\ & = -(\mu_M + \alpha)\frac{Y_P^*}{I^*} I_{MD} + (\mu_M + \alpha) Y_P \\ & = \frac{\mu_M + \alpha}{I^*} \left(Y_P I^* - Y_P^* I_{MD} \right) > 0. \end{aligned} \tag{5.37}$$

Therefore, in this case $EE_{MD}^{(1)}$ and $EE_{MD}^{(2)}$ are both in the male scarcity region. Hence, they are also equilibria of (5.17).

If $Y_P < Y_P^*$ and $I_{MD} > I^*$, considering (5.34), then using the same method as in (5.37) we obtain

$$Y_P + Y_{MD} - \gamma M_{MD} < 0. \tag{5.38}$$

Therefore, $EE_{MD}^{(2)}$ is not in the male scarcity region. Hence, it is not an equilibrium of (5.17).

Taking into consideration the above results regarding $EE_{MD}^{(1)}$ and $EE_{MD}^{(2)}$ we obtain the following theorem for the model (5.17).

Theorem 5.4.3. *Let $Y_P > 0$. The following holds for model (5.17):*

a) TE is an asymptotically stable equilibrium.

b) If $0 < Y_P < Y_P^*$ there are two positive equilibria $EE_{MD}^{(1)}$ and $EE^{\#}$, where $EE^{\#}$ is asymptotically stable.

c) If $Y_P^* < Y_P < Y_P^{**}$ *there are two positive equilibria* $EE_{MD}^{(1)}$ *and* $EE_{MD}^{(2)}$.

d) If $Y_P > Y_P^{**}$ *there is no positive equilibrium.*

Obtaining theoretically the stability properties of the equilibria $EE_{MD}^{(1)}$ and $EE_{MD}^{(2)}$ is not easy considering the complexity of the system. The numerical simulations indicate that $EE_{MD}^{(1)}$ is unstable while $EE_{MD}^{(2)}$ is asymptotically stable, and that the equilibria are the only invariant set of the system on $\mathbb{R}_4^+$. Further, when $Y_P > Y_P^{**}$, TE is globally asymptotically stable. The equilibria and their properties are presented on the bifurcation diagram in Figure 5.5. The equilibrium values of $Y+F$ are given as function of the bifurcation parameter Y_P. The solid line represents stable equilibria, while the dotted line represents unstable equilibria.

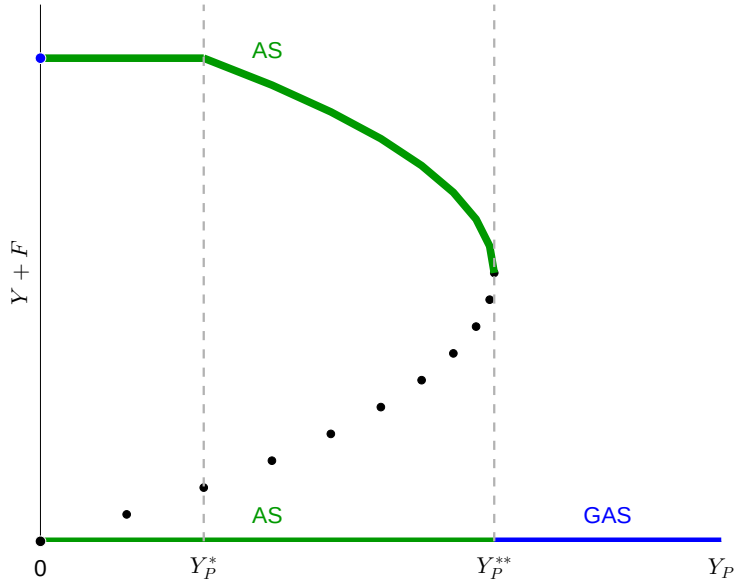

Figure 5.5: Bifurcation diagram of the values of $Y+F$ at equilibrium with respect to the values of Y_P for system (5.17).

5.4.3.3 Global asymptotic stability of the trivial equilibrium for sufficiently large Y_P

Theorem 5.4.3 shows that for $Y_P < Y_P^{**}$ the insect population persists at substantial endemic level. Hence, the numerically observed global asymptotic stability of TE for $Y_P > Y_P^{**}$ is of significant practical importance. This section deals with the mathematical proof of this result. More precisely, we will establish global asymptotic stability of TE under

slightly stronger condition $Y_P > \tilde{Y}_P^{**}$ where $\tilde{Y}_P^{**} > Y_P^{**}$. We also show that $\tilde{Y}_P^{**}$ is a close approximation for Y_P^{**}.

The asymptotic analysis for system (5.17) cannot be conducted in the same way as for the other systems considered so far, since it is not a monotone system. More precisely due to the term $-\nu_Y \frac{\gamma M}{Y+Y_P} Y$ in the equation for the Y compartment, the right hand side of (5.17) is not quasi-monotone. In order to obtain the practically important result mentioned above, we consider an auxiliary system which is monotone and provides upper bounds for the solutions of (5.17). The system is obtained by removing the mentioned term in the second equation and replacing $\min\{\frac{\gamma M}{Y+Y_P}, 1\}$ by $\frac{\gamma M}{Y+Y_P}$ in the third equation. In vector form it is given as

$$\frac{dx}{dt} = \tilde{h}(x), \tag{5.39}$$

where $x = (I, Y, F, M)^T$ and

$$\tilde{h}(x) = \begin{pmatrix} b\left(1-\frac{I}{K}\right)F - (\nu_I + \mu_I)\, I \\ r\nu_I I - \mu_Y Y + \delta F \\ \nu_Y \frac{\gamma M}{Y+Y_P} Y - \delta F - \mu_F F \\ (1-r)\nu_I I - (\mu_M + \alpha \frac{Y_P}{Y+Y_P}) M \end{pmatrix}. \tag{5.40}$$

Theorem 5.4.4. *a) The system of ODEs (5.39) defines a positive dynamical system on* $\mathbb{R}^4_+$.

b) TE is asymptotically stable equilibrium.

c) There exists a threshold value $\tilde{Y}_P^{**}$ *such that*

i) if $Y_P > \tilde{Y}_P^{**}$, *TE is globally asymptotically stable on* $\mathbb{R}^4_+$;

ii) if $0 < Y_P < \tilde{Y}_P^{**}$, *the system has three equilibria,* TE *and two positive equilibria* $\tilde{E}^{(1)}$ *and* $\tilde{E}^{(2)}$ *such that* $\tilde{E}^{(1)} < \tilde{E}^{(2)}$. *The basin of attraction of* TE *contains the set* $\{x \in \mathbb{R}^4_+ : 0 \le x < \tilde{E}^{(1)}\}$. *The basin of attraction of* $\tilde{E}^{(2)}$ *contains the set* $\{x \in \mathbb{R}^4_+ : x \ge \tilde{E}^{(2)}, I \le K\}$.

Proof. a) and b) are proved similarly to a) and b) in Theorem 5.4.2.

c) Setting the first, second and fourth component of $\tilde{h}$ to zero, we have

$$Y = \frac{r\nu_I I + \delta F}{\mu_Y}, \quad F = \frac{\nu_I + \mu_I}{b\left(1-\frac{I}{K}\right)} I, \quad M = \frac{(1-r)\nu_I}{\mu_M Y + (\mu_M + \alpha) Y_P} I.$$

Setting the third component of $\tilde{h}$ to zero and substituting the expressions for Y, F and M above, we obtain an equation for I in the form

$$\tilde{\psi}(I) := I\xi(I)\tilde{\phi}(I) = \eta(Y_P, I). \tag{5.41}$$

where $\xi(I)$ and $\eta(Y_P, I)$ are the linear expression given in (5.24) and (5.26) and

$$\tilde{\phi}(I) = r\nu_I b\left(1 - \frac{I}{K}\right) + \delta(\nu_I + \mu_I). \tag{5.42}$$

Therefore the non-trivial equilibria of (5.39) are of the form

$$\begin{aligned} \tilde{Y} &= \frac{1}{\mu_Y}\left(r\nu_I + \frac{\delta(\nu_I+\mu_I)}{b\left(1-\frac{\tilde{I}}{K}\right)}\right)\tilde{I}, \\ \tilde{F} &= \frac{\nu_I+\mu_I}{b\left(1-\frac{\tilde{I}}{K}\right)}\tilde{I}, \\ \tilde{M} &= \frac{(1-r)\nu_I}{\mu_M + \alpha\frac{Y_P}{\tilde{Y}+Y_P}}\tilde{I}, \end{aligned} \tag{5.43}$$

with $\tilde{I}$ a positive root of (5.42). The roots of (5.42) correspond to the values of I where the graph of the cubic polynomial $\tilde{\psi}$ and the straight line $\eta(Y_P, \cdot)$ intersect. It is clear that the straight line $\eta(Y_P, \cdot)$ intersects the I axis at $I = K$. Note that the state where I greater is than K is not sustainable, and therefore not biologically relevant. From the factorization of $\tilde{\psi}$ in (5.42), it is clear that I_0 and I_1 given in (5.31) and

$$\tilde{I}_2 = \left(1 + \frac{\delta(\nu_I+\mu_I)}{r\nu_I b}\right)K \tag{5.44}$$

are roots of $\tilde{\psi}$. Clearly, we have

$$0 < I_1 < K < \tilde{I}_2.$$

Therefore, the graph of the cubic polynomial $\tilde{\psi}$ is as given in Figure 5.6.

Considering the inequalities (5.30) and (5.45), only the points of intersection of the straight line $\eta(Y_P, \cdot)$ with the section of the graph of $\tilde{\psi}$ for $0 < I < I_1$ are of relevance to the equilibria of the model. Note that $\tilde{\psi}$ is independent of Y_P while the gradient of $\eta(Y_P, \cdot)$ is a multiple of Y_P. We denote by $\tilde{Y}_P^{**}$ the value of Y_P such that the line η is tangent to the indicated section of the graph of $\tilde{\psi}$, see Figure 5.6. Then, it is clear that for $Y_P > \tilde{Y}_P^{**}$ there is no intersection between $\eta(Y_P, \cdot)$ and $\tilde{\psi}$ on $[0, I_1]$ while if $0 < Y_P < \tilde{Y}_P^{**}$ there are two such points of intersection.

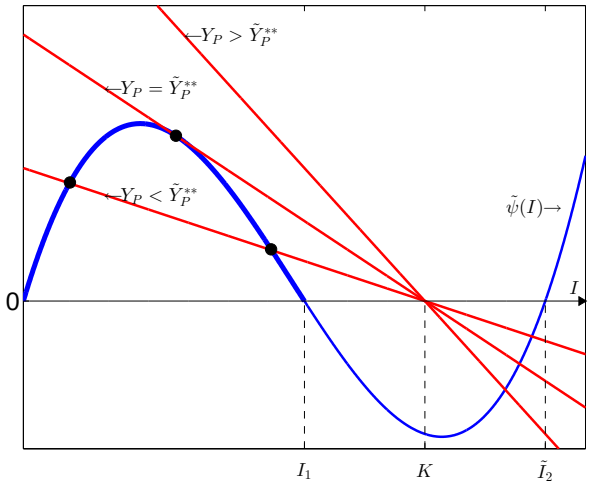

Figure 5.6: Intersections between the graphs of $\eta(Y_P, \cdot)$ (in red) and ψ (in blue) for different values of Y_P. The black dots represent the intersection points on the interval $[0, I_1]$.

i) Let $Y_P > \tilde{Y}_P^{**}$. Consider the point

$$\tilde{y}_q = \begin{pmatrix} K \\ \frac{1}{\mu_Y}\left(r\nu_I + \frac{\delta\nu_Y\gamma(1-r)\nu_I}{(\delta+\mu_F)\mu_M}\right)q \\ \frac{\nu_Y\gamma(1-r)\nu_I}{(\delta+\mu_F)\mu_M}q \\ \frac{(1-r)\nu_I}{\mu_M}q \end{pmatrix}, \tag{5.45}$$

where $q \in \mathbb{R}, q \geq K$. It is easy to see that $\tilde{h}(\tilde{y}_q) \leq 0$. Then by Theorem 5.5.4, TE is GAS on $[\mathbf{0}, \tilde{y}_q]$. Therefore, TE is GAS on $\Omega_K = \cup_{q\geq K}[\mathbf{0}, \tilde{y}_q]$ as well. Similarly to Theorem 5.3.1, Ω_K is an absorbing set. Hence TE is GAS on $\mathbb{R}^4_+$.

ii) Let $0 < Y_P < \tilde{Y}_P^{**}$. Denote the two equilibria by $\tilde{E}^{(j)} = (\tilde{I}^{(j)}, \tilde{Y}^{(j)}, \tilde{F}^{(j)}, \tilde{M}^{(j)})^T$, $j = 1, 2$, where $\tilde{I}^{(1)} < \tilde{I}^{(2)}$. Since $\tilde{Y}$, $\tilde{F}$, $\tilde{M}$ as given in (5.43) are increasing functions of $\tilde{I}$, we have $0 < \tilde{E}^{(1)} < \tilde{E}^{(2)}$ (Figure 5.7). Considering $\tilde{y}_q$ in (5.45) we have

$$\tilde{h}(\tilde{E}^{(2)}) = 0 \leq \tilde{h}(\tilde{y}_q).$$

Then by Theorem 5.5.4 $\tilde{E}^{(2)}$ is GAS on $[\tilde{E}^{(2)}, \tilde{y}_q]$. Therefore, $\tilde{E}^{(2)}$ is GAS on $\cup_{q\geq K}[\tilde{E}^{(2)}, \tilde{y}_q] = \{x \in \mathbb{R}^4_+ : x \geq \tilde{E}^{(2)}, I \leq K\}$. We obtain the statements about the basin of attraction of TE by using Theorem 5.5.5. Indeed, TE being asymptotically stable, attracts some solutions initiated in $[TE, \tilde{E}^{(1)}]$. Then it follows from Theorem 5.5.5 that all solutions initiated in $\{x \in \mathbb{R}^4_+ : x < \tilde{E}^{(1)}\}$ converge to TE. □

The implication of Theorem 5.4.4 for the system (5.17) are stated in the following theorem which extends the results of Theorem 5.4.3.

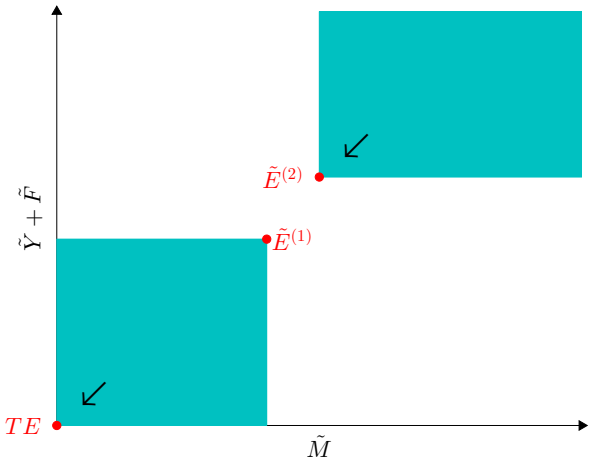

Figure 5.7: Positive invariant sets, when $0 < Y_P < \tilde{Y}_P^{**}$.

Theorem 5.4.5. *Let $Y_P > 0$. Then the following hold for the model (5.17).*

a) If $0 < Y_P \leq \tilde{Y}_P^{**}$, then the basin of attraction of TE contains $\{x \in \mathbb{R}_+^4 : x < \tilde{E}^{(1)}\}$.

b) If $Y_P > \tilde{Y}_P^{**}$, then TE is GAS on $\mathbb{R}_+^4$.

Proof. Using Theorem 5.5.2 with x being the solution of (5.39) and y being the solution of (5.17) we obtain that any solution of (5.39) is an upper bound of the solution of (5.17) with the same initial point. This implies that the basin of attraction of TE as an equilibrium of (5.17) contains the sets indicated in Theorem 5.4.4 c) (i) and ii)), thus proving a) and b) respectively. □

Theorem 5.4.5 characterises the benefit from the control effort represented by Y_P as follows:

- Increasing the effort Y_P in the range $0 < Y_P < Y_P^{**}$ does not lead to elimination of an established population. In fact, as shown on Figure 5.5, the reduction is not proportional to the effort. However, $\tilde{E}^{(1)}$ increases at least linearly with $\tilde{I}^{(1)}$. Hence, increasing Y_P enlarges the basin of attraction of TE, providing better opportunity for controlling an invading population.
- Effort Y_P stronger than $\tilde{Y}_P^{**}$ eliminates any established or invading population.

5.5 Numerical Simulation and Discussion

We use numerical simulations to illustrate the results of Theorems 5.4.3 and 5.4.5 and discuss the biological meaning of the results. The numerical simulations are done using the **ode23tb** solver of Matlab [171] which solves system of stiff ODEs using a trapezoidal rule and second order backward differentiation scheme (TR-BDF2) [12, 134]. The values of the parameters used for the numerical simulations are those of Table 5.1.

Using (5.5), we compute the basic offspring number, $\mathcal{N}_0 = 122$. $\mathcal{N}_0 > 1$, therefore, the population establishes to the positive endemic equilibrium EE^* which we have shown to be GAS on $\mathbb{R}^4_+ \setminus \{TE\}$ (Theorem 5.3.1 c)). Figure 5.8 represents the trajectories of a set of solutions of system (5.1), or equivalently system (5.17) with $Y_P = 0$ and $\alpha = 0$, in the $M \times (Y + F)$ plane. The dots represent the points at which the solutions are initiated. The solutions initiated on $\mathbb{R}^4_+ \setminus \{TE\}$ all converge to the point $EE^* = (992, 319, 1407, 1498)^T$, represented by the green square. Here, TE is also an equilibrium, but it is unstable (Theorem 5.3.1 c)), and therefore it is not represented in Figure 5.8. In the following, we confirm

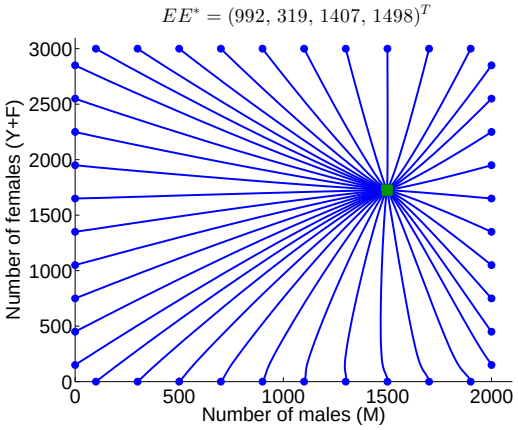

Figure 5.8: Trajectories of a set solutions of system (5.1) in the $M \times (Y + F)$-plane initiated at the dots. The green square represents the stable equilibrium EE^*.

numerically the theoretical results of Theorems 5.4.3 and 5.4.5 with respect to the values of the mating disruption thresholds mentioned in those theorems, Y_P^* and Y_P^{**}. We also investigate the impact of the trapping effort, α, on the population. Using (5.19) and solving numerically the system

$$\begin{cases} \psi(I) &= \eta(Y_P, I) \\ \frac{d\psi}{dI}(I) &= \frac{d\eta}{dI}(Y_P, I) \end{cases}$$

with ψ and $\eta(Y_P, \cdot)$ as defined in (5.23), we obtain respectively the thresholds values Y_P^* and Y_P^{**} as functions of α as represented in Figure 5.9. One can observe that a small trapping

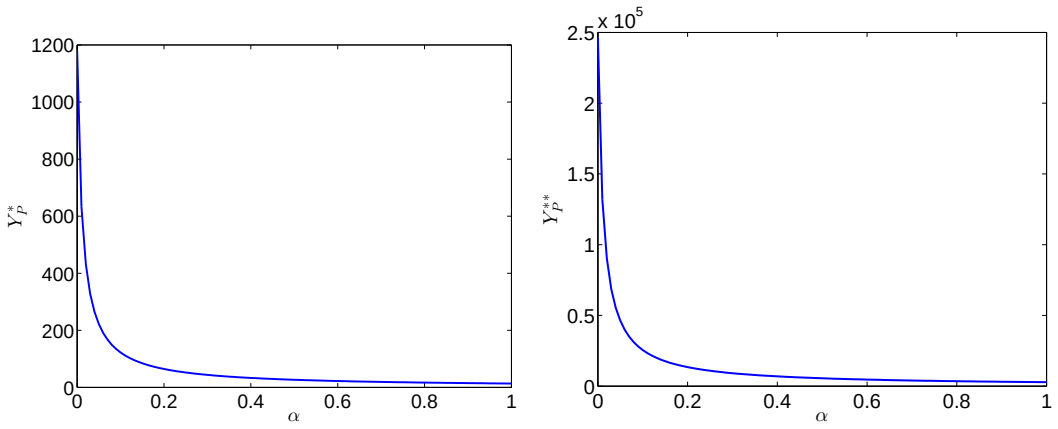

(a) Y_P^* as a function of α (b) Y_P^{**} as a function of α

Figure 5.9: Mating disruption thresholds as function of the trapping parameter α.

effort reduces the mating disruption thresholds in a non-linear manner. Adding trapping to mating disruption allows to reduce the amount of the lure for equivalent control efficiency. In particular, for $\alpha = 0$, we have $Y_P^* = 5673$ and $Y_P^{**} = 987735$, while for $\alpha = 0.1$, we have $Y_P^* = 588$ and $Y_P^{**} = 102462$. Thus, increasing the trapping effort by 10% reduces both Y_P^* and Y_P^{**} by 90%.

Figure 5.10 illustrates the trajectories of the solutions of system (5.17) when the mating disruption level is below the threshold Y_P^* for $\alpha = 0$ and $\alpha = 0.1$. The dots represent the initial points and the green squares represent the asymptotically stable equilibria. In this case, the system has one positive equilibrium, $EE^{\#}$ (Theorem 5.4.3 b)), with value given in the figure. One can observe that when there is no trapping, $EE^{\#} = EE^*$ (Figure 5.10 (a)). This means that the positive endemic equilibrium of the population is not affected by the control. When trapping occurs, we observe in Figure 5.10 (b) that the positive equilibrium is shifted to the left. In fact, the control allows to reduce the number of males but not sufficiently to disrupt the fertilisation of the females. Therefore, the control is not efficient on an established population as the number of females at equilibrium is not reduced. However, when $Y_P > 0$, TE is asymptotically stable, which means that a population can be controlled if it is small enough. Figure 5.11 (a), represents the basin of attraction of TE (the red dots) for a small population in the same setting as for the experiments in Figure 5.10 (a). We observe that there is a set of solutions, for which the initial population is small enough, that converge to TE, hence, a small population can be eradicated for $Y_P > 0$. Further, as shown

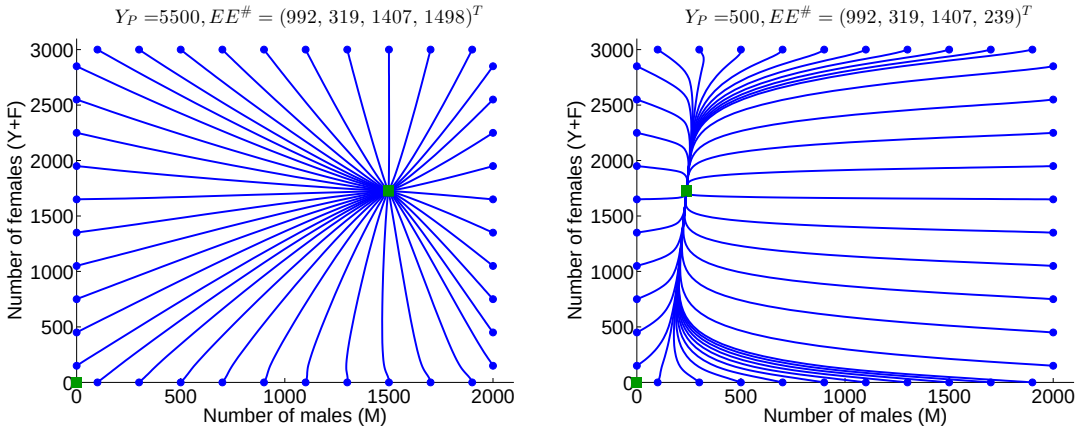

(a) $\alpha = 0$ (b) $\alpha = 0.1$

Figure 5.10: Trajectories of a set solutions of system (5.17) in the $M \times (Y + F)$-plane initiated at the dots. The green squares represent the asymptotically stable equilibria TE and $EE^{\#}$.

in Figure 5.11 (b), adding trapping ($\alpha = 0.1$) with the same mating disruption effort as for Figure 5.11 (a), enlarges the basin of attraction of TE. In other words, for identical mating disruption effort, larger populations can be drawn to extinction when trapping occurs.

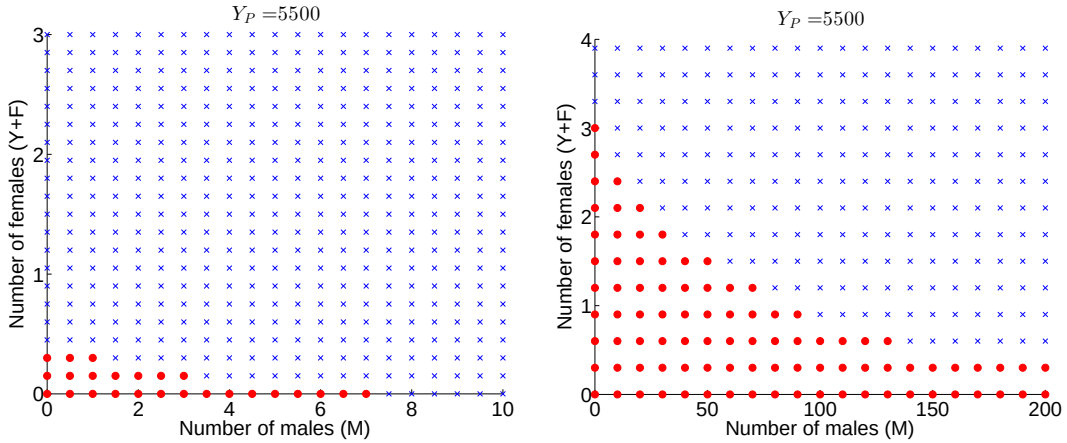

(a) $\alpha = 0$. (b) $\alpha = 0.1$.

Figure 5.11: Effect of α on the basin of attraction of TE. The solutions initiated at the points represented by the red dots converge to TE while the blue crosses represent initial points for which the solution converges to $EE^{\#}$.

In order to observe a reduction in the number of females, the mating disruption effort

has to be increased above the threshold Y_P^*. This is the case in Figure 5.12 ((a) and (b)), where $Y_P = 0.9999 \times Y_P^{**} < Y_P^*$, for $\alpha = 0$ and $\alpha = 0.1$, respectively. We can see that there is a positive asymptotically stable equilibrium, $EE_{MD}^{(2)}$ represented with a green square (Theorems 5.4.3 c)). The blue lines represent the trajectories of the solutions of (5.17) initiated at the blue points which converge to $EE_{MD}^{(2)}$, while the red lines represent the trajectories of the solutions initiated at the red points which converge to TE. With $Y_P > Y_P^*$, the number of females at equilibrium is reduced, however, the impact of the control is not proportional to the effort. Indeed comparing the experiments in Figure 5.10 and Figure 5.12, we observe that in order to reduce the number of females at equilibrium by 49%, the amount of the lure has to be increased by 17857% when $\alpha = 0$ and by 20390% when $\alpha = 0.1$. Further,

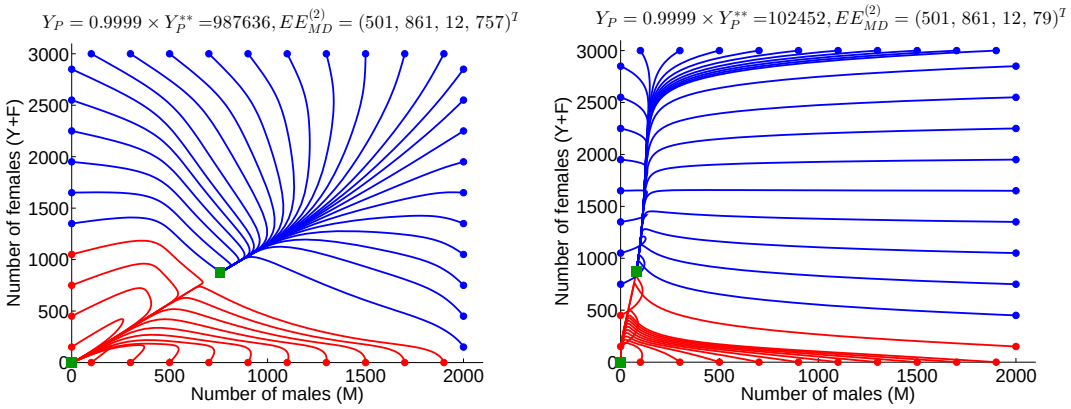

(a) $\alpha = 0$. (b) $\alpha = 0.1$

Figure 5.12: Trajectories of a set solutions of system (5.17) in the $M \times (Y + F)$-plane initiated at the dots. The green squares represent the asymptotically stable equilibria.

comparing the red dots in Figure 5.11 and the red trajectories in Figure 5.12, we can see that the basin of attraction of the trivial equilibrium becomes larger as the value of Y_P increases.

Finally, $Y_P > Y_P^{**}$ allows a full control of the population leading it to extinction no matter how big it is. In Figure 5.13, Y_P is above Y_P^{**} by 0.01%, and we can see that all the trajectories converge to TE. This shows the GAS nature of TE when $Y_P > Y_P^{**}$.

Note that in Theorem 5.4.5, the GAS of TE is established for $Y_P > \tilde{Y}_P^{**}$, however, we show numerically that the GAS property of TE holds for $Y_P > Y_P^{**}$. From Figure 5.14 we can see that the error between $\tilde{Y}_P^{**}$ and Y_P^{**} is of order 10^4 which is small compared to the values of $\tilde{Y}_P^{**}$ and Y_P^{**} which are of order 10^6.

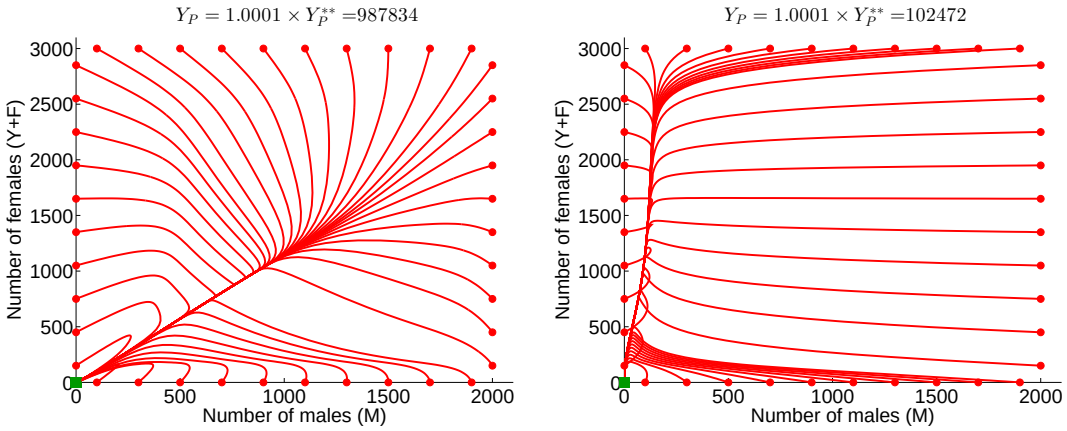

(a) $\alpha = 0$. (b) $\alpha = 0.1$

Figure 5.13: Trajectories of a set solutions of system (5.17) in the $M \times (Y + F)$-plane initiated at the dots. The green squares represent the asymptotically stable equilibria.

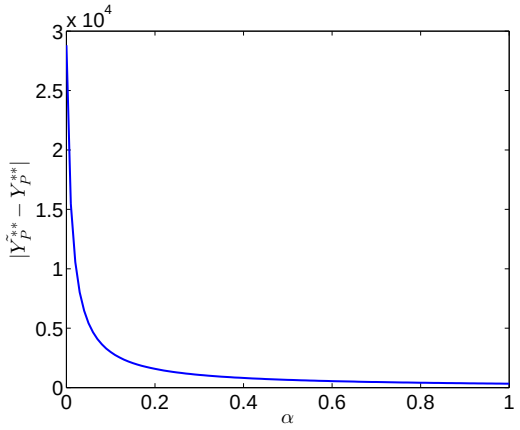

Figure 5.14: Error between the thresholds $\tilde{Y}_P^{**}$ and Y_P^{**} as function of α.

Conclusion and Perspectives

Controlling insect pest population in environmentally respectful manner is a main challenge in IPM programs. Mating disruption using female sex-pheromone based lures falls within IPM requirements as it is species specific and leaves no toxic residues in the produce grown. In this work, we build a generic model, governed by a system of ODEs to simulate the dynamics of a pest population and its response to mating disruption control with trapping. From the theoretical analysis of the model, we identify two threshold values of biological interest for the strength of the lure. The first threshold, Y_P^*, corresponds to a minimum amount of pheromone necessary for mating disruption to have an effect on the population.

However, we show that the control can only be fully efficient, that is, drive an established population to extinction, for an amount of pheromone above a second threshold, Y_P^{**}. We also show asymptotic stability of the trivial equilibrium, TE, whenever $Y_P > 0$. In other words, a small amount of pheromone can be efficient on a very small population, like at invasion stage. Despite the different modelling approach and control method considered, similar results were found by Barclay and Mackauer [17], where a threshold for the size of the release of sterile males was identified, below which two positive equilibria were found, the larger one being stable and the smaller one being unstable, and above which SIT control is fully effective. These theoretical results are consistent with field observation, where the failure of mating disruption is often attributed to a wrong dosage of the pheromone and/or to an excessive population density [4, 178]. Further, we show that increasing the capture efficiency of the traps can reduce considerably these threshold values. From practical point of view this suggests that there is an optimal combination of the strength of the pheromone attractant and the capture efficiency of the traps to optimise the control of the pests in terms of population control and cost. These results support the conclusions of Yamanaka [257] stipulating that in the case where the lure used for mating disruption is strong enough, then additional trapping is not necessary, while otherwise, the author advise to rather focus the effort on the trapping efficiency. In a more realistic setting, this optimised control corresponds to an optimal setting of traps releasing the pheromone. Alternative approaches, such as individual based models (IBM), have been considered to study the impact of mating disruption, incorporating a spatial component where the attraction of males is governed by the pheromone plume [258], or by the effective attraction radius (EAR) which corresponds to the probability of finding the source [40]. A next step for this work is to add a spatial component to investigate how traps should be set, how many should be used, and how far from each other they should be positioned. Investigation on trap settings and their interactions have been studied in a parallel work dealing with parameter estimation [81] and extended in [5], where spatio-temporal trapping models are governed by advection-diffusion-reaction processes.

Another perspective is the validation of the model using field data obtained by Mark-Release-Recapture (MRR) experiments. MRR consists of releasing marked insects in the wild population and recapture them in traps. In such experiments, the number of insects released, as well as the position of the release and the position of the traps are known. Therefore, comparing the trapping data obtained with the model with those obtained using MRR experiments would enable us to validate the model. Then, following the protocol proposed in [5], unknown parameters of the model could be estimated.

Acknowledgements

This work has been supported by the French Ministry of Foreign Affairs and International Development and the South African National Research Foundation in the framework of the PHC PROTEA 2015 call. The support of the DST-NRF Centre of Excellence in Mathematical and Statistical Sciences (CoE-MaSS) towards this research is hereby acknowledged. Opinions expressed and conclusions arrived at, are those of the authors and are not necessarily to be attributed to the CoE.

Appendix A: Computation of the basic offspring number

The basic offspring number, sometimes called "net reproduction rate or ratio" [28], is defined as the expected number of females originated by a single female in a lifetime [212]. The computation can be done using a similar method as for the computation of the "basic reproduction number" in epidemiological model which determines the number if secondary infections produced by a single infectious individual [242, 77]. Let

- $\mathcal{R}_i(x)$ be the rate of recruitment of new individuals in compartment i,
- $\mathcal{T}_i^+(x)$ be the transfer of individuals into compartment i, and
- $\mathcal{T}_i^-(x)$ be the transfer of individuals out of compartment i.

Our system can be written in the form:

$$\dot{x}_i = \mathcal{R}_i(x) - \mathcal{T}_i(x),$$

with

$$\mathcal{T}_i = \mathcal{T}_i^-(x) - \mathcal{T}_i^+(x),$$

$i = 1, .., 4$. When $\gamma M > Y + Y_P$, system (5.17) is reduced to system (5.18) and it can be written as

$$\dot{x} = \mathcal{R}(x) - \mathcal{T}(x),$$

with

$$\mathcal{R}(x) = \begin{pmatrix} b(1 - \frac{I}{K})F \\ 0 \\ 0 \\ 0 \end{pmatrix},$$

end

$$\mathcal{T}(x) = \begin{pmatrix} (\nu_I + \mu_I)I \\ (\nu_Y + \mu_Y)Y - r\nu_I I - \delta F \\ (\delta + \mu_F)F - \nu_Y Y \\ \mu_M M - (1-r)\nu_I I \end{pmatrix}.$$

To obtain the next generation operator, we compute the Jacobian matrices of $\mathcal{R}$ and $\mathcal{T}$, respectively, $J_{\mathcal{R}}$ and $J_{\mathcal{T}}$. Then, from [125, 242], the next generation operator is defined as RT^{-1} where $R = J_{\mathcal{R}}(TE)$ and $T = J_{\mathcal{T}}(TE)$. Here, we have

$$R = \begin{pmatrix} 0 & 0 & b & 0 \\ 0 & 0 & 0 & 0 \\ 0 & 0 & 0 & 0 \\ 0 & 0 & 0 & 0 \end{pmatrix}, \text{ and } \quad T = \begin{pmatrix} \nu_I + \mu_I & 0 & 0 & 0 \\ r\nu_I & \nu_Y + \mu_Y & -\delta & 0 \\ 0 & -\nu_Y & \delta + \mu_F & 0 \\ (1-r)\nu_I & 0 & 0 & \mu_M \end{pmatrix}.$$

The basic offspring number is obtained by computing the spectral radius of the next generation operator [242, 77]:

$$\mathcal{N}_0 = \rho(RT^{-1}) = \frac{br\nu_I\nu_Y}{(\mu_I + \nu_I)\left((\nu_Y + \mu_Y)(\delta + \mu_F) - \delta\nu_Y\right)}.$$

Appendix B: Computation of the endemic equilibrium

We seek for (I^*, Y^*, F^*, M^*) such that

$$\begin{cases} \frac{dI^*}{dt} &= 0, \\ \frac{dY^*}{dt} &= 0, \\ \frac{dF^*}{dt} &= 0, \\ \frac{dM^*}{dt} &= 0, \end{cases}$$

that is

$$\begin{cases} b\left(1 - \frac{I^*}{K}\right)F^* - (\nu_I + \mu_I)I^* &= 0, \\ r\nu_I I^* - (\nu_Y + \mu_Y)Y^* + \delta F^* &= 0, \\ v_Y Y^* - (\delta + \mu_F)F^* &= 0, \\ (1-r)\nu_I I^* - \mu_M M^* &= 0. \end{cases} \tag{5.46}$$

Thus, starting from the bottom:

$$M^* = \frac{(1-r)\nu_I}{\mu_M} I^*,$$

$$F^* = \frac{\nu_Y Y^*}{(\delta + \mu_F)},$$

$$r\nu_I I^* - (\nu_Y + \mu_Y)Y^* + \frac{\delta\nu_Y Y^*}{(\delta + \mu_F)} = 0,$$

$$\Leftrightarrow \quad Y^* = \frac{r\nu_I(\delta + \mu_F)}{(\upsilon_Y + \mu_Y)(\delta + \mu_F) - \delta\nu_Y} I*,$$

and therefore,

$$F^* = \frac{r\nu_I\nu_Y}{(\upsilon_Y + \mu_Y)(\delta + \mu_F) - \delta\nu_Y} I*.$$

Using the first equation of (5.46),

$$b\left(1 - \frac{I^*}{K}\right) F^* - (\nu_I + \mu_I)I^* = 0$$

$$\Leftrightarrow \quad b\left(1 - \frac{I^*}{K}\right) \frac{\nu_Y Y^*}{(\delta + \mu_F)} - (\nu_I + \mu_I)I^* = 0$$

$$\Leftrightarrow \quad b\left(1 - \frac{I^*}{K}\right) \frac{\nu_Y}{(\delta + \mu_F)} \frac{r\nu_I(\delta + \mu_F)}{(\upsilon_Y + \mu_Y)(\delta + \mu_F) - \delta\nu_Y} I^* - (\nu_I + \mu_I)I^* = 0$$

$$\Leftrightarrow \quad b\left(1 - \frac{I^*}{K}\right) \frac{r\nu_I\nu_Y}{(\upsilon_Y + \mu_Y)(\delta + \mu_F) - \delta\nu_Y} - (\nu_I + \mu_I) = 0$$

$$\Leftrightarrow \quad b\left(1 - \frac{I^*}{K}\right) \frac{r\nu_I\nu_Y}{(\upsilon_Y + \mu_Y)(\delta + \mu_F) - \delta\nu_Y} - \frac{(\nu_I + \mu_I)((\upsilon_Y + \mu_Y)(\delta + \mu_F) - \delta\nu_Y)}{(\upsilon_Y + \mu_Y)(\delta + \mu_F) - \delta\nu_Y} = 0$$

$$\Leftrightarrow \quad b\left(1 - \frac{I^*}{K}\right) r\nu_I\nu_Y - (\nu_I + \mu_I)((\upsilon_Y + \mu_Y)(\delta + \mu_F) - \delta\nu_Y) = 0$$

$$\Leftrightarrow \quad br\nu_I\nu_Y I^* = (-(\nu_I + \mu_I)((\upsilon_Y + \mu_Y)(\delta + \mu_F) - \delta\nu_Y) + br\nu_I\nu_Y)K$$

$$\Leftrightarrow \quad I^* = \frac{-(\nu_I + \mu_I)((\upsilon_Y + \mu_Y)(\delta + \mu_F) - \delta\nu_Y) + br\nu_I\nu_Y}{b\nu_I\nu_Y} K$$

$$\Leftrightarrow \quad I^* = \frac{-(\nu_I + \mu_I)((\upsilon_Y + \mu_Y)(\delta + \mu_F) - \delta\nu_Y)}{b\nu_I\nu_Y} K + K$$

$$\Leftrightarrow \quad I^* = \left(1 - \frac{1}{\mathcal{N}_\delta}\right) K.$$

Appendix C: Preliminaries on monotone dynamical systems

Consider the autonomous system of ODEs

$$\frac{dx}{dt} = f(x) \tag{5.47}$$

where $f : D \longrightarrow \mathbb{R}^n$, $D \subset \mathbb{R}^n$. We assume that f is locally Lipshitz so that local existence and uniqueness of the solution is assured. We will use the following notations. Denote

$$x(x_0, t)$$

the solution of (5.47) initiated in x_0. Further, for $x, y \in \mathbb{R}^n_+$, we have:

$$x \leq y \Longleftrightarrow x_i \leq y_i, \forall i \in \{1, 2, \ldots, n\},$$

Definition 5.5.1. *System (5.47) is said to be cooperative if for every $i = 1, ..., n$ the function $f_i(x)$ is monotone increasing with respect to all x_j, $j = 1, ..., n$, $j \neq i$.*

Theorem 5.5.1. *If f is differentiable on D then the system (5.47) is cooperative if and only if*

$$\frac{\partial f_i}{\partial x_j}(x) \geq 0, \quad i \neq j, \quad x \in D.$$

Theorem 5.5.2. *Let (5.47) be a cooperative system and let $x(x_0, t)$ be a solution of (5.47) on $[0, T)$. If $y(t)$ is a differentiable function on $[0, T)$ satisfying*

$$\frac{dy}{dt} \leq f(y), \quad y(0) \leq x_0,$$

then

$$y(t) \leq x(x_0, t), \quad t \in [0, T).$$

[248, Theorem II, 12, II]

Theorem 5.5.3. *Let (5.47) be a cooperative system, and $a, b \in D$. If $a \leq b$ and if for $t > 0$, $x(a, t)$ and $x(b, t)$ are defined, then $x(a, t) \leq x(b, t)$.*

([225, Prop. 1.1 p32])

Theorem 5.5.4. *Let $a, b \in D$, such that $a \leq b, [a, b] \subseteq D$ and $f(a) \leq \mathbf{0} \leq f(b)$. Then (5.47) defines a positive dynamical system on $[a, b]$. Moreover, if $[a, b]$ contains a unique equilibrium p then, p is globally asymptotically stable (GAS) on $[a, b]$.*

([225, Thm. 3.1 p18], [6, Thm. 6])

Theorem 5.5.5. *Let $a, b \in D$, such that $a \leq b$, $[a, b] \subseteq D$ and $f(a) = f(b) = 0$ for (5.47). Then*

a) (5.47) defines a positive dynamical system on $[a, b]$.

b) If a and b are the only equilibria of the dynamical system on $[a, b]$, then all non-equilibrium solutions initiated in $[a, b]$ converge to one of them, that is, either all converge to a or all converge to b.

Proof. a) The proof follows from Theorem 5.5.4.

b) Assume that there exist in the interior of the order interval $[a, b]$ two points x_1 and x_2 such that $\lim_{t\to\infty} x(x_1, t) = a$ and $\lim_{t\to\infty} x(x_2, t) = b$. Then with some technical considerations we deduce that a and b are asymptotically stable. Then by [225, Thm. 2.3.2, Prop. 2.2.1] there is a unique equilibrium in $interior([a, b])$. This contradiction shows that all trajectories converge either all to a or all to b. □

Chapter 6

Conclusion and perspectives

6.1 Overview

The control of pest insects is a matter of main economical, environmental and health concern. IPM programs aim to develop control strategies in order to maintain the pest at a low-impact level while satisfying environmentally respectful requirements. In this context, more and more attention is given to pest-specific methods such as biological control, involving natural enemies of the pest, SIT control, and/or behavioural methods, as mating disruption. The success of such methods relies on accurate knowledge of the pest's biology and ecology as well as a good understanding of its interactions with its environment and its response to the control methods. Much of this knowledge can be obtained via field observations, typically collected via trapping, that are usually costly and time consuming and provide information in the specific setting of the experiment. In order to gain understanding on the biological processes observed in the field in a more generic manner and test various hypothesis, mathematical modelling is a very useful tool.

This study was conducted to set a mathematical framework for the development of control strategies against pest insects. In this prospect this research is focused on the following.

(1) Mathematical models for the pest's dynamics based on biological assumptions and processes, and its response to trapping.

(2) Use of the models to simulate trapping data and compare with field data in order to propose a protocol for accurate and reliable estimation of parameters, such as the insect population size and distribution, and its dispersal rate as well as other parameters related to the traps.

(3) Study of the impact of a specific control method, mating disruption and trapping, and identify thresholds related to the effort of the control method for extinction of the population.

In this chapter, we first recall the major findings of this thesis, their practical implications and the methodology (section 6.2). Then, we discuss the limits and perspectives of this study (section 6.3).

6.2 Major findings of the thesis

6.2.1 Construction of trap-insect models

The first objective of this thesis was to model the dynamics of an insect population responding to attractive traps in order to simulate trapping data to be compared with field data. The modelling choices were driven by biological and ecological knowledge and/or assumptions related to the species, as well as by the research question addressed. For more accuracy given the purpose of the model, we accounted for some heterogeneity and we considered structured population models.

On the one hand, the models built in chapters 3 and 4 are spatio-temporal models. They were used to investigate trapping strategies in terms of positioning of the traps in order to estimate population parameters. Further, in the model of chapter 4, the spatial component allows to account for spatial distribution of the insect species. In these models, we only accounted for an adult population of flying insects which can respond to the traps. There, the trapping of insects is governed by an advection-diffusion-reaction model formulated by PDEs. The diffusion term accounts for random movements of insects when they are not responding to any stimulus, while the advection term governs the attraction of the insects towards the traps. The reaction term models the demography (births, deaths) and the trapping. In the model of chapter 4 we consider that the insects are compartmented in “free” or “captured” insects where the transfer from free to captured occurs in the reaction term of the equation modelling the dynamics of the free insects. In chapter 3 we assume that the concentration of the chemical attractant is static, determined over a disk centred at the trap which increases as the distance to the trap gets smaller. This approach suggests that the trapping occurs when the distribution of the chemical has reached some equilibrium state, and thus does not change with time. In contrast, in chapter 4, we couple the dynamics of the insects with the spread of the chemical attractant which is itself modelled by a diffusion-reaction process. Then, the force and direction of attraction of the insects towards the traps depends on the chemical concentration and its gradient. In chapters 3 and 4 the dynamics of the insects and

their responses to attractive traps is model via advection-diffusion-reaction processes defined via PDEs. The theoretical study of these models was done considering the problems in their variational form and applying the theory of Lions. The general theoretical background is provided in chapter 2, section 2.3. The numerical approximations of the solutions were obtained via the method of lines, where the problem is first discretized with respect to the space variable which reduces the problem to a system of ODEs. The space discretization of the solution in chapter 3 was obtained via approximations of the derivatives using a finite difference scheme. In order to carry out computations on a unstructured mesh, which allows a finer refinement around the traps, the space discretization of the solution in chapter 4 is performed on the variational form of the solution via the finite element method considering first order polynomials.

On the other hand, the purpose of the model presented in chapter 5 is to study the impact of a specific control strategy which consists in disrupting the mating between males and females using female-pheromone traps. Since the pheromone traps only attract males, and that the control affects the fertilisation of females we assumed that the population is structured in four compartments that each have a specific contribution to the dynamics of the whole population. More precisely, we considered a compartment for the aquatic stage (I) gathering eggs, larvae and pupae, one for adult males (M), another one for females available for mating (Y), and finally one for fertilised females (F). The transfer rate from the Y compartment to the F compartment depends on the abundance of males available for mating. When the males are in sufficient abundance, this rate is maximal and constant, while when the males are scarce, the rate accounts for the proportion of females that were able to mate with a male. Following the approach in [18], we related the amount of pheromones released by the traps to an equivalent number of females (Y_P). The males attracted to the pheromone traps become unavailable for mating. Given all these consideration, the model governing the insect population dynamics is formulated by a system of four coupled ODEs. A deep theoretical study of this model was carried out using the theory of monotone dynamical recalled in chapter 2, section 2.4. It allowed to identify pheromone threshold values that ensure an effective control of the population.

6.2.2 Protocol for the estimation of population parameters

The models built in chapters 3 and 4 were used to estimate population parameters, more precisely, the initial population size, its dispersal rate and other parameter values related to the attractiveness of the traps.

In chapter 3, the model allowed to investigate the influence of the number of parameters

estimated simultaneously as well as the positioning of the traps on the quality of the estimations. As a result, we found that, the more parameters are estimate simultaneously, less accurate and reliable are the estimates. Further, we found that the trap setting plays an important role in the quality of the estimations. More precisely, using data from interacting traps provided better results than non-interacting traps (or equivalently, using a single trap). In our experiments, the trap setting C stood out providing significantly better estimation of the parameter values than the other settings regardless the number of parameters estimated simultaneously. This suggests the existence of an optimal setting of interacting traps that would allow an accurate and reliable simultaneous estimation of several parameters.

The population size and distribution, its dispersal rate and the parameters related to the traps may depend on environmental changes (temperature, humidity, wind, etc.) and thus vary in time. In chapter 4 we develop a protocol for the estimation of the population parameters using data over a short period of time during which the parameter values may be assumed to be constant. This protocol is structured in three steps, three (short) experiments, in which we minimize the number of parameters to estimate simultaneously for a more accurate and reliable estimations.

The first step of this protocol consists in estimating the dispersal rate using data obtained from a MMR experiment with non-attractive traps. In this experiment, the initial population size and distribution of marked insects is known since they are released in a specific location. In chapter 4, we studied numerically the influence of the size of the release, as well as its distance to the trap for 3 and 5 days of data. We found that 5 days of data do not provide significantly better estimates of the dispersal rate. Further, we showed that farther releases from the trap (50 meters) provided less accurate estimates but can be compensated by increasing the size of the release. For closer releases (10 meters and 30 meters), increasing the size of the release did not improve significantly the quality of the estimation.

The second step consists in estimating the parameters related to the traps. Here, we have two parameters α and β which account for the strength of attraction of the trap. To estimate α and β we use a MRR experiment with attractive traps, and the value of the dispersal rate estimated in the first step of the protocol. Similarly as for the estimation of the dispersal rate, we show that it is preferable to do the release close to the trap and that larger releases increase the quality of the estimations. However, here, the estimations obtained with 5 days of data were less accurate than those obtained with 3 days of data, thus the estimation of the trap parameters can be done using a short period of time.

The final step is the estimation of the population size, U_0, which is the integral of the initial condition of the problem, u_0, over the spatial domain Ω. While in the work of chapter 3, the initial distribution of insects was assumed homogeneous over the domain, here we

account for heterogeneous distributions of insets. Trapping data were simulated considering three different distributions. Then, the population size was estimated using "guessed" initial distributions with unknown population size with 3 days, and 5 days of data. The results suggested that 5 days of data produces more accurate estimations, however, if the initial guessed distribution is close enough to the real distribution, 3 days of data can be sufficient to obtain accurate distribution. In other words, with a good understanding and knowledge about the insect's ecology, its distribution and interactions with the environment, we can expect accurate estimation of its population size, even with data collected over a short period of time.

The numerical approximations of the solutions allowed to simulate trapping data used to estimate parameter values. The estimation of the parameters consists in solving an optimization problem in the least-square sense, where we minimize an objective function which is defined by the sum of the squares of the difference between the observed data and the simulated data. This minimization problem is solved numerically using the Levenberg-Marquardt algorithm. However, since the latter algorithm is a local minimization problem, the minimization problem was solved several times with initial values picked (uniformly) randomly in a specified interval. When several local minima are found, we choose the set of parameters that yields the smallest value of the minimized objective function.

6.2.3 Identification of thresholds for mating disruption and trapping control

A preliminary study of the model of chapter 5 with no control allowed to compute the basic offspring number $\mathcal{N}_0$ which determines whether the population is viable or not. To study this model, we first studied the case when males were in sufficient abundance following the same approach as in [82], then we studied the model in the case when males were scares. Combining the results of both cases we concluded that when $\mathcal{N}_0 \leq 1$ the only equilibrium of the model with no control is the trivial equilibrium (TE) which is GAS on $\mathbb{R}^4_+$, thus the population is not viable. When $\mathcal{N}_0 > 1$, we found that the model has 2 equilibria, TE which is unstable, and a positive endemic equilibrium EE^* which is GAS on $\mathbb{R}^4_+ \backslash \{x \in \mathbb{R}^4_+ : I = F = 0\}$, thus the population can establish.

The study of the model with control was carried out assuming that the population could establish $\mathcal{N}_0 > 1$. As for the study of the model with no control, properties of the equilibria in the male abundance region and in the male scarcity region were studied independently in order to determine the properties of the whole system. Two threshold values of Y_P were identified, Y_P^* and Y_P^{**} which determine the behaviour of the system and have important

consequences on the efficacy of the control.

First, we found that whenever $Y_P > 0$, TE is asymptotically stable, thus a population could be driven to extinction if it is small enough, such as at invasion stage. Then, we identified a threshold Y_P^{**} such that whenever $0 < Y_P < Y_P^{**}$, the system has two positive equilibria. Numerically, we found that one is unstable while the other one is asymptotically stable. In addition, we found another threshold value $Y_P^* < Y_P^{**}$ under which the control has no effect on an established population. More precisely, when $0 < Y_P < Y_P^*$, the males remain in sufficient abundance and the control does not affect the endemic equilibrium of the females. On the other hand, for $Y_P^* < Y_P < Y_P^{**}$, the control has an effect on an established population, the abundance of females at equilibrium is reduced but can remain high. However when $Y_P > Y_P^{**}$, we observe a "jump" in the behaviour of the system where the population is driven to extinction. Theoretically, we show that there is a threshold value of Y_P above which TE is GAS.

It is typically difficult to understand why mating disruption is a success in some cases [48, 58] while it fails in others [4, 178]. The failure in mating disruption experiments often attributed to a wrong dosage of the pheromone and/or to over-abundant population [4, 178]. These results show that a full control of the population can only be achieved if the dosage is above a certain threshold. Below this threshold, the control may be efficient on a small (i.e. invading) population but may have only a small or no impact on an established population.

6.3 Limits and perspectives

This study provides outputs of importance in the prospect of pest-insect control resulting from the theoretical analysis and simulations of trap-insect mathematical models. The next major step of this work is the validation and application of the obtained results using field data. In this perspective, a certain number of limitations need to be considered.

In chapters 3 and 4, for instance, homogeneous Neumann boundary conditions were considered. This condition implies that the domain is assumed isolated, such that there is no flux of insects on its boundary. In other words, when using homogeneous Neumann boundary conditions, we assume that, at the boundary, immigration compensate emigration, or that the domain is sufficiently large so that the dynamics at the boundary have a negligible impact on the dynamics within the domain. However, such assumption is seldom verified in the field. Indeed, immigration can play a crucial role to prevent species extinction, particularly in small habitats [188]. A possible way to account for migration is to consider non-homogeneous conditions at the boundary of the domain. Other types of boundary conditions, such as Robin

conditions involving the flux and the density at the boundary, could be considered, or even mixed boundary conditions where different types of conditions are modelled on different parts of the boundary. However, these approaches require to quantify the flux at the boundary, which is often difficult. Another commonly used boundary condition is the homogeneous Dirichlet condition which has been used to model the spread of the chemical attractant in the model of chapter 4. The use of Dirichlet boundary condition implies that the surrounding environment is totally hostile, such that the density modelled is equal to zero. In the case of the spread of the chemical attractant, it was convenient as we assumed that the concentration of the chemical had vanished by the time it reached the boundary. However, we highlight here that the use of homogeneous Neumann or Dirichlet boundary conditions can be suitable provided that the domain is assumed large enough. Alternatively migration can be accounted for in the reaction term of the model similarly as for the demography (births and death) of the population. This approach can be relevant to model migration due to long-distance dispersal, or inter-layer migrations in the case of a 2D model restricted to a specific layer. But here again, the knowledge on the migration rates would be required.

In addition, the model of chapter 4 does not account for spatial heterogeneity in the diffusion and advection coefficients. However such parameter values are expected to vary when the landscape is heterogeneous. Adding spatial heterogeneity in the coefficients would allow more realistic simulations and possibly link the model with GIS data. In particular, although heterogeneous spatial distribution of insects was assumed in chapter 4, we did not take into account the factor leading to such a distribution in the model, such as attractiveness to hosts (trees, shaded areas, etc.). The spatial distribution of insects can be decisive in the effectiveness of control methods. These models could be extended to account for the dynamics governing the heterogeneity in the initial distributions, like interactions between pests and hosts.

Besides, in the protocol for parameter estimation proposed in chapter 4, the first step consists in estimating the diffusion parameter using non-attractive traps, and thus assuming that the movement of insects is only driven by diffusion. Although it is possible to obtain simulated trapping data in such a case, practically it is not realistic to capture insects assuming only the isotropic random walk process with passive traps. Typically, insects are also receptive to visual cues, like colour, size or shape, which give direction to their displacements. The work of chapter 4 aimed to focus on the chemical cues via a chemotaxis process. However, in order to be more consistent with field experiments, an additional advection term could be considered to account for other drift parameters such as visual attraction, attraction to host fruits or wind transport. In a previous work [80], host attraction and breeding sites were accounted for in a mosquito model to simulate their spatio-temporal distribution.

Furthermore, modelling the trapping via a diffusion-advection-reaction process has its

challenges of its own as the attraction towards the traps can lead to an accumulation of insects in a very localised area of the domain which can produce singularities and compromise the well-posedness of the problem. To overcome this difficulty, in chapter 3, we assumed that the value of the diffusion coefficient was very small inside the traps to avoid "escapes" of insects via the diffusion process due to the accumulation of insects inside the traps. Alternatively, in chapter4, we considered a "trapped-insect" compartment and we had to define a transfer rate from free to trapped insects. Another possible approach of mathematical interest would be to consider a domain with singularities, where traps would be modelled by holes in the domain as represented in Figure 6.1. Then, flux at the boundaries of the traps letting insect go exclusively in the traps (outside the domain) would account for the trapping of insects.

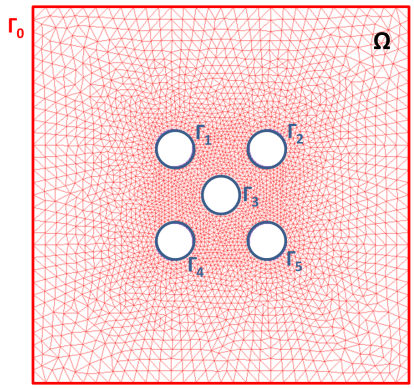

Figure 6.1: Domain Ω, where traps are modelled via holes with boundaries Γ_1, Γ_2, Γ_3, Γ_4 and Γ_5.

Moreover, the mating disruption model of chapter 5 has allowed a deep theoretical study due to its ODE formulation. Such model is relevant in a spatially homogeneous environment, or in a local area, for instance at the scale of a tree. In order to model the dynamics of the pest population at the scale of a crop, individual trees could be seen as homogeneous interacting patches on which we could consider a meta-population model. This approach would allow to study the impact of the control in a spatially structured crop in order to adapt and/or optimize control strategies. Another significant aspect to investigate is the positioning of the traps given the concentration of the lure used in the prospect of finding an optimal setting of the traps. This aspect could be addressed following a similar approach as in the study of chapter 3 with interacting traps, where the ODE model would be extended to a PDE model to account explicitly for the spatial variable.

Another relevant perspective is the combination of mating disruption and trapping with other methods in order to optimise control strategies in terms of efficiency and cost. Further, combination of several methods would be more flexible to adapt with environmental

changes and avoid dependence to a single method that might work only in specific conditions. Such other control methods may involve natural enemies such as weaver ants, used in Benin [243], or using parasitoids as in French Polynesia [159], involving *Fopius arisanus* and *Diachasmimorpha longicauda* for the control of fruit flies.

The present work gives a mathematical framework to model the dynamics of insects responding to attractive traps. Although the models presented here can be made more realistic by adding complexity, their relative simplicity allowed to carry out theoretical mathematical studies and simulations providing biologically relevant and applicable results useful for the development of pest-insect control tool satisfying the requirements of IPM programs.

Bibliography

[1] V. V. Akimenko, Y. V. Zahorodnii, and A. L. Boyko. Identification of parameters of evolutionary model of monocyclic cells aggregation with the hop plants example. Computers & Mathematics with Applications, 66(9):1547–1553, 2013.

[2] L. Alphey and N. Alphey. Five things to know about genetically modified (gm) insects for vector control. PLoS Pathogens, 10(3):e1003909, 2014.

[3] M. Aluja and P. Liedo. Fruit Flies: Biology and Management. Springer Science & Business Media, 2013.

[4] B. G. Ambrogi, E. R. Lima, and L. Sousa-Souto. Efficacy of mating disruption for control of the coffee leaf miner leucoptera coffeella (guérin-méneville)(lepidoptera: Lyonetiidae). BioAssay, 1(8):1–5, 2006.

[5] R. Anguelov, C. Dufourd, and Y. Dumont. Simulations and parameter estimation of a trap-insect model using a finite element approach. Mathematics and Computers in Simulation, 133:47 – 75, 2017.

[6] R. Anguelov, Y. Dumont, and J. Lubuma. Mathematical modeling of sterile insect technology for control of anopheles mosquito. Computers and Mathematics with Applications, 64(3):374–389, 2012.

[7] R. Anguelov, Y. Dumont, and J. M.-S. Lubuma. On nonstandard finite difference schemes in biosciences. AIP Conference Proceedings, 1487(1):212–223, 2012.

[8] R. Anguelov and E. D. Popova. Topological structure preserving numerical simulations of dynamical models. Journal of Computational and Applied Mathematics, 235(2):358–365, 2010.

[9] J. L. Apple and R. F. (Eds.) Smith. Integrated Pest Management. New-York: Plenum Press, 1976.

[10] J. Arino, A. Ducrot, and P. Zongo. A metapopulation model for malaria with transmission-blocking partial immunity in hosts. Journal of Mathematical Biology, 64(3):423–448, 2012.

[11] P. Auger, E. Kouokam, G. Sallet, M. Tchuente, and B. Tsanou. The ross–macdonald model in a patchy environment. Mathematical Biosciences, 216(2):123–131, 2008.

[12] R. E. Bank, W. M. Coughran Jr, W. Fichtner, E. H. Grosse, D. J. Rose, and R. K. Smith. Transient simulation of silicon devices and circuits. Computer-Aided Design of Integrated Circuits and Systems, IEEE Transactions on Electron Devices, 4(4):436–451, 1985.

[13] C. J. Banks and E. S. Brown. A comparison of methods of estimating population density of adult sunn pest, eurygaster integriceps put.(hemiptera, scutelleridae) in wheat fields. Entomologia Experimentalis et Applicata, 5(4):255–260, 1962.

[14] H. Banks, J. Crowley, and K. Kunisch. Cubic spline approximation techniques for parameter estimation in distributed systems. Automatic Control, IEEE Transactions on Automatic Control, 28(7):773–786, 1983.

[15] H. T. Banks and P. Kareiva. Parameter estimation techniques for transport equations with application to population dispersal and tissue bulk flow models. Journal of Mathematical Biology, 17(3):253–273, 1983.

[16] H. T. Banks, P. M. Kareiva, and L. Zia. Analyzing field studies of insect dispersal using two-dimensional transport equations. Environmental Entomology, 17(5):815–820, 1988.

[17] H. Barclay and M. Mackauer. The sterile insect release method for pest control: a density-dependent model. Environmental Entomology, 9(6):810–817, 1980.

[18] H. Barclay and P. Van den Driessche. Pheromone trapping models for insect pest control. Researches on Population Ecology, 25(1):105–115, 1983.

[19] H. J. Barclay and J. Hendrichs. Models for assessing the male annihilation of bactrocera spp. with methyl eugenol baits. Annals of the Entomological Society of America, 107(1):81–96, 2014.

[20] H. J. Barclay and G. J. R. Judd. Models for mating disruption by means of pheromone for insect pest control. Researches on Population Ecology, 37(2):239–247, 1995.

[21] R. J. Bartell. Mechanisms of communication disruption by pheromone in the control of lepidoptera: a review. Physiological Entomology, 7(4):353–364, 1982.

[22] M. A. Bateman. The ecology of fruit flies. Annual Review of Entomology, 17(1):493–518, 1972.

[23] N. Becker and K. R. S. Ascher. The use of bacillus thuringiensis subsp. israelensis (bti) against mosquitoes, with special emphasis on the ecological impact. Israel Journal of Entomology, 32:63–69, 1998.

[24] N. Becker, D. Petrić, C. Boase, J. Lane, M. Zgomba, C. Dahl, and A. Kaiser. Mosquitoes and Their Control, volume 2. Springer, 2010.

[25] R. Bellini, M. Calvitti, A. Medici, M. Carrieri, G. Celli, and S. Maini. Use of the sterile insect technique against aedes albopictus in italy: First results of a pilot trial. In Area-Wide Control of Insect Pests, pages 505–515. Springer, 2007.

[26] L. Berec. Techniques of spatially explicit individual-based models: construction, simulation, and mean-field analysis. Ecological Modelling, 150(1):55–81, 2002.

[27] H. C. Berg. Random Walks in Biology. Princeton University Press, 1993.

[28] L. C. Birch. The intrinsic rate of natural increase of an insect population. The Journal of Animal Ecology, 17(1):15–26, 1948.

[29] P.-A. J. Bliman, M. S. Aronna, F. C. Coelho, and M. A. H. B. da Silva. Ensuring successful introduction of wolbachia in natural populations of aedes aegypti by means of feedback control. arXiv preprint arXiv:1503.05216, 2015.

[30] S. Bloem, J. Carpenter, and H. Hofmeyr. Area-wide control tactics for the false codling moth thaumatotibia leucotreta in south africa: a potential invasive species. In Area-Wide Control of Insect Pests, pages 351–359. Springer, 2007.

[31] M. Bonizzoni, G. Gasperi, X. Chen, and A. A. James. The invasive mosquito species aedes albopictus: current knowledge and future perspectives. Trends in Parasitology, 29(9):460–468, 2013.

[32] W. H. Bossert and E. O. Wilson. The analysis of olfactory communication among animals. Journal of Theoretical Biology, 5(3):443–469, 1963.

[33] M. Branco, H. Jactel, J. C. Franco, and Z. Mendel. Modelling response of insect trap captures to pheromone dose. Ecological Modelling, 197(1):247–257, 2006.

[34] F. Brauer and C. Castillo-Chavez. Mathematical Models in Population Biology and Epidemiology, volume 40. Springer, 2011.

[35] S. C. Brenner and R. Scott. The Mathematical Theory of Finite Element Methods, volume 15. Springer, 2008.

[36] H. Brezis. Functional Analysis, Sobolev Spaces and Partial Differential Equations. Springer, 2011.

[37] S. R. Broadbent and D. G. Kendall. The random walk of trichostrongylus retortaeformis. Biometrics, 9(4):460–466, 1953.

[38] S. T. Buckland, D. R. Anderson, K. P. Burnham, and J. L. Laake. Distance Sampling. Wiley Online Library, 2005.

[39] M. Burger. Parameter identification. Lecture Notes, 2005.

[40] J. A. Byers. Simulation of mating disruption and mass trapping with competitive attraction and camouflage. Environmental Entomology, 36(6):1328–1338, 2007.

[41] J. A. Byers. Active space of pheromone plume and its relationship to effective attraction radius in applied models. Journal of Chemical Ecology, 34(9):1134–1145, 2008.

[42] J. A. Byers. Modeling distributions of flying insects: Effective attraction radius of pheromone in two and three dimensions. Journal of Theoretical Biology, 256(1):81–89, 2009.

[43] J. A. Byers, O. Anderbrant, and J. Löqvist. Effective attraction radius. Journal of Chemical Ecology, 15(2):749–765, 1989.

[44] P. Cailly. Modélisation de la Dynamique Spatio-Temporelle d'une Population de Moustiques, Sources de Nuisances et Vecteurs d'Agents Pathogènes. PhD thesis, Oniris, Ecole Nationale Vétérinaire, Agroalimentaire et de l'Alimentation Nantes Atlantique; Université Nantes Angers Le Mans (UNAM), 2011.

[45] G. L. Campbell, A. A. Marfin, R. S. Lanciotti, and D. J. Gubler. West nile virus. The Lancet infectious diseases, 2(9):519–529, 2002.

[46] B. Cantrell, B. Chadwick, and A. Cahill. Fruit Fly Fighters: Eradication of the Papaya Fruit Fly. CSIRO Publishing, 2002.

[47] R. T. Carde. Principles of mating disruption. Behavior-Modifying Chemicals for Pest Management: Applications of Pheromones and Other Attractants. Marcel Dekker, New York, pages 47–71, 1990.

[48] R. T. Carde and A. K. Minks. Control of moth pests by mating disruption: successes and constraints. Annual Review of Entomology, 40(1):559–585, 1995.

[49] H. Caswell. Matrix Population Models. Wiley Online Library, 2006.

[50] F. Catteruccia, T. Nolan, T. G Loukeris, C. Blass, C. Savakis, F. C. Kafatos, and A. Crisanti. Stable germline transformation of the malaria mosquito anopheles stephensi. Nature, 405(6789):959–962, 2000.

[51] K.-L. Chan et al. Life table studies of aedes albopictus (skuse). Sterility principles for insect control or eradication. International Atomic Energy Agency, Vienna, Austria, pages 131–144, 1971.

[52] R. Choquet, L. Rouan, and R. Pradel. Program e-surge: a software application for fitting multievent models. In Modeling Demographic Processes in Marked Populations, pages 845–865. Springer, 2009.

[53] I. Chou and E. O. Voit. Recent developments in parameter estimation and structure identification of biochemical and genomic systems. Mathematical Biosciences, 219(2):57–83, 2009.

[54] D. Cianci, J. Van Den Broek, B. Caputo, F. Marini, A. Della Torre, H. Heesterbeek, and N. Hartemink. Estimating mosquito population size from mark–release–recapture data. Journal of Medical Entomology, 50(3):533–542, 2013.

[55] P. G. Ciarlet. The Finite Element Method for Elliptic Problems, volume 40. Siam, 2002.

[56] L. R. Clark, P. W. Geier, R. D. Hughes, R. F. Morris, et al. The Ecology of Insect Populations in Theory and Practice. London, Methuen & Co. Ltd., 1967.

[57] A. N. Clements. The Biology of Mosquitoes: Development, Nutrition, and Reproduction. The Biology of Mosquitoes. Chapman & Hall, 1992.

[58] A. Cocco, S. Deliperi, and G. Delrio. Control of *Tuta absoluta* (meyrick)(lepidoptera: Gelechiidae) in greenhouse tomato crops using the mating disruption technique. Journal of Applied Entomology, 137(1-2):16–28, 2013.

[59] M. L. Cornelius, J. J. Duan, and R. H. Messing. Visual stimuli and the response of female oriental fruit flies (Diptera: Tephritidae) to fruit-mimicking traps. Journal of Economic Entomology, 92(1):121–129, 1999.

[60] R. Couilloud. Cryptophlebia leucotreta (Meyrick) (Lepidoptera: Tortricidae). In Insect Pests of Cotton, pages 207–213. CAB International, Wallingford, UK, 1994.

[61] J. Crank. The Mathematics of Diffusion. Oxford university press, 1979.

[62] J. Crank and P. Nicolson. A practical method for numerical evaluation of solutions of partial differential equations of the heat-conduction type. In Mathematical Proceedings of the Cambridge Philosophical Society, volume 43, pages 50–67. Cambridge Univ Press, 1947.

[63] M. Cristofol, J. Garnier, F. Hamel, and L. Roques. Uniqueness from pointwise observations in a multi-parameter inverse problem. arXiv preprint arXiv:1105.5570, 2011.

[64] B. Cummins, R. Cortez, I. M. Foppa, J. Walbeck, and J. M. Hyman. A spatial model of mosquito host-seeking behavior. PLoS Computational Biology, 8(5):e1002500, 2012.

[65] R. T. Cunningham and H. M. Couey. Mediterranean fruit fly (diptera: Tephritidae): distance/response curves to trimedlure to measure trapping efficiency. Environmental Entomology, 15(1):71–74, 1986.

[66] T. Czárán. Spatiotemporal Models of Population and Community Dynamics, volume 21. Springer Science & Business Media, 1998.

[67] C. C. Daiber. A survey of male flight of the false codling moth, cryptophlebia leucotreta meyr., by the use of the synthetic sex pheromone. Phytophylactica, 10(2):65–72, 1978. 7.

[68] C. C. Daiber. A study of the biology of the false codling moth (cryptophlebia leucotreta (meyr.)): the cocoon. Phytophylactica, 11(4):151–157, 1979. 8.

[69] C. C. Daiber. A study of the biology of the false codling moth (cryptophlebia leucotreta (meyr.)): the egg. Phytophylactica, 11(3):129–132, 1979. 4.

[70] C. C. Daiber. A study of the biology of the false codling moth (cryptophlebia leucotreta (meyr.)): the larva. Phytophylactica, 11(3):141–144, 1979. 9.

[71] C. C. Daiber. A study of the biology of the false codling moth cryptophlebia leucotreta (meyr.): the adult and generations during the year. Phytophylactica, 12(4):187–193, 1980. 10.

[72] R. Dautray and J.-L. Lions. Mathematical Analysis and Numerical Methods for Science and Technology: Volume 2: Functional and Variational Methods. Springer, 2000.

[73] R. Dautray and J.-L. Lions. Mathematical Analysis and Numerical Methods for Science and Technology: Volume 5 Evolution Problems I. Springer-Verlag Berlin Heidelberg, 1 edition, 2000.

[74] P. N. Daykin, F. E. Kellogg, and R. H. Wright. Host-finding and repulsion of *Aedes aegypti*. The Canadian Entomologist, 97(3):239–263, 1965.

[75] D. L. DeAngelis and W. M. Mooij. Individual-based modeling of ecological and evolutionary processes. Annual Review of Ecology, Evolution, and Systematics, pages 147–168, 2005.

[76] H. Delatte, G. Gimonneau, A. Triboire, and D. Fontenille. Influence of temperature on immature development, survival, longevity, fecundity, and gonotrophic cycles of aedes albopictus, vector of chikungunya and dengue in the indian ocean. Journal of Medical Entomology, 46(1):33–41, 2009.

[77] O. Diekmann, J. A. P. Heesterbeek, and M. G. Roberts. The construction of next-generation matrices for compartmental epidemic models. Journal of the Royal Society Interface, page rsif20090386, 2009.

[78] R. A. I. Drew, K. Tsuruta, I. M. White, et al. A new species of pest fruit fly (Diptera: Tephritidae: Dacinae) from sri lanka and africa. African Entomology, 13(1):149–154, 2005.

[79] C. Dufourd and Y. Dumont. Modeling and simulations of mosquito dispersal. The case of *Aedes albopictus*. Biomath, 1(2):128–134, 2012.

[80] C. Dufourd and Y. Dumont. Impact of environmental factors on mosquito dispersal in the prospect of sterile insect technique control. Computers & Mathematics with Applications, 66(9):1695–1715, 2013.

[81] C. Dufourd, C. Weldon, R. Anguelov, and Y. Dumont. Parameter identification in population models for insects using trap data. Biomath, 2:1–10, 2013.

[82] Y. Dumont and J. M. Tchuenche. Mathematical studies on the sterile insect technique for the chikungunya disease and *Aedes albopictus*. Journal of Mathematical Biology, 65(5):809–855, 2012.

[83] J. B. Dunning Jr, D. J. Stewart, B. J. Danielson, B. R. Noon, T. L. Root, R. H. Lamberson, and E. E. Stevens. Spatially explicit population models: current forms and future uses. Ecological Applications, 5(1):3–11, 1995.

[84] R. Durrett and S. Levin. The importance of being discrete (and spatial). Theoretical Population Biology, 46(3):363–394, 1994.

[85] R. Durrett and S. A. Levin. Stochastic spatial models: a user's guide to ecological applications. Philosophical Transactions of the Royal Society of London B: Biological Sciences, 343(1305):329–350, 1994.

[86] V. A. Dyck, J. Hendrichs, and A. S. Robinson. Sterile Insect Technique. Springer, 2005.

[87] L. Edelstein-Keshet. Mathematical Models in Biology, volume 46. Siam, 1988.

[88] J. M. Edington and M. A. Edington. Ecology, Recreation and Tourism. CUP Archive, 1986.

[89] S. Ekesi, P. W. Nderitu, and I. Rwomushana. Field infestation, life history and demographic parameters of the fruit fly bactrocera invadens (diptera: Tephritidae) in africa. Bulletin of Entomological Research, 96(04):379–386, 2006.

[90] A. M. El-Sayed, D. M. Suckling, C. H. Wearing, and J. A. Byers. Potential of mass trapping for long-term pest management and eradication of invasive species. Journal of Economic Entomology, 99(5):1550–1564, 2006.

[91] J. S. Elkinton and R. T. Cardé. Odor dispersion. In W. J. Bell and R. T. Cardé, editors, Chemical Ecology of Insects, pages 73–91. Sinauer Associates Sunderland, 1984.

[92] W. R. Enkerlin. Impact of fruit fly control programmes using the sterile insect technique. In Sterile Insect Technique, pages 651–676. Springer, 2005.

[93] Nancy D Epsky and Robert R Heath. Exploiting the interactions of chemical and visual cues in behavioral control measures for pest tephritid fruit flies. Florida Entomologist, pages 273–282, 1998.

[94] A. Ern. Theory and Practice of Finite Elements, volume 159. Springer, 2004.

[95] G. Evans, J. Blackledge, and P. Yardley. Numerical methods for partial differential equations. Springer Science & Business Media, 2012.

[96] L. C. Evans. Partial Differential Equations, volume 19 of Graduate Studies in Mathematics. Providence, Rhode Island, 1998.

[97] J. Z. Farkas and P. Hinow. Structured and unstructured continuous models for *Wolbachia* infections. Bulletin of Mathematical Biology, 72(8):2067–2088, 2010.

[98] M. E. Fisher, P. Van Den Driessche, and H. J. Barclay. A density dependent model of pheromone trapping. Theoretical Population Biology, 27(1):91–104, 1985.

[99] R. Fletcher. Practical Methods of Optimization. John Wiley & Sons, 2013.

[100] D. Fontenille, M. Traore-Lamizana, M. Diallo, J. Thonnon, J. P. Digoutte, and H. G. Zeller. New vectors of rift valley fever in west africa. Emerging infectious diseases, 4(2):289, 1998.

[101] A. Fortin and A. Garon. Les éléments finis: de la théorie à la pratique, 2011. Université Laval.

[102] A. Friedman. Partial Differential Equations. Holt, Rinehart and Winston, 1969.

[103] D. M. Fry. Reproductive effects in birds exposed to pesticides and industrial chemicals. Environmental Health Perspectives, 103(Suppl 7):165, 1995.

[104] P. Gabrieli, A. Smidler, and F. Catteruccia. Engineering the control of mosquito-borne infectious diseases. Genome Biology, 15(11):1, 2014.

[105] C. Geuzaine and J.-F. Remacle. Gmsh: A 3-d finite element mesh generator with built-in pre-and post-processing facilities. International Journal for Numerical Methods in Engineering, 79(11):1309–1331, 2009.

[106] H. Gillet. F. de Laroussilhe—Le Manguier. Techniques agricoles et productions tropicales. Journal d'Agriculture Traditionnelle et de Botanique Appliquée, 27(3-4):277–278, 1980.

[107] H. C. J. Godfray. Parasitoids: Behavioral and Evolutionary Ecology. Princeton University Press, 1994.

[108] L. C. Gouagna, Dehecq. J.-S., D. Fontenille, Y. Dumont, and S. Boyer. Seasonal variation in size estimates of aedes albopictus population based on standard mark-release-recapture experiments in an urban area on reunion island. Acta Tropica, 143(0):89 – 96, 2015.

[109] F. Gould and P. Schliekelman. Population genetics of autocidal control and strain replacement. Annual Reviews in Entomology, 49(1):193–217, 2004.

[110] G. Grard, M. Caron, I. M. Mombo, D. Nkoghe, S. M. Ondo, D. Jiolle, D. Fontenille, C. Paupy, and E. M. Leroy. Zika virus in gabon (central africa)–2007: a new threat from aedes albopictus? PLoS Neglected Tropical Diseases, 8(2):e2681, 2014.

[111] E. M. Griebeler and A. Seitz. An individual based model for the conservation of the endangered large blue butterfly, maculinea arion (lepidoptera: Lycaenidae). Ecological Modelling, 156(1):43–60, 2002.

[112] P. Gros. La représentation de l'espace dans les modèles de dynamique des populations(modèles dynamiques déterministes à temps et espace continus). Bilans & Prospectives- IFREMER, 2001.

[113] S. Gubbins, C. A. Gilligan, and A. Kleczkowski. Population dynamics of plant–parasite interactions: thresholds for invasion. Theoretical Population Biology, 57(3):219–233, 2000.

[114] D. J. Gubler and G. G. Clark. Dengue/dengue hemorrhagic fever: the emergence of a global health problem. Emerging Infectious Diseases, 1(2):55, 1995.

[115] R. A. Haack, R. C. Wilkinson, J. L. Foltz, and J. A. Corneil. Spatial attack pattern, reproduction, and brood development of *Ips-calligraphus* (Coleoptera: Scolytidae) in relation to slash pine phloem thickness, a field-study. Environmental Entomology, 16(2):428–436, 1987.

[116] P. A. Hancock and H. C. J. Godfray. Modelling the spread of wolbachia in spatially heterogeneous environments. Journal of the Royal Society Interface, page rsif20120253, 2012.

[117] I. Hanski. Metapopulation dynamics. Nature, 396(6706):41–49, 1998. 1179.

[118] I. Hanski. Metapopulation Ecology. Oxford University Press, 1999.

[119] A. W. Hartstack and J. A. Witz. Estimating field populations of tobacco budworm moths from pheromone trap catches. Environmental Entomology, 10(6):908–914, 1981.

[120] M. P. Hassell, H. N. Comins, and R. M. May. Spatial structure and chaos in insect population dynamics. Nature, 353(6341):255–258, 1991.

[121] A. Hastings. Models of spatial spread: is the theory complete? Ecology, 77(6):1675–1679, 1996.

[122] W. A. Hawley. The biology of aedes albopictus. Journal of the American Mosquito Control Association. Supplement, 1:1–39, 1988.

[123] F. Hecht. New development in freefem++. Journal of Numerical Mathematics, 20(3-4):251–265, 2012.

[124] F. Hecht, O. Pironneau, A. Le Hyaric, and K. Ohtsuka. Freefem++ manual, 2005.

[125] J. A. P. Heesterbeek. Mathematical Epidemiology of Infectious Diseases: Model Building, Analysis and Interpretation, volume 5. John Wiley & Sons, 2000.

[126] G. A. Hepburn and H. J. Bishop. Control of false codling moth by means of insecticidal sprays. Farming in South Africa, 26:375–8, 1951. 0.

[127] T. Hillen and K. J. Painter. A user's guide to pde models for chemotaxis. Journal of Mathematical Biology, 58(1-2):183–217, 2009.

[128] M. W. Hirsch and S. Smale. Differential Equations, Dynamical Systems, and Linear Algebra, volume 60. Academic press, 1974.

[129] A. A. Hoffmann, B. L. Montgomery, J. Popovici, I. Iturbe-Ormaetxe, P. H. Johnson, F. Muzzi, M. Greenfield, M. Durkan, Y. S. Leong, Y. Dong, et al. Successful establishment of *Wolbachia* in aedes populations to suppress dengue transmission. Nature, 476(7361):454–457, 2011.

[130] A. A. Hoffmann, P. A. Ross, and G. Rašić. *Wolbachia* strains for disease control: ecological and evolutionary considerations. Evolutionary Applications, 8(8):751–768, 2015.

[131] J. H. Hofmeyr, J. E. Carpenter, and S. Bloem. Developing the sterile insect technique for *Cryptophlebia leucotreta* (Lepidoptera: Tortricidae): Influence of radiation dose and release ratio on fruit damage and population growth in field cages. Journal of Economic Entomology, 98(6):1924–1929, 2005.

[132] J. H. Hofmeyr and K. L. Pringle. Resistance of false codling moth, *Cryptophlebia leucotreta* (Meyrick)(Lepidoptera: Tortricidae), to the chitin synthesis inhibitor, triflumuron. African Entomology, 6(2):373–375, 1998.

[133] C. S. Holling. Some characteristics of simple types of predation and parasitism. The Canadian Entomologist, 91(07):385–398, 1959.

[134] M. E. Hosea and L. F. Shampine. Analysis and implementation of TR-BDF2. Applied Numerical Mathematics, 20(1):21–37, 1996.

[135] P. E. Howse, I. D. R. Stevens, and O. T. Jones. Insect Pheromones and their Use in Pest Management. Chapman & Hall, 1998.

[136] W. H. Hundsdorfer and J. G. Verwer. Numerical Solution of Time-Dependent Advection-Diffusion-Reaction Equations, volume 33. Springer Verlag, 2007.

[137] N. J. B. Isaac, K. L. Cruickshanks, A. M. Weddle, M. J. Rowcliffe, T. M. Brereton, R. L. H. Dennis, D. M. Shuker, and C. D. Thomas. Distance sampling and the challenge of monitoring butterfly populations. Methods in Ecology and Evolution, 2(6):585–594, 2011.

[138] R. E. Jones. Movement patterns and egg distribution in cabbage butterflies. The Journal of Animal Ecology, pages 195–212, 1977.

[139] S. A. Juliano and P. L. Lounibos. Ecology of invasive mosquitoes: effects on resident species and on human health. Ecology Letters, 8(5):558–574, 2005.

[140] P. M. Kareiva and N. Shigesada. Analyzing insect movement as a correlated random walk. Oecologia, 56(2-3):234–238, 1983.

[141] E. F. Keller and L. A. Segel. Model for chemotaxis. Journal of Theoretical Biology, 30(2):225–234, 1971.

[142] L. Kelly and J. Sellers. Abundance and distribution of the invasive ant, *Solenopsis invicta* (Hymenoptera: Formicidae), in Cypress savannas of north carolina. Annals of the Entomological Society of America, 107(6):1072–1080, 2014.

[143] J. S. Kennedy. The excitant and repellent effects on mosquitos of sub-lethal contacts with ddt. Bulletin of Entomological Research, 37(04):593–607, 1947.

[144] W. O. Kermack and A. G. McKendrick. A contribution to the mathematical theory of epidemics. In Proceedings of the Royal Society of London A: Mathematical, Physical and Engineering Sciences, volume 115, pages 700–721. The Royal Society, 1927.

[145] F. M. Khamis, N. Karam, S. Ekesi, M. De Meyer, A. Bonomi, L. M. Gomulski, F. Scolari, P. Gabrieli, P. Siciliano, D. Masiga, et al. Uncovering the tracks of a recent and rapid invasion: the case of the fruit fly pest bactrocera invadens (diptera: Tephritidae) in africa. Molecular Ecology, 18(23):4798–4810, 2009.

[146] E. F. Knipling. Possibilities of insect control or eradication through the use of sexually sterile males. Journal of Economic Entomology, 48(4):459–462, 1955.

[147] E. F. Knipling. Sterile-male method of population control. Science, 130(3380):902–904, 1959.

[148] E. F. Knipling. Sterile-male method of population control successful with some insects, the method may also be effective when applied to other noxious animals. Science, 130(3380):902–904, 1959.

[149] E. F. Knipling et al. The basic principles of insect population suppression and management. Agriculture Handbook. USDA, (512), 1979.

[150] E. F. Knipling, J. U. McGuire, et al. Population Models to Test Theoretical Effects of Sex Attractants Used for Insect Control. Agricultural Research Service, US Dept. of Agriculture, 1966.

[151] J. Koiller, M. Da Silva, M. Souza, C. Codeço, A. Iggidr, and G. Sallet. Aedes, Wolbachia and Dengue. PhD thesis, Inria Nancy-Grand Est (Villers-lès-Nancy, France), 2014.

[152] J. Koyama, T. Teruya, and K. Tanaka. Eradication of the oriental fruit fly (Diptera: Tephritidae) from the Okinawa Islands by a male annihilation method. Journal of Economic Entomology, 77(2):468–472, 1984.

[153] C. J. Krebs et al. Ecological Methodology, volume 620. Benjamin/Cummings Menlo Park, California, 1999.

[154] L. A. Krumholz. Reproduction in the western mosquitofish, gambusia affinis affinis (baird & girard), and its use in mosquito control. Ecological Monographs, pages 1–43, 1948.

[155] D. R. Lance and D. O. McInnis. Biological basis of the sterile insect technique. In Sterile Insect Technique, pages 69–94. Springer, 2005.

[156] D. Lanser and J. G. Verwer. Analysis of operator splitting for advection–diffusion–reaction problems from air pollution modelling. Journal of Computational and Applied Mathematics, 111(1):201–216, 1999.

[157] M. M. Lavrent'ev, V. G. Romanov, and S. P. Shishatskii. Ill-Posed Problems of Mathematical Physics and Analysis, volume 64. American Mathematical Society, 1986.

[158] L. Leblanc, R. I. Vargas, B. MacKey, R. Putoa, and J. C. Piñero. Evaluation of cue-lure and methyl eugenol solid lure and insecticide dispensers for fruit fly (diptera: Tephritidae) monitoring and control in tahiti. Florida Entomologist, 94(3):510–516, 2011.

[159] L. Leblanc, R. I. Vargas, and R. Putoa. From eradication to containment: invasion of French Polynesia by *Bactrocera dorsalis* (Hendel)(Diptera: Tephritidae) and releases of two natural enemies: a 17-year case study. In Hawaiian Entomological Societey, volume 45. 2013.

[160] L. P. Lefkovitch. The study of population growth in organisms grouped by stages. Biometrics, 21(1):1–18, 1965.

[161] P. H. Leslie. On the use of matrices in certain population mathematics. Biometrika, 33(3):183–212, 1945.

[162] S. A. Levin. Dispersion and population interactions. American Naturalist, 108(960):207–228, 1974.

[163] C. C. Lord. Modeling and biological control of mosquitoes. Journal of the American Mosquito Control Association, 23(2 Suppl):252, 2007.

[164] S. A. Lux, R. S. Copeland, I. M. White, A. Manrakhan, and M. K. Billah. A new invasive fruit fly species from the *Bactrocera dorsalis* (Hendel) group detected in East Africa. International Journal of Tropical Insect Science, 23(04):355–361, 2003.

[165] C. Magaña, P. Hernández-Crespo, F. Ortego, and P. Castañera. Resistance to malathion in field populations of *Ceratitis capitata*. Journal of Economic Entomology, 100(6):1836–1843, 2007.

[166] N. C. Manoukis, B. Hall, and S. M. Geib. A computer model of insect traps in a landscape. Scientific Reports, 4:1–8, 2014.

[167] A. Manrakhan, V. Hattingh, J. H. Venter, and M. Holtzhausen. Eradication of *Bactrocera invadens* (Diptera: Tephritidae) in Limpopo Province, South Africa. African Entomology, 19(3):650–659, 2011.

[168] A. Manrakhan and C. Kotze. Attraction of *Ceratitis capitata*, *C. rosa* and *C. cosyra* (Diptera: Tephritidae) to proteinaceous baits. Journal of Applied Entomology, 135(1-2):98–105, 2011.

[169] D. W. Marquardt. An algorithm for least-squares estimation of nonlinear parameters. Journal of the Society for Industrial & Applied Mathematics, 11(2):431–441, 1963.

[170] M. Martcheva. An Introduction to Mathematical Epidemiology, volume 61 of Texts in Applied Mathematics. Springer US, 1 edition, 2015.

[171] MATLAB. version 7.14.0.739 (R2012a). The MathWorks Inc., Natick, Massachusetts, 2012.

[172] R. M. May and R. M. Anderson. Population biology of infectious diseases: Part ii. Nature, 280(5722):455–461, 1979.

[173] H. McCallum. Population Parameters: Estimation for Ecological Models, volume 3. John Wiley & Sons, 2008.

[174] E. McCauley, W. G. Wilson, and A. M. de Roos. Dynamics of age-structured and spatially structured predator-prey interactions: individual-based models and population-level formulations. American Naturalist, 142(3):412–442, 1993.

[175] A. Meats and C. J. Smallridge. Short-and long-range dispersal of medfly, ceratitis capitata (dipt., tephritidae), and its invasive potential. Journal of Applied Entomology, 131(8):518–523, 2007.

[176] J. M. Medlock, K. M. Hansford, F. Schaffner, V. Versteirt, G. Hendrickx, H. Zeller, and W. V. Bortel. A review of the invasive mosquitoes in europe: ecology, public health risks, and control options. Vector-Borne and Zoonotic Diseases, 12(6):435–447, 2012.

[177] M. Megharaj, D. Kantachote, I. Singleton, and R. Naidu. Effects of long-term contamination of ddt on soil microflora with special reference to soil algae and algal transformation of ddt. Environmental Pollution, 109(1):35–42, 2000.

[178] M. Michereff Filho, E. F. Vilela, G. N. Jham, A. Attygalle, A. Svatos, and J. Meinwald. Initial studies of mating disruption of the tomato moth, *Tuta absoluta* (Lepidoptera: Gelechiidae) using synthetic sex pheromone. Journal of the Brazilian Chemical Society, 11(6):621–628, 2000.

[179] R. E. Mickens. Nonstandard Finite Difference Models of Differential Equations. World Scientific Pub Co Inc, 1994.

[180] R. E. Mickens. Applications of Nonstandard Finite Difference Schemes. World Scientific, 2000.

[181] A. G. M'Kendrick. Applications of mathematics to medical problems. Proceedings of the Edinburgh Mathematical Society, 44:98–130, 1925.

[182] C. Mocenni, D. Madeo, and E. Sparacino. Linear least squares parameter estimation of nonlinear reaction diffusion equations. Mathematics and Computers in Simulation, 81(10):2244–2257, 2011.

[183] J. G. Morse, R. F. Luck, and D. J. Gumpf. Citrus Pest Problems and their Control in the Near East. Number 135. Food & Agriculture Organisation, 1996.

[184] M. W. Mwatawala, M. De Meyer, R. H. Makundi, and A. P. Maerere. Seasonality and host utilization of the invasive fruit fly, *Bactrocera invadens* (Dipt., Tephritidae) in central Tanzania. Journal of Applied Entomology, 130(9-10):530–537, 2006.

[185] K. Nakmura and K. Kawasaki. The active space of the *Spodoptera litura* (F.) sex pheromone and the pheromone component determining this space. Applied Entomology and Zoology, 12(2):162–177, 1977.

[186] T. Nishida, H. A. Bess, et al. Studies on the Ecology and Control of the Melon Fly *Dacus* (Strumeta) *cucurbitae* Coquillett (Diptera: Tephritidae). Number 34. Hawaii Agricultural Experiment Station, University of Hawaii, 1957.

[187] E. V. Nordheim, D. B. Hogg, and S.-Y. Chen. Leslie matrix models for insect populations with overlapping generations. In Estimation and Analysis of Insect Populations, pages 289–298. Springer, 1989.

[188] A. Okubo. Diffusion and Ecological Problems: Mathematical Models, volume 10. Springer-Verlag Berlin, 1980.

[189] F. Östrand and O. Anderbrant. From where are insects recruited? a new model to interpret catches of attractive traps. Agricultural and Forest Entomology, 5(2):163–171, 2003.

[190] H. G. Othmer, S. R. Dunbar, and W. Alt. Models of dispersal in biological systems. Journal of Mathematical Biology, 26:263–298, 1988. 10.1007/BF00277392.

[191] S. N. Ouedraogo. Dynamique Spatio-Temporelle des Mouches des Fruits (Diptera Tephritidae) enFfonction des Facteurs Biotiques et Abiotiques dans les Vergers de Manguiers de l'Ouest du Burkina Faso. PhD thesis, Université Paris, 2011.

[192] A. Pazy. Semigroups of Linear Operators and Applications to Partial Differential Equations. Springer-Verlag, New York, 1983.

[193] A. Perasso. Identifiabilité de Paramètres pour des Systèmes Décrits par des Equations aux Dérivées Partielles. Application à la Dynamique des Populations. PhD thesis, Université Paris Sud-Paris XI, 2009.

[194] N. Petrovskaya, S. Petrovskii, and A. K. Murchie. Challenges of ecological monitoring: estimating population abundance from sparse trap counts. Journal of the Royal Society Interface, 9(68):420–435, 2012.

[195] S. Petrovskii, D. Bearup, D. A. Ahmed, and R. Blackshaw. Estimating insect population density from trap counts. Ecological Complexity, 10:69–82, 2012.

[196] G. Pialoux, B.-A. Gaüzère, S. Jauréguiberry, and M. Strobel. Chikungunya, an epidemic arbovirosis. The Lancet Infectious Diseases, 7(5):319–327, 2007.

[197] R. E. Plant and R. T. Cunningham. Analyses of the dispersal of sterile Mediterranean fruit flies (Diptera: Tephritidae) released from a point source. Environmental Entomology, 20(6):1493–1503, 1991.

[198] K. H. Pollock, J. D. Nichols, C. Brownie, and J. E. Hines. Statistical inference for capture-recapture experiments. Wildlife Monographs, (107):3–97, 1990.

[199] P. Pommois, P. Brunetti, V. Bruno, A. Mazzei, V. Baldacchini, and S. Di Gregorio. Flysim: a cellular automata model of *Bactrocera oleae* (olive fruit fly) infestation and first simulations. In Cellular Automata, pages 311–320. Springer, 2006.

[200] A. Prieto-Langarica, H. V. Kojouharov, and B. M. Chen-Charpentier. Upscaling from discrete to continuous mathematical models of two interacting populations. Computers & Mathematics with Applications, 66(9):1606–1612, 2013.

[201] M. H. Protter and H. F. Weinberger. Maximum Principles in Differential Equations. Springer, 1984.

[202] H. Ranson, B. Jensen, J. M. Vulule, X. Wang, J. Hemingway, and F. H. Collins. Identification of a point mutation in the voltage-gated sodium channel gene of Kenyan *Anopheles gambiae* associated with resistance to DDT and pyrethroids. Insect Molecular Biology, 9(5):491–497, 2000.

[203] J. N. Reddy. An Introduction to the Finite Element Method, volume 2. McGraw-Hill New York, 1993.

[204] E. Rexstad and K. P. Burnham. User's Guide for Interactive Program CAPTURE. Color. Cooperative Fish and Wildlife Research Unit, 1991.

[205] R.-D. Richtmyer and K.-W. Morton. Difference methods for initial-value problems. SIAM Review, 10(3):381–383, 1967.

[206] D. C. Robacker. Effects of shape and size of colored traps on attractiveness to irradiated, laboratory-strain Mexican fruit flies (Diptera: Tephritidae). Florida Entomologist, pages 230–241, 1992.

[207] D. C. Robacker, D. S. Moreno, and D. A. Wolfenbarger. Effects of trap color, height, and placement around trees on capture of Mexican fruit flies (Diptera: Tephritidae). Journal of Economic Entomology, 83(2):412–419, 1990.

[208] I. D. Rojnić, R. Bažok, and J. I. Barčić. Reduction of olive fruit fly damage by early harvesting and impact on oil quality parameters. European Journal of Lipid Science and Technology, 117(1):103–111, 2015.

[209] L. Roques, M.-A. Auger-Rozenberg, and A. Roques. Modelling the impact of an invasive insect via reaction-diffusion. Mathematical Biosciences, 216(1):47–55, 2008.

[210] R. Ross. Malaria prevention in greece. British Medical Journal, 1(2735):1186, 1913.

[211] I. Rwomushana, S. Ekesi, I. Gordon, and C. K. P. O. Ogol. Host plants and host plant preference studies for *Bactrocera invadens* (Diptera: Tephritidae) in Kenya, a new invasive fruit fly species in Africa. Annals of the Entomological Society of America, 101(2):331–340, 2008.

[212] G. Sallet. R_0, 2010. INRIA & IRD EPICASA09, Avril 2010.

[213] G. Sallet and A. H. B. S. Moacyr. Monotone dynamical systems and some models of wolbachia in *Aedes aegypti* populations. Revue Africaine de la Recherche en Informatique et Mathématiques Appliquées, 20:145–176, 2015.

[214] F. Schlyter. Sampling range, attraction range, and effective attraction radius: Estimates of trap efficiency and communication distance in coleopteran pheromone and host attractant systems. Journal of Applied Entomology, 114(1-5):439–454, 1992.

[215] M. K. Schutze, N. Aketarawong, W. Amornsak, K. F. Armstrong, A. A. Augustinos, N. Barr, W. Bo, K. Bourtzis, L. M. Boykin, C. Caceres, et al. Synonymization of key pest species within the *Bactrocera dorsalis* species complex (Diptera: Tephritidae): taxonomic changes based on a review of 20 years of integrative morphological, molecular, cytogenetic, behavioural and chemoecological data. Systematic Entomology, 40(2):456–471, 2015.

[216] M. K. Schutze, K. Mahmood, A. Pavasovic, W. Bo, J. Newman, A. R. Clarke, M. N. Krosch, and S. L. Cameron. One and the same: integrative taxonomic evidence that bactrocera invadens (diptera: Tephritidae) is the same species as the oriental fruit fly bactrocera dorsalis. Systematic Entomology, 40(2):472–486, 2015.

[217] A. Schwartz, W. J. du Toit, and W. J. Du Toit. Improvements to the mass rearing technique for the Mediterranean fruit-fly *Ceratitis capitata* (Wied.). Citrus and Subtropical Fruit Journal, (540):7–12, 1978. 0.

[218] C. J. Schwarz and G. A. F. Seber. Estimating animal abundance: Review iii. Statistical Science, 14(4):pp. 427–456, 1999.

[219] Scilab Enterprises. Scilab: Le logiciel open source gratuit de calcul numérique. Scilab Enterprises, Orsay, France, 2012.

[220] N. Shigesada and K. Kawasaki. Biological Invasions: Theory and Practice. Oxford University Press, UK, 1997.

[221] M. D. F. Shirley and R. M. Sibly. Metapopulation dynamics of fruit flies undergoing evolutionary change in patchy environments. Ecology, 82(11):3257–3262, 2001.

[222] J. G. Skellam. Random dispersal in theoretical populations. Biometrika, 38(1):196–218, 1951.

[223] R. Slimi, S. El Yacoubi, E. Dumonteil, and S. Gourbiere. A cellular automata model for chagas disease. Applied Mathematical Modelling, 33(2):1072–1085, 2009.

[224] D. Smith and D. F. Papacek. Studies of the predatory mite *Amblyseius victoriensis* (Acarina: Phytoseiidae) in citrus orchards in south-east Queensland: Control of *Tegolophus australis* and *Phyllocoptruta oleivora* (Acarina: Eriophyidae), effect of pesticides, alternative host plants and augmentative release. Experimental & Applied Acarology, 12(3-4):195–217, 1991.

[225] H. L. Smith. Monotone Dynamical Systems: an Introduction to the Theory of Competitive and Cooperative Systems. Number 41. American Mathematical Society, 2008.

[226] T. R. E. Southwood and P. A. Henderson. Ecological Methods. John Wiley & Sons, 2009.

[227] T. R. E. Southwood and M. J. Way. Ecological background to pest management. Concepts of Pest Management, 6:28, 1970.

[228] F. Spitzer. Principles of Random Walk, volume 34. Springer, 1976.

[229] G. C. Steyskal. History and use of the McPhail trap. Florida Entomologist, pages 11–16, 1977.

[230] R. E. Stinner, C. S. Barfield, J. L. Stimac, and L. Dohse. Dispersal and movement of insect pests. Annual Review of Entomology, 28(1):319–335, 1983.

[231] F. J. Stofberg. Larval structure as a basis for certain identification of false codling moth (Argyroploce leucotreta, Meyr.) larvae. Journal of the Entomological Society of Southern Africa, 11:68–75, 1948. 3.

[232] R. L. Stotter. Spatial and Temporal Distribution of False Codling mMoth across Landscapes in the Citrusdal area (Western Cape Province, South Africa). PhD thesis, Stellenbosch: University of Stellenbosch, 2009.

[233] J. Strikwerda. Finite difference schemes and partial differential equations. Siam, 2007.

[234] D. D. Thomas, C. A. Donnelly, R. J. Wood, and L. S. Alphey. Insect population control using a dominant, repressible, lethal genetic system. Science, 287(5462):2474–2476, 2000.

[235] J. W. Thomas. Numerical Partial Differential Equations: Finite Difference Methods, volume 22. Springer Science & Business Media, 2013.

[236] A. N. Tikhonov. Solution of Ill-Posed Problems. Winston & Sons, 1977.

[237] D. Tilman and P. M. Kareiva. Spatial ECology: the Role of Space in Population Dynamics and Interspecific Interactions, volume 30. Princeton University Press, 1997.

[238] P. Turchin. Quantitative Analysis of Movement: Measuring and Modeling Population Redistribution in Animals and Plants. Sinauer Associates Sunderland, 1998.

[239] A. M. Turing. The chemical basis of morphogenesis. Philosophical Transactions of the Royal Society of London B: Biological Sciences, 237(641):37–72, 1952.

[240] V. Turusov, V. Rakitsky, and L. Tomatis. Dichlorodiphenyltrichloroethane (DDT): ubiquity, persistence, and risks. Environmental Health Perspectives, 110(2):125, 2002.

[241] R. Tyson, H. Thistlewood, and G. J. R. Judd. Modelling dispersal of sterile male codling moths, *Cydia pomonella*, across orchard boundaries. Ecological Modelling, 205(1):1–12, 2007.

[242] P. Van den Driessche and J. Watmough. Reproduction numbers and sub-threshold endemic equilibria for compartmental models of disease transmission. Mathematical Biosciences, 180(1):29–48, 2002.

[243] P. Van Mele, J.-F. Vayssières, E. Van Tellingen, and J. Vrolijks. Effects of an African weaver ant, *Oecophylla longinoda*, in controlling mango fruit flies (Diptera: Tephritidae) in Benin. Journal of Economic Entomology, 100(3):695–701, 2007.

[244] J.-F. Vayssieres, A. Sinzogan, S. Korie, I. Ouagoussounon, and A. Thomas-Odjo. Effectiveness of spinosad bait sprays (gf-120) in controlling mango-infesting fruit flies (diptera: Tephritidae) in benin. Journal of Economic Entomology, 102(2):515–521, 2009.

[245] V. Volpert. Elliptic Partial Differential Equations: Volume 2: Reaction-Diffusion Equations, volume 104. Springer, 2014.

[246] H. von Foerster. Some Remarks on Changing Populations. In The Kinetics of Cellular Proliferation, pages 382–407. Grune and Stratton, 1959.

[247] C. Wall and J. N. Perry. Range of action of moth sex-attractant sources. Entomologia experimentalis et applicata, 44(1):5–14, 1987.

[248] W. Walter. Differential and Integral Inequalities, volume 55. Springer Science & Business Media, 2012.

[249] M. Watson. The Prevention of Malaria in the Federated Malay States: a Record of Twenty Years' Progress. EP Dutton & Company, 1921.

[250] M. J. Way and H. F. Van Emden. Integrated pest management in practice—pathways towards successful application. Crop Protection, 19(2):81–103, 2000.

[251] J. H. Werren. Biology of *Wolbachia*. Annual Review of Entomology, 42(1):587–609, 1997.

[252] G. C. White. Noremark: population estimation from mark-resighting surveys. Wildlife Society Bulletin, pages 50–52, 1996.

[253] G. C. White and K. P. Burnham. Program mark: survival estimation from populations of marked animals. Bird Study, 46(S1):120–139, 1999.

[254] S. Wiggins. Introduction to Applied Nonlinear Dynamical Systems and Chaos, volume 2. Springer Science & Business Media, 2003.

[255] A. B. B. Wilke and M. T. Marrelli. Paratransgenesis: a promising new strategy for mosquito vector control. Parasites & Vectors, 8(1):1–9, 2015.

[256] P. Witzgall, P. Kirsch, and A. Cork. Sex pheromones and their impact on pest management. Journal of Chemical Ecology, 36(1):80–100, 2010.

[257] T. Yamanaka. Mating disruption or mass trapping? numerical simulation analysis of a control strategy for lepidopteran pests. Population Ecology, 49(1):75–86, 2007.

[258] T. Yamanaka, S. Tatsuki, and M. Shimada. An individual-based model for sex-pheromone-oriented flight patterns of male moths in a local area. Ecological Modelling, 161(1):35–51, 2003.

[259] Q.-H. Zhang and F. Schlyter. High recaptures and long sampling range of pheromone traps for fall web worm mothhyphantria cunea (lepidoptera: Arctiidae) males. Journal of Chemical Ecology, 22(10):1783–1796, 1996.

[260] A. A. Zhigljavsky and J. Pintér. Theory of Global Random Search. Springer Netherlands, 1991.